

D65-92
HIS

MODELLING OF SURFACE ACOUSTIC WAVE SIGNAL PROCESSING DEVICES

A THESIS

submitted in fulfilment of the
requirements for the award of the degree

of

DOCTOR OF PHILOSOPHY

in

ELECTRONICS AND COMPUTER ENGINEERING

By

HISHAM AL-RAWI



DEPARTMENT OF ELECTRONICS & COMPUTER ENGINEERING
UNIVERSITY OF ROORKEE
ROORKEE-247 667 (INDIA)
SEPTEMBER, 1992



DEDICATED TO

Beloved PARENTS

Dear Wife MANAA

Dear Son MUSTAFA

Dear Daughter NOOR

AND to all relatives and friends
who encouraged and helped me
Morally and/or Materially inspite
of their suffering during and
after the so called

1991-1992

Roorkee Sep. 1992


Wisham Al-Rawi

CANDIDATE'S DECLARATION

I hereby certify that the work which is being presented in the thesis entitled ' Modelling Of Surface Acoustic Wave Signal Processing Devices ' in fulfilment of the requirement for the award of the Degree of Doctor of Philosophy and submitted in the Department Of Electronics And Computer Engineering of the University is an authentic record of my own work carried out during a period from August 1989 to September 1992 under the supervision of Dr. Jai Krishna Gautam.

The matter presented in this thesis has not been submitted by me for the award of any other degree of this or any other University.

Date: 22 Sep. 1992



22/9/92 (Hisham Al-Rawi)
Candidate


This is to certify that the above statement made by the candidate is correct to the best of my knowledge.


Date: 22 Sep. 1992


(Dr. Jai Krishna Gautam)
Supervisor 20/9/92

The Ph.D Viva-Voce examination of Hisham Al-Rawi, Research Scholar, Has been held on 23.1.1993 at 10:30 AM.


Signature of Supervisor 23/1/93


Signature of H.O.D.


Signature of External Examiner

ACKNOWLEDGMENTS

My first and foremost thanks are due to Dr. Jai Krishna Gautam, for his supervision of my work and for his helpful suggestions, fruitful discussions, and continuous encouragement and support. It is only because of his continuous efforts to make work facilities available for me and his keen interest in my work that brought this work into existence.

I wish to express my thanks to the past and present Heads and all Staff and Faculty members of the *Department of Electronics and Computer Engineering* of this university for what ever help they afforded even with a 'smile' and 'Good Morning' I used to start my day with. Special thanks to staff and O.C.s of Communication Systems and P.C. labs.

I would like to acknowledge gratefully the continuous support and encouragement of my Wife; who made a lot of sacrifice since we started our trip toward this country, tried her best to allow me maximum time for research and never complained inspite of hardships.

The blessings and prayers of my Mother and Father, and their continuous support, inspite the distance between us and their problems, were among the most important boosts for me to complete this work.

I would like to thank all Relatives and Friends who wrote to me and encouraged me. And I do not forget to thank All The Good People I met here in this country since the first day I landed.

Roorkee. September 1992.

Hisham Al-Rawi.

ABBREVIATIONS

<i>Apodization Type Number</i>	APD
<i>Acoustic Transmission Loss</i>	ATL
<i>Bidirectional InterDigital Transducer</i>	BIDT
<i>Bandwidth</i>	BW
<i>Chain Matrix Model</i>	CHAIN MAT
<i>Coupled Of Modes Theory</i>	COM
<i>Electronic</i>	ESM
<i>Fall Bandwidth Support Measurs</i>	FB
<i>Finite Impulse Response</i>	FIR
<i>Group UniDirectional Transducer</i>	GUDT
<i>InterDigital Transducer</i>	IDT
<i>Interdigitated InterDigital Transducer</i>	IIDT
<i>Infinite Impulse Response</i>	IIR
<i>Insertion Loss</i>	IL
<i>Lift Side lobe Level</i>	LSL
<i>Modified Bessel Function</i>	MBF
<i>Modified type GUDT</i>	MGUDT
<i>Normal type GUDT</i>	NGUDT

<i>New type GUDT</i>	NUGUDT
<i>Pass Band Ripples</i>	R_p
<i>Phase Shifter</i>	PS
<i>Quadreture Amplitude Modulation</i>	QAM
<i>Quadreture Phase UniDirectional Transducer</i>	QPUDT
<i>Rise Bandwidth</i>	RB
<i>Rejection Bandwidth</i>	RJ
<i>Right Side lobe Level</i>	RSL
<i>Surface Acoustic Wave</i>	SAW
<i>Scattering Matrix Model</i>	SCAT MAT
<i>Transition Bandwidth</i>	TB
<i>Three Phase UniDirectional Transducer</i>	TPUDT
<i>Transfer Matrix Model</i>	TRANS MAT
<i>Triple Transit Echo</i>	TTE
<i>UniDirectional Transducer</i>	UDT

TABLE OF CONTENTS

DEDICATION.	(ii)
CANDIDATE'S DECLARATION.	(iii)
ACKNOWLEDGEMENT.	(iv)
LIST OF ABBREVIATIONS.	(vi)
ABSTRACT.	7
CHAPTER ONE	
TO BEGIN WITH..	
1.1 <i>Introduction.</i>	11
1.2 <i>Surface Acoustic Wave Interdigital Transducer.</i>	12
1.3 <i>Unidirectional Transducers.</i>	14
1.4 <i>Models For The Analysis Of Surface Acoustic Wave Devices.</i>	15
1.5 <i>Equivalent Circuit Theory Approach Models.</i>	17
1.6 <i>Field Theory Approach Models.</i>	18
1.7 <i>Merits Of SAW Devices.</i>	20
1.8 <i>Statement Of The Problem.</i>	22
1.9 <i>Organization Of The Dissertation.</i>	24
1.10 <i>Notes To The Reader.</i>	25

CHAPTER TWO	SCATTERING MATRIX APPROACH.	
	2.1 Introduction.	28
	2.2 Modelling Of An IDT.	29
	2.3 Modelling Of IDT From A Single Finger-Pair.	33
	2.3.1 Junction.	37
	2.3.2 Combination Of Two Radiators /Scatterers.	40
	2.4 Modelling Of A UDT.	44
	2.5 Understanding The Scattering Matrix Parameters.	50
	2.6 Calculations Of Scattering Matrix Parameters.	53
	2.7 Computations.	58
	2.8 Conclusion.	60
CHAPTER THREE	TRANSFER MATRIX APPROACH.	
	3.1 Introduction.	64
	3.2 Modelling Of An IDT.	64
	3.3 Single Finger Transfer Matrix.	67
	3.4 Basic-Unit Transfer Matrix.	77
	3.5 Positive And Negative Voltage derived Fingers.	79
	3.6 Computations.	81
	3.7 Conclusion.	85

CHAPTER FOUR	CHAIN MATRIX APPROACH.	
4.1	Introduction.	88
4.2	Chain Matrix Approach Explanation.	89
4.3	Modelling Of Chain matrix Approach Basic-Unit.	92
4.4	Modelling Of Transducer And Filter.	97
4.5	Modelling Of Unidirectional Transducers.	102
4.5.1	Group Type Unidirectional Transducer.	102
4.5.2	Three Phase Unidirectional Transducer.	107
4.6	Computations.	112
4.7	Performance Of Group Type Unidirectional Transducers.	115
4.8	Performance Of Three Phase Unidirectional transducers.	118
4.9	Filters Of Pair Of Identical Transducers.	119
4.10	Filters Of Combinations Of Group Unidirectional Transducers.	125
4.11	Filters Of Combinations Of GUDTs And TPUDTs.	132
4.12	Conclusion.	138

CHAPTER FIVE	APODIZATION AND WINDOWING.	
	5.1 Introduction.	143
	5.2 Apodization.	144
	5.3 Filter Design Specifications.	147
	5.4 SINC Apodization Computations.	151
	5.5 SINC Apodized Group Unidirectional Transducers.	151
	5.6 SINC Apodized Three Phase Unidirectional transducers.	155
	5.7 Filters Of Uniform And SINC Apodized GUDTs.	157
	5.8 Filters Of Uniform And SINC Apodized TPUDTs.	167
	5.9 Filters Of Combinations Of Uniform And SINC Apodized GUDT And TPUDT Transducers.	175
	5.10 Windowing.	183
	5.11 COSINE Windowing Computations.	186
	5.12 SINC Weighted - COSINE Windowed Apodized GUDTs.	188
	5.13 SINC Weighted - COSINE Windowed Apodized TPUDTs.	194
	5.14 Filters Of Uniform And SINC Weighted - COSINE Windowed (Apodized) GUDTs.	194

5.15	<i>Filters Of Uniform And SINC Weighted - COSINE Windowed (Apodized) TPUDTs.</i>	204
5.16	<i>Filters Of Combinations Of Uniform And SINC Weighted - COSINE Windowed (Apodized) GUDTs and TPUDTs.</i>	214
5.17	<i>Conclusion.</i>	224
CHAPTER SIX	MODIFIED BESSEL FUNCTION WINDOW FAMILY.	
6.1	<i>Introduction.</i>	233
6.2	<i>Windows For SAW Transducers.</i>	234
6.3	<i>Modified Bessel Function Window Family.</i>	236
6.4	<i>Computation Of Modified Bessel Function Window Family.</i>	237
6.5	<i>Characteristics Of Different MBF Windows.</i>	240
6.6	<i>New Apodization Profiles Using MBF Windows.</i>	243
6.7	<i>Apodized GUDTs. (SINC-COSINE-MBF Profiles).</i>	252
6.8	<i>Apodized TPUDTs. (SINC-COSINE-MBF Profiles).</i>	257

6.9	<i>Filters With Uniform And (SINC - COSINE - MBF Profiles) Apodized GUDTs.</i>	261
6.10	<i>Filters With Uniform And (SINC - COSINE - MBF Profiles) Apodized TPUDTs.</i>	275
6.11	<i>Filters With Uniform TPUDTs And (SINC - COSINE - MBF Profiles) Apodized GUDTs.</i>	284
CHAPTER SEVEN	RECAPITULATION AND CONCLUSION.	
7.1	<i>Introduction.</i>	295
7.2	<i>Modelling Of SAW Devices.</i>	295
7.3	<i>Simulation And Study Of Performances Of Different Types Of SAW Transducers And Filters.</i>	298
7.4	<i>Discussing The Goals.</i>	304
7.5	<i>Future Scope.</i>	305
7.6	<i>Concluding Words.</i>	306
APPENDIX	CHAIN MAT SIMULATOR	307
REFERENCES.		311
VITA OF THE AUTHOR.		317

ABSTRACT

Surface Acoustic Wave (SAW) devices are finding applications in many diverse electronic equipment. Analysis and synthesis of any operational device (like a SAW device) associated with a complicated physics can be performed by some equivalent model. Many models have been developed for the analysis of SAW devices. There are two approaches for such modelling namely; field theory approach and circuit theory approach. The existing models are such as the Delta function model, the Impulse model, the Equivalent Circuit model, the Green's function model, the Coupling Of Modes model,..etc.

The main goal of this study is to try to find out a proper model that can describe different types of SAW signal processing devices, specially low loss transducers and filters. It also aims to simulate different types of filters and study the techniques for improving the performances of these filters. The model which is aimed to be developed is supposed to be an aidfull tool to the designers of signal processing equipments using SAW devices.

The crossed field equivalent circuit model has been studied in three approaches for modelling SAW transducers and filters.

Using the scattering matrix theory and the simplified equivalent circuit model of Smith; the possibility of calculating the scattering matrix of a finger pair directly from the simplified equivalent circuit and building up the full transducer has been studied, and the relevant computations have been done. The scattering matrix for Group-type Uni-Directional Transducer (GUDT) as an example for Uni-Directional Transducer has been derived under tuned and matched conditions. The different losses and the frequency responses of matched and tuned BI-directional

Inter Digital Transducers (BIDTs) with different number of finger pairs have been computed. It has been found that the scattering matrix method can directly give many informations that can not be calculated directly using other methods, such as the Electric Mismatch losses, Triple Transit Echo, Acousto Electric Transmission loss, etc.

In the second approach, a single SAW IDT finger has been modeled by a 3×3 transfer matrix. A pair of fingers has been represented by cascading a positive and a negative voltage derived fingers. It has been found that the model can be used to analyze successfully different types of BIDTs, split-finger BIDTs, CHIRP and COMB filters. The frequency responses of filters of BIDTs with single and split fingers have been computed for different number of finger pairs.

A chain matrix was used to model BIDT, GUDT and Three Phase Uni- Directional Transducer (TPUDT) with 4×4 , 6×6 and 8×8 matrices, respectively. Forward and backward frequency responses, directivities and input and output admittances, phases, conductances and susceptances of filters with various possible combinations and types of unidirectional transducers have been computed. Normal/Modified/New-type GUDTs and TPUDTs with different number of active finger pairs, groups and periodic sections in various possible combinations were used at the transmitting as well as the receiving ends with both transducers properly tuned and matched.

The results obtained using the three approaches are quite good and give good agreement with experimental results available in literature. Moreover, using different types of transducers at both ends gave interesting results in terms of 3dB bandwidth and stopband rejection

Apodization is another way to get filters with lower insertion losses, good bandwidths and larger side-lobe suppressions. The usual practice is to have a low insertion loss, wide band, uniform transducer at one end and a narrower bandwidth,

low insertion loss, higher side-lobe suppression, apodized transducer at the other end. Forward, backward frequency responses and relative directivities of different filters having one uniform and one apodized transducer at the two ends with different combinations of Normal/Modified/New- type GUDTs and TPUDTs have been computed. The apodized transducer's effective apertures were apodized using SINC function weighting. The results obtained were interesting in terms of bandwidth and side-lobe suppression.

The SINC function is an Infinite Impulse Response (IIR) function (of infinite time duration) and since an IDT has finite number of fingers in it (similar to FIR filters); it is always the practice that the SINC function is truncated, hence some Gibbs may appear in the frequency response of the filter. If a COSINE window function is additionally included to modify the IDT apodization these Gibbs can be eliminated or the frequency response can be improved to some extent. In this case, a longer part of the SINC function can be used. The responses of the filters mentioned above were computed using a COSINE window along with different lengths of the SINC function. Good results have been obtained.

This windowing technique can also be used to improve the stopband rejection. A Modified Bessel Function (MBF) window family was considered.

Filters of different combinations of UDTs, having different number of periodic sections, active fingers and groups have been computed using different types of windows. It has been found that proper selection of number of periodic sections or groups is very essential in getting good responses.

The software modelling package that has been developed seem to be promising and expandable to include the modelling of more SAW signal processing devices and it is expected to be useful and helpful to the designers of SAW devices for signal processing applications.

CHAPTER ONE

1

To Begin With..

- 1.1 Introduction.
- 1.2 Surface Acoustic Wave
Interdigital Transducer.
- 1.3 Unidirectional Transducers.
- 1.4 Models For The Analysis of
Surface Acoustic Wave Devices.
- 1.5 Equivalent Circuit Theory
Approach Models.
- 1.6 Field Theory Approach Models.
- 1.7 Merits Of SAW Devices.
- 1.8 Statement Of The Problem.
- 1.9 Organization Of The Dissertation.
- 1.10 Notes To The Reader.

To BEGIN WITH..

1.1 INTRODUCTION :

Last few years have seen considerable research interest in electronic applications include surface wave delay lines, acousto-optical devices, and other signal processing devices operating in a frequency range extending from 1 MHz into the microwave region. Most surface acoustic wave (SAW) devices employ some form of interdigital transducer (IDT) proposed by White and Voltmer [1] for the generation and detection of acoustic surface waves on piezoelectric substrates.

Surface acoustic signal processing devices are finding nowadays applications in many diverse electronic equipments. Every modern UHF/VHF communication receiver (mobile/stationed) usually contains at least one SAW filter. Many telecommunication systems - particularly satellite systems - can not do away without extremely high performance SAW filters. Large radar systems as well as smaller ones (on an increasing extent) utilize pulse compression

SAW filters. In addition to many applications, high frequency SAW oscillators and SAW convolvers are also in use. Low loss SAW transducers filters are very much essential for designing signal processing devices/equipments.

In this chapter a brief introduction to bidirectional and unidirectional transducers is given. The different approaches for modeling SAW devices are given with brief discussions on different models for analyzing SAW devices. Some of the merits and applications of SAW devices are also presented. Finally the statement of the problem is declared.

1.2 SURFACE ACOUSTIC WAVE INTERDIGITAL TRANSDUCER :
--

The conventional surface acoustic wave interdigital transducer consists of an array of thin metal fingers (usually of gold or aluminum) deposited on the polished surface of a piezoelectric substrate. Alternate fingers are connected together, so that each transducer has a single electrical port. If an electrical signal generator is connected to the electrical port the resulting electric field within the piezoelectric material causes an acoustic surface wave to be generated beneath the transducer and to propagate along the surface in two directions perpendicular to the fingers. Conversely, if the electrical port

is connected to a load the electric field associated with an incident acoustic surface wave produces a voltage between the electrical terminals, and power is delivered to the load.

Since its introduction, this type of transducer has gained wide acceptance because of its high efficiency and ease of fabrication by conventional microcircuits technology. In its original form, the interdigital transducer was applicable only to piezoelectric substrates. However, similar electrode arrays have been used in conjunction with piezoelectric overlays to launch and receive surface waves on non-piezoelectric materials [2].

The interdigital transducer is frequency-dependent, operating most efficiently at the synchronous frequency, at which the centre to centre spacing of adjacent fingers is one half surface acoustic wave length [3-4]. Interdigital transducers are attractive for variety of filter applications, because the variation of phase shift and loss with frequency may be controlled by varying the spacing and amplitude weighting of the fingers along the array. The weighting may be controlled by varying the finger overlap or to a limited extent by varying the finger width [5-7].

The conventional interdigital transducer has two important disadvantages; bidirectionality and the presence of triple transit echoes. The transducer is regarded as having two acoustic ports, corresponding to the two directions of wave propagation. With equal loading at the acoustic ports, power incident at the

electrical port of an input transducer is divided equally between the two acoustic ports, and thus half of the input power is usually lost because it is radiated away from the receiving transducer. This results in a minimum loss of 3 dB per transducer.

1.3 UNIDIRECTIONAL TRANSDUCERS:

For reducing this minimum loss of 3db per transducer in Bi-Directional Transducers (*BIDTs*) described in the previous section one of the proposals was to place two identical receiving transducers with the electrical ports connected in parallel, at equal distance on either sides of the input transducer. This method of interdigitated interdigital transducer (*IIDT*) can be extended to $n+1$ output *IDTs* interlaced with n input *IDTs*. As more *IDTs* are added the minimum insertion loss reduces [8].

Another method for overcoming the problems of conventional bidirectional transducers is the use of Uni-Directional Transducers (*UDTs*), which radiate acoustic power in only one direction [9,10]. Conversely, an ideal unidirectional transducer may be used to pick up all the power incident at one acoustic port and deliver it to a load, there is then no reflected acoustic wave and triple transit echoes are eliminated.

Several different methods for obtaining unidirectional

operation of an interdigital transducer have been described. Engan [11] was the first to propose a simple unidirectional transducer structure while later on it was developed by Collins et al [9] and is commonly known as Quadrature Phase unidirectional transducer (*QPUDT*).

The Three Phase unidirectional transducer (*TPUDT*) was reported by Potter and Hartmann [12]. The Group type unidirectional transducer (*GUDT*) was developed by Yamanochi et al [13] as a new *QPUDT*. Some different structures have been proposed for *GUDT* such as the Modified *GUDT* (*MGUDT*)[13] and the New type *GUDT* (*NUGUDT*) [14]. Single Phase unidirectional transducer (*SPUDT*) was proposed by Hartmann et al [15] where no phase shifting of the electrical signal is required and the unidirectionality is performed by the use of reflecting gratings.

This dissertation considers bidirectional transducers, three phase unidirectional transducers and different types of group unidirectional transducers, for signal processing applications.

1.4 MODELS FOR THE ANALYSIS OF SURFACE ACOUSTIC WAVE DEVICES :

Analysis and synthesis of any operational device (like a *SAW* device) associated with a complicated physics can be performed by

some equivalent model. The behaviour of surface acoustic wave interdigital transducers is in general very complex, involving complicated electrostatic effects, the presence of variety of acoustic modes and electrodes interactions which cause propagating waves to be perturbed by electrodes under which they pass. A further complication is the variety of features to be analyzed; the amplitude of waves generated the transducer admittance, and for acoustic waves incident on the transducer the scattering parameters for conversion, reflection and transmission.

The complexity of the problem has resulted in a variety of theoretical models for analysis which mostly make simplifying assumptions. Almost always it is assumed that the only acoustic mode present is a non-leaky surface wave, and it is also common to ignore electrode interactions..etc.

The methods or models that have been developed for the analysis of SAW devices are either one of the two approaches; field theory approach and circuit theory approach. the existing models are such as the Delta function model [6], the Impulse response model [16], the Equivalent circuit model [17,18], the Green's function model [19], the Coupling of modes model [15]..etc.

The simplifying assumptions that have been made in each of the above models were to get a model that gives results as accurate as possible with less computational effort and simpler procedures.

The delta function model provides basic information in the transfer function response of a *SAW* filter [6]. It can only cater to some of the second order effects. It can not provide information on filter input/output impedance level, circuit loading factor, harmonic operation, bulk wave interference or diffraction. Its basic modelling concept that it approximates the complex electric field distribution between adjacent fingers of an exited *IDT* as a discrete number of delta function sources.

The impulse response model developed by Hartmann, Bell and Rosenfeld [16] yields additional information on the *SAW* transducer response over that given by the simple delta function model, in that circuit impedances and matching networks can be included. It also provides ready insight into frequency scaling that must be employed in the determination of apodization quantities for broadband or chirp *SAW* filters. In essence, the impulse response model uses fourier transform pair relations to determine the impulse response $h(t)$ of a *SAW* filter, given its desired frequency response $h(f)$.

The crossed field equivalent circuit model is derived from the Mason's equivalent circuit employed for modelling acoustic bulk wave piezoelectric devices [17]. In this model the electric

field distribution under the electrode of an exited *IDT* is approximated as being normal to the piezoelectric surface, as if between the plates of a capacitor. There is also an alternative model, known as the in line field equivalent circuit model. Experimentally [20] it has been found that the crossed field model yields better agreement with experiment than the in line one for *IDTs* fabricated on high electromechanical coupling piezoelectric substrate such as lithium niobate. The in line model is readily applicable, however to *IDT* designs on quartz substrates.

The delta function model, the impulse response model are analytical in approach and the crossed field model is of the equivalent circuit approach. Each of them reveals an important factor for *SAW* filter design. The delta function model relates the restriction placed on apodizing both *IDTs* in *SAW* filters. The crossed field model yields information on *IDT* input and output impedance levels, and on triple transit interference levels in the filter passband. The impulse response model also provides information on input and output impedance levels as well as on the frequency sensitivity of exited *IDT* electrodes.

1.6 FIELD THEORY APPROACH MODELS :

Generally speaking, Field theory approach models for the analysis of *SAW* devices are usually more accurate than circuit

theory approach models, but in the same time they suffer usually from the enormous computation time involved and the complexity. These drawbacks are different from one model to another as per the accuracy involved. Such types of models include the normal mode model [21], the Coupling of modes model and greens function model.

The coupling of modes (COM) theory has earlier been applied extensively to the design of optical devices [22,23]. Later on it has been applied to SAW devices [15]. The coupling of modes theory (model) describes the acoustic field distribution in the SAW device in terms of forward and backward waves [24]. It assumes that the metal film is thin (compared to the wave length). Different equations are to be obtained which hold for the amplitudes of the two coupled waves propagating forwards and backwards in the structure. The solution of these differential equations, subject to boundary conditions, describe the behaviour of the SAW device including second order effects.

The green's function model takes almost full account of electrostatic effects, electrode interactions, electrode mass and resistance and couples to bulk modes as well as surface modes [19,25]. It gives highly accurate modelling with high coupling materials. several researchers are working on different green's function models such as the simplified Green's function model [25] and the two dimensional Green's function model [26] depending upon the goal whether reducing the computation time or increasing the accuracy. The Green's function model involves complex and time

consuming numerical computations, and it ignores diffraction effect.

A lot of research work is going on nowadays on coupling of modes [27,28] and Green's function models [29] because of the high accuracy and the ability to model a wide range of SAW devices.

1.7 MERITS OF SAW DEVICES :

Many SAW based devices and systems have several excellent features when compared to competing technologies. Apart from usual merits, these includes the following:

1. SAW devices can generally be designed to provide quite complex signal processing functions with a single package contained on a single piezoelectric substrate with superimposed thin film input and output interdigital transducers
2. SAW devices can be mass produced using semiconductor microfabrication techniques. As a result they can be made to be cost competitive in mass volume applications.
3. SAW devices can have outstanding reproducibility in performance from device to device. Indeed, the practical

implementation of channeled receivers for spectral analysis of signals in electronics support measures (ESM) has only been possible since the arrival of SAW devices.[21].

4. Since they can often be implemented in small rugged, light and power efficient modules, they are finding ever increasing applications in mobile and space-borne communication systems.
5. Although SAW devices are analog devices, they can be implemented in many digital communications systems; such as the use of SAW Nyquist filters in quadrature amplitude modulation (QAM) digital radio modems. Feldman et al [30] have given many such examples.
6. SAW filters can be made to operate very efficiently at high harmonic modes. As a result giga hertz frequency-range devices can be fabricated using relatively inexpensive photolithographic techniques rather than the process involving electron beam lithography.

SAW devices are having nowadays so many signal processing applications due to the merits mentioned above. Campbell [21] has outlined many of SAW devices signal processing applications.

1.8 STATEMENT OF THE PROBLEM :

The main goal of this study has been to try to find out a proper model that could describe different types of SAW signal processing devices, specially low loss transducers and filters. It also aimed to simulate different types of filters and study the techniques for improving the performances of these filters. The model aimed to be developed is supposed to be an aidfull tool to the designers of signal processing equipment using SAW devices, so that they could use the model to simulate and afterwards select the proper design as per their requirements.

It has been thought that if a model is to be used as a quick and accurate (up to some extent) tool for such designing tasks then the computation speed is a very important factor. The crossed field equivalent circuit model - although it is not the most ideal one - seems to be most appropriate as far as a compromise between complexity and computational effort required is concerned and with comparable results with that of experiments. Based on this; the crossed field equivalent circuit has been selected as the basic ground for this study.

The problem undertaken is stated as follow :

- a: Study the possibility and work to develop a fast and accurate model (based on the crossed field equivalent

circuit model) that is able to represent, predict the performance and give as much information as possible about the different parameters (of as wide range as possible) of different types of *SAW* transducers and filters.

- b: Develop a software simulating package based on the model to be developed. The simulator is to be developed in a way that it can be used as an aidfull tool to the designers of *SAW* devices for signal processing applications so that they will be able to simulate their designs and find out its performances and the different related responses and parameters before fabricating. This is to ease the design process and eliminate errors before fabrication.

- c: Study ways and techniques for getting different *SAW* transducers/filters performances for signal processing applications such as apodization and windowing. See the possibility of modelling/simulating filters with both apodized unidirectional transducers (by say chanalization method [6]).

- d: Look into some new window techniques and try to apply it on *SAW* apodized transducers and make use of it in getting good *SAW* filters responses for signal processing applications.

- e: Simulate different types of *SAW* filters from combinations

of same and different types of transducers and study the different parameters affecting filters performances.

1.9 ORGANIZATION OF
THE DISSERTATION :

Chapter two deals with the scattering matrix modelling approach. Two models are presented. Models derivations and relation between different scattering parameters are given. Results of some modelled transducers are reported and discussed.

The transfer matrix approach is presented in chapter three. The derivation of the basic modelling unit is given. The conventional IDT is modelled by cascading positive and negative voltage derived basic-units. Results of some transducers and filters are reported and discussed.

A third approach for modelling SAW signal processing devices (Chain matrix approach) is presented in chapter four. Different combinations of SAW transducers and filters are simulated and results are reported, studied and discussed.

In Chapters five and six, simulator package is used to study ways to improve and control the performances of SAW transducers and filters for signal processing applications. Apodization and windowing techniques are used in chapter five to achieve such

improvements. A variety of apodization profiles are worked out in chapter six and used to modify SAW transducers and filters responses to obtain the required performances suitable for signal processing applications.

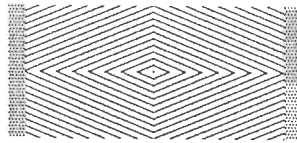
Finally, recapitulation, conclusions and future work suggestions are presented in chapter seven.

1.10 NOTES TO THE READER:

Before terminating this chapter and proceeding to the next it is desirable that the reader may kindly note the following:

1. The crossed field equivalent circuit model is the basic ground for the models presented in this dissertation.
2. In these modelling approaches various parasitic losses such as diffraction loss, beam-steering loss, electrode resistance loss, air-loading loss, mass loading loss, propagation loss, apodization loss..etc. have been neglected as they do not contribute more than 1 dB of loss combined together.
3. A 128° rotated Y-cut X-propagating LiNbO_3 was selected as the material on which various types of SAW transducers have been assumed to be fabricated. The material was

selected for its high electromechanical coupling coefficient compared to any other material available in the market [30,31]. It has an inherent property of suppressing undesired side-lobes to a great extent. It has the disadvantage of a high temperature coefficient. It is also possible to use the model presented in this dissertation with any other material by providing the required changes in the substrate data.



CHAPTER TWO

2

Scattering Matrix Approach.

- 2.1 Introduction.
- 2.2 Modelling Of An IDI.
- 2.3 Modelling Of IDI From
A Single Finger-Pair.
 - 2.3.1 Junction.
 - 2.3.2 Combination Of Two
Radiator/Scatterer.
- 2.4 Modelling Of A UDI.
- 2.5 Understanding The Scattering
Matrix Parameters.
- 2.6 Calculations Of Scattering
Parameters.
- 2.7 Computations.
- 2.8 Conclusion.

SCATTERING MATRIX APPROACH

2.1 INTRODUCTION:

An IDT can be considered as a radiator of the acoustic energy when it is operating in the transmitting mode, and as a scatterer of the acoustic energy when it is operating in the receiving mode. In this chapter the transducer is represented/ modeled by scattering matrix. The derivation and the relations between the different scattering parameters of the scattering matrix modeling the transducer are given. Another scattering matrix model approach is proposed and derived based on a single finger-pair unit. The same approach is used to model a unidirectional transducer. The differences between IDT and UDT scattering matrices as well as the different losses in the two types of transducers are studied. The procedure and the required equations for calculating the different scattering parameters of an IDT from the simplified Smith's equivalent circuit are presented. Results are reported and discussed.

When a surface acoustic wave is incident on an electrically loaded interdigital transducer a part of the wave energy is absorbed, a part is transmitted forward and a part is reflected. The IDT thus can be considered as a scatterer of surface acoustic wave. Let the interdigital transducer to be assumed to possess one of the two kinds of symmetry illustrated in Fig 2.1. In The bilaterally symmetric (S) case, the comb pattern map onto their mirror images seen in a surface normal plane containing the center line C'-C". In the bilaterally antisymmetric (A) case, the self mapping corresponds to 180° rotation around the surface normal axis passing through the center point C. The two cases cover unweighted transducers and transducers with bilaterally symmetric weighting through finger withdrawal or apodization of finger overlaps. Such an IDT can be represented by a three-port network having one electric port (*port 1*) and two acoustic ports (*port 2 and port 3*). The electric port can either be a source of energy with some source resistance or a load. The acoustic ports are symmetrical in the sense that they appear identical as viewed from the electric port. If b_i and a_j are the (complex) amplitudes of waves incident on the j th port and leaving the i th port, the three outputs are related to the three inputs by the linear equation

$$b_i = \sum_{j=1}^3 S_{ij} a_j \quad \dots (2.1)$$

or

$$\mathbf{b} = \mathbf{S} \cdot \mathbf{a} \quad \dots(2.2)$$

where S_{ij} is an element of 3x3 scattering matrix \mathbf{S} that tells how a set of input waves \mathbf{a} ($a_1, a_2, a_3..$) is scattered into a set of output waves \mathbf{b} ($b_1, b_2, b_3..$). Using polar notation with real amplitudes and phases, (2.2) can be written as;

$$S_{ij} = \sigma_{ij} \exp(J\vartheta_{ij}) \quad \dots(2.3)$$

where σ_{ij}^2 is the ratio of power leaving the junction or the network through port i to the incoming power available at port j . σ_{ij}^2 should not exceed unity ($\sigma_{ij}^2 \leq 1$) for a passive network. The scattering phase shifts ϑ_{ij} are defined as though the transducer were a point scatterer or a point wave radiator located at c'-c" in Fig. 2.1. Note that positive ϑ_{ij} correspond to a scattering phase lag in (2.3) when time factors are written as $\exp(J\omega t)$.

From equation (2.1) the wave-scattering matrix \mathbf{S} has nine different elements S_{ij} of the complex form (2.3), for a total of 18 real parameters, as in the case of a general three-port network. However, in the case of IDT the matrix is simplified due to the bilateral symmetry.

Reciprocity makes the \mathbf{S} matrix symmetric about its main diagonal, so that

$$S_{ij} = S_{ji} \quad \dots(2.4)$$

As a result of bilateral symmetry the acoustic ports are indistinguishable, so that

$$S_{22} = S_{33} \quad \dots (2.5)$$

$$S_{23} = S_{32} \quad \dots (2.6)$$

$$S_{12} = S_{13} \quad \dots (2.7)$$

The relations (2.5)-(2.7) eliminate all but four complex scattering parameters, to leave the S matrix in the form

$$S = \begin{bmatrix} S_{11} & S_{12} & S_{12} \\ S_{12} & S_{22} & S_{23} \\ S_{12} & S_{23} & S_{22} \end{bmatrix} \quad \dots (2.8)$$

Just for the sake of simplicity and clarity we write (2.3) as follows

$$S_{11} = R \exp(J\rho) \quad \dots (2.9)$$

$$S_{12} = T \exp(J\theta) \quad \dots (2.10)$$

$$S_{22} = S \exp(J\sigma) \quad \dots (2.11)$$

$$S_{23} = G \exp(J\gamma) \quad \dots (2.12)$$

(2.2) can be written as

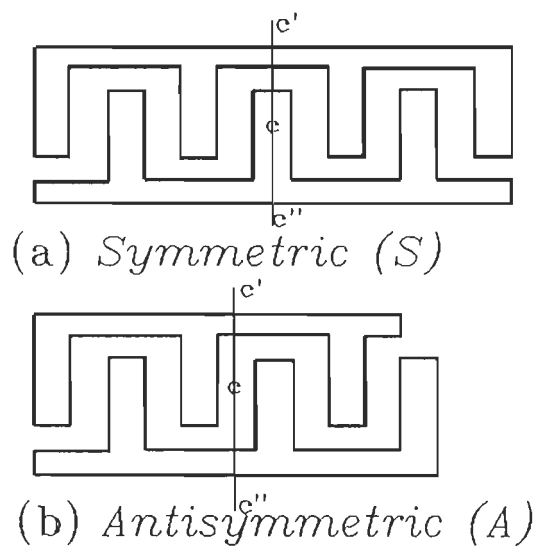


Fig. 2.1 IDTs symmetry types treated. Transducer can be represented by a point radiator/scatterer located on $c'-c''$

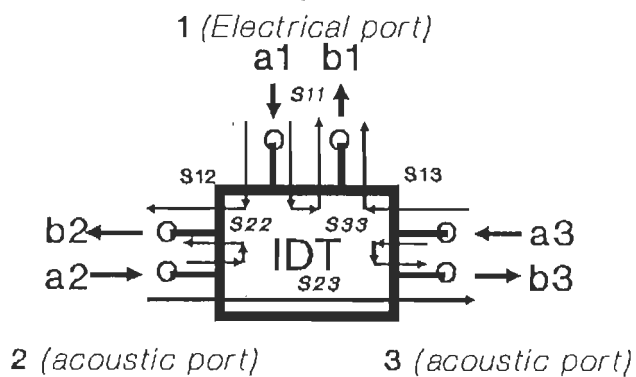


Fig. 2.2 IDT 3-port network representation. Identification of port number, scattering parameters and waves entering and leaving the transducer ports.

$$\begin{bmatrix} b_1 \\ b_2 \\ b_3 \end{bmatrix} = \begin{bmatrix} R \exp(J\rho) & T \exp(J\vartheta) & T \exp(J\vartheta) \\ T \exp(J\vartheta) & S \exp(J\sigma) & G \exp(J\gamma) \\ T \exp(J\vartheta) & G \exp(J\gamma) & S \exp(J\sigma) \end{bmatrix} \cdot \begin{bmatrix} a_1 \\ a_2 \\ a_3 \end{bmatrix} \quad (2.13)$$

where $R, T, S, G, \rho, \vartheta, \sigma, \gamma$ are all real.

The interdigital transducer, therefore, can be represented by (2.13), and the individual scattering parameters are identified in Fig. 2.2. S_{11} is reflection coefficient at electric port, S_{22} is wave reflection coefficient at acoustic port 2 and 3, S_{23} is transmission coefficient between acoustic ports, and S_{12} is mixed transmission coefficient between electric and acoustic ports.

The physical requirements of reciprocity and conservation of energy impose the condition on S that it is unitary, i.e.

$$S S^* = I \quad \dots (2.14)$$

where asterisk $*$ denotes complex conjugation, and I is unit matrix.

The following relationships are obtained as a consequence;

$$T^2 + S^2 + G^2 = 1 \quad \dots (2.15)$$

$$2T^2 + R^2 = 1 \quad \dots (2.16)$$

$$S_{22} S_{23}^* + S_{22}^* S_{23} + T^2 = 0 \quad \dots (2.17)$$

$$(S_{22} + S_{23}) S_{12}^* + S_{12} S_{11}^* = 0 \quad \dots (2.18)$$

Equations (2.15) and (2.16) are energy conservation conditions for the scattering of a single input wave entering port 3 or port 2. Equations (2.17) and (2.18) are scattering interference conditions that must also be satisfied for energy conservation when waves enter second or third ports [32].

2.3 MODELING OF IDT FROM A SINGLE FINGER-PAIR:

A single finger-pair can be represented similar to an M finger-pair IDT by equation (2.13). The single finger-pair IDT can be considered as a point scatterer or a point radiator located at the center of the finger-pair. The whole transducer may be regarded as an array of scatterers or radiators, which may be identical with one another or may be different. The performance of the transducer may be deduced, in principle, from the performances of the individual radiators, also the performances of systems of more than one transducer. The whole transducer can then be considered as a point scatterer or a point radiator located at the center of the transducer, as discussed in section 2.2.

From the above discussion let us consider the two radiators (two finger-pair) transducer sketched in Fig. 2.3a. If S_1 and S_2

are the scattering matrices representing radiator 1 and radiator 2, respectively, then if these two matrices are cascaded using a suitable method we may get the scattering matrix S that represents the whole transducer.

The radiators (in Fig. 2.3b) are essentially localized three-port devices, separated by a length l , and if β is the phase constant of acoustic waves, there is a phase difference βl between the radiators. The electric ports 1 and 4 of the radiators are connected by line sections of virtually zero length at E. A suitable representation of this electrical connection is required.

Waldron [33,34] was suggesting that this electrical connection can be represented as another three-port device (Fig. 2.4). He considered this electrical connection like three transmission lines meeting at a point, and the junction to be symmetrical with respect to all leads.

The electrical connection (junction) proposal is adopted here, and full transducer model has been derived in the coming lines, also the model has been verified verified.

Let us consider the transducer of Fig. 2.3a to be having identical finger-pairs (radiators), and let SR_1 , SR_2 and SJ to be the scattering matrices of radiator 1, radiator 2 and the electrical connection (junction), respectively.

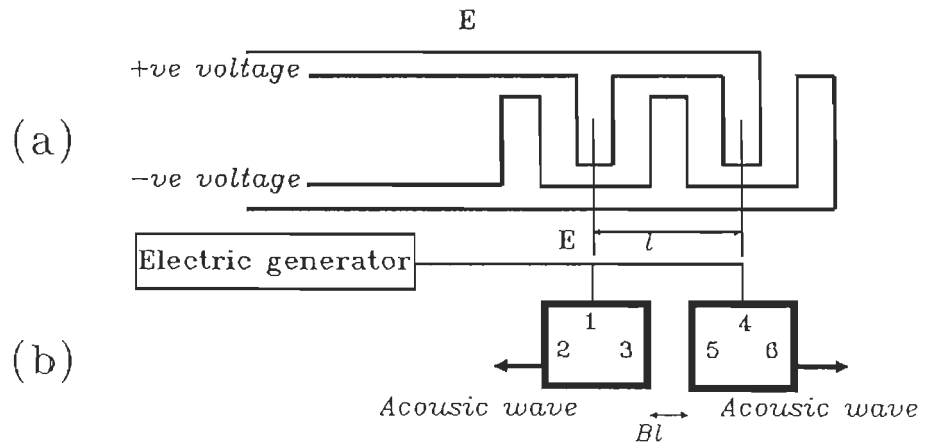


Fig. 2.3 A two finger-pair transducer.

(a) Actual transducer.

(b) 3-port representation for each radiator/scaterer with a phase difference of Bl

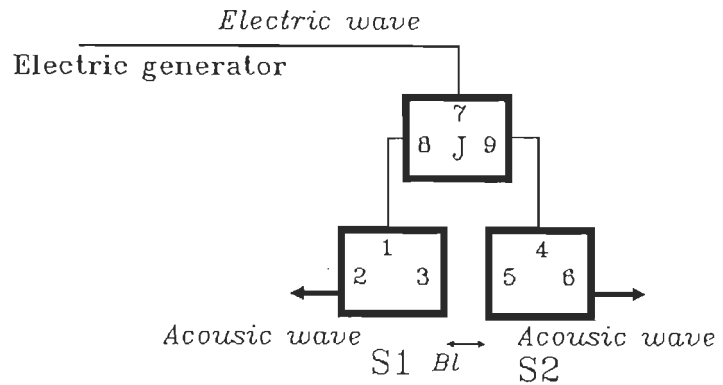


Fig. 2.4 3-port network representation of the electrical connection.

SR1 and SR2 can be written as;

$$SR1 = SR2 = \begin{bmatrix} A & B & B \\ B & C & D \\ B & D & C \end{bmatrix} \dots (2.19)$$

and due to symmetry SJ can be written as;

$$SJ = \begin{bmatrix} J_{11} & J_{12} & J_{13} \\ J_{12} & J_{22} & J_{23} \\ J_{13} & J_{23} & J_{33} \end{bmatrix} \dots (2.20)$$

2.3.1 JUNCTION :

If Z_{o1} , Z_{o2} and Z_{o3} are the characteristic impedances of the three transmission lines meeting at a point A in Fig. 25, which represents the electrical connection, and if

$$Z_1 = Z_{o2} Z_{o3} / Z_{o1}^2$$

$$Z_2 = Z_{o2} / Z_{o1}$$

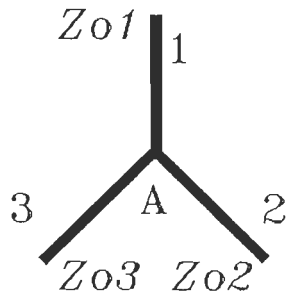


Fig. 2.5 The electrical connection can be considered like three transmission lines 1, 2, and 3 meeting at point A with characteristic impedances Z_{o1} , Z_{o2} and Z_{o3}

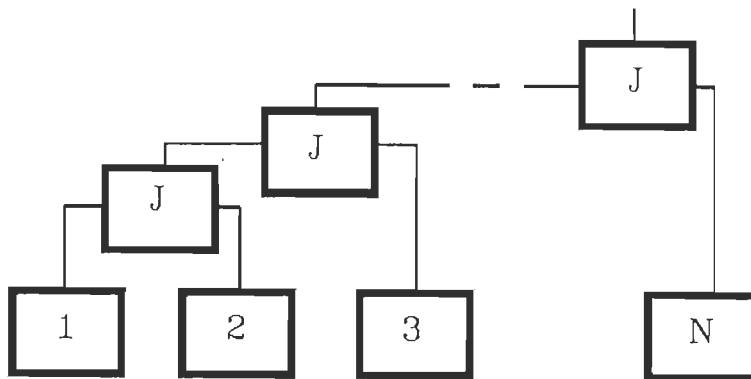


Fig. 2.6 Cascading of N finger-pairs to construct an IDT.

$$Z_3 = Z_{o3} / Z_{o1}$$

$$Z = Z_1 + Z_2 + Z_3$$

Then

$$J_{11} = \frac{Z_1 - Z_2 - Z_3}{Z} \quad \dots (2.21)$$

$$J_{22} = \frac{Z_3 - Z_2 - Z_1}{Z} \quad \dots (2.22)$$

$$J_{33} = \frac{Z_2 - Z_1 - Z_3}{Z} \quad \dots (2.23)$$

$$J_{12} = \frac{2 \times Z_3 \sqrt{Z_2}}{Z} \quad \dots (2.24)$$

$$J_{13} = \frac{2 \times Z_2 \sqrt{Z_3}}{Z} \quad \dots (2.25)$$

$$J_{23} = \frac{2 \times \sqrt{Z_1}}{Z} \quad \dots (2.26)$$

Hence

$$SJ = \begin{bmatrix} -1/3 & 2/3 & 2/3 \\ 2/3 & -1/3 & 2/3 \\ 2/3 & 2/3 & -1/3 \end{bmatrix} \quad \dots (2.27)$$

2.3.2 COMBINATION OF TWO
RADIATORS/SCATTERERS:

Referring to Fig. 2.4 and according to the results obtained earlier, the scattering matrices representing the Three-port networks J, S1 and S2 in terms of the waves leaving and entering the different ports are as follow;

Network S1

$$\begin{bmatrix} b_1 \\ b_2 \\ b_3 \end{bmatrix} = \begin{bmatrix} A & B & B \\ B & C & D \\ B & D & C \end{bmatrix} \begin{bmatrix} a_1 \\ a_2 \\ a_3 \end{bmatrix} \quad \dots (2.28)$$

Network S2

$$\begin{bmatrix} b_4 \\ b_5 \\ b_6 \end{bmatrix} = \begin{bmatrix} A & B & B \\ B & C & D \\ B & D & C \end{bmatrix} \begin{bmatrix} a_4 \\ a_5 \\ a_6 \end{bmatrix} \quad \dots (2.29)$$

Network J

$$\begin{bmatrix} b_7 \\ b_8 \\ b_9 \end{bmatrix} = \begin{bmatrix} -1/3 & 2/3 & 2/3 \\ 2/3 & -1/3 & 2/3 \\ 2/3 & 2/3 & -1/3 \end{bmatrix} \begin{bmatrix} a_7 \\ a_8 \\ a_9 \end{bmatrix} \quad \dots (2.30)$$

If the two radiators/ scatterers are placed as in Fig. 2.4 with the electrical connections through junction J, then the following equations can be deduced from figure;

$$a_1 = b_8$$

$$a_8 = b_1$$

$$a_4 = b_9$$

$$a_9 = b_4$$

and if

$$K = \exp(j\beta l) , \text{ as is the case ;}$$

then

$$a_3 = K b_5$$

$$a_5 = K b_3$$

Eliminating port 3 and port 5

$$\begin{bmatrix} b_1 \\ b_2 \\ b_4 \\ b_6 \end{bmatrix} = \frac{1}{E1} \begin{bmatrix} x_{11} & x_{12} & x_{13} & x_{14} \\ x_{12} & x_{22} & x_{14} & x_{24} \\ x_{13} & x_{14} & x_{11} & x_{12} \\ x_{14} & x_{24} & x_{12} & x_{22} \end{bmatrix} \begin{bmatrix} a_1 \\ a_2 \\ a_4 \\ a_6 \end{bmatrix} \quad \dots (2.31)$$

where

$$x_{11} = A + (K^2 B^2 C)/E1$$

$$x_{12} = B + (K^2 B C D)/E1$$

$$x_{13} = K B^2/E1$$

$$x_{14} = K B D/E1$$

$$x_{22} = C (1 + K^2 D^2/E1)$$

$$x_{24} = K D^2/E1$$

$$E1 = 1 - K^2 C^2$$

Now eliminating ports 1 and 8 we get

$$\begin{bmatrix} b_2 \\ b_4 \\ b_6 \\ b_7 \\ b_9 \end{bmatrix} = \frac{1}{E2} \begin{bmatrix} y_{11} & y_{12} & y_{13} & y_{14} & y_{14} \\ y_{12} & y_{22} & y_{23} & y_{24} & y_{24} \\ y_{13} & y_{23} & y & y_{33} & y_{34} \\ y_{14} & y_{24} & y_{34} & y_{44} & y_{45} \\ y_{14} & y_{24} & y_{34} & y_{45} & y_{44} \end{bmatrix} \begin{bmatrix} a_2 \\ a_4 \\ a_6 \\ a_7 \\ a_9 \end{bmatrix} \quad \dots (2.32)$$

where

$$y_{11} = E_2 x_{22} - x_{12}^2$$

$$y_{12} = E_2 x_{14} - x_{12} x_{13}$$

$$y_{13} = E_2 x_{24} - x_{12} x_{14}$$

$$y_{14} = x_{12}$$

$$y_{22} = E_2 x_{11} - x_{13}^2$$

$$y_{23} = E_2 x_{12} - x_{13} x_{14}$$

$$y_{24} = 2x_{13}$$

$$y_{33} = E_2 x_{22} - x_{14}^2$$

$$y_{34} = 2x_{14}$$

$$y_{44} = 1/3 (6x_{11} - E_2)$$

$$y_{45} = 2/3 (3x_{11} + E_2)$$

$$E_2 = 3E_1 + x_{11}$$

finally, let us eliminate ports 4 and 9 and rearrange the matrix. We get

$$\begin{bmatrix} b_7 \\ b_2 \\ b_6 \end{bmatrix} = \frac{1}{E_4} \begin{bmatrix} \mathcal{A} & \mathcal{B} & \mathcal{B} \\ \mathcal{B} & \mathcal{C} & \mathcal{D} \\ \mathcal{B} & \mathcal{D} & \mathcal{C} \end{bmatrix} \begin{bmatrix} a_7 \\ a_2 \\ a_6 \end{bmatrix} \quad \dots (2.33)$$

where

$$A = E_4 y_{44} + y_{24}(E_3 y_{45} + y_{24} y_{44}) + y_{45}(E_3 y_{24} + y_{22} y_{45})$$

$$B = E_4 y_{34} + y_{24}(E_3 y_{34} + y_{23} y_{44}) + y_{45}(E_3 y_{23} + y_{22} y_{34})$$

$$C = E_4 y_{33} + y_{24}(E_3 y_{34} + y_{23} y_{44}) + y_{34}(E_3 y_{23} + y_{22} y_{34})$$

$$D = E_4 y_{13} + y_{12}(E_3 y_{34} + y_{23} y_{44}) + y_{14}(E_3 y_{23} + y_{22} y_{34})$$

The final matrix (2.33) we ended with is very much similar to that of equation (2.13). This procedure may be continued by adding a radiator each time up to the full number of finger-pairs of the transducer, as shown in Fig. 2.6. We conclude that this model starting from a single finger-pair basic unit and cascading up to the full transducer gives the expected scattering matrix that is similar in form to that of the full transducer discussed earlier.

2.4 MODELING OF A UDT :

Here we would like to try , as we did in the case of BIDT, to model or to derive the scattering matrix model for a unidirectional transducer. Because our basic-unit is the finger-pair and not the single finger, then it seems to be difficult to model any type of UDT starting from this basic unit. GUDT is one type of UDTs that the finger-pair basic unit can be used to build it. The GUDT is selected for this reason to be an example for UDT modeling using the scattering matrix junction approach.

Let us consider the identical BIDTs of Fig. 2.7a, with the driving voltage of one BIDT 90° phase shifted using a proper phase shifter. As concluded in the last section, both BIDTs can be represented by

$$\begin{bmatrix} b_1 \\ b_2 \\ b_3 \end{bmatrix} = \begin{bmatrix} A_0 & B_0 & B_0 \\ B_0 & C_0 & D_0 \\ B_0 & D_0 & C_0 \end{bmatrix} \begin{bmatrix} a_1 \\ a_2 \\ a_3 \end{bmatrix} \quad \dots (2.34)$$

for the 0° section and

$$\begin{bmatrix} b_4 \\ b_5 \\ b_6 \end{bmatrix} = \begin{bmatrix} A_0 & B_0 & B_0 \\ B_0 & C_0 & D_0 \\ B_0 & D_0 & C_0 \end{bmatrix} \begin{bmatrix} a_4 \\ a_5 \\ a_6 \end{bmatrix} \quad \dots (2.35)$$

for the 90° section

Whereas the phase shifter may be represented by the scattering matrix P as

$$\begin{bmatrix} b_{10} \\ b_{11} \end{bmatrix} = \begin{bmatrix} F_1 & F_2 \\ F_2 & F_1 \end{bmatrix} \begin{bmatrix} a_{10} \\ a_{11} \end{bmatrix} \quad \dots (2.36)$$

where

$$F_1 = J f(1 + Jf)$$

$$F_2 = 1/(1 + Jf)$$

f is frequency.

Eliminating ports 4 and 11 we get

$$\begin{bmatrix} b_{10} \\ b_5 \\ b_6 \end{bmatrix} = \begin{bmatrix} A_{90} & B_{90} & B_{90} \\ B_{90} & C_{90} & D_{90} \\ B_{90} & D_{90} & C_{90} \end{bmatrix} \begin{bmatrix} a_{10} \\ a_5 \\ a_6 \end{bmatrix} \quad \dots (2.37)$$

where

$$A_{90} = (E F_1 + A_0 F_2^2)/E$$

$$B_{90} = B_0 F_2/E$$

$$C_{90} = (E C_0 + F_1 B_0^2)/E$$

$$D_{90} = (E D_0 + F_1 B_0^2)/E$$

Fig. 2.8a reduces to Fig. 2.7b. From figure we have

$$a_4 = b_9$$

$$a_9 = b_4$$

$$a_8 = b_1$$

$$a_1 = b_8$$

and if $K = \exp(J\beta l)$ then

$$F_1 = J f(1 + Jf)$$

$$F_2 = 1/(1 + Jf)$$

f is frequency.

Eliminating ports 4 and 11 we get

$$\begin{bmatrix} b_{10} \\ b_5 \\ b_6 \end{bmatrix} = \begin{bmatrix} A_{90} & B_{90} & B_{90} \\ B_{90} & C_{90} & D_{90} \\ B_{90} & D_{90} & C_{90} \end{bmatrix} \begin{bmatrix} a_{10} \\ a_5 \\ a_6 \end{bmatrix} \quad \dots (2.37)$$

where

$$A_{90} = (E F_1 + A_0 F_2^2)/E$$

$$B_{90} = B_0 F_2/E$$

$$C_{90} = (E C_0 + F_1 B_0^2)/E$$

$$D_{90} = (E D_0 + F_1 B_0^2)/E$$

Fig. 2.8a reduces to Fig. 2.7b. From figure we have

$$a_4 = b_9$$

$$a_9 = b_4$$

$$a_8 = b_1$$

$$a_1 = b_8$$

and if $K = \exp(J\beta_1)$ then

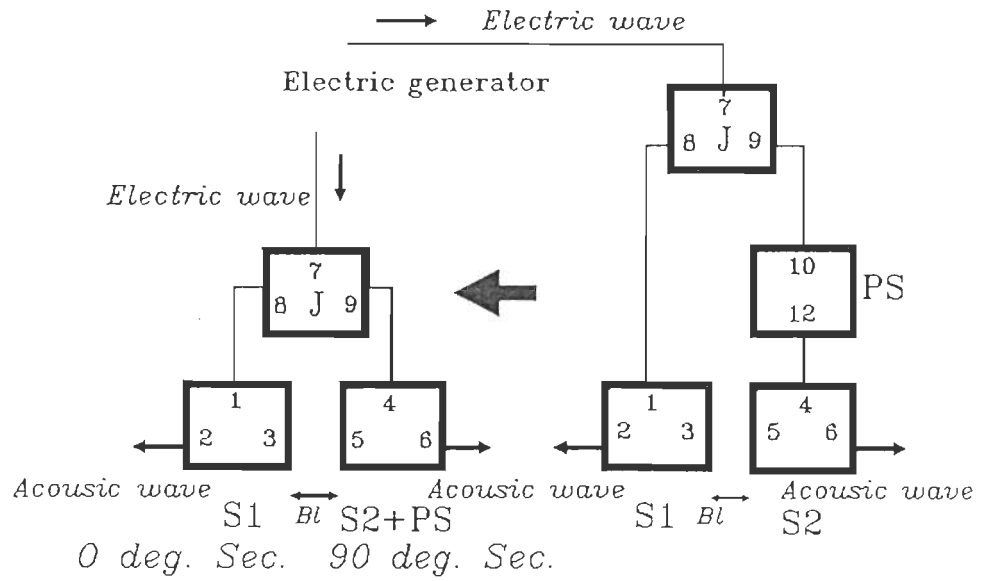


Fig. 2.7 Representation of a single group GUDT.

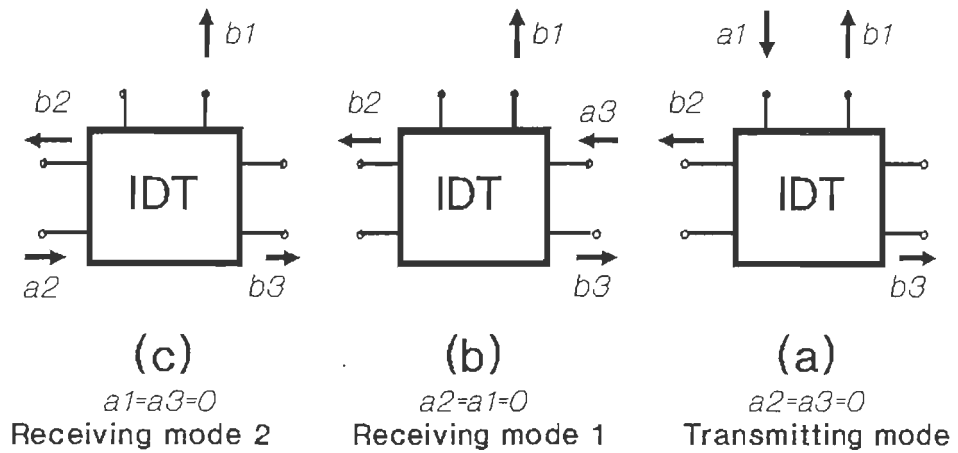


Fig. 2.8 Transducer in transmitting and receiving modes.

$$a_3 = K b_5$$

$$a_5 = K b_3$$

Eliminating ports 4 and 9 we get

$$\begin{bmatrix} b_5 \\ b_6 \\ b_7 \\ b_8 \end{bmatrix} = \frac{1}{E_1} \begin{bmatrix} w & x_1 & y_1 & y_1 \\ x_1 & w & y_1 & y_1 \\ y_1 & y_1 & y_3 & y_4 \\ y_1 & y_1 & y_4 & y_3 \end{bmatrix} \begin{bmatrix} a_5 \\ a_6 \\ a_7 \\ a_8 \end{bmatrix} \dots (2.38)$$

where

$$E_1 = 1 + A_{90} / 3$$

$$w = E_1 C_{90} - (B_{90}^2 / 3)$$

$$x_1 = E_1 D_{90} - (B_{90}^2 / 3)$$

$$y_1 = 2 B_{90} / 3$$

$$y_3 = (4 A_{90} / 9) - (E_1 / 3)$$

$$y_4 = (4 A_{90} / 9) + (2 E_1 / 3)$$

Now eliminating ports 1 and 8

$$\begin{bmatrix} b_2 \\ b_4 \\ b_5 \\ b_6 \\ b_7 \end{bmatrix} = \frac{1}{E_2} \begin{bmatrix} F_1 & G_1 & H_1 & H_1 & J_1 \\ G_1 & F_1 & H_1 & H_1 & J_1 \\ H_1 & H_1 & H_3 & I_3 & J_3 \\ H_1 & H_1 & I_3 & H_3 & J_3 \\ J_1 & J_1 & J_3 & J_3 & J_5 \end{bmatrix} \begin{bmatrix} a_2 \\ a_3 \\ a_5 \\ a_6 \\ a_7 \end{bmatrix} \dots (2.39)$$

where

$$E_2 = E_1 - y_2$$

$$F_1 = E_2 C_0 + B_0^2 Y_3$$

$$G_1 = E_2 D_0 + B_0^2 Y_3$$

$$H_3 = E_2 w + A_0 Y_1^2$$

$$I_3 = E_2 x_1 + A_0 Y_1^2$$

$$J_3 = E_2 y_1 + A_0 Y_1 y_4$$

$$J_5 = E_2 y_3 + A_0 Y_4^2$$

By eliminating ports 5 and 3 we finally get

$$\begin{bmatrix} b_7 \\ b_2 \\ b_6 \end{bmatrix} = \frac{1}{E_4} \begin{bmatrix} A & B_1 & B_2 \\ B_1 & C_1 & D \\ B_2 & D & C_2 \end{bmatrix} \begin{bmatrix} a_7 \\ a_2 \\ a_6 \end{bmatrix} \quad \dots (2.40)$$

where

$$E_3 = (E_2 - KH_1)/K$$

$$E_4 = E_3^2 - F_1 H_3$$

$$A = E_4 J_5 + J_1 (E_3 J_3 + J_1 H_3)$$

$$B_1 = E_4 J_1 + J_1 (E_3 H_1 + G_1 H_3) + J_3 (E_3 G_1 + H_1 F_1)$$

$$B_2 = E_4 J_3 + J_1 (E_3 I_3 + H_1 H_3) + J_3 (E_3 H_1 + I_3 F_1)$$

$$C_1 = E_4 F_1 + G_1 (E_3 H_1 + G_1 H_3) + H_1 (E_3 G_1 + H_1 F_1)$$

$$C_2 = E_4 H_3 + H_1 (E_3 I_3 + H_1 H_3) + I_3 (E_3 H_1 + I_3 F_1)$$

$$D = E_4 H_1 + G_1 (E_3 I_3 + H_1 H_3) + H_1 (E_3 H_1 + I_3 F_1)$$

Equation (2.40) is the scattering matrix representation of one group GUDT. Similarly we can continue by cascading groups up to the required number of groups to get the final GUDT representation, which is easy to show in the same way that it has similar form to equation (2.40).

From the matrix of (2.40), we find that for a unidirectional transducer we have six independent scattering parameters, while we have only four in the case of BIDT. That can be explained by the acoustic symmetry in BIDT, while in UDT the acoustic wave is radiated unequally from the two acoustic ports. This has been clarified in the next section with more details.

2.5 UNDERSTANDING THE SCATTERING MATRIX PARAMETERS :

Consider a transducer in the transmitting mode, where the only source of energy is through the electric port 1. i.e. $a_2 = a_3 = 0$, as shown in Fig. 2.8a. Then, equation (2.1) can be written as

$$\begin{bmatrix} b_1 \\ b_2 \\ b_3 \end{bmatrix} = \begin{bmatrix} A \\ B1 \\ B2 \end{bmatrix} \begin{bmatrix} a_1 \end{bmatrix} \quad \dots (2.41)$$



245872.

Then the Electro-Acoustic power loss or Insertion loss IL can be written as

$$IL = (b_3 / a_1)^2$$

$$IL = B_2^2 \quad \dots(2.42)$$

and if we consider the required output to be from port 2 then

$$IL = (b_2 / a_1)^2$$

$$IL = B_1^2 \quad \dots(2.43)$$

In the case of a bidirectional transducer, like that of Fig 2.3 and due to bidirectionality, the acoustic waves of the two ports b_2 and b_3 are equal, hence B_2 has to be equal to B_1 . If the transducer is unidirectional, then according to the directivity of the transducer, the wave radiated from one acoustic port is to be more than that radiated from the other port, hence we will have two IL s or Electro-acoustic transmission losses, one is for the forward direction and the other for the backward direction.

It is clear that B_1 and B_2 can be used as a measure to the directivity of a transducer. If both B_1 and B_2 are equal then the directivity of the transducer is zero, i.e. it is bidirectional, otherwise if one of the B s is larger than the other then there is certain directivity toward one side of the transducer depending on the port to which B of the larger value belongs.

Now consider the transducer in the receiving mode, where the only source of energy is through an incident acoustic wave on one of the two acoustic ports; say port 3, i.e. $a_1 = a_2 = 0$, as shown in Fig. 2.8b . Then we can write

$$\begin{bmatrix} b_1 \\ b_2 \\ b_3 \end{bmatrix} = \begin{bmatrix} B_2 \\ D \\ C_2 \end{bmatrix} \begin{bmatrix} a_1 \end{bmatrix} \quad \dots (2.44)$$

Hence the Triple Transit Echo (TTE) loss may be written as

$$T.T.E._3 = (b_3 / a_3)^2$$

$$T.T.E._3 = C_2^2 \quad \dots (2.45)$$

and the Acoustic Transmission Loss *A.T.L.* as

$$A.T.L. = (b_2 / a_3)^2$$

$$A.T.L. = D^2 \quad \dots (2.46)$$

Similarly if a_2 is the energy source and $a_1 = a_3 = 0$ then *T.T.E* of port 2 will be written as

$$T.T.E._2 = C_1^2 \quad \dots (2.47)$$

If the device is bidirectional then $C_1 = C_2 = C$

2.6 CALCULATIONS OF
SCATTERING PARAMETERS :

For the calculation of IDT scattering parameters, it is possible to find out experimentally sufficient number of independent parameters and then by using equations (2.15)-(2.18) the rest can be calculated. This method is not useful in the first design steps, where the transducer is to be designed and then fabricated. It may be useful if the transducer is there and some more information on its performance is required. Constructing the scattering matrix through calculation may be used as a good tool during designing process and later on fabricate the device as per the requirements.

Joshi et al [35] derived three scattering parameters, Acoustic reflection coefficient r , Acoustic transmission coefficient t and power absorption coefficient p as follows

$$r = G_a / Y_{tot}$$

$$t = 1 - (G_a / Y_{tot})$$

$$p = (2 G_a \operatorname{Re} Y_l) / Y_{tot}$$

where G_a is the transducer conductance.

Y_{tot} is total transducer admittance,

and Y_l is load admittance

If we consider Smith's simplified equivalent circuit [17] shown in Fig. 2.9 where $G_a(f)$ is the transducer conductance, $B_a(f)$ is the transducer susceptance and C_T is the transducer capacitance, then we can write the scattering matrix coefficients as follow

Referring to Fig. 2.10

$$a_i = \frac{1}{2 \sqrt{Z_l}} (U_i + Z_l I_i) \quad \dots (2.48)$$

$$b_i = \frac{1}{2 \sqrt{Z_l}} (U_i - Z_l I_i) \quad \dots (2.49)$$

where a_i , b_i are wave vectors of port i ,

U_i and I_i are voltage and current, respectively,

Z_l is transducer source or load impedance.

Or we can write (2.48) and (2.49) in the form

$$U_i = \sqrt{Z_l} (a_i + b_i)$$

$$I_i = (1 / \sqrt{Z_l}) (a_i - b_i)$$

Then we can write the Electric Mismatch Loss S_{11} as

$$S_{11} = R \exp(j\rho) = \frac{b_1}{a_1} = \frac{U_1 - Z_l I_1}{U_1 + Z_l I_1}$$

$$= \frac{Z_{in} - Z_l}{Z_{in} + Z_l}$$

where Z_{in} is transducer input impedance.

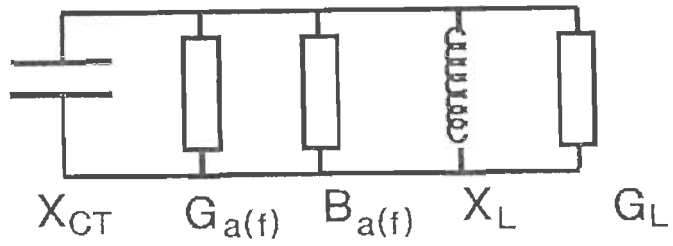


Fig. 2.9 *Smith's cross-field equivalent circuit model for an IDT.*

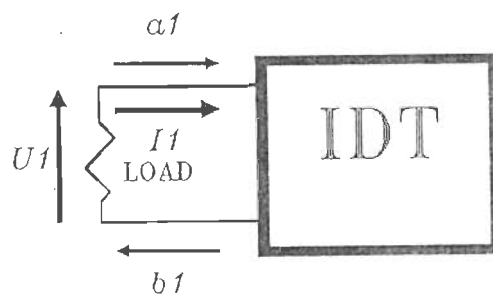


Fig. 2.10 *Electrically loaded IDT; voltage, current and waves entering and leaving the electric port.*

Assuming real load and source impedances and matched condition;

$$Z_l = R_s = R_l = G_a(f_0)$$

Let us rewrite $G_a(f)$ and $B_a(f)$ as follow

(With $x = N_p \pi \Delta f / f_0$)

$$G_a(f) = (\sin x / x) G_0 / G_l \quad \dots (2.50)$$

$$B_a(f) = \left(\frac{\sin 2x - 2x}{2x^2} \right) G_0 / G_l$$

Hence Input Admittance $Y_{in} = G_a(f) + B_a(f) + X_{C_T}$

Let us now define the transducer electric quality factor Q_e [25,35].

$$Q_e = \frac{\omega_0 C_T}{G_a(f_0)}$$

$$Q_e = \frac{\pi \Delta f}{4 K^2 f} G_0 / G_l$$

$$\text{but } \Delta f / f \approx \frac{1}{1.12 N_p}$$

then

$$Q_e = \frac{\pi}{4 K^2 1.12 N_p} G_0 / G_l$$

Input admittance of the transducer

$$Y_{in} = G_a(f) + (B_a(f) + Q_e f)$$

If the transducer is tuned using the tuning coil shown in Fig. 2.9 JX will be

$$JX = J \left[\omega C_T - \frac{1}{\omega L} \right] = J \left[\omega C_T - \frac{1}{\omega / (\omega_0^2 C_T)} \right]$$

$$JX = J G_0 Q_e \left[\frac{f}{f_0} - \frac{f_0}{f} \right] \quad \dots (2.51)$$

Then

$$Y_{in} = G_a(f) + J(B_a(f) + Q_e (f/f_0 - f_0/f)) \quad \dots (2.52)$$

Finally, the scattering parameters can be calculated from the following equations

$$S_{11} = R \exp(J\rho) = \frac{Z_{in} - Z_l}{Z_{in} + Z_l} \quad \dots (2.53)$$

where $Z_{in} = 1/Y_{in}$

$$S_{12} = T \exp(J\theta) = \frac{\sqrt{2 G_a(f)}}{Y_T} \quad \dots (2.54)$$

where $Y_T = 1 + Y_{in}$

$$S_{22} = S \exp(J\sigma) = \frac{-G_a(f)}{Y_T} \quad \dots (2.55)$$

$$S_{23} = G \exp(J\gamma) = 1 + S_{22} \quad \dots (2.56)$$

Note that all quantities above are normalized to G_1 . G_0 is the transducer conductance at f_0 (i.e. equal to $G_a(f_0)$).

If the transducer is matched then $G_0 / G_1 = 1$.

2.7 COMPUTATIONS :

For the purpose of modeling IDTs, FORTRAN 77 program was developed to interpret the mathematical modeling presented in the earlier sections. Different BIDTs with different number of finger-pairs were simulated and the relevant scattering matrices were computed. Different transducer's losses were plotted versus frequency for a frequency range from 0.9 to 1.1 of the operating frequency.

Figures 2.11 and 2.12 show the plots of Electro-Acoustic Losses (Transducers Frequency Responses), Triple Transit Echo Losses, Acoustic Transmission Losses and Electric Mismatch Losses for two bidirectional transducers having 30 and 60 finger-pairs, respectively.

Such information, that can be deduced directly from the scattering matrix model , no other model can give the same directly, and this is one of the major advantages of scattering matrix model over other models.

Fig. 2.11 Different losses of BIDT having 30 finger-pairs calculated using SCAT MAT approach. Aperture is $2.099E-4$ m.

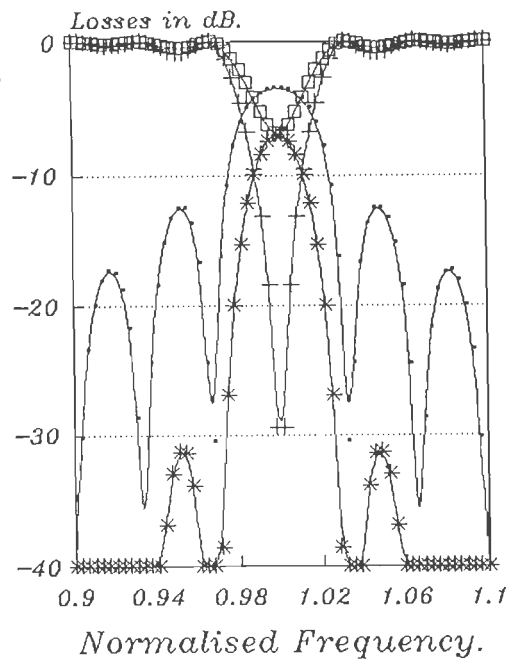
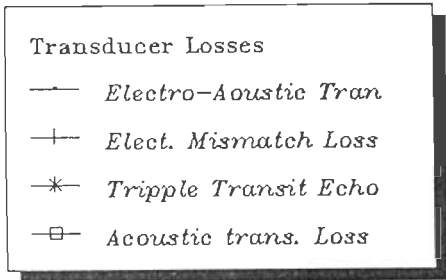
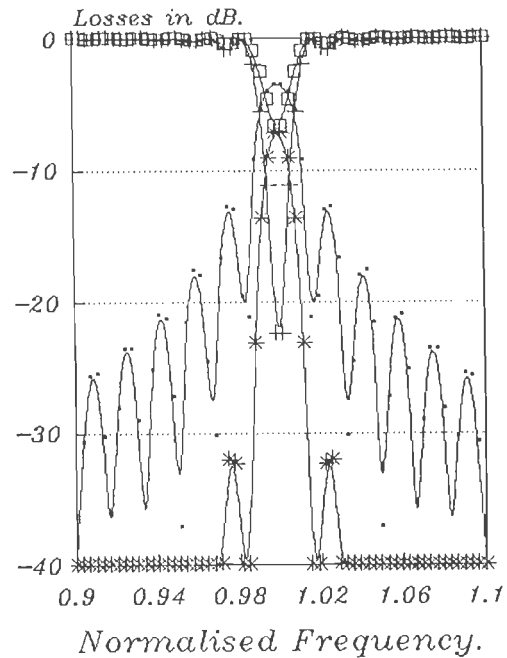
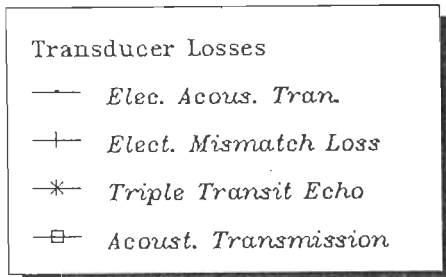


Fig. 2.12 Different losses of BIDT having 60 finger-pairs calculated using SCAT MAT approach. Effec. Aperture is $5.247E-5$ m.



The Junction Scattering Matrix modeling, or the pair by pair scattering matrix model, was also included in the program to see the differences of the two approaches. The program is to calculate the scattering matrix of the basic unit - The finger-pair - using the simplified smith's equivalent circuit. This basic unit is to be cascaded several times, depending on the number of periodic sections and as discussed earlier. The results obtained indicated that the model expressed the transducer ideally but only at the center frequency and very much close to it, where the transducer is matched and tuned. The scattering parameters for the two BIDTs with 30 and 60 finger-pairs at center frequency and very close to it have been found to be identical to what have been obtained from the previous approach. Yet this approach failed to give the frequency response of the transducer little bit far from the center frequency. One or more of the relationships (2.15) to (2.18) may fail when the transducer is operating under unmatched and untuned conditions (i.e. far from f_0).

2.8 CONCLUSION :

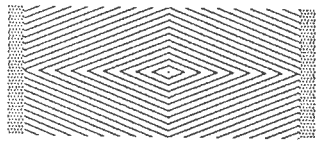
The interdigital transducer has been represented by 3x3 scattering matrix of four independent scattering parameters, and treated as if it is a point scatterer located at the center of the transducer. A single finger-pair basic unit scattering matrix approach has also been considered. BIDT has been modeled by cascading the finger-pair scattering matrix number of times equal

to the number of periodic sections. A GUDT has been selected, to be modeled by the same approach, as an example for unidirectional transducers. It has been found that two more complex independent scattering parameters are present in the representation of GUDT compared to that of BIDT. This difference in the number of independent scattering parameters is due to the difference in directionality in the two types of transducers, as it has been clarified. It has been found that the scattering matrix model provides much information regarding the performance of transducers, Forward and backward responses, directivity, triple transit echo, acoustic transmission loss and electric mismatch loss.

The different scattering parameters of an IDT have been derived from the simplified equivalent circuit of Smith. A FORTRAN 77 program has been developed to interpret the two scattering matrix approaches. BIDTs with different number of finger-pairs have been simulated. Plots of performances and losses of these transducers for a certain range of frequencies have been presented. It has been found that the junction scattering matrix approach is limited to the matched and tuned condition. The approach represents the transducer only at the operating frequency f_0 and very close to it.

The scattering matrix model has been found to be very fast in terms of computation time requirements in addition to giving many informations regarding the performances of transducers that no

other model can give directly, yet it is limited in its capability of representing many types of SAW transducers.



CHAPTER THREE

3

Transfer Matrix Approach.

3.1 Introduction.

3.2 Modelling Of An IDI.

3.3 Single Finger Transfer
Matrix.

3.4 Basic Unit Transfer Matrix

3.5 Positive And Negative Voltage
Derived Fingers.

3.6 Computations.

3.7 Conclusion.

3.1 INTRODUCTION :

The three-port network representation of an IDT is translated in this chapter into mixed transfer matrix starting from a single finger basic unit. The basic modeling unit is selected to be a single finger bounded by two gaps. The transfer matrix of this basic unit is derived and used to construct the full transducer transfer matrix model. The cascading of acoustic quantities of the acoustic ports of the basic units is performed in wave terms, while the electrical quantities are treated differently in terms of voltage and current. Positive and negative voltage derived basic units transfer matrix representations are presented for the modeling of different types of bidirectional transducers. Performances of normal BIDTs and split-finger BIDTs are reported. Effect of finger splitting on transducer and filter performances are also discussed.

Due to the limitations in modeling IDTs using the scattering matrix approach we thought of finding some other approach also based on the cross-field equivalent circuit model - for reasons discussed earlier -.One of the main limitations of any model is the basic unit from which the modeled device is to be built up. In the junction scattering matrix approach, it is obviously not possible to model a transducer like the TPUDT due to the finger-pair basic unit. With the Junction scattering matrix representation , we have seen that the model was limited to the matched and tuned condition and very close to it.

These limitations were studied carefully and a new approach for modeling the IDT is thought of using transfer matrix. The basic unit is chosen to be a combination of a single finger and gaps on both sides of the finger. This basic unit is to be cascaded according to the type of the transducer and the number of fingers in it differently than what has been proposed in the scattering matrix approach.

An IDT may be represented by the three-port network shown in Figure 3.1, with two acoustic ports (*ports 1 and 2*) and one electric port (*port 3*). The two acoustic ports can be expressed by acoustic waves leaving and entering the two terminals, while the electric port can be expressed by electrical quantities,

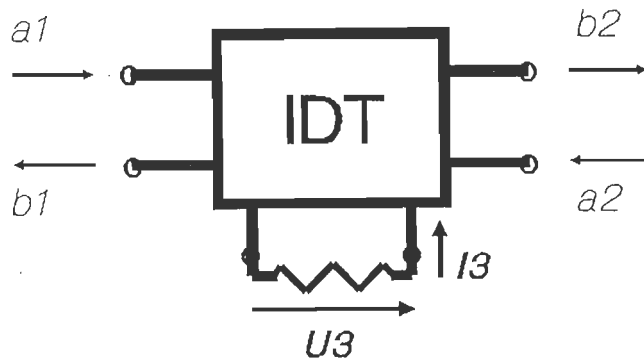


Fig. 3.1 Three-port representation of an IDT. Ports numbering and notations for TRANS MAT approach are indicated.

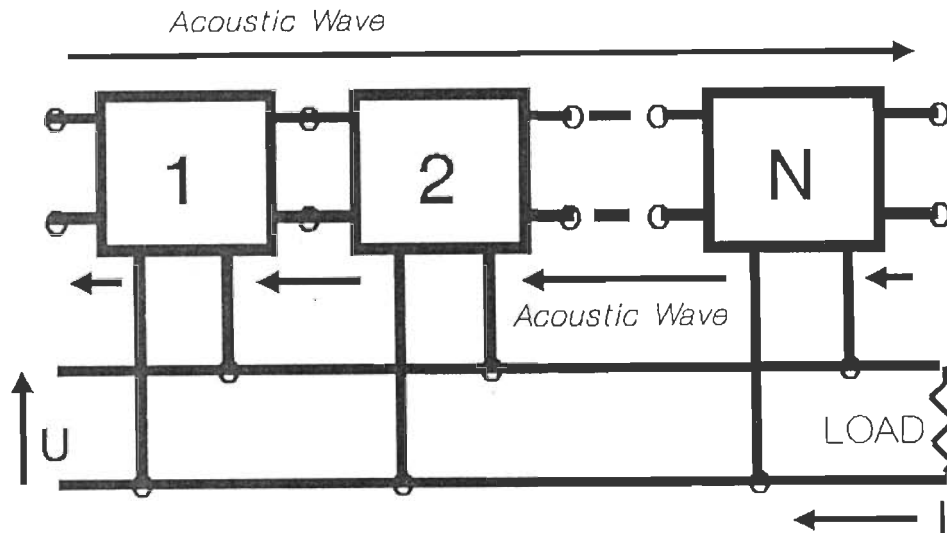


Fig. 3.2 Cascading IDT fingers to construct full transducer. Electric ports are treated in electrical terms, Voltage and Current.

current entering the transducer and voltage across it. The basic unit of the model (i.e. the finger with left and right side gaps) can be represented by a similar network. The fingers of the transducers are to be cascaded acoustically in wave terms as far as the acoustic ports are concerned and the electric quantities of the electric ports are to be treated differently by direct electric circuit connections to the positive and negative voltage sources, as in Figure 3.2.

The basic unit consists of one metalized portion (or finger) and two unmetalized portions (or gaps) on both sides of the first. The unmetalized portions can be considered as unmetalized fingers. Both metalized and un-metalized fingers are to be treated in the same way, taking into consideration the differences between the two types of acoustic wave paths due to the difference of metal and the distance of each path. Also some inversing or transforming network representations are required on the edges of the metalized finger, which are function of metal thickness and other metal constants. The different types of network representations are to be cascaded together according to the sequence shown in Figure 3.3 to model the basic unit. A sketch of the actual basic unit of the model is also shown in the Figure.

3.3 SINGLE FINGER TRANSFER MATRIX :
--

Before proceeding into the derivations of the single finger transfer matrix [36] let us define some of the notations used in

the calculation of the basic modeling unit. (Figure 3.3).

l is the metalized portion length of the basic unit,

U_3 and I_3 are the voltage applied and the current passing through the basic unit.

a_1 & a_2 and b_1 & b_2 are the acoustic waves entering and leaving the acoustic terminal 1 and 2.

Angles ϑ and ϕ are defined as follow

$$\vartheta = \frac{\omega}{v_0} \cdot \frac{l}{2} \quad \dots (3.1)$$

$$\phi = \frac{\omega}{v_0} l \quad \dots (3.2)$$

Now with the aid of smith's equivalent circuit model [17] we can draw the equivalent circuit for a single finger as in Figure 3.4. The general equations for such circuits are;

$$U_2 = \left(1 + \frac{Z_1}{Z_2}\right) U_1 - (Z_1 + 2Z_2) \frac{Z_1}{Z_2} I_1 - \frac{Z_1}{Z_2} r U_3 \quad \dots (3.3)$$

$$I_2 = \frac{1}{Z_2} U_1 - \left(1 + \frac{Z_1}{Z_2}\right) I_1 - \frac{r}{Z_2} U_3 \quad \dots (3.4)$$

$$I_3 = \frac{r}{Z_2} U_1 - \frac{Z_1}{Z_2} r I_1 - \frac{r^2}{Z_2} U_3 \quad \dots (3.5)$$

Where U , I and Z are voltage, current and impedance, respectively.

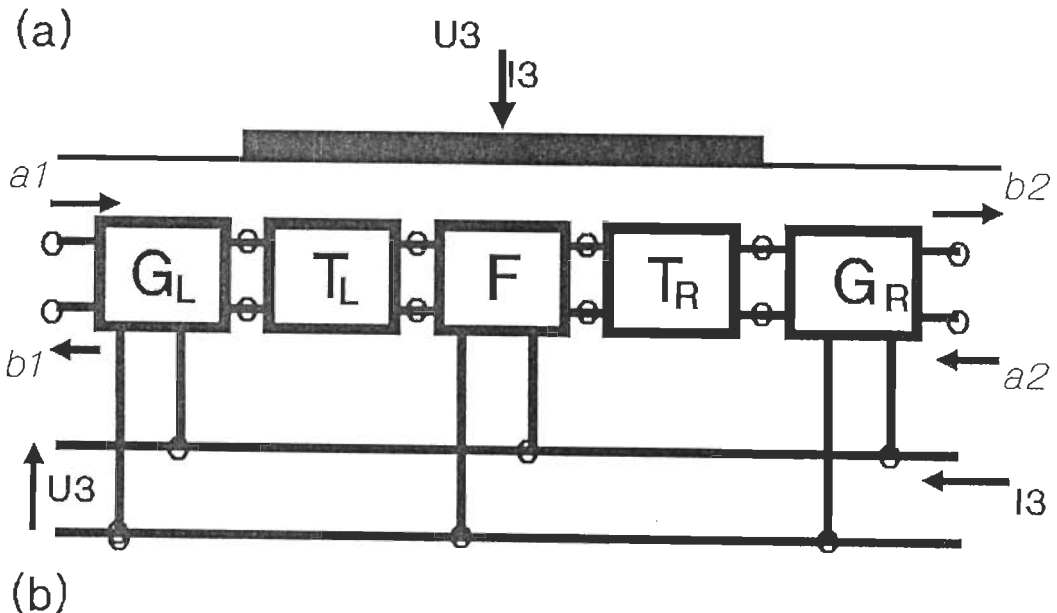


Fig. 3.3 Basic Modelling Unit.
 a) Actual shape.
 b) Constructing the Basic Unit Through cascading.

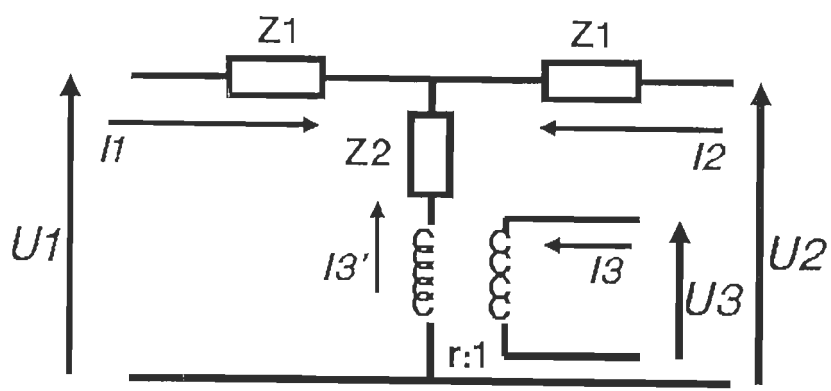


Fig. 3.4 Single finger equivalent circuit.

Numbering is as shown in Figure 3.4.

r is transformer turn ratio which is function of material, section length and capacitance. [37]

Now if we define the periodic section transit angle as ϑ_T [17] and ψ to be equal to $\vartheta/2$, then we can write Z_1 and Z_2 in terms of ψ

$$Z_1 = jZ_o \frac{1 - \cos \psi}{\sin \psi} \quad \dots (3.6)$$

$$Z_2 = \frac{Z_o}{j \sin \psi} \quad \dots (3.7)$$

$$\frac{Z_1}{Z_2} = \cos \psi - 1$$

where Z_o is the substrate characteristic impedance.

Then substituting equations (3.6) and (3.7) in equations (3.3) up to (3.5), the later can be written in a matrix form as

$$\begin{bmatrix} U_2 \\ I_2 \\ I_3 \end{bmatrix} = \begin{bmatrix} \cos \psi & -jZ_o \sin \psi & r(1 - \cos \psi) \\ jY_o \sin \psi & -\cos \psi & -jrY_o \sin \psi \\ -jrY_o \sin \psi & r(\cos \psi - 1) & jr^2 Y_o \sin \psi \end{bmatrix} \begin{bmatrix} U_1 \\ I_1 \\ U_3 \end{bmatrix} \quad \dots (3.8)$$

where $Y_o = 1/Z_o$

Introducing the wave vectors a_i and b_i

$$a_i = \frac{1}{2 \sqrt{Z_o}} (U_i + Z_o I_i) \quad \dots (3.9)$$

$$b_i = \frac{1}{2\sqrt{Z_o}}(U_i - Z_o I_i) \quad \dots (3.10)$$

Or

$$a_i + b_i = U_i / \sqrt{Z_o} \quad \dots (3.11)$$

$$a_i - b_i = I_i \sqrt{Z_o} \quad \dots (3.12)$$

we can write equation (3.8) in a mixed T-matrix form

$$\begin{bmatrix} b_2 \\ a_2 \\ I_3 \end{bmatrix} = \begin{bmatrix} F_{11} & F_{12} & F_{13} \\ F_{21} & F_{22} & F_{23} \\ F_{31} & F_{32} & F_{33} \end{bmatrix} \begin{bmatrix} a_1 \\ b_1 \\ U_3 \end{bmatrix} \quad \dots (3.13)$$

where

$$F_{11} = \exp(-j\psi) \quad \dots (3.14)$$

$$F_{12} = 0 \quad \dots (3.15)$$

$$F_{13} = \frac{r}{2\sqrt{Z_o}} [1 - \exp(-j\psi)] \quad \dots (3.16)$$

$$F_{21} = 0$$

$$F_{22} = \exp(j\psi)$$

$$F_{23} = \frac{r}{2\sqrt{Z_o}} [1 - \exp(j\psi)]$$

$$F_{31} = \frac{-r}{\sqrt{Z_o}} [1 - \exp(-j\psi)]$$

$$F_{23} = \frac{r}{\sqrt{Z_o}} [1 - \exp(j\psi)]$$

$$F_{33} = jr^2 Y_o \sin \psi \quad \dots (3.17)$$

Simplifying (3.13) the finger mixed transfer matrix can be written as

$$F = \begin{bmatrix} F_{11} & F_{12} & F_{13} \\ F_{12} & F_{11}^* & F_{13}^* \\ -2F_{13} & 2F_{13}^* & F_{33} \end{bmatrix} \quad \dots (3.18)$$

where

$$F_{21} = F_{12}$$

$$F_{22} = F_{11}^*$$

$$F_{31} = -2 F_{13}$$

$$F_{32} = 2 F_{13}$$

hence F has only three independent elements.

Now let us add the two inverse networks of Figure 3.5a to the left acoustic port and that of Figure 3.5b to the right acoustic port of the finger. [38].

The chain matrix for the left inverse network is

$$\begin{bmatrix} U_1 \\ I_1 \end{bmatrix} = \begin{bmatrix} n & 0 \\ Y/n & -1/n \end{bmatrix} \begin{bmatrix} U_2 \\ I_2 \end{bmatrix} \quad \dots (3.19)$$

Introducing wave vectors using equations (3.9)-(3.12) the left side inverse network transfer matrix can be written as

$$T_L = \begin{bmatrix} T_{11} & T_{12} \\ T_{21} & T_{22} \end{bmatrix} \quad \dots (3.20)$$

where

$$T_{11} = \frac{1}{n} + n - \frac{Z_o}{n} Y$$

$$T_{12} = \frac{1}{n} - n - \frac{Z_o}{n} Y$$

$$T_{21} = \frac{1}{n} - n + \frac{Z_o}{n} Y$$

$$T_{22} = \frac{1}{n} + n + \frac{Z_o}{n} Y$$

The chain matrix of the right side inverse network is

$$\begin{bmatrix} U_1 \\ I_1 \end{bmatrix} = \begin{bmatrix} n & 0 \\ Y/n & -1/n \end{bmatrix} \begin{bmatrix} U_2 \\ I_2 \end{bmatrix} \quad \dots (3.21)$$

and in a similar way the network mixed transfer matrix can be written as

$$T_R = \begin{bmatrix} T_{11} & -T_{12} \\ -T_{21} & T_{22} \end{bmatrix} \quad \dots (3.22)$$

Y is taken to be a purely imaginary element and equal to jB .

T_L and T_R can be written as

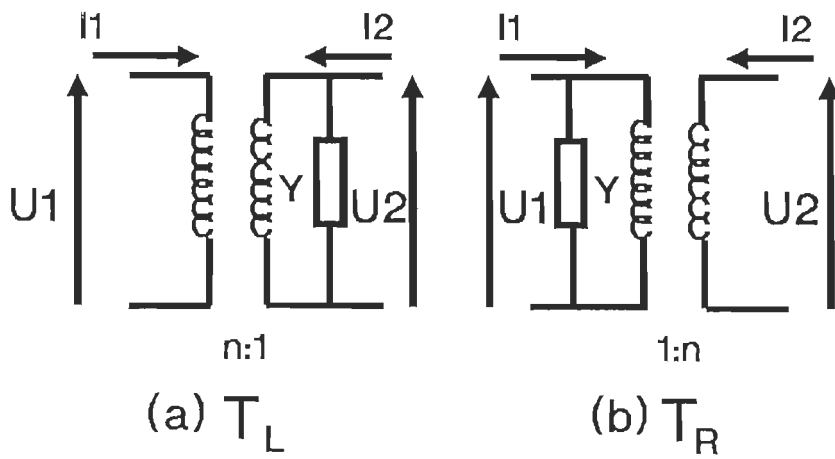


Fig. 3.5 Inverse networks to the right and left of finger equivalent circuit.

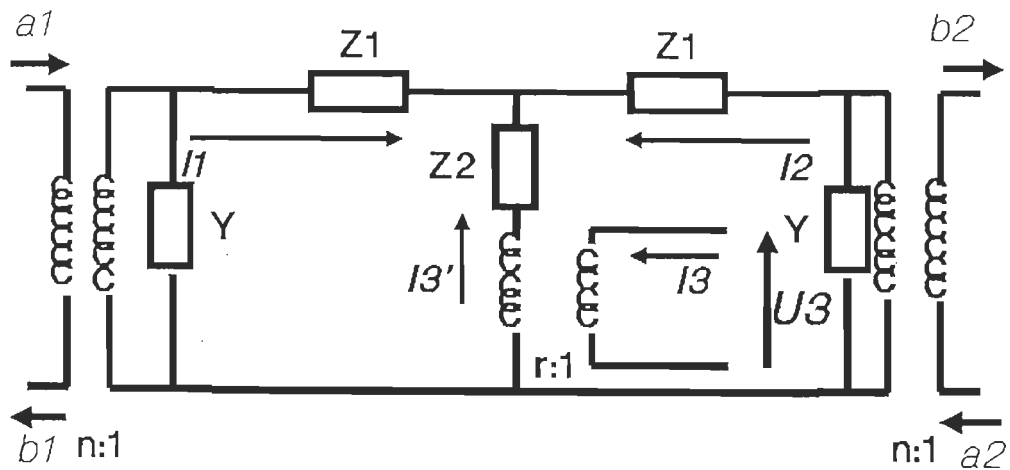


Fig. 3.6 Equivalent circuit of the metalised portion of the basic unit.

$$T_L = 1/2 \begin{bmatrix} T_{11} & T_{12} \\ T_{12}^* & T_{11}^* \end{bmatrix} \quad \dots (3.23)$$

and

$$T_R = 1/2 \begin{bmatrix} T_{11} & -T_{12}^* \\ -T_{12} & T_{11}^* \end{bmatrix} \quad \dots (3.24)$$

where

$$T_{11} = n + \frac{1}{n} - jB, \quad 1 \quad \dots (3.25)$$

$$T_{12} = n - \frac{1}{n} - jB, \quad 1 \quad \dots (3.26)$$

$$T_{21} = T_{12}^*$$

$$T_{21} = T_{11}^*$$

$$B = B / Y_0 = Z_0 B$$

The overall equivalent circuit representation of the metalized portion of the basic unit will be as in Figure 3.6, and the overall mixed transfer matrix H of the unit will be

$$H = T_L F T_R \quad \dots (3.27)$$

where the acoustic quantities are to be cascaded in wave terms while the electric terms are to be treated separately.

Here we have

$$a_3 = b_2$$

$$a_2 = b_3$$

$$a_5 = b_4$$

$$a_4 = b_5$$

$$b_4 = F_{11} a_3 + F_{13} U_7$$

$$a_4 = F_{11}^* b_3 + F_{13}^* U_7$$

$$I_7 = -2F_{13} a_3 + 2F_{13}^* b_3 + F_{33} U_7$$

Using the above equations we can derive the matrix H as

$$H = \begin{bmatrix} H_{11} & H_{12} & H_{13} \\ -H_{12} & H_{11}^* & H_{13}^* \\ -H_{13} & H_{13}^* & H_{33} \end{bmatrix} \quad \dots (3.28)$$

with four independent elements. Where

$$H_{11} = \frac{1}{2} (F_{11} T_{11}^2 - F_{11}^* T_{12}^2) \quad \dots (3.29)$$

$$H_{12} = \frac{1}{2} (T_{11}^* T_{12} F_{11}^* - T_{11} T_{12}^* F_{11}) \quad \dots (3.30)$$

$$H_{13} = T_{11} F_{13} + T_{12} F_{13}^* \quad \dots (3.31)$$

$$H_{21} = -H_{12}$$

$$H_{22} = H_{11}^*$$

$$H_{23} = H_{13}^*$$

$$H_{31} = -H_{13}$$

$$H_{32} = H_{13}^*$$

$$H_{33} = F_{33} \quad \dots (3.32)$$

3.4 BASIC UNIT TRANSFER MATRIX :

For getting the final model of the basic-unit it is required to add the gap areas on both sides of the finger. As mentioned before, a gap can be treated as unmetallized finger. A similar three-port network as that representing metallized finger portion of the unit may be used to represent the unmetallized gap portion of the unit if differences in acoustic wave propagation in the two paths (metallized and unmetallized paths) are considered. Figure 3.7 shows three-port network and equivalent circuit representations for a gap.

Gap transfer matrix can be written similar to (3.18) as

$$G = \begin{bmatrix} G_{11} & G_{12} & G_{13} \\ G_{12} & G_{11}^* & G_{13}^* \\ -2G_{13} & 2G_{13}^* & G_{33} \end{bmatrix} \quad \dots (3.33)$$

where

$$G_{11} = \exp(-j\theta)$$

$$G_{13} = \frac{1}{2\sqrt{Z_0}} (1 - \exp(j\vartheta))$$

$$G_{33} = jr^2 Y_0 \sin \vartheta$$

Adding the two gaps to the right and left of the finger, i.e.

$$U = G H G \quad \dots (3.34)$$

we get

$$\begin{bmatrix} b_2 \\ a_2 \\ I_3 \end{bmatrix} = \begin{bmatrix} U_{11} & U_{12} & U_{13} \\ -U_{12} & U_{11}^* & U_{13}^* \\ -2U_{13} & 2U_{13}^* & U_{33} \end{bmatrix} \begin{bmatrix} a_1 \\ b_1 \\ U_3 \end{bmatrix} \quad \dots (3.35)$$

where

$$U_{11} = G_{11}^2 H_{11} \quad \dots (4.36)$$

$$U_{12} = H_{12} \quad \dots (3.37)$$

$$U_{13} = G_{11} (G_{13} H_{11} + G_{13}^* H_{12} + H_{13}) + G_{13} \quad \dots (3.38)$$

$$U_{21} = -U_{12}$$

$$U_{22} = U_{11}^*$$

$$U_{23} = U_{13}^*$$

$$U_{31} = -2U_{13}$$

$$U_{32} = 2U_{13}^*$$

$$U_{33} = H_{33} + 2G_{33} + j4 \operatorname{Im} [G_{13}^* (2H_{13}^* + G_{13}^* H_{11}^* - G_{13} H_{12})] \quad \dots (3.39)$$

Final basic-unit mixed transfer matrix has only four independent elements. G , H , F and T have been defined earlier. ϕ , ϕ , a_1 , a_2 , b_1 , b_2 , I_3 and U_3 are defined in Figure 3.3.

3.5 POSITIVE AND NEGATIVE
VOLTAGE DERIVED FINGERS :

The derivations for the basic-unit model of the transfer matrix approach carried out in the previous sections led to the mixed transfer matrix U of equation (3.35) which consists of four independent elements. This matrix represents a basic-unit finger derived by a positive voltage U_3 applied to it. For the sake of modeling a BIDT it is required to have two types of voltage derived fingers, a positive derived and a negative derived finger units. Now if we go through the same procedure followed earlier to calculate the mixed transfer matrix for a negative voltage derived unit we will get the matrix U_- shown below with U_+ for comparison.

$$U_+ = \begin{bmatrix} U_{11} & U_{12} & U_{13} \\ U_{21} & U_{22} & U_{23} \\ U_{31} & U_{32} & U_{33} \end{bmatrix} \quad \dots (3.40)$$

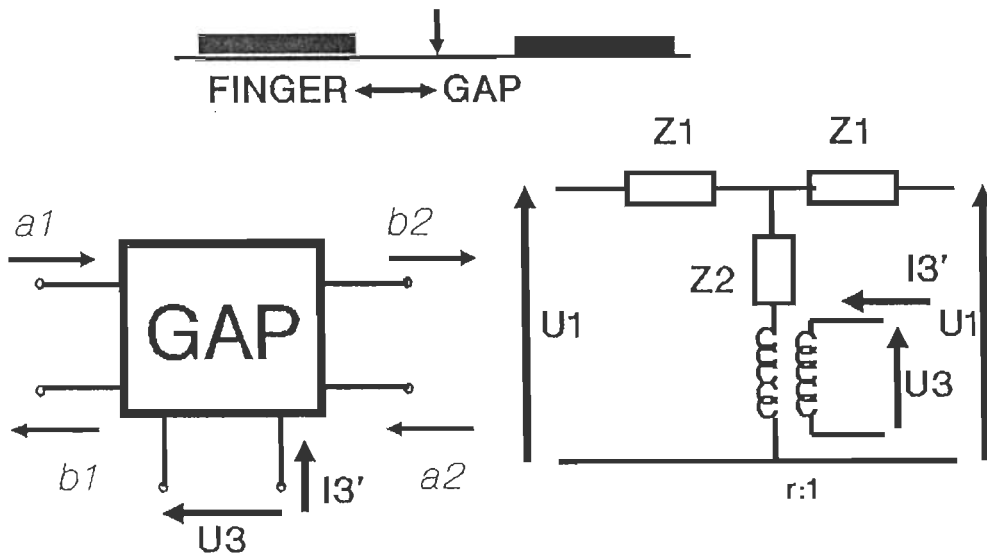
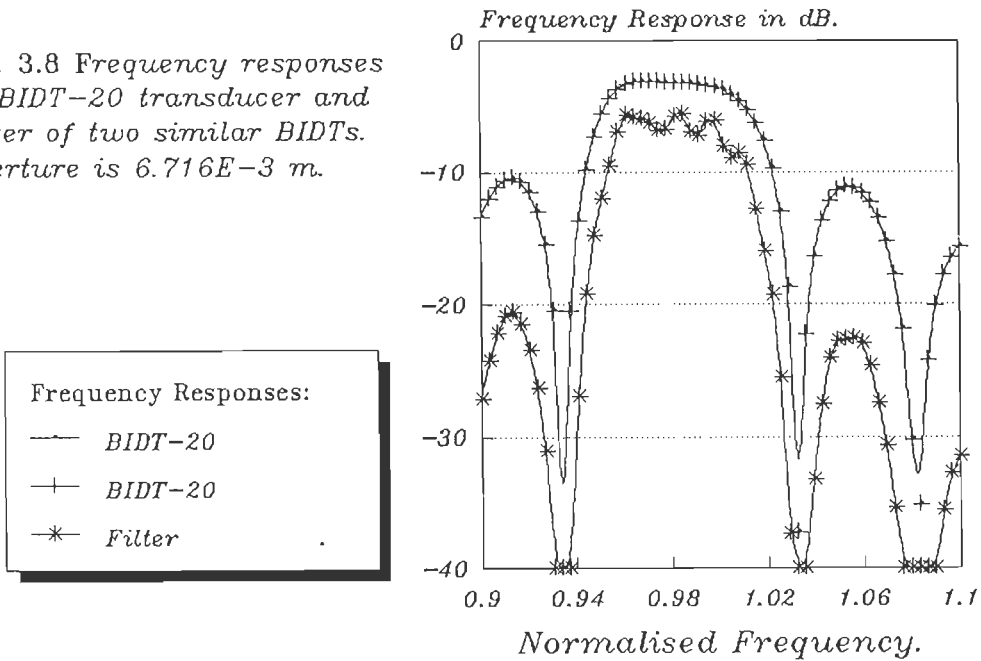


Fig. 3.7 Gap three-port representation and equivalent circuit.

Fig. 3.8 Frequency responses of BIDT-20 transducer and filter of two similar BIDTs. Aperture is $6.716E-3$ m.



$$U_- = \begin{bmatrix} U_{11} & U_{12} & -U_{13} \\ U_{21} & U_{22} & -U_{23} \\ -U_{31} & -U_{32} & U_{33} \end{bmatrix} \quad \dots (3.41)$$

The two matrices U_+ and U_- are to be cascaded in wave terms for the acoustic quantities and electrically by direct electric circuit connections similar to the procedure followed so far in this chapter. Now if the transducer is having identical finger-pairs then this finger-pair can be cascaded N_p times, where N_p is the number of periodic sections otherwise each finger-pair has to be calculated separately and then all the finger-pairs are to be cascaded to represent the full matrix (in the case of CHIRP transducers).

3.6 COMPUTATIONS :

The mathematical derivations and modeling carried out in this chapter so far were interpreted into a software package using FORTRAN 77 programming language. The software was aimed to model different types of bidirectional transducers. Due to the proper selection of the basic modeling unit and the possibilities available in the modeling approach to represent different (not identical) finger-pairs, the program was extended to include the

Fig. 3.9 Frequency responses of BIDT of 40 finger-pairs and two BIDTs Filter Using TRANS MAT approach. Effec. Apert. is $1.679E-3$ m

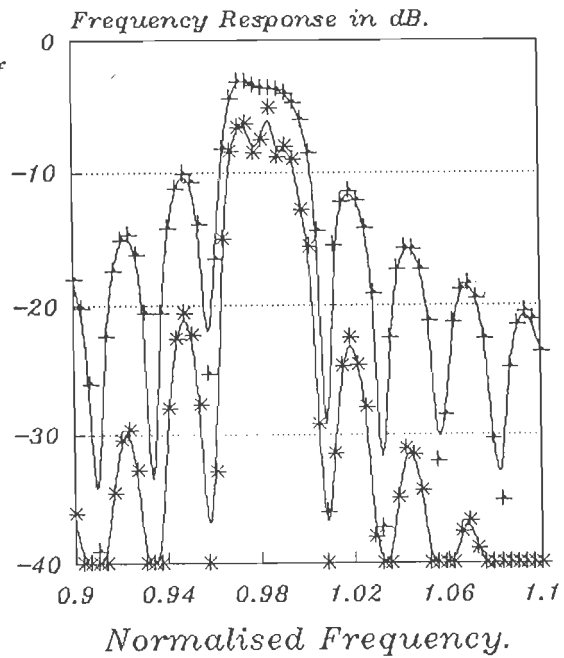
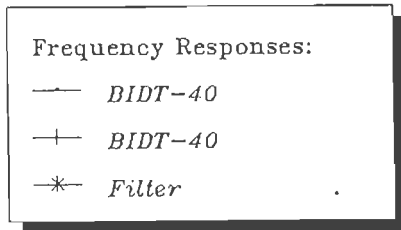
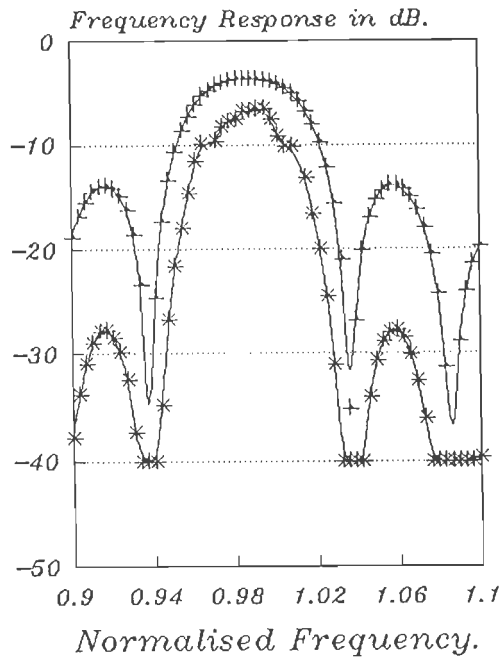
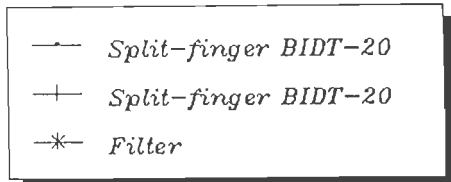


Fig. 3.10 Frequency responses of 20 periodic sections, Split-finger BIDT and two Split-finger BIDTs Filter modeled using TRANS MAT approach. Aperture is $5.721E-3$ m.



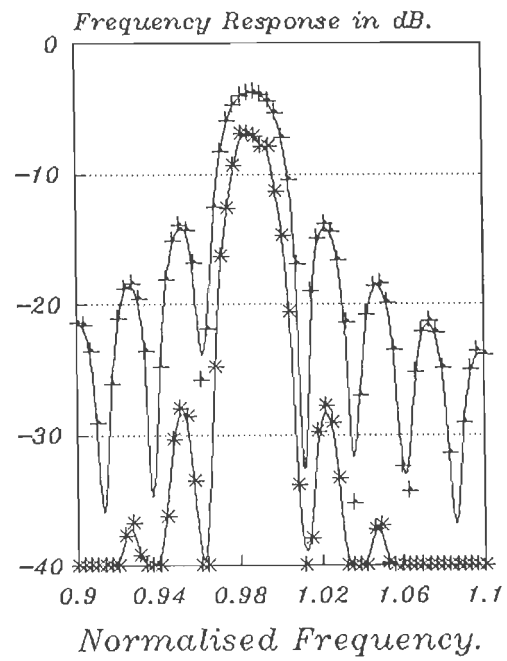
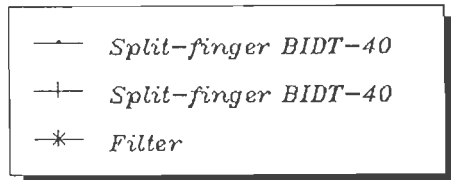
modeling of many types of bidirectional transducers such as normal BIDT, split finger BIDT, CHIRP transducers and filters and COMB transducers and filters.

Different types of these bidirectional transducers and filters of similar pairs of transducers were simulated with different number of finger-pairs. Typical performances of such transducers and filters are shown in Figure 3.8 to Figure 3.11. Figures 3.8 and 3.9 are plots of frequency responses of normal BIDTs of 20 and 40 finger-pairs and the frequency responses of filters simulated from identical pairs of BIDTs. A 3dB insertion loss can be seen due to bidirectionality. It can be seen also from filters responses that the main lobes are not smooth for the two filters shown due to triple transit echo.

One method for improving the filter response by reducing the triple transit echo loss is by splitting the transducer's fingers into a pair of splitted fingers each, both are to be derived by the same voltage as a single finger. The performances of two split-finger BIDT transducers and filters of identical pairs of these transducers with 20 and 40 periodic sections, each section of 4 fingers (two splitted fingers), are shown in Figure 3.10 and Figure 3.11. The improvement in the smoothness of filters responses are very much clear.

The transfer matrix approach succeeded in breaking off some of the modeling limitations in the scattering matrix approach, yet

Fig. 3.11 Frequency responses of 40 periodic sections Split-finger BIDT and Two Split-finger BIDTs Filter modeled using TRANS MAT approach.
 Effec. Apert. is $1.43E-3$ m.



the approach although able to model a variety of bidirectional transducers and filters, it is not able in its present form to model unidirectional transducers such as GUDT and TPUDT because for each of these transducers the basic unit has to be derived again according to the modifications required. For modeling GUDT and TPUDT a new derivations for earthed and phase shifted voltage derived fingers are to be carried out. Similar derivations are required whenever a new transducer or device is to be included.

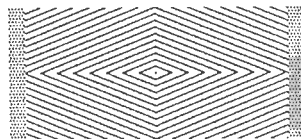
3.7 CONCLUSION :

A basic modeling unit, of a single IDT finger and two gaps on both sides of the finger, has been selected for the modeling of many kinds of SAW transducers using transfer matrix approach. The gaps between IDT fingers have been considered as unmetallized fingers. The differences in acoustic wave propagation in the two metallized (finger) and unmetallized (gap) paths have been taken into account while modeling the two assumed types of fingers. Both have been represented by three-port networks with the acoustic ports 1 and 2 expressed in terms of waves and the electric port 3 expressed in electric terms, voltage and current. A 3x3 mixed transfer matrices have been derived - based on the equivalent circuit of a finger - to model single finger and gap. The combination Gap-Finger-Gap transfer matrix has been considered as

the basic unit matrix from which the full transfer matrix representing the full transducer can be derived through cascading this basic unit.

A FORTRAN 77 program has been developed by interpreting the derivations of the transfer matrix approach into a programming algorithm for the purpose of modeling different kinds of SAW transducers. The selection of the basic modeling unit allowed the approach to include the modeling of many bidirectional transducers such as normal BIDT, split-finger BIDT, CHIRP and COMB transducers and filters. The software succeeded in simulating and finding out the performances of these types of transducers. Performances of filters constructed from simulated identical BIDTs and split-finger BIDTs have been reported and the effect of splitting fingers on the filter performance has been looked into.

The approach was able to model many types of bidirectional transducers from combinations of negative and positive voltage derived fingers. For modeling of UDTs, the approach is not able to include the modeling of such transducers unless some more types of voltage derived basic units such as the earthed finger unit and the phase shifted voltage derived finger unit are modeled. The next chapter looks into some other approach that has the ability of including the modeling of such types of transducers.



CHAPTER FOUR

4

Chain Matrix Approach

- 4.1 Introduction.
- 4.2 Chain Matrix Approach Explanation.
- 4.3 Modelling Of Chain Matrix Approach
Basic Unit.
- 4.4 Modelling Of Transducer And Filter.
- 4.5 Modelling Of Unidirectional Transducers.
 - 4.5.1 Group Type Unidirectional Transducers.
 - 4.5.2 Three Phase Unidirectional Transducers.
- 4.6 Computation.
- 4.7 Performances Of Group Type Unidirectional
Transducers.
- 4.8 Performances Of Three Phase Unidirectional
Transducers.
- 4.9 Filters Of Pairs Of Identical Transducers.
- 4.10 Filters Of Combinations Of Group UDTs.
- 4.11 Filters Of Combinations Of GUDTs And FPUDTs.
- 4.12 Conclusion.

CHAIN MATRIX APPROACH

4.1 INTRODUCTION :

For the purpose of having a model that is able to simulate a large variety of SAW devices and due to the limited capabilities of the two approaches discussed in the previous chapters, a new approach is presented here aiming to model a wide range of SAW transducers and filters this will enable the designers to simulate their designed transducers or filters and study its performances and select the proper design up to the best of their requirements, avoiding spending much money and effort on fabricating a device that may not be up to the required performance.

In this approach the basic unit is modeled in a different way than that of the SCAT MAT and TRANS MAT basic modeling units. Modeling of bidirectional transducers having identical or different periodic sections is presented. The modeling of unidirectional transducers is also included. Different types of

group unidirectional transducers namely; Normal, Modified and new type GUDTs are modeled. In a similar way to two-phase transducers three phase unidirectional transducers are also modeled.

Many types of transducers and filters are simulated and performance results are reported. a study to improve the performances of two-transducer filters in terms of insertion loss, bandwidths and side-lobes suppression is carried out. Many filters of different types of transducers are simulated and their performances are reported and studied.

4.2 CHAIN MATRIX APPROACH EXPLANATION :
--

In the previous two approaches it was not possible to include the modeling of unidirectional transducers together with the bidirectional ones. The main reason was the basic modeling unit. In scattering matrix approach finger-pair unit can not be used to represent transducers having sections other than finger-pairs such as Quadreture-Phase or Three-Phase Unidirectional Transducers. In the case of transfer matrix approach different types of basic units are required for different driving voltages to represent sections of different finger combinations. Here in chain matrix approach we are trying to overcome the drawbacks of the previous two approaches in order to get a model that is able to represent a

wide range of SAW devices specially low-loss transducers and filters.

For the sake of obtaining good approximation several kinds of equivalent circuits have been proposed for the analysis of uniform overlap electrodes such as that shown in Figure 4.1. Smith et al, Jones et al and Krairojananan et al are among those who suggested different equivalent circuits for IDT [17,18,39,40].

However smith's equivalent circuit reported later [18] seems to be enable the prediction of the experimental results more precisely than others. As shown in Figure 4.2 the circuit representation for a single finger and gaps is different than the old type Smith's circuit reported earlier [17] in the sense that it includes such an acoustic impedance discontinuity as the characteristic impedance Z_{om} in the metalized portion and Z_{og} in the unmetalized portion of what is considered as the basic modeling unit of this approach shown in Figure. The ratio (Z_{om}/Z_{og}) is proportional to the ratio (v_m/v_g) where v_m is the acoustic velocity in metalized region and v_g is the acoustic velocity in unmetalized or gap region.

In this approach the acoustic terminals of the equivalent circuit of Figure 4.2 are expressed in some different terms than that in the equivalent circuits considered so far in this dissertation, that is the acoustic Force \bar{F} and the particle

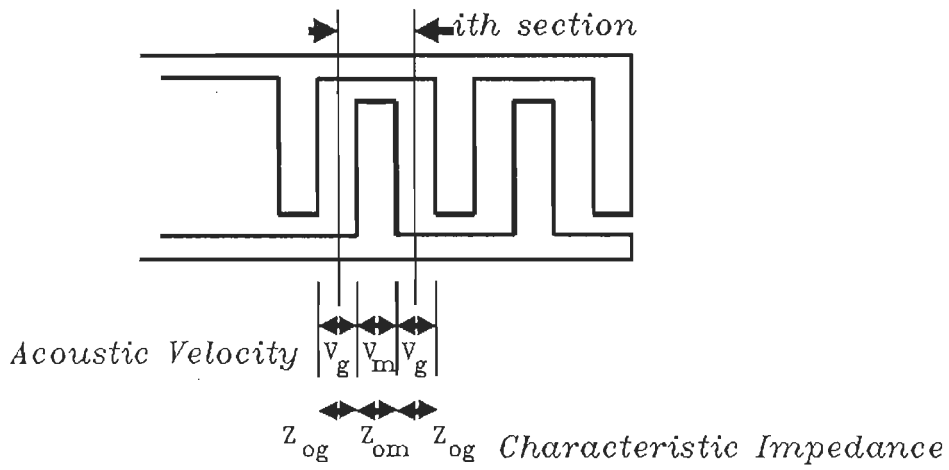


Fig. 4.1 Uniform overlap transducer section.
Acoustic velocities and characteristic impedances are shown

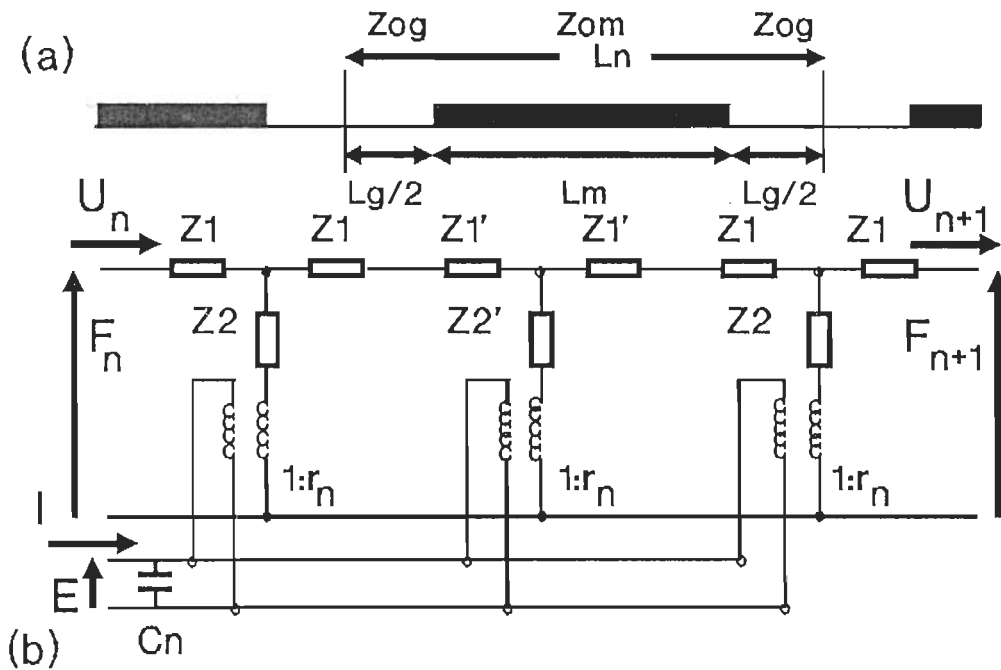


Fig. 4.2 Basic modeling Unit for CHAIN MAT approach.
a) actual shape. b) equivalent circuit.

velocity \bar{U} . For this purpose electromechanical transformation ratio ϕ_o is defined in the next section.

4.3 MODELING OF
CHAIN MATRIX APPROACH
BASIC UNIT :

Let us first define the electromechanical transformation ratio ϕ_o . For a crossed field model we can write ϕ_o as [41]

$$\phi_o = k \sqrt{\frac{2 f_o C_o Z_o}{1 - k^2}} \quad \dots(4.1)$$

where f_o is center frequency

C_o is Clamped Capacitance

Z_o is Characteristic impedance in basic section

k is Electromechanical coupling coefficient.

Now we can write transformed mechanical quantities \bar{F} and \bar{U} in electrical equivalents as

$$F = \phi_o \bar{F} \quad \dots(4.2)$$

$$U = \bar{U} / \phi_o \quad \dots(4.3)$$

Referring to Figure 4.2. In metalized portion we have

$$Z'_1 = j Z_{om} \tan (\psi_n / 2) \quad \dots (4.4)$$

$$Z'_2 = -j Z_{om} \operatorname{cosec} (\psi_n) \quad \dots (4.5)$$

where

$$\psi_n = 2 \pi f l_m / v_m$$

f is frequency,

l_m is metalized portion length.

In unmetalized portion we have

$$Z_1 = j Z_{og} \tan (\psi_n / 2) \quad \dots (4.6)$$

$$Z_2 = -j Z_{og} \operatorname{cosec} (\psi_n) \quad \dots (4.7)$$

$$Z_{og} / Z_{om} = v_g / v_m \approx 1 + \frac{1}{2} k^2 \quad \dots (4.8)$$

Electromechanical transformation ratio r_n for crossed field model

$$r_n = (-1)^n \sqrt{2 f_n C_n k^2 Z_{om}} \left[\frac{K (2^{-1/2})}{K (q_n)} \right] \dots (4.9)$$

where

$$q_n = \sin (\pi/2 l_m / l_n)$$

K is the complete elliptical integral of the first kind.

The basic modeling unit is represented by a four-port network with two acoustic ports and two electric ports for input and output [42]. The i th unit in an IDT is represented in Figure 4.3.

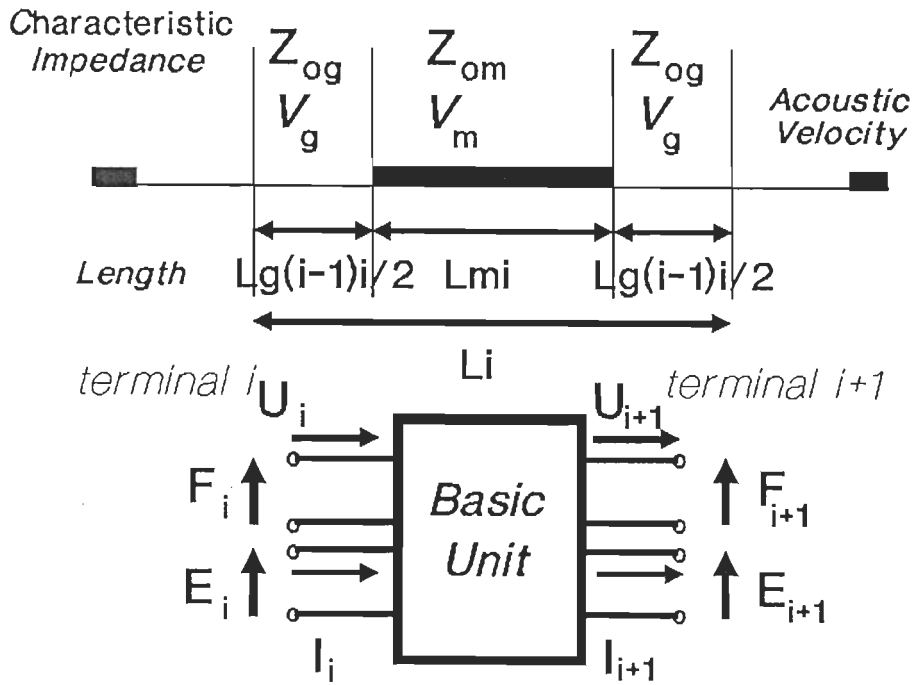


Fig. 4.3 Four-port network representation for CHAIN MAT basic unit.

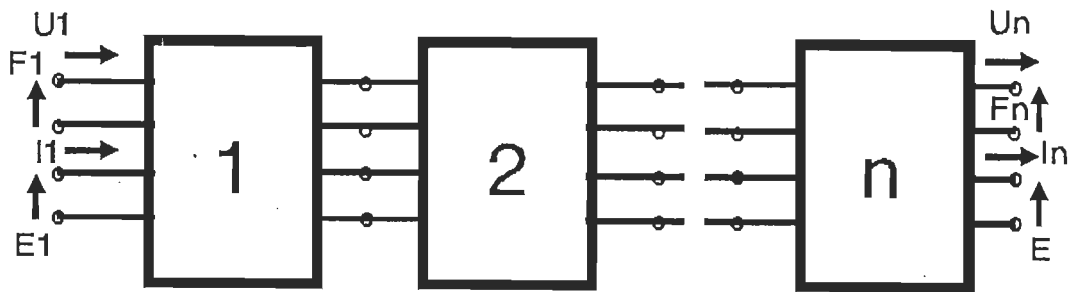


Fig. 4.4 Cascading Basic Modeling Unit to perform a section or a full transducer.

The additional electrical port is added to make the cascade connection easy. For a particular transducer the required number of fingers per section are first cascaded giving one section and these are cascaded to give the whole transducer. This procedure can be followed even if the various sections are of different types.

The four port network of the basic unit can be described by the use of Sittig's [43] chain matrix. In ordinary chain matrix representations for a network the input and output potentials and currents are related together by a chain matrix that represents various impedance and admittance elements that may be joined together in a particular manner inside that network. Sittig's chain matrix representation relates the input and output electric quantities (potential and current) with the acoustic input and output quantities (force and displacement) in the following form

$$\begin{bmatrix} F_i \\ U_i \\ E_i \\ I_i \end{bmatrix} = \begin{bmatrix} U_{11} & U_{12} & U_{13} & U_{14} \\ U_{21} & U_{22} & U_{23} & U_{24} \\ U_{31} & U_{32} & U_{33} & U_{34} \\ U_{41} & U_{42} & U_{43} & U_{44} \end{bmatrix} \begin{bmatrix} F_{i+1} \\ U_{i+1} \\ E_{i+1} \\ I_{i+1} \end{bmatrix} \quad \dots (4.10)$$

Let us define now the following

$$q = Z_{og} / Z_{om}$$

$$\beta_m = \omega / v_m$$

$$\vartheta_i = \beta_m l_{mi}$$

$$\beta_g = \omega / v_g$$

$$\psi_{-i} = \beta_g (l_{g(i-1)i} / 2)$$

$$\psi_{i+1} = \beta_g (l_{g(i+1)i} / 2)$$

$$\psi_{oi} = \psi_{-i} + \psi_{i+1}$$

ω is angular frequency.

From the equivalent circuit of Figure 4.2 and equations 4.4 to 4.7 we can write the chain matrix U of equation 4.10 as follows

$$U = \begin{bmatrix} A_i & B_i & (1-A_i)N_i & 0 \\ C_i & D_i & -C_i N_i & 0 \\ 0 & 0 & 1 & 0 \\ -C_i N_i & (1-D_i)N_i & (N_i^2) \left(\frac{Y_i}{2} + C_i \right) & 1 \end{bmatrix} \dots (4.11)$$

where

$$A_i = \cos \vartheta_i \cos \psi_{oi} - \sin \vartheta_i (q b + c/q) \dots (4.12)$$

$$B_i = j\zeta [\cos \vartheta_i \sin \psi_{oi} + \sin \vartheta_i (q a - d/q) \dots (4.13)$$

$$C_i = j(1/\zeta) [\cos \vartheta_i \sin \psi_{oi} + \sin \vartheta_i (a/q - q d) \dots (4.14)$$

$$D_i = \cos \vartheta_i \cos \psi_{oi} - \sin \vartheta_i (q c + b/q) \dots (4.15)$$

$$a = \cos \psi_{+1} \cos \psi_{-1}$$

$$b = \cos \psi_{+1} \cos \psi_{-1}$$

$$c = \sin \psi_{+1} \cos \psi_{-1}$$

$$d = \sin \psi_{+1} \sin \psi_{-1}$$

$$Y_i = j \omega C_{oi}$$

$$N_i = Q_i / Q_o = \sqrt{\frac{f_{io} C_{oi} Z_{om}}{f_o C_o Z_o}} \frac{K(1/\sqrt{2})}{K(r_i)} \quad \dots (4.16)$$

$$r_i = \sin(-\pi/2 \quad l_{mi} / l_i) \quad \dots (4.17)$$

$$(f_{io})^{-1} \cong \left(\frac{l_{mi}}{v_m} + \frac{l_i - l_{mi}}{v_g} \right)$$

$$\phi_o = k \sqrt{\frac{2 f_o C_o Z_o}{1 - k^2}} \quad \dots (4.18)$$

$$\zeta = Z_{og} / \phi_o^2 \quad \dots (4.19)$$

k is Electromechanical coupling coefficient,

$K(x)$ is complete elliptical integral of the first kind.

Equation 4.11 is the chain matrix representation of the basic modeling unit of this approach.

4.4 MODELING OF TRANSDUCER AND FILTER :

The chain matrix representation for a full transducer of uniform overlap electrodes can be obtained by connecting the

four-port networks in cascade , that is multiplying such chain matrices one after another as shown in Figure 4.4. Also different types of periodic sections can be built up by cascading the required number of these basic-unit networks and by cascading these sections different types of transducers can be modeled.

Several kinds of transmission characteristics can be analyzed by giving suitable mechanical and electrical terminal conditions to the network. In the case of two-transducer type filter each backside of the transducers is joined to infinite space. when the characteristic impedance Z_{og} is connected to the back side terminals of the transducers and the one side electrode is open, the network is simplified into two-port network as shown in figure 4.5.

If the electrodes are formed periodically with equal pitch (i.e Normal BIDT) the chain matrix of this equivalent two-port network is given by

$$\begin{bmatrix} E \\ I \end{bmatrix} = \begin{bmatrix} A_t & \zeta B_t \\ C_t / \zeta & D_t \end{bmatrix} \begin{bmatrix} F_n \\ U_n \end{bmatrix} \quad \dots (4.20)$$

where A_t , B_t , C_t and D_t are undimensional constants which are dependent on N , k and f but are not dependent on the clamped capacitance C_o [41].

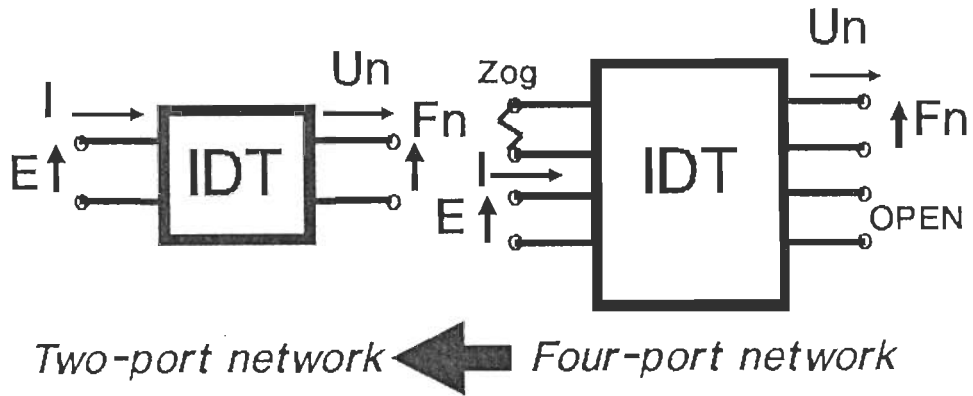


Fig. 4.5 By terminating one acoustic port by free space characteristic impedance the four-port network representation may be reduced to Two Port Network representation.

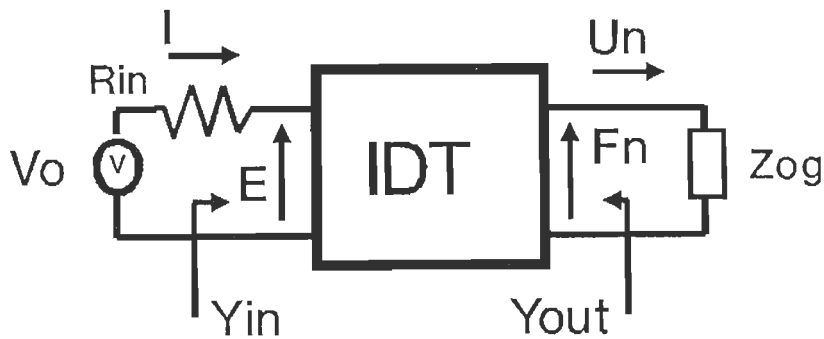


Fig. 4.6 Model for calculating the performance of single transducer.

The performance of the transducer can be calculated when the acoustic power from the transducer radiates into the infinite medium with the characteristic impedance Z_{og} as represented in Figure 4.6. Input and output admittances are as indicated.

Whereas in the usual case of two-transducer filter where one transducer acts as a transmitter and the other as a receiver and both are connected by an assumed uniform transmission line with a characteristic impedance Z_{oT} , the representation can be as in Figure 4.7. R_{in} is the inner resistance of the source and R_l is the load resistance. The chain matrix representation of the whole filter is given by the product of all the chain matrices representing all parts as follows

$$\begin{bmatrix} T_{11} & \zeta T_{12} \\ T_{21}/\zeta & T_{22} \end{bmatrix} = \begin{bmatrix} A_{t1} & \zeta B_{t1} \\ C_{t1}/\zeta & D_{t1} \end{bmatrix} \begin{bmatrix} \cosh \gamma l & Z_{oT} \sinh \gamma l \\ \sinh \gamma l / Z_{oT} & \cosh \gamma l \end{bmatrix} \begin{bmatrix} D_{t2} & \zeta B_{t2} \\ C_{t2}/\zeta & A_{t2} \end{bmatrix} \dots (4.21)$$

where $Z_{oT} = \zeta$ in case of loss less transmission,

$$\gamma = j\beta = \omega / v_g$$

The total insertion loss of the filter can be given by

$$I.L. = \left| \frac{R_l T_{11} + \zeta T_{12} + R_i R_l \zeta^{-1} T_{21} + R_i T_{22}}{2 \sqrt{R_i R_l}} \right| \dots (4.22)$$

$$\text{Insertion loss } I.L. = 20 \log (I.L.) \dots (4.23)$$

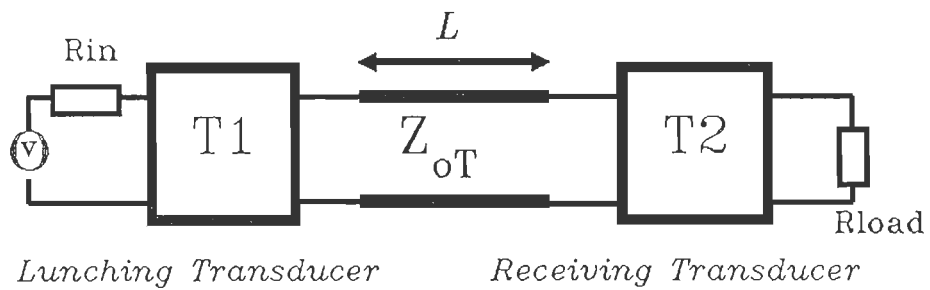


Fig. 4.7 Model for calculating the performance of a two transducers filter.

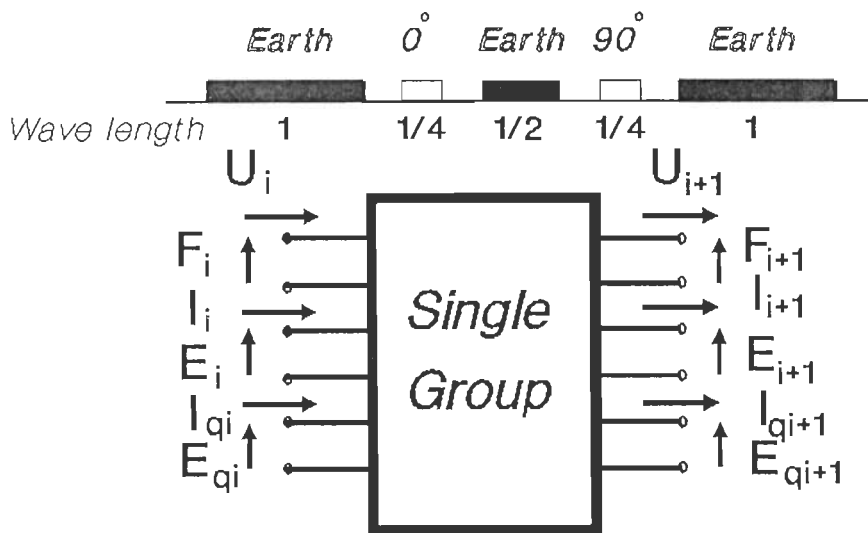


Fig. 4.8 Six-port single group GUDT representation.

4.5 MODELING OF UNIDIRECTIONAL TRANSDUCERS :

As described earlier it is possible to cascade the basic modeling unit according to requirements to construct any type of sections which can be used later to construct different types of transducers in the same way i.e. by cascading sections. In the next subsections two types of unidirectional transducers (namely Group type and Three Phase type unidirectional transducers) are modeled using this approach.

4.5.1. GROUP TYPE UNIDIRECTIONAL TRANSDUCERS :

A single group of a group type transducer can be represented by the six-port network shown in Figure 4.8. Two (input and output) ports are added for the 90° phase shifted section. This basic group can be cascaded several times up to the total number of groups of the transducer to construct the full GUDT transducer.

The three types of Group unidirectional transducers (Normal, Modified and New-type GUDTs shown in Figure 4.9) can be modeled in

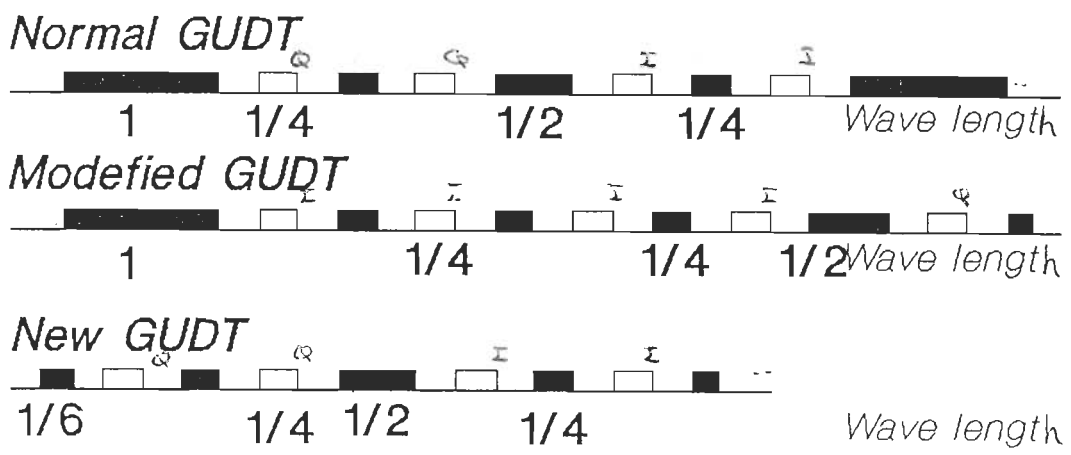


Fig. 4.9 Differences between the three types of **GUDTs**.
 Note that the figure is not necessarily showing a full group nor the beginning of the group.

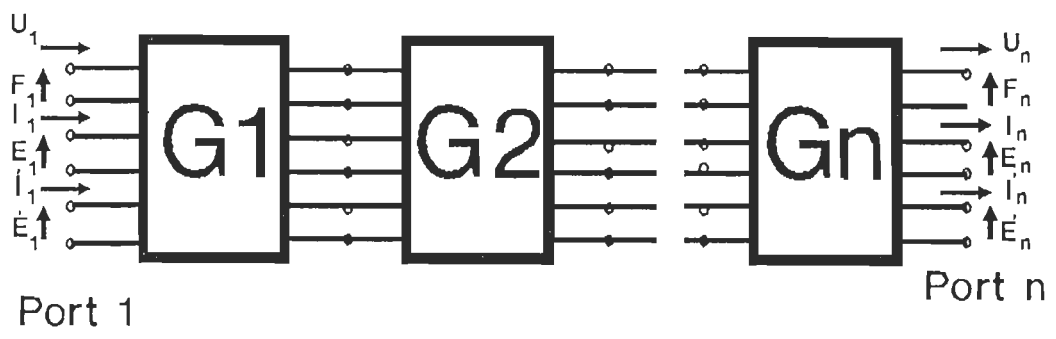


Fig. 4.10 Cascading **GUDT** groups to perform the full transducer model.

the same way by starting cascading the basic-unit in a proper way to perform a single group of the type intended to be modeled, taking into consideration the different earthed metalized portions, and proceed by cascading this single group number of times to model the transducer of full required number of groups as in Figure 4.10.

The six-port network representation of a group type transducer may be expressed by a 6x6 chain matrix

$$\begin{bmatrix} F_i \\ U_i \\ E_{0i} \\ I_{0i} \\ E_{90i} \\ I_{90i} \end{bmatrix} = \begin{bmatrix} G_{11} & G_{12} & G_{13} & G_{14} & G_{15} & G_{16} \\ G_{21} & G_{22} & G_{23} & G_{24} & G_{25} & G_{26} \\ G_{31} & G_{32} & G_{33} & G_{34} & G_{35} & G_{36} \\ G_{41} & G_{42} & G_{43} & G_{44} & G_{45} & G_{46} \\ G_{51} & G_{52} & G_{53} & G_{54} & G_{55} & G_{56} \\ G_{61} & G_{62} & G_{63} & G_{64} & G_{65} & G_{66} \end{bmatrix} \begin{bmatrix} F_{i+1} \\ U_{i+1} \\ E_{0i+1} \\ I_{0i+1} \\ E_{90i+1} \\ I_{90i+1} \end{bmatrix} \quad \dots (4.24)$$

where E_0 , I_0 , E_{90} and I_{90} are electric potential and current for the 0° and 90° sections, respectively.

According to the type of operation required, whether forward operated GUDT or backward operated GUDT, the acoustic ports may be terminated by the free space characteristic impedance Z_{og} as shown in Figure 4.11.

This will reduce equation 4.24 into a 4x4 chain matrix in a

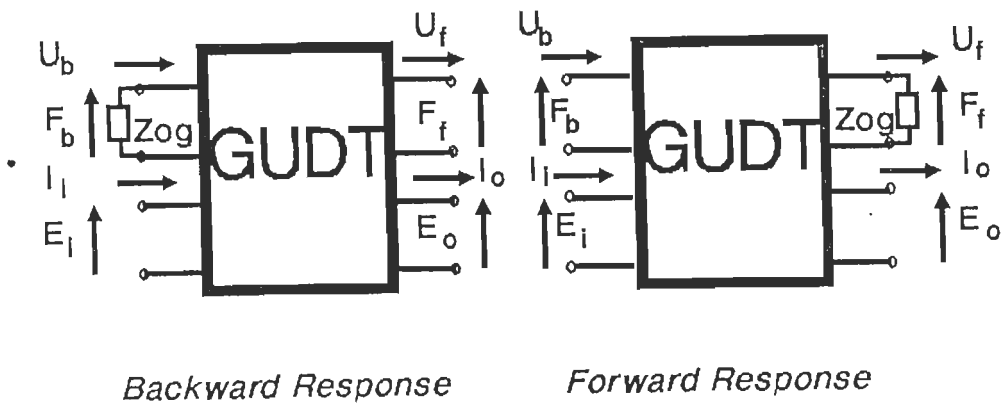


Fig. 4.11 Model for Forward and Backward performances of GUDT.

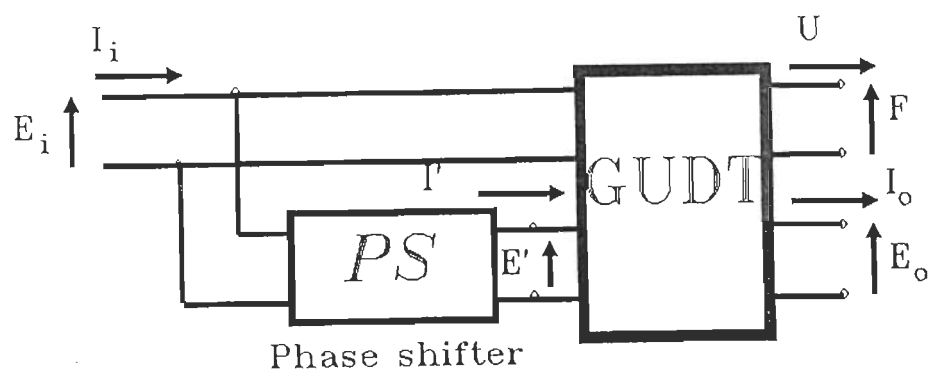


Fig. 4.12 Simplifying GUDT network representation by including The 90 degrees phase shifter to eliminate phase shifted signal electric port.

similar way to that described in previous section.

$$\begin{bmatrix} E_o \\ I_o \\ E_{90} \\ I_{90} \end{bmatrix} = \begin{bmatrix} F_{11} & F_{12} & F_{13} & F_{14} \\ F_{21} & F_{22} & F_{23} & F_{24} \\ F_{31} & F_{32} & F_{33} & F_{34} \\ F_{41} & F_{42} & F_{43} & F_{44} \end{bmatrix} \begin{bmatrix} F_i \\ U_i \\ E_{90i+1} \\ I_{90i+1} \end{bmatrix} \quad \dots (4.25)$$

E_{90} and I_{90} can be eliminated if we introduce to the network a proper phase shifter as in Figure 4.12. Equation (4.25) will be reduced to

$$\begin{bmatrix} E \\ I \end{bmatrix} = \begin{bmatrix} T_{11} & T_{12} \\ T_{21} & T_{22} \end{bmatrix} \begin{bmatrix} F \\ U \end{bmatrix} \quad \dots (4.26)$$

The values of the different elements of equations (4.24) to (4.26) depend upon the type of operation whether forward or backward.

Different types of phase shifters can be used while modeling the different types of group unidirectional transducers by introducing the chain matrix of the selected type of phase shifter in the computation of the transducer model. The phase shifter used in all results presented in this dissertation corresponding to GUDTs is the one shown in Figure 4.13, where

R is the radiation resistance of each section.

R_{in} is the inner source resistance,

C_D is inter electrode capacitance,

C_f is stray capacitance,

L is coil inductance and

r is coil resistance.

The chain matrix of the phase shifter used is

$$\begin{bmatrix} E_1 \\ I_1 \end{bmatrix} = \begin{bmatrix} (1-\omega L\omega C)+jr\omega C & r+j\omega C \\ (-r\omega L\omega C)+j[\omega C(2-\omega L\omega C)] & (1-\omega L\omega C)+jr\omega C \end{bmatrix} \begin{bmatrix} E_2 \\ I_2 \end{bmatrix} \dots (4.27)$$

where

$$C = C_D + C_f$$

$$\omega = 2\pi f$$

4.5.2 THREE PHASE
UNIDIRECTIONAL TRANSDUCER :

In case of three-phase unidirectional transducer the single periodic section, which consists of three fingers derived by

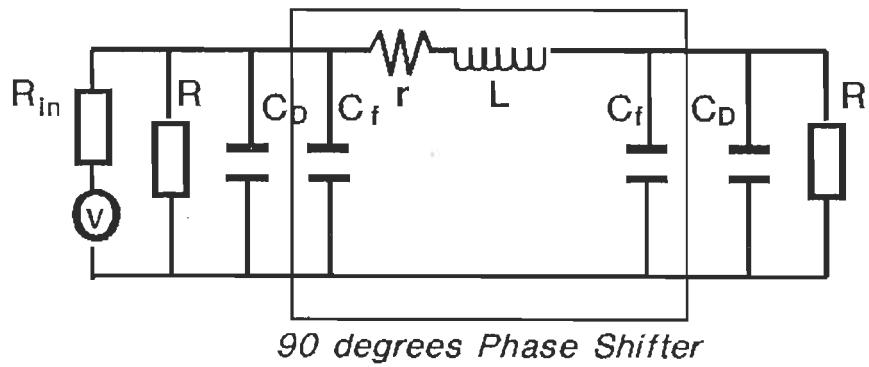


Fig. 4.13 Phase shifter type used in GUDT.

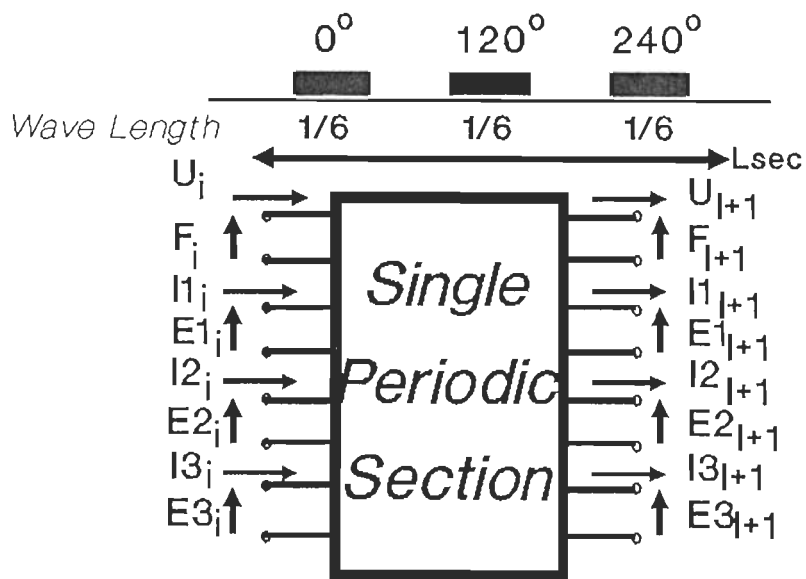


Fig. 4.14 Eight-port representation of a single periodic section of TPUDT.

voltages of three different phases of 120° phase shifts each, can be represented by the eight-port network of Figure 4.14 with two acoustic ports for acoustical input and output and three electrical input and three electrical output ports for the three phases.

This section may be repeated several times depending on the number of periodic sections in the full transducer to be modeled. The sections are to be cascaded in the same way as in the case of bidirectional transducer and group type unidirectional transducer, as shown in Figure 4.14, to get the final eight-port network representation of the full TPUDT transducer.

The TPUDT transducer may be expressed by 8x8 chain matrix as given below

$$\begin{bmatrix} F_i \\ U_i \\ E_{1i} \\ I_{1i} \\ E_{2i} \\ I_{2i} \\ E_{3i} \\ I_{3i} \end{bmatrix} = \begin{bmatrix} P_{11} & P_{12} & P_{13} & P_{14} & P_{15} & P_{16} & P_{17} & P_{18} \\ P_{21} & P_{22} & P_{23} & P_{24} & P_{25} & P_{26} & P_{27} & P_{28} \\ P_{31} & P_{32} & P_{33} & P_{34} & P_{35} & P_{36} & P_{37} & P_{38} \\ P_{41} & P_{42} & P_{43} & P_{44} & P_{45} & P_{46} & P_{47} & P_{48} \\ P_{51} & P_{52} & P_{53} & P_{54} & P_{55} & P_{56} & P_{57} & P_{58} \\ P_{61} & P_{62} & P_{63} & P_{64} & P_{65} & P_{66} & P_{67} & P_{68} \\ P_{71} & P_{72} & P_{73} & P_{74} & P_{75} & P_{76} & P_{77} & P_{78} \\ P_{81} & P_{82} & P_{83} & P_{84} & P_{85} & P_{86} & P_{87} & P_{88} \end{bmatrix} \begin{bmatrix} F_{i+1} \\ U_{i+1} \\ E_{1i+1} \\ I_{1i+1} \\ E_{2i+1} \\ I_{2i+1} \\ E_{3i+1} \\ I_{3i+1} \end{bmatrix} \quad \dots (4.28)$$

where E_1, E_2, E_3 and I_1, I_2, I_3 are potentials and currents of the three phases.

Similar to the procedure followed in the previous section, according to the type of operation of the transducer, whether forward operated TPUDT or backward operated TPUDT, the acoustic ports may be terminated by the free space characteristic impedance Z_{og} . A suitable phase shifter also can be introduced to the electric input ports. The eight-port network representing the transducer may be simplified to a two-port network representation as shown in Figure 4.15, similar to the two-port representation of BIDT and GUDT discussed earlier.

The chain matrix of the two-port network representation of TPUDT may be written as

$$\begin{bmatrix} E \\ I \end{bmatrix} = \begin{bmatrix} PT_{11} & PT_{12} \\ PT_{21} & PT_{22} \end{bmatrix} \begin{bmatrix} F \\ U \end{bmatrix} \quad \dots (4.29)$$

The values of different elements in equation (4.29) depend upon the type of operation of the transducer whether forward or backward.

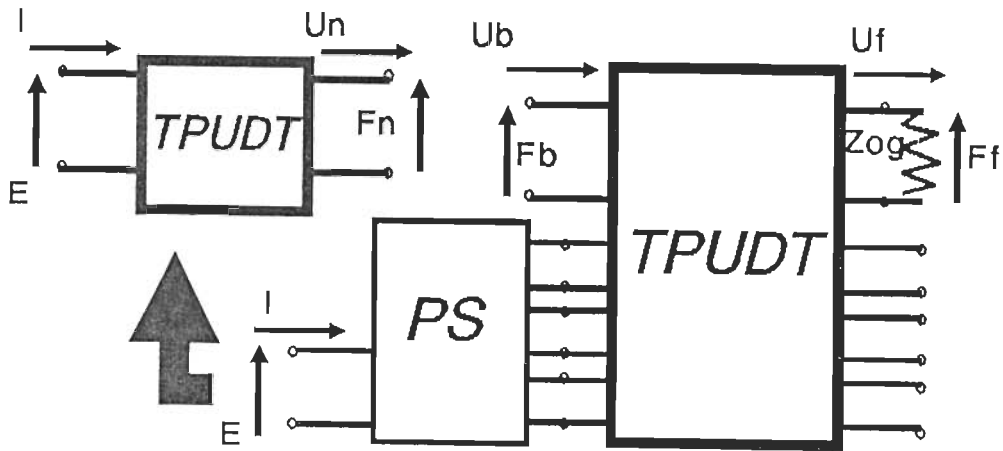


Fig. 4.15 Simplifying TPUDT representation into two port network by including the phase shifter and terminating acoustic port by Z_{og} .

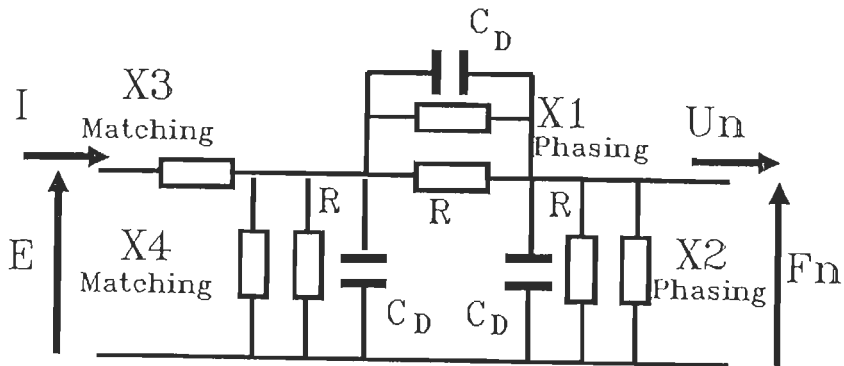


Fig 4.16 Type of Phase shifting and Matching of TPUDT.

Different types of phase shifters can be used while modeling three phase unidirectional transducers. The only requirement is to write the chain matrix representing the phase shifter and use it in the computation of transducer model. The phase shifter and the matching network used in all TPUDTs that its performances are reported in this dissertation are as shown in Figure 4.16 with the following chain matrices representing them;

$$\begin{bmatrix} E_1 \\ I_1 \end{bmatrix} = \begin{bmatrix} 1 - (1/j\omega^2 LC) & -j/\omega C \\ -j/\omega L & 1 \end{bmatrix} \begin{bmatrix} E_2 \\ I_2 \end{bmatrix} \quad \dots (4.30)$$

For the phase shifter , and

$$\begin{bmatrix} E_1 \\ I_1 \end{bmatrix} = \begin{bmatrix} 1 & j\omega L \\ j\omega C & 1 - \omega^2 LC \end{bmatrix} \begin{bmatrix} E_2 \\ I_2 \end{bmatrix} \quad \dots (4.31)$$

for the matching network.

4.6 COMPUTATION :

For the purpose of modelling and simulating different types of SAW devices with the aid of CHAIN MATRIX approach so that the approximate actual performances of different types of transducers

and filters could be found out before fabrication , a software package has been developed using FORTRAN 77 programming language. The package is found to be able to simulate successfully different types of bidirectional transducers as well as different types of unidirectional transducers. The three types of group unidirectional transducers namely; Normal, Modified and New type GUDTs were included in the package and the differences in performances using different number of active fingers per group and groups can be known by running the software. Simulation of three phase unidirectional transducers with different periodic sections were also included in the package.

In the following sections we present the performances of some of the transducers and filters that have been modeled and simulated with the aid of chain matrix approach by using the said package. Before proceeding into these results let us have a look on Figure 4.17 which clarify some of the notations used later on in the analysis of filter and transducers. The figure shows a typical unidirectional transducer forward frequency response with zero insertion loss at center frequency and close to it. The transducer bandwidth (BW) is taken to be the bandwidth measured at 3dB line. Rise bandwidth (RB) and fall bandwidth (FB) are shown in figure with their relation to first left side-lobe level (LSL) and first right side-lobe level (RSL). Theoretically transducer response is symmetrical therefore rise bandwidth and fall bandwidth are equal and naturally the first side-lobe level on

Fig. 4.17 Typical transducer response.

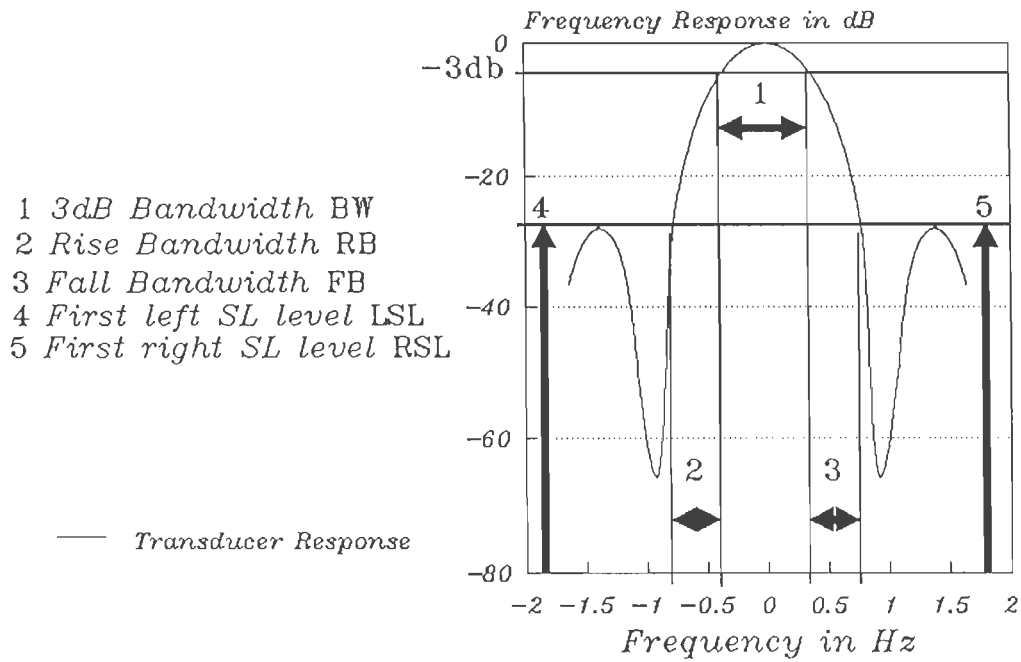
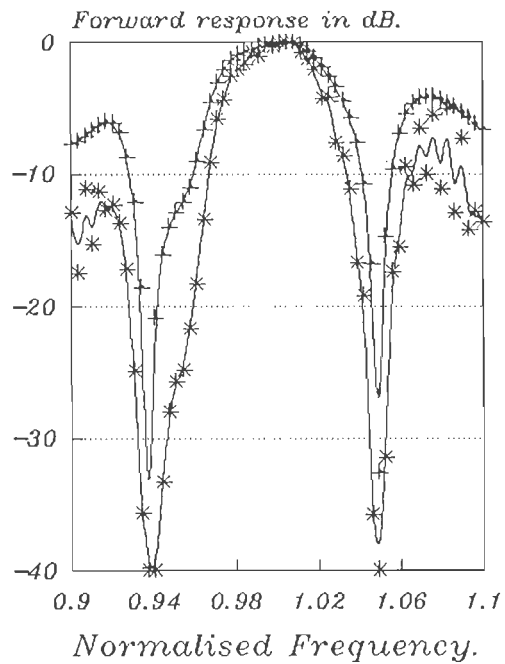


Fig. 4.18 Forward frequency responses of a pair of NGUDT transducers and a filter of both transducers. Number of active fingers and groups are indicated below. Aperture is $7.3798E-4$ m.

Frequency Responses:
 — GUDT N-8-2
 + GUDT N-8-2
 * FILTER



both sides are same. Yet there is some deviation from this practically as will be seen from the results of simulated transducers.

4.7 PERFORMANCES OF GROUP TYPE UNIDIRECTIONAL TRANSDUCERS:

From many group unidirectional transducers that have been modeled and simulated we present in Table {4.1}, {4.2} and {4.3} some of the results related to bandwidths and side-lobes levels of some of these transducers. Table {4.1} lists the results obtained from three Normal-type GUDT transducers with number of active fingers per group and groups as indicated in Table.

It is obvious that the bandwidth generally decreases with the increase in active fingers - groups product number. It is also seen that with the same number of fingers - groups product the bandwidth reduces with the increase in the number of groups (number of fingers is decreased by the same factor group number is increased).

A similar conclusion can be obtained from Table {4.2} where a number of Modified type GUDT transducers were presented. By comparing the two types of transducers (Normal and Modified), it

Table {4.1}

*Computational results of some Normal type Group
UniDirectional Transducers.*

Transducer type	Aperture in meter	RB per cent	3dB BW per cent	FB per cent	LSL in dB	RSL in dB
N-8-2	7.3798E-4	0.402	5.8099	0.279	6.	4.04
N-4-4	7.3798E-4	1.2178	5.419	1.329	10.48	7.16
N-4-8	4.8449E-4	0.268	2.5139	0.335	7.24	8.

Table {4.2}

*Computational results of some Modified type Group
UniDirectional Transducers.*

Transducer type	Aperture in meter	RB per cent	3dB BW per cent	FB per cent	LSL in dB	RSL in dB
M-8-2	7.3798E-4	0.9161	7.195	2.513	6.4	9.2
M-4-4	7.3798E-4	0.558	6.469	0.5027	5.6	9.2
M-4-6	3.2799E-4	0.4469	4.67	0.469	6.08	6.2

Table {4.3}

*Computational results of some New type Group
UniDirectional Transducers.*

Transducer type	Aperture in meter	RB per cent	3dB BW per cent	FB per cent	LSL in dB	RSL in dB
NU-8-2	7.3798E-4	0.8268	6.2	0.469	6.88	4.2
NU-2-8	7.3798E-4	3.1396	5.9775	0.916	14.2	9.24
NU-8-3	5.5977E-4	0.782	4.525	0.391	8.	4.72
NU-8-4	4.8449E-4	0.4469	3.452	0.648	7.52	6.8

Table {4.4}

*Computational results of some Three Phase
UniDirectional Transducers.*

Transducer type	Aperture in meter	RB per cent	3dB BW per cent	FB per cent	LSL in dB	RSL in dB
T-13	7.3798E-4	1.6312	10.1897	1.	10.	6.68
T-15	5.5977E-4	1.307	7.92	0.67	9.	5.69
T-20	3.1487E-4	0.8156	6.292	0.5698	8.36	6.2

is clear that the later is having a larger bandwidth and in most of the cases a less rise and fall bandwidths but with a little bit higher side-lobe levels.

From the Table one can see also that although the rise and fall bandwidths decreases with the increase of fingers - groups product number, for the same fingers - groups product number it seems that these bandwidths decreases with the increase of number of groups. The relation may not be linear as it can be concluded from the fall bandwidth values.

New type GUDT transducer performance in terms of bandwidths and side-lobe levels can be considered as in between Normal and Modified types GUDTs as Table {4.3} tells us. The conclusions concerning relations between the three bandwidths and number of fingers - groups product and number of groups are the same for New-type GUDT as with the other types.

4.8 PERFORMANCE OF THREE PHASE UNIDIRECTIONAL TRANSDUCERS :
--

In Table {4.4} three TPUDT transducers with 13, 15 and 20 periodic sections are presented. It is clear from figures that rise bandwidth, 3dB bandwidth and fall bandwidth are decreasing

with the increase of number of periodic sections. First left side-lobe level is increasing as the number of periodic sections increases, but the right side-lobe level does not seem to be following the same.

4.9 FILTERS OF PAIRS OF IDENTICAL TRANSDUCERS :

We present here two filters listed in Table {4.5}. Identical pair of Normal type GUDT transducers with 8-active fingers per group and 2-groups have been simulated and a two-transducer type filter has been built from. Performances of filter and transducers are given in Figure 5-18 to Figure 5-20 and some of the results are summerised in table {4.5}. Another filter has been built from two identical simulated TPUDT transducers with 20 periodic sections. Some of the filter characteristics are summerised in the said Table and the performances of transducer and filter are shown in Figure 4.25 to Figure 4.27.

Figure 4.18 shows forward frequency responses of the NGUDT filter and transducer. From the backward frequency response shown in Figure 4.19 and the relative directivity shown in Figure 4.20 of both transducer and filter, it is clear that transducer and

Table {4.5}

*Computational results of Normal type Group
UniDirectional Transducers filter and Three
Phase unidirectional transducers filter with
identical transducers in each filter.*

Transdu- cer type	Aperture in meter	RB per cent	3dB BW per cent	FB per cent	LSL in dB	RSL in dB
N-8-2	7.3798E-4	1.1173	5.273	0.983	12.12	7.6
T-20	3.1487E-4	1.564	5.296	1.128	16.6	11.92

Fig. 4.19 Backward frequency responses of a pair of NGUDT transducers and a filter of both transducers. Number of active fingers and groups are indicated below. Aperture is $7.3798E-4$ m.

Frequency Responses:
 — GUDT N-8-2
 + GUDT N-8-2
 * Filter

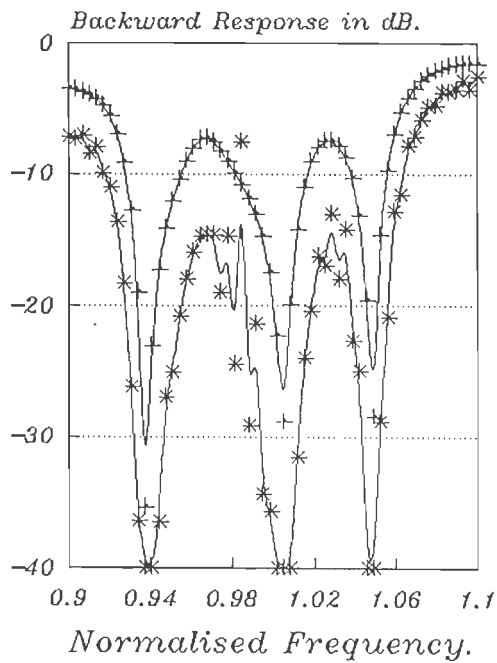


Fig. 4.20 Relative directivities of a pair of NGUDT transducers and a filter of both transducers. Number of active fingers and groups are indicated below. Aperture is $3.798E-4$ m.

Relative Directivities:
 — GUDT N-8-2
 + GUDT N-8-2
 * Filter

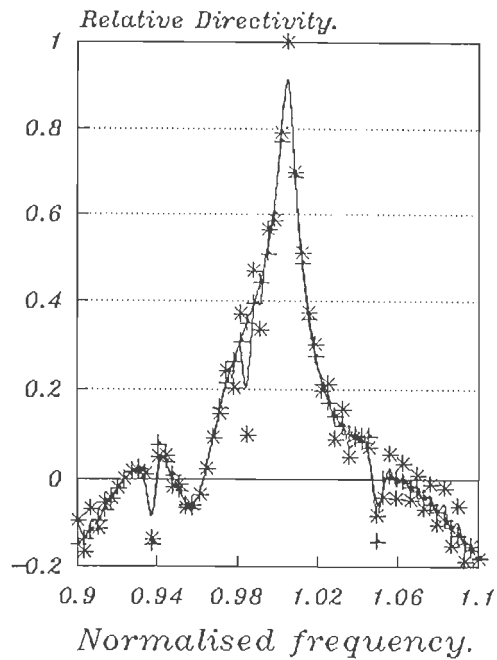


Fig. 4.21 Input admittances of a pair of NGUDT transducers and a filter of both transducers. Number of active fingers and groups are indicated below. Aperture is $7.3798E-4$ m.

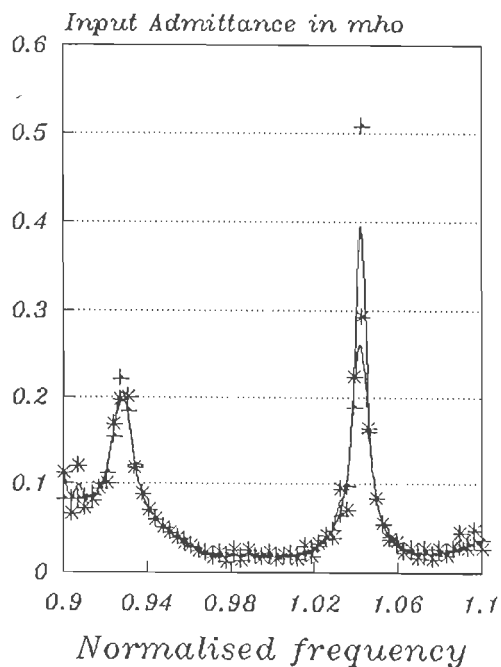
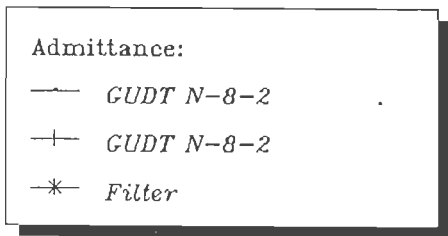


Fig. 4.22 Change of phase of input admittances of a pair of NGUDT transducers and a filter of both transducers. Number of active fingers and groups are given below. Aperture is $7.3798E-4$ m.

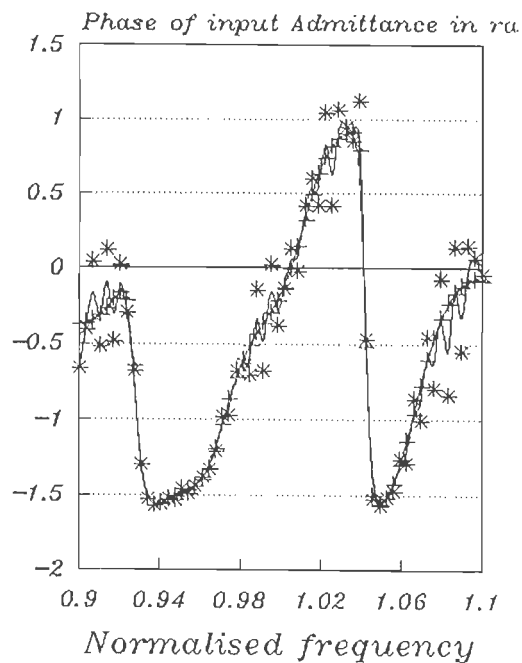
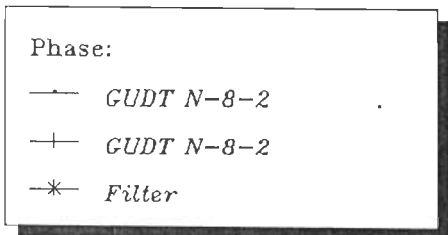


Fig. 4.23 Output admittances of a pair of NGUDT transducers and a filter of both transducers. Number of active fingers and groups are indicated below. Aperture is $7.3798E-4$ m.

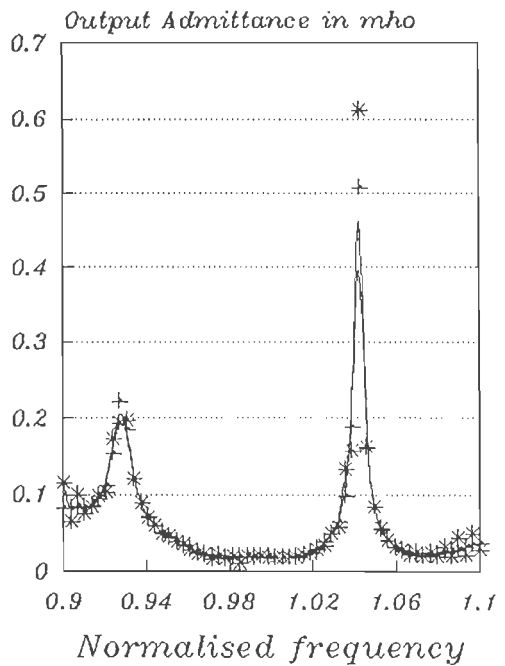
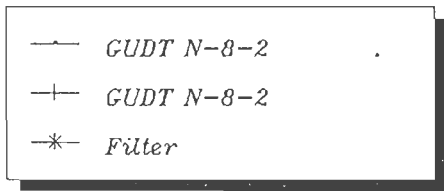


Fig. 4.24 Change of phase of output admittances of a pair of NGUDT transducers and a filter of both transducers. Number of active fingers and groups are indicated below. Aperture is $7.3798E-4$ m.

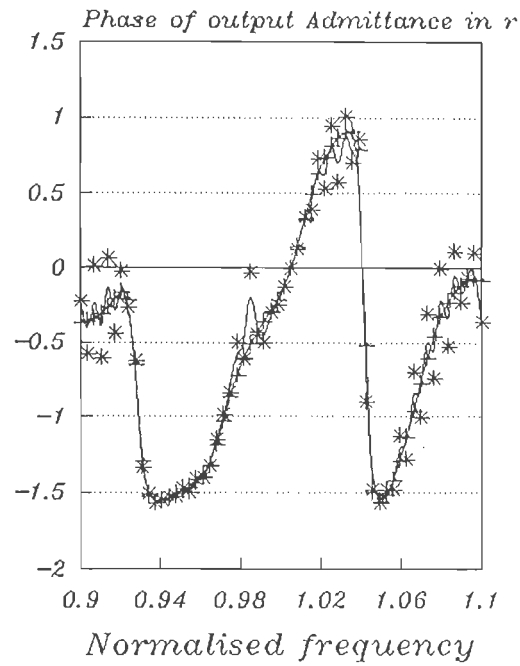
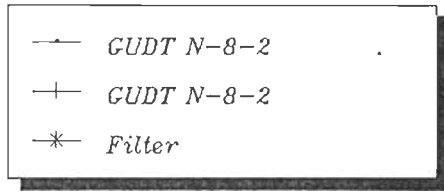


Fig. 4.25 Forward frequency responses of TPUDT-20 transducer and a filter of a pair of transducers of same type. Aperture is $3.1487E-4$ m

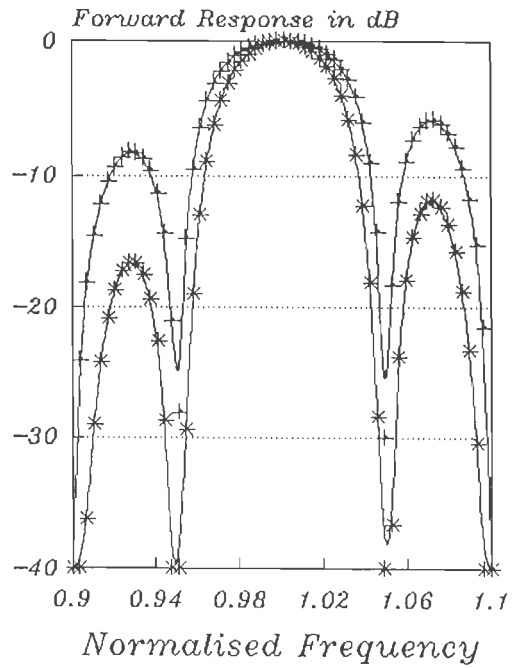
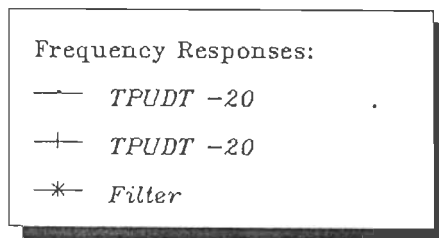
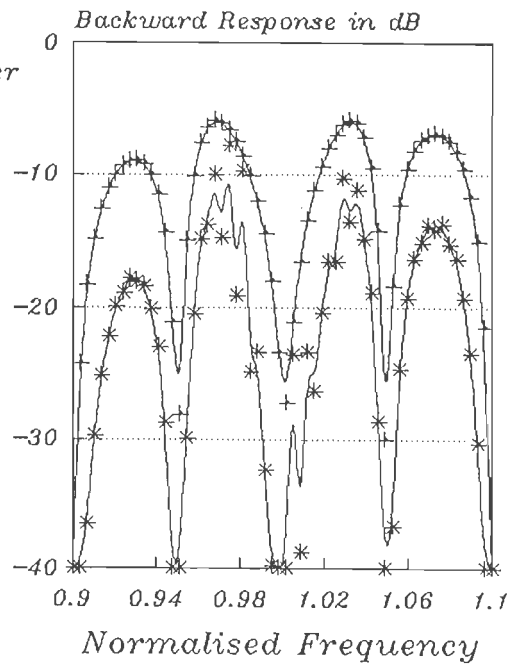
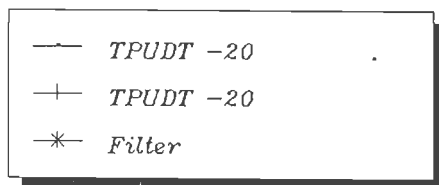


Fig. 4.26 Backward frequency responses of TPUDT-20 transducer and filter of a pair of same transducers. Aperture is $3.1487E-4$ m



filter have some bidirectional operating points. Also it can be seen that at some frequencies both transducer and filter are operating in reverse direction (negative directivity) giving certain frequency responses but with high insertion loss.

Figures 4.21 to 4.24 show the variation of input and output admittances, and input and output phases of both transducer and filter. It can be seen that in all figures the region approximately between 0.95 to 1.05 normalized frequency is containing the pass band, low admittance, phase linearity, proper directivity and low insertion loss.

Forward and backward frequency responses, directivities, input admittance, conductance and susceptance of TPUDI-20 transducer and filter are shown in Figures 4.25 to 4.30.

4.10 FILTERS OF COMBINATIONS OF GROUP UNIDIRECTIONAL TRANSDUCERS :

In order to get better filter performances in terms of bandwidth, insertion loss and lower side-lobes levels, filter of combinations of different types of group unidirectional transducers have been simulated to find out the extent of such improvement in filter performances. Four such types of filters

Fig. 4.27 Normalised directivities of TPUDT-20 transducer and filter of pair of same transducers. Aperture is $3.1487E-4$ m.

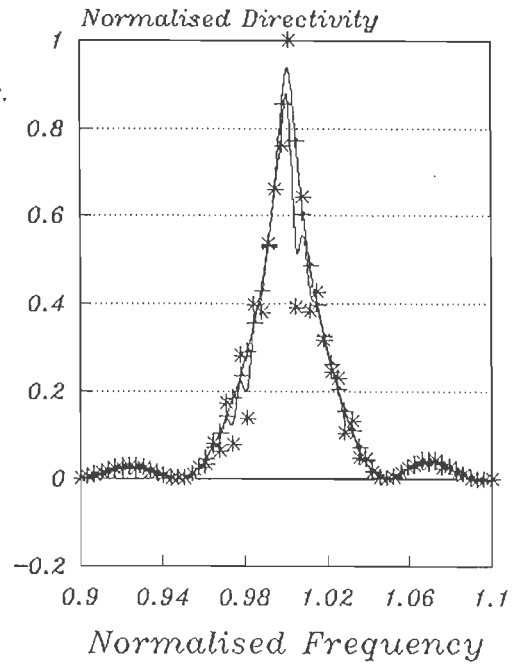
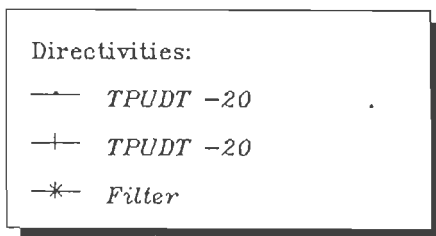


Fig. 4.28 Input conductances of TPUDT-20 transducer and filter of pair of same transducers. Aperture is $3.1487E-4$ m.

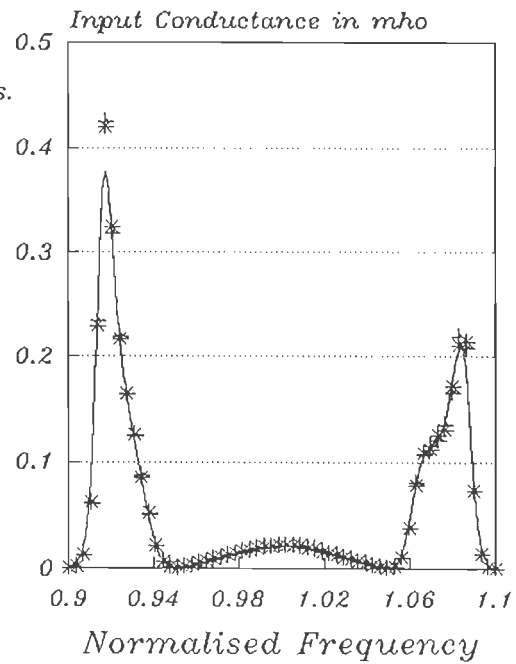
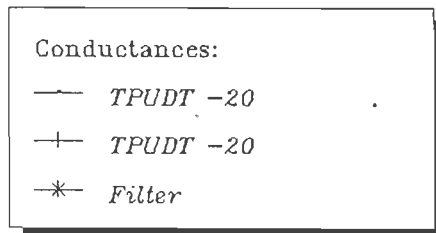


Fig. 4.29 Input susceptances of TPUDT-20 transducer and filter of pair of same transducers. Aperture is $3.1487E-4$ m.

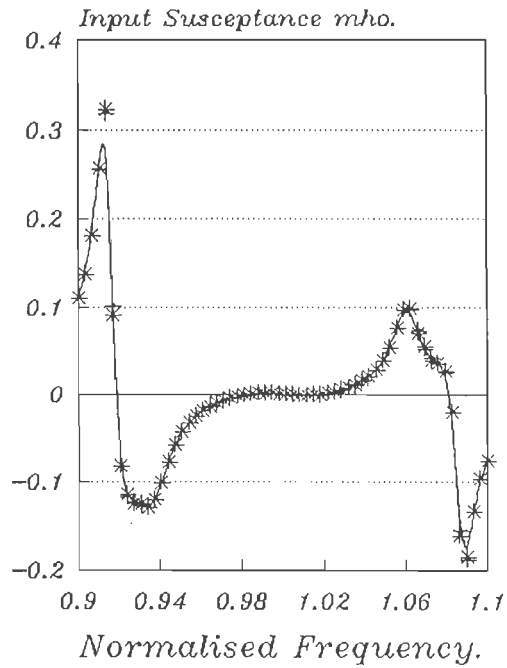
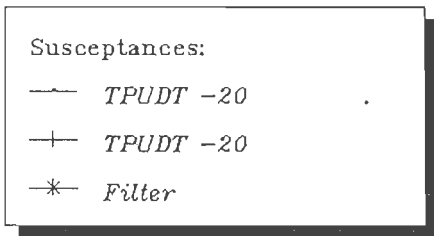


Fig. 4.30 Input admittances of TPUDT-20 transducer and filter of pair of same transducers. Aperture is $3.1487E-4$ m.

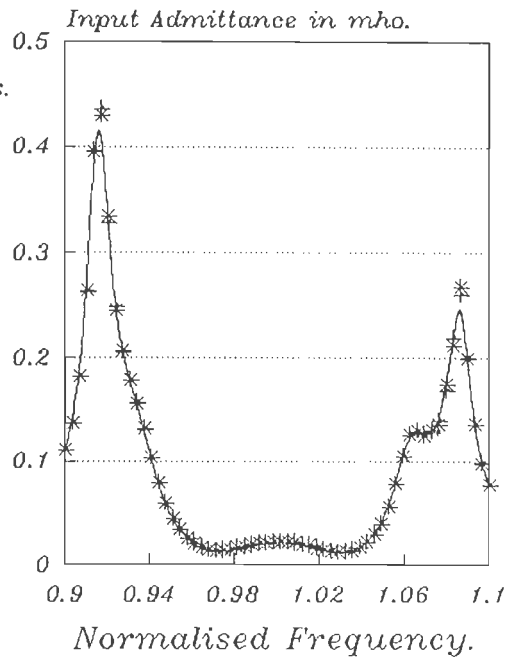
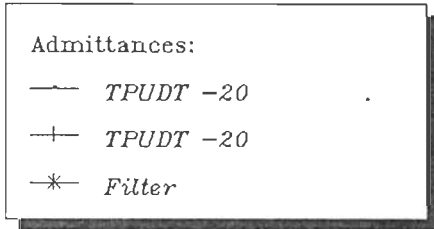


Table {4.6}

*Computational results of filters of combinations
of Group UniDirectional Transducers.
(Normal, Modified and New type GUDTs).*

Transducer type	Aperture in meter	RB per cent	3dB BW per cent	FB per cent	LSL in dB	RSL in dB
N-8-2	7.3798E-4	1.575	4.268	1.329	17.6	11.32
N-4-4						
M-4-4	7.3798E-4	1.407	5.35	1.698	12.44	14
M-8-2						
NU-8-4	4.8449E-4	0.670	2.346	1.0279	15.6	19.16
N-4-4						
NU-8-2	7.3798E-4	2.904	4.368	1.6647	21.2	13.68
NU-2-8						

with the corresponding computational results are listed in table {4.6} and the forward frequency responses of transducers and filters are shown in Figures 4.31 to 4.34. Two types of combinations have been used;

pair of same type of transducer with different number of active fingers per group and different number of groups (but same number of fingers - groups product) or

pair of different types of GUDTs with different number of active fingers per group and different number of groups (but same number of fingers - groups product to secure matching).

From computational results of table {4.6} and forward frequency responses of filters shown in Figures 4.31 to 4.34, good improvement in side-lobes suppression has been achieved. If we compare the performance of normal type GUDT filter of identical transducer pair of N-8-2 with the filter of same type transducers (ie. NGUDT) but with N-8-2 and N-4-4 number of fingers and groups we can see the difference in side-lobes levels with little sacrifice in the 3dB fractional bandwidth. A side-lobe suppression up to 21 dB has been achieved using New-type GUDT transducers of NU-2-8 and NU-8-2. In all cases an increase in the rise and fall bandwidths can be observed.

Fig.4.31 Forward frequency responses of NGUDT-4-4, NGUDT-8-2 and filter of both transducers. Aperture is $7.3789E-4$ m

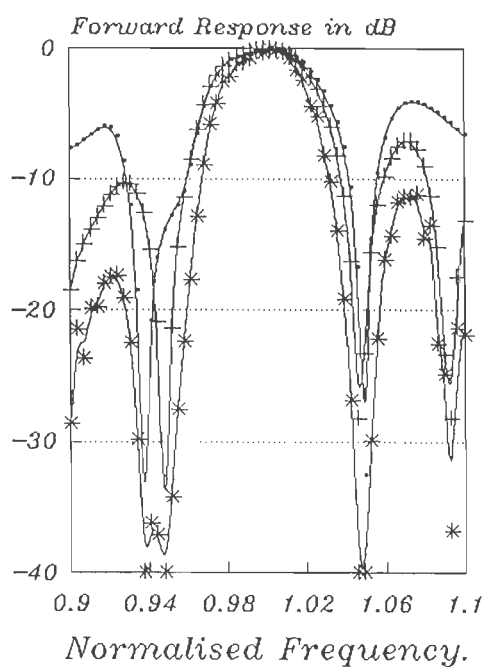
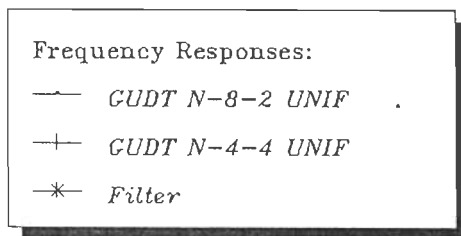


Fig. 4.32 Forward frequency responses of MGUDT-4-4, MGUDT-8-2 and filter of both transducers. Aperture is $7.3798E-4$ m

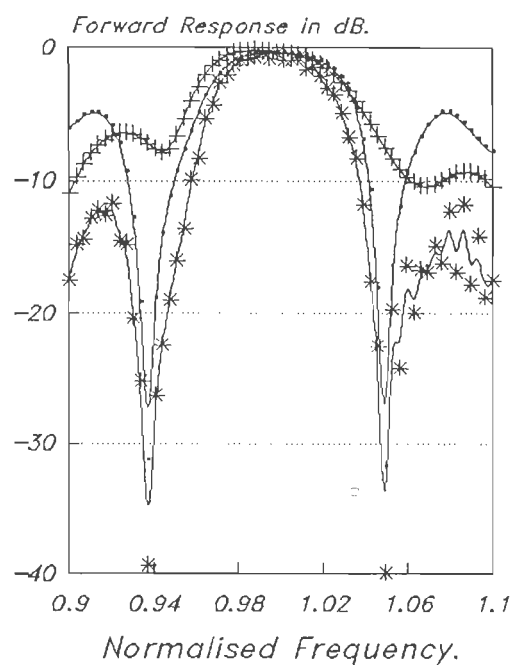
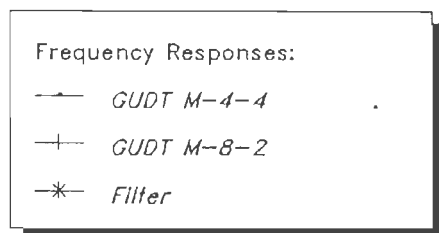


Fig. 4.33 Forward frequency responses of NUGUDT-8-4, NGUDT-4-8 and filter of both transducers. Aperture is $1.8449E-4$ m

Frequency Responses:
 — GUDT NU-8-4 UNIF
 + GUDT N-4-8 UNIF
 * Filter

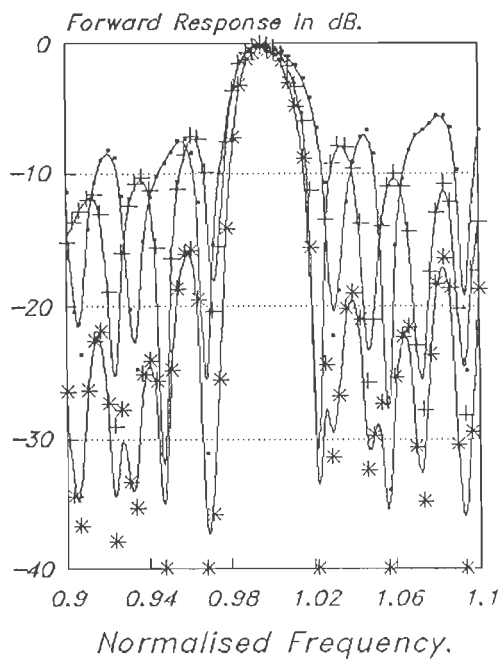
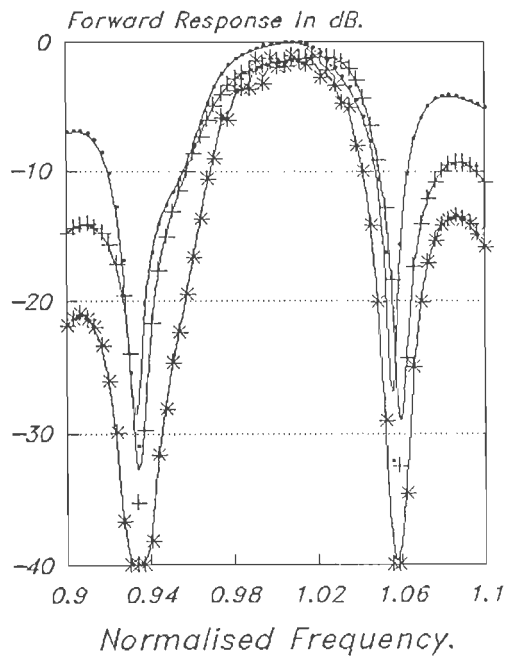


Fig. 4.34 Forward frequency responses of NUGUDT-8-2, NUGUDT-2-8 and filter of both transducers. Aperture is $7.3798E-4$ m

Frequency Responses:
 — GUDT NU-8-2
 + GUDT NU-2-8
 * Filter



From the plots of forward frequency responses of NUGUDT-8-4 and NGUDT-4-8 and filter of their combination shown in Figure 4.33 it can be seen how greatly side-lobe levels have been reduced due to the different frequency locations of side-lobes of the two transducers. A better selection of the combination can cause a great reduction in side-lobe levels due to the cancellation of side-lobes of each transducer by different frequency locations of side-lobes of the other transducer. That is why this much of level reduction and this much of distance from the main lobe is there in the first right side-lobe of filter shown in Figure.

4.11 FILTERS OF COMBINATIONS OF GUDTs AND TPUDTs :

For the same goal of achieving better filter performances, filters of combinations of group unidirectional transducers and three phase unidirectional transducers have been simulated. Different types of GUDT transducers with different number of fingers per group and different number of groups have been used, either in transmitting or receiving modes with TPUDT transducers with different number of periodic sections. The number of fingers - groups product of GUDT or number of periodic sections of TPUDT of one of the filter transducers (either the one in receiving or the one in transmitting modes) is to be calculated by the package to secure matching.

Some of these filters are listed in Table {4.7} with the corresponding computational results of rise, fall, 3dB bandwidths and side-lobe levels. Figures 4.35 to 4.37 represent forward, backward frequency responses and relative directivities of NGUDT-8-2 transducer, TPUDT-13 transducer and filter of both transducers. Figure 4.38 is a plot of forward frequency responses of TPUDT-15 transducer, NUGUDT-8-3 transducer and filter of both. Figure 4.39 shows forward frequency response of filter, simulated from a pair of MGUDT-4-6 transducer and TPUDT-20 transducer, and responses of both transducers.

From Table and Figures it can be seen that using such combinations high side-lobe suppression up to 26 dB has been achieved with a good 3dB fractional bandwidth. It can be seen also that rise and fall bandwidths are remarkably high.

The effect of using high bandwidth transducer with another lower bandwidth transducer, both with minimal insertion loss (unidirectional transducers) in constructing a filter on improving the performance of that filter is very much clear from the examples given here as well as the ones given in previous section. The filter 3db fractional bandwidth is usually very close to that of the narrower bandwidth transducer. If both the transducers are unidirectional then the insertion loss of the filter is zero (at f_0 and close to it) or negligible fraction. First left and right

Table {4.7}

*Computational results of filter of combinations
of Group and Three Phase UniDirectional Transducers*

Transducer type	Aperture in meter	RB per cent	3dB BW per cent	FB per cent	LSL in dB	RSL in dB
N-8-2 T-13	7.3798E-4	3.05	5.329	1.653	26.44	12
T-15 NU-8-3	5.5977E-4	0.96	4.3	1.25	15.4	14.84
M-4-6 T-20	3.2799E-4	1.508	4.234	1.284	20	19.32

Fig. 4.35 Forward frequency responses of NGUDT-8-2, TPUDT-13 and filter of both transducers. Aperture is $7.3798E-4$ m

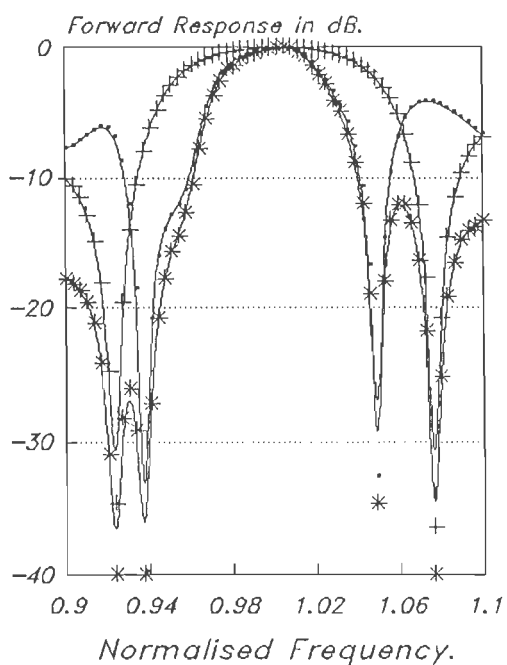
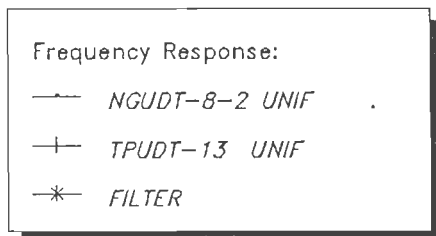


Fig. 4.36 Backward frequency responses of NGUDT-8-2, TPUDT-13 and filter of both transducers. Aperture is $7.3789E-4$ m.

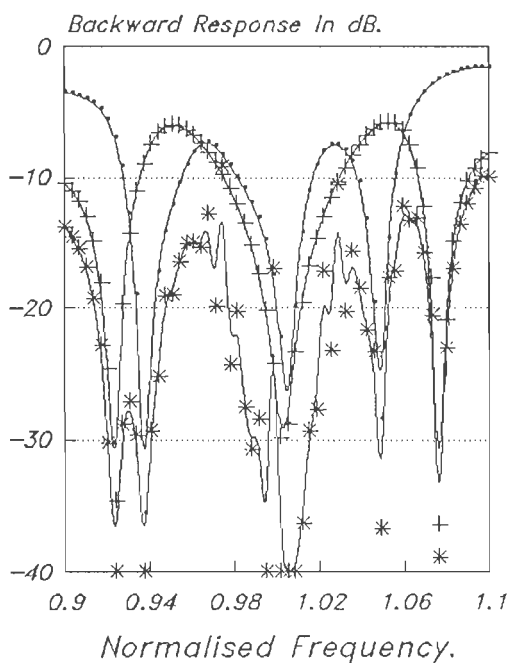
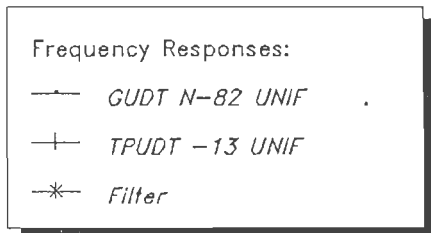


Fig. 4.37 Relative directivities of NGUDT-8-2, TPUDT-13 and filter of both transducers. Aperture is $7.3798E-4$ m.

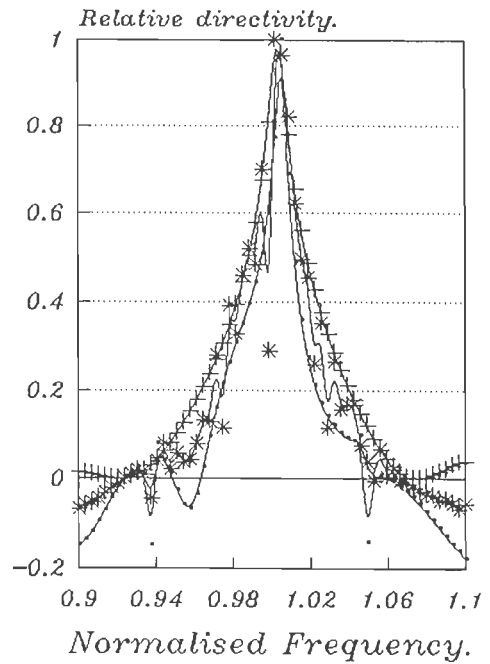
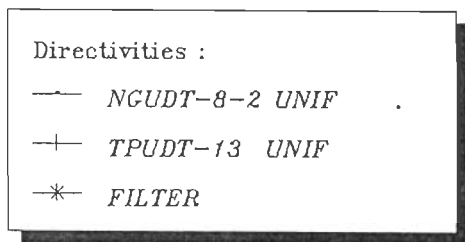


Fig. 4.38 Forward frequency responses of TPUDT-15, NUGUDT-8-3 and filter of both transducers. Aperture is $5.5977E-4$ m.

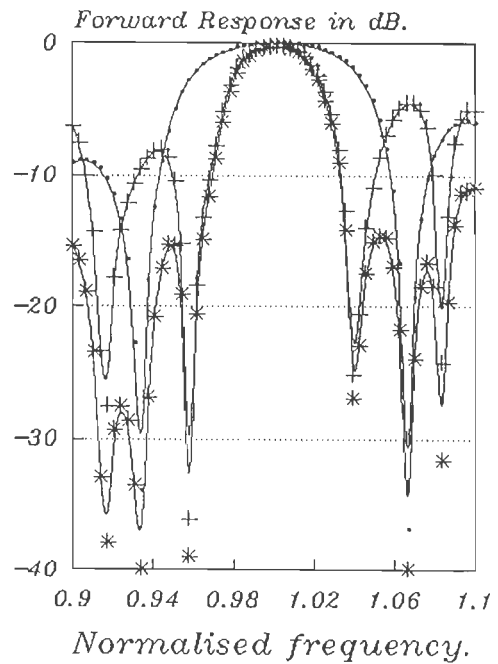
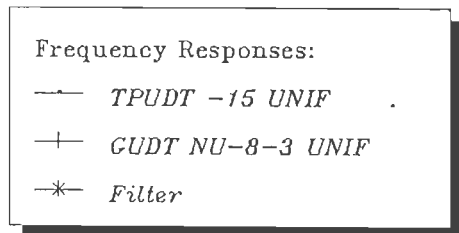
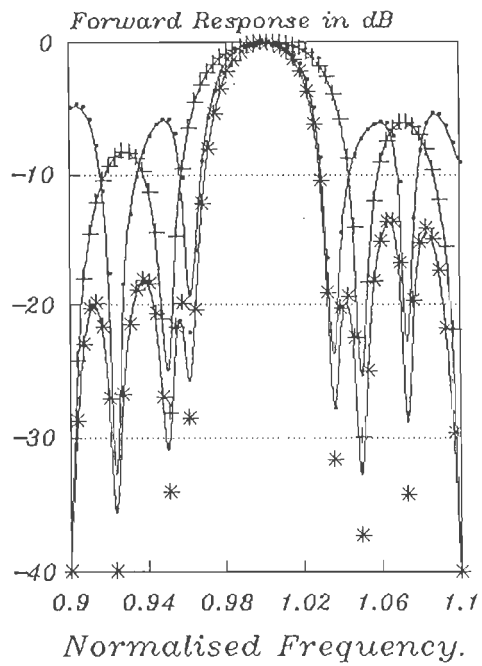


Fig. 4.39 Forward frequency responses of MGUDT-4-6, TPUDT-20 and filter of both transducers. Aperture is $3.2799E-4$ m

Frequency Responses:
 — GUDT M-4-6 UNIF
 + TPUDT -20 UNIF
 * Filter



side-lobes are usually very low (Suppressed) and it is possible to have negative or positive side-lobes roll off depending upon the selection of transducers combination.

4.12 CONCLUSION :

Due to the limited capabilities of SCAT MAT and TRANS MAT models, and for the sake of having a model that is able to describe the performances of large variety of SAW signal processing devices, CHAIN MAT approach has been developed and presented in this chapter. The basic modeling unit of this approach has been represented by a four-port network and a 4x4 chain matrix. With the use of this basic-unit the modeling of an IDT has been worked out. The model for two-transducer type filters has also been considered.

Modeling of bidirectional transducers as well as unidirectional transducers have been included. Different type of group unidirectional transducers (Normal, Modified and New type GUDTs) as well as three phase unidirectional transducers have been modeled. Group type unidirectional transducers have been represented by six-port networks and a 6x6 chain matrix, while three phase unidirectional transducers have been represented by eight-port network and 8x8 chain matrix. A single group of GUDT and a single section of TPUOT have been modeled by cascading the basic modeling unit of this approach number of times equal to the

number of fingers per group or sections. full GUDT and full TPUdT transducers have been constructed by cascading the groups or section number of times as number of groups or number of sections per transducer is required.

A SAW model simulator has been developed to model and simulate different types of bidirectional and unidirectional transducers and filters built from different combinations of these simulated transducers. The simulator proved to be a very helpful tool for designers of SAW devices. It allows the designer to simulate his device and test its performance under different operational conditions by changing different parameters such as electrical loading, aperture, material,..etc. before fabricating the device, thus saving money and effort that may be spent on fabricating a device with performance characteristics not up to the requirements.

With the aid of this CHAIN MAT simulator different types of transducers and filters have been modeled and simulated. Some of the performances of different group types unidirectional transducers (Normal, Modified and New type) with different number of active fingers per group and different number of groups have been reported and studied. Performances of some of the three phase unidirectional transducers that have been simulated with different periodic sections have been reported and studied too.

A study has been carried out to improve the performances of two-transducer type filters in terms of good bandwidths and side-lobe suppression. Quite useful results have been obtained by using different combinations of unidirectional transducers to construct filters. Performances (in terms of forward and backward frequency responses and directivities) of filters of (a) two identical unidirectional transducers, (b) combinations of group types unidirectional transducers and (c) combinations of group unidirectional transducers and three phase unidirectional transducers have been reported and studied.

For getting good performance filters it has been found that combinations of unidirectional transducers with one wide bandwidth transducer and the other with narrower bandwidth give very good filter performances if the side-lobes of the two transducers are acceptably low. It has been noticed that the difference in side-lobes frequency locations of the two transducers causes cancellation or great reduction in filter side-lobes levels.

Results concerning input and output admittances, conductances, susceptances and phases of some transducers and filters as function of frequency have also been reported.

The study of ways to improve the performances of SAW filters in terms of bandwidth and side-lobe suppression is continued in the coming chapters of this dissertation.

Apodization and Windowing

- 5.1 *Introduction.*
- 5.2 *Apodization.*
- 5.3 *Filter Design Specifications.*
- 5.4 *PFNC Apodization Computations.*
- 5.5 *PFNC Apodized Group Unidirectional Transducers.*
- 5.6 *PFNC Apodized Three Phase Unidirectional Transducers.*
- 5.7 *Filters Of Uniform And PFNC Apodized GUDTs.*
- 5.8 *Filters Of Uniform And PFNC Apodized JPUDTs.*
- 5.9 *Filters Of Combinations Of Uniform And Apodized GUDT and JPUDT Transducers.*

- 5.10 Windowing.
- 5.11 Cosine Windowing Computations.
- 5.12 *SINC*-Weighted *COSINE*-Windowed Apodized *SUDTs*.
- 5.13 *SINC*-Weighted *COSINE*-Windowed Apodized *IPUDTs*.
- 5.14 Filters Of Uniform And *SINC* Weighted-*COSINE* Windowed (Apodized) *SUDTs*.
- 5.15 Filters Of Uniform And *SINC* Weighted-*COSINE* Windowed (Apodized) *IPUDTs*.
- 5.16 Filters Of Combinations Of Uniform And *SINC* Weighted-*COSINE* Windowed (Apodized) *SUDTs* And *IPUDTs*.
- 5.17 Conclusion.

APODIZATION AND WINDOWING

5.1 INTRODUCTION :

There are certain response requirements that are considered in filter design as goals. Generally a filter response is required to be very close to a brick shape response. There are some applications that require responses of different shape than that of the brick. In this chapter two methods of improving the performances of SAW transducers/filters are considered. These are apodization and windowing techniques.

Apodization of SAW transducers is discussed briefly and SINC function finger weighting apodization type is considered. Different transducer/filter performance parameters and basic requirements for a good transducer/filter performance are discussed.

Additional development has been carried out on the simulator package reported and discussed in the previous chapter. Different types of SINC apodized unidirectional transducer are simulated and

results related to its performances are presented. Filters of one uniform and one apodized transducers are also simulated. Results related to filters of GUDTs, TPUUDTs and combinations of both types of transducers are reported and discussed.

Windowing as one way of improving the apodized transducers performances is discussed in brief. It eliminates the gibbs caused by the truncation of the SINC weighting function. It also improves the the transducer/filter response up to some extent depending upon the type of window. Mainly COSINE windowing is considered in this chapter. Different SINC weighted-COSINE windowed apodized transducers are simulated and their relative performances in tabular and graphical forms are reported. Forward, backward responses, admittance (magnitude and phase) responses..etc. of different filters having one uniform and one SINC weighted-COSINE windowed apodized transducers at the two ends with different combinations of GUDT and TPUUDT transducers are computed, reported and discussed.

5.2 APODIZATION :

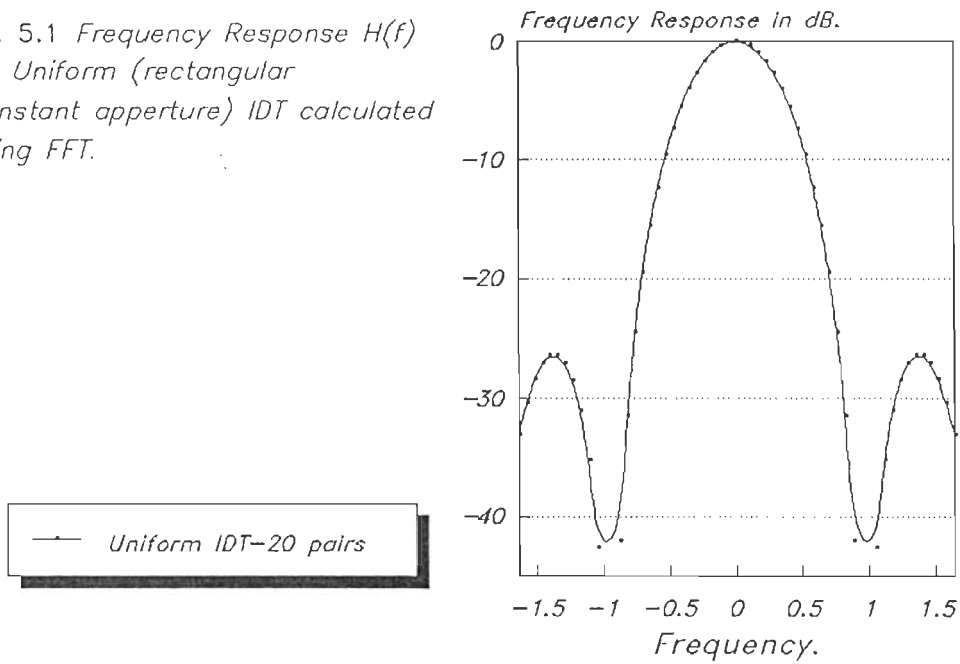
SAW transducers/filters can be considered as finite impulse response (FIR) filters (in the absence of any feedback). The geometric pattern of an interdigital transducer is a unique feature of SAW filter design. It corresponds to a spatially sampled replica of the IDT impulse response. So far we have

studied the frequency responses of different types of SAW transducers using different models aiming to achieve close simulation of the real transducers performances so that to enable the designers to study the performance of the simulated transducers/filters before fabrication and to ease the studies regarding improving SAW transducers/filters performances. Now this simulator is used to study the impulse responses, performances under different conditions of these transducers/filters and ways to improve these performances.

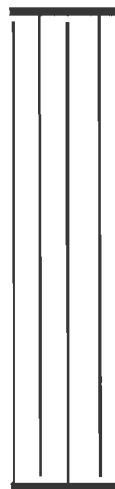
Let us consider an ideal lossless uniform (constant finger overlap) interdigital transducer with 20 finger pairs operating at frequency f_0 . If we calculate the magnitude of the frequency response $|H(f)|$ using fourier transform, by considering the transducer as a rectangular time domain function of duration from $-T$ to $+T$ with 20 samples per $2T$, we will get a result similar to that shown in Figure 5.1. Examining the overall response it is seen that it is infinite and same as the SINC function response.

If we are interested in getting a rectangular response filter then it is easy to find out from fourier transform theory that this can be achieved if the transducer finger overlaps follow a SINC function. Instead of using the uniform IDT with constant overlap apodization - that we were using so far in this study - let us consider the case of SINC function finger overlap apodization. It can be anticipated that the frequency response of one such IDT should now approximate a rectangular bandpass

Fig. 5.1 Frequency Response $H(f)$ of Uniform (rectangular constant aperture) IDT calculated using FFT.



UNIFORM



APODIZED

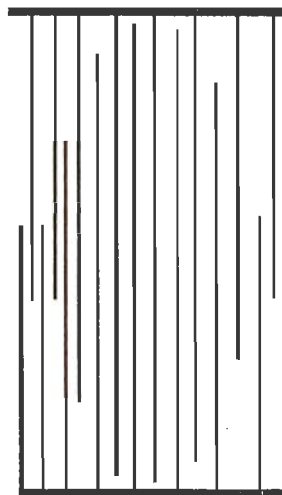


Fig. 5.2 Schematic diagram showing two transducers filter with one apodised and another uniform.

response. Ideally the frequency response would have the rectangular bandpass form if the impulse response of the SAW filter was of infinite time duration which is not the case in practice since it is truncated by the ends of the IDT.

Figure 5.2 shows a typical SAW transversal filter with one SINC apodized transducer and another uniform transducer. here it should be noted that the acoustic wave is not uniform normal to its direction of propagation due to the variation of aperture.

5.3 FILTER DESIGN SPECIFICATIONS :

Before proceeding into the simulation of apodized transducers/filters and study their performances let us see what are the basic requirements in a good transducer/filter performance.

We refer to Figure 5.3 that shows a plot of a filter frequency response and indicates some design parameters required for specifying the desired performance of a SAW transducer/filter. These parameters are :

1. *Insertion loss I.L.*; which is always required to be as minimum as possible and this is usually achieved by using low loss transducers (Unidirectional transducers).

2. *Pass band bandwidth BW*; which is usually (in case of UDTs) is considered to be the 3dB bandwidth.
3. *Pass band ripple R_p* ; These ripples are either due to Triple Transit Echo in Bidirectional transducers or (what is called Gibbs) due to truncation of the SINC weighting function of apodized transducers.
4. *Transition bandwidths: Rise bandwidth R_B and Fall bandwidth F_B* ; generally they are required to be as small as possible and equal if the transducer/filter response is required to be close to the brick shape.
5. *Side lobes rejection level*; required to be as high as possible in most of the applications.
5. *Phase ripple*; for getting a linear and smooth phase response in the pass band region it is required that the phase ripple should be minimal.

7. *Rejection bandwidth RJ*; an arbitrary bandwidth selected to calculate the shape factor of the transducer/filter. It may be taken as the 40dB, 60dB, 100dB bandwidths or any other. For our analysis we will take it as the 40dB bandwidth.

8. *Shape factor S* ; is a relative measure of the filter or transducer selectivity. As the transition bandwidths approach zero S approaches 1. When each of the transition bandwidths is equal to the transducer/filter bandwidth S will be equal to 0.3333. A higher shape factor indicates how close is the transducer/filter response to that of the brick shape.

Shape factor has many definitions and can be somewhat misleading. Some definitions are TBW_{0-60dB} , TBW_{3-60dB} , TBW_{60-3dB} , TBW_{0-40dB} , TBW_{3-40dB} , etc. [20,44]. For theoretical analysis and comparison we will use the definition TBW_{3-40dB} .

Fig. 5.3 Trans./Filter design specifications.

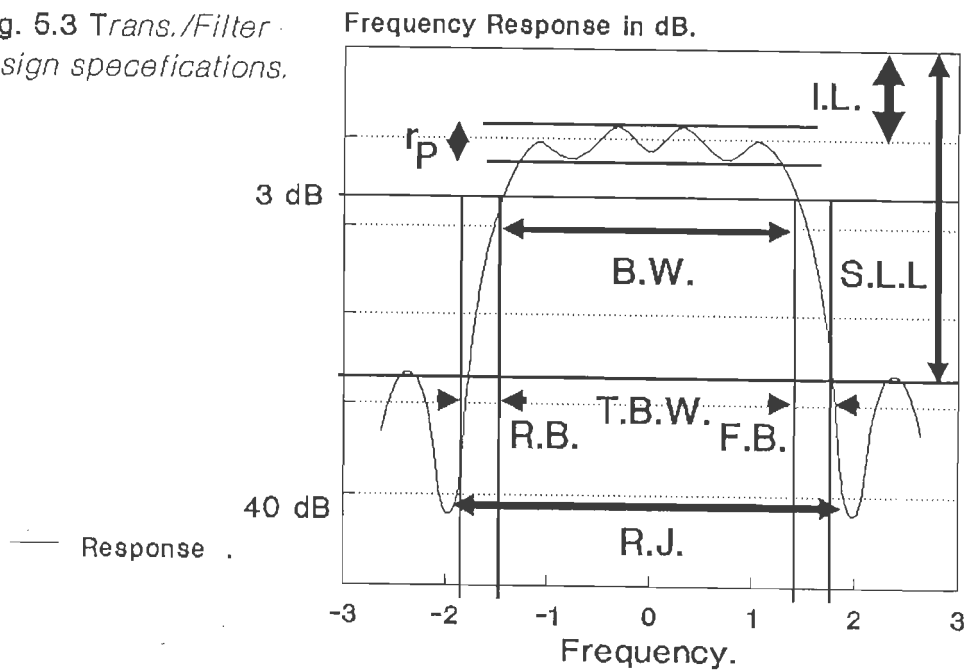
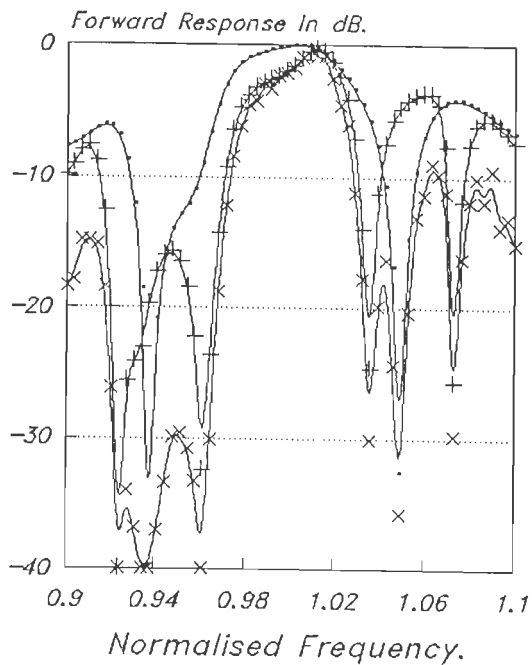


Fig. 5.4 Forward Frequency response of uniform NGUDT-8-2, apodised NGUDT-8-3 (one zero crossing) and filter of both transducers.

Max. Aperture is $7.3798E-4$ m

Frequency Responses:

- NGUDT-8-2 UNIF
- + NGUDT-8-3 APD; 31
- * FILTER



5.4 SINC APODIZATION COMPUTATIONS :

To include the modeling and simulation of SINC apodized transducers and filter having one uniform and one apodized transducers, some additional developing has been carried out on the CHAIN MAT modeling software package.

Number of filter having one apodized and one uniform transducers have been simulated in order to study the effect of SINC apodization on transducers/filters performances.

The software used for these simulations has been developed in a way that it calculates the proper number of finger-pairs (BIDT), periodic sections (TPUDT), and active fingers per group or number of groups (GUDT) for either the uniform or apodized transducers to secure matching.

5.5 SINC APODIZED GROUP UNIDIRECTIONAL TRANSDUCERS :

Different types of apodized group unidirectional transducers have been simulated using the above mentioned package. Computational results of some of these transducers are given in Table {5.1}. In all the transducers tabulated the SINC function is truncated at its first or second zero crossing on both ends of

Table {5.1}
*Computed Rise, 3dB and Fall bandwidths
of SINC weighted Group
type UniDirectional Transducers.*

Transducer type	Apodization type	Aperture in meter	RB per cent	3dB BW per cent	FB per cent
N-8-3	31	7.3798E-4	2.022	3.53	0.1675
N-4-5	31	7.3798E-4	1.1173	4.4915	0.4469
N-4-6	31	4.9199E-4	1.3407	3.564	0.2122
N-4-7	32	7.4525E-4	1.486	2.6815	0.1452
N-4-8	31	3.1487E-4	0.5698	2.9943	0.1340
N-2-10	31	7.3798E-4	0.6368	3.7988	0.4022

Table {5.2}
*Computed first left and right side lobes levels
of SINC weighted Group Unidirectional Transducers*

Transducer type	Apodization type	Aperture in meter	LSL in dB	RSL in dB
N-8-3	31	7.3798E-4	15.92	3.8
N-4-5	31	7.3798E-4	10.	5.6
N-4-6	31	4.9199E-4	10.	4.4
N-4-7	32	7.4525E-4	10.	4.4
N-4-8	31	3.1487E-4	8.6	5.2
N-2-10	31	7.3798E-4	9.2	4.8

transducers as indicated in table for each transducer. The apodization is performed by changing the finger overlap or aperture per group, i.e. group apodization. Fingers in each group have the same overlap (aperture).

Computational results corresponding to 3dB bandwidth, transit bandwidths and side-lobes levels are given in Table 5.1 and Table 5.2, respectively. Rejection bandwidths and shape factor of each of these group type apodized transducers are given in Table 5.3. Generally it seems that for same number of fingers per group-groups product the increase in number of groups raises side-lobes levels and decrease transition bandwidth.

Comparing GUDT-4-5 and GUDT-4-7 normal type transducers, where the SINC function in the later transducer is truncated at the second zero crossing, there is a great difference in the rise to 3dB bandwidths ratios of the two transducers. Due to lengthening of the weighting part of the SINC function, an increase in rise bandwidth and a decrease in both 3dB and fall bandwidths is caused. This in turn affects negatively the shape factor of the transducer (Table{5.3}). A relation can be sensed between the these three bandwidths (transition and 3dB bandwidths) and the amount of used (or truncated) length of the SINC weighting function. This is to be considered in more details in the coming sections of this chapter.



Table {5.3}

Computed Rejection bandwidth and Shape factor of SINC weighted Group type Unidirectional Transducers

Transducer type	Apodization type	Aperture in meter	RJ per cent	SHAPE factor
N-8-3	31	7.3798E-4	7.3518	0.48
N-4-5	31	7.3798E-4	7.824	0.574
N-4-6	31	4.9199E-4	6.569	0.542
N-4-7	32	7.4525E-4	5.698	0.4705
N-4-8	31	3.1487E-4	5.0278	0.5955
N-2-10	31	7.3798E-4	6.6479	0.5714

Table {5.4}

Computed Rise, 3dB and Fall bandwidths of SINC Weighted Three Phase Unidirectional transducer

Transducer type	Apodization type	Aperture in meter	RB per cent	3dB BW per cent	FB per cent
T-17	31	7.3798E-4	1.4525	7.9329	0.5586
T-20	31	4.9199E-4	0.916	6.6144	0.3351
T-33	32	7.3798E-4	0.8938	2.3240	0.0558

5.6 SINC APODIZED THREE PHASE UNIDIRECTIONAL TRANSDUCERS:
--

Many apodized three phase unidirectional transducers with different number of periodic sections have been simulated. The apodization has been performed by changing aperture per sections keeping the finger overlap of each section constant. Different truncations of the SINC weighting function have been considered.

Computational results of some of these simulated three phase unidirectional transducers are listed in Tables 5.4, 5.5 and 5.6. The effect of increasing number of sections is clear (Table 5.4) on decreasing transition and 3dB bandwidths.

Considering the results related to increasing used length of the SINC weighting function such as the case of apodized TPUDT-33, with its (section) aperture follows a SINC function truncated at second zero crossing, the effect of such lengthening is clear from results. It is to be noted that the increased number of sections is to keep the transducer impedance same as TPUDT-20 with a single zero crossing SINC apodization. Comparing the result of the two transducers it can be seen that although transition bandwidths have been reduced and side-lobes levels have been lowered due to the combined effect of increasing SINC function length and the number of sections, yet the shape factor of the transducer is quit low. This deterioration in the shape factor is due to the

Table {5.5}

Computed first left and right side lobes levels of SINC weighted Three Phase type UniDirectional Transducers.

Transducer type	Apodization type	Aperture in meter	LSL in dB	RSL in dB
T-17	31	7.3798E-4	6.8	8.4
T-20	31	4.9199E-4	7.12	6.08
T-33	32	7.3798E-4	10.8	6.76

Table {5.6}

Computed Rejection bandwidth and Shape factor of SINC weighted Three Phase type UniDirectional Transducers.

Transducer type	Apodization type	Aperture in meter	RJ per cent	SHAPE factor
T-17	31	7.3798E-4	11.899	0.6666
T-20	31	4.9199E-4	9.8323	0.6727
T-33	32	7.3798E-4	6.1563	0.3774

increased rise to 3dB bandwidths ratio caused by lengthening the used part of the SINC function in weighting the transducer.

It has been found that for compensating the effect of increasing the SINC function weighting length more increase in the number of sections is required, and to keep the input impedance of the transducer constant (for matching purposes) while increasing the number of sections for the same apodization pattern the maximum effective aperture of the transducer has to be reduced. This we will consider again in the coming sections with some more examples.

Proper selection of the SINC weighting function length and proper number of sections is very much essential in the design of apodized SAW TPUDT transducers for getting a good performance up to the requirements.

5.7 FILTERS OF UNIFORM AND SINC APODIZED GUDTs :

In order to find the effect of apodization on improving SAW GUDT filter performance, many types of filters have been simulated from different combinations of uniform and apodized group unidirectional transducers. In each filter one uniform wide band and another apodized narrower band GUDT transducers have been used. Tables {5.7}, {5.8} and Table {5.9} list the computational results of some of these simulated filters.

Table {5.7}

*Computed Rise, 3dB and Fall bandwidths of filters
of uniform and SINC apodized GUDTs.*

Transducer type	Apodization type	Aperture in meter	RB per cent	3dB BW per cent	FB per cent
N-8-2	1	7.3798E-4	2.4357	3.005	1.229
N-8-3	31				
N-8-2	1	7.3798E-4	1.7765	3.8547	1.564
N-4-5	31				
NU-8-2	1	7.3798E-4	1.2737	3.4077	0.8044
N-2-10	31				

Table {5.8}

*Computed left and right side lobes levels of filters
of uniform and SINC apodized GUDTs.*

Transducer type	Apodization type	Aperture in meter	LSL in dB	RSL in dB
N-8-2	1	7.3798E-4	30.5	16.4
N-8-3	31			
N-8-2	1	7.3798E-4	25.2	22.4
N-4-5	31			
NU-8-2	1	7.3798E-4	21.2	12.4
N-2-10	31			

Table {5.9}

Computed Rejection bandwidth and Shape factor of filters of uniform and SINC apodized GUDTs.

Transducer type	Apodization type	Aperture in meter	RJ per cent	SHAPE factor
N-8-2	1	7.3798E-4	7.3518	0.4087
N-8-3	31			
N-8-2	1	7.3798E-4	7.8211	0.4928
N-4-5	31			
NU-8-2	1	7.3798E-4	6.6479	0.5125
N-2-10	31			

Generally the main lobe of the filter response is very close to that of the apodized transducer, therefore, the 3dB bandwidth of the filter and the apodized transducer is very close to each other. Increasing the number of fingers per group - groups product of the apodized transducer decreases the 3dB bandwidth of the filter, but not necessarily improves the shape factor which depends on how much the difference in bandwidths between the uniform and the apodized transducers. For the same number of fingers per group - groups product of the apodized transducer and the same uniform transducer an increase in the number of groups of the apodized transducer with the same apodization pattern causes a reduction in the 3dB bandwidth as well as improvement in the shape factor of the filter. These are some of the observations that can be anticipated from the mentioned tables.

Side-lobes levels of filters depend on side-lobes levels and side-lobes frequency locations of the two uniform and apodized transducers. Side-lobes level up to 30.5 dB is reported in Table {5.8}. This is due to the low side-lobes level of the apodized transducer as well as frequency locations of first both sides lobes inside the main lobe of the uniform transducer as shown in Figure 5.4. The Figure represents the forward frequency response of uniform GUDT-8-2, apodized GUDT-8-3 and filter of both normal type transducers.

Figure 5.5 shows the input admittance response of the above mentioned transducers and filter. The input admittance of the

Fig. 5.5 *Input admittance of uniform NGUDT-8-2, apodized NGUDT-8-3 and filter of both transducers.*
 Max Aperture is $7.3798E-4$ m.

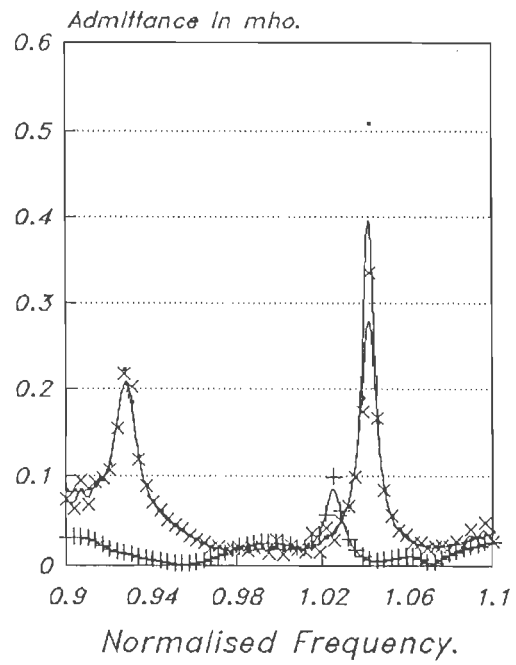
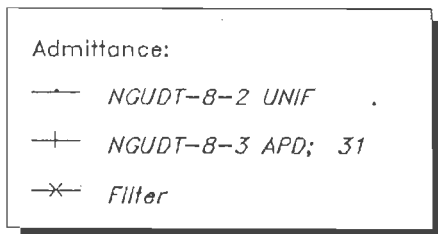
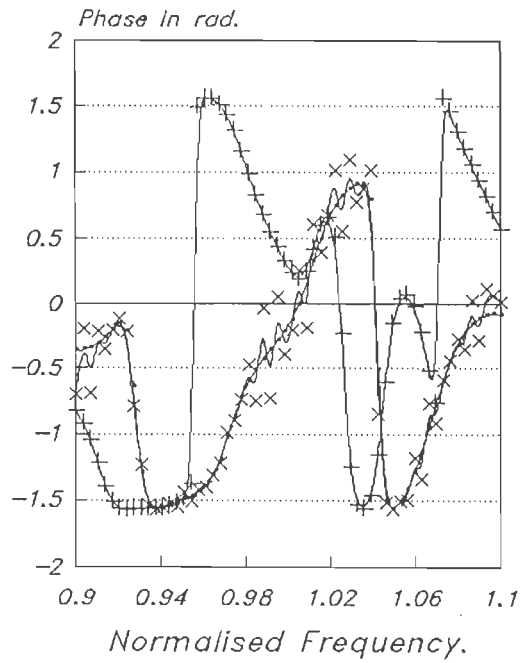
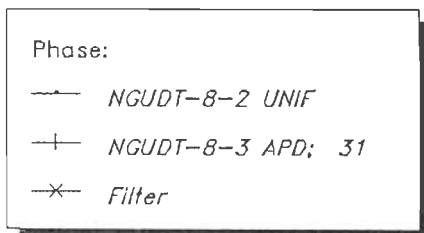


Fig. 5.6 *Input phase response of uniform NGUDT-8-2, apodized NGUDT-8-3 and filter of both.*



filter follows the input admittance of the uniform transducer which is used as the transmitting transducer in this filter. There is a dip or a high ripple destoring the linearity of the phase response of the apodized transducer that causes small oscillations or ripples in the filter phase response as shown in Figure 5.6. The linear and smaller ripple phase response of the transducer/filter leads to lesser signal distortion due to frequency dispersion. This phase ripple caused by apodization can be eliminated or reduced by the use of dummy fingers.

It has been found from the different simulated apodized transducers and filters -which is not possible to report all its performances and results here- that if we measure both transition bandwidths on the same line (say either LSL level or RSL level) then we can see that rise bandwidth and fall bandwidth behaviors are inversely proportional to each other. When the rise bandwidth is large the response may fall sharply giving a low fall bandwidth and vice versa. It is even noted that when the rise bandwidth is large enough the response may fall sharply before it rises above the 3dB line giving higher insertion loss performance and zero or very low 3dB bandwidth.

It has been found that the rise bandwidth of an apodized GUDT transducer is function of number of fingers per group - groups product, number of apodized groups and length of SINC weighting function. The rise bandwidth increases with the increase of the SINC weighting function length. It decreases with the increase of

Fig 5.7 Forward frequency response of uniform NUGDT-8-2, apodized NGUDT-2-10 (one zero crossing) and filter of both transducers.
Max. Aperture is $7.3798E-4$ m

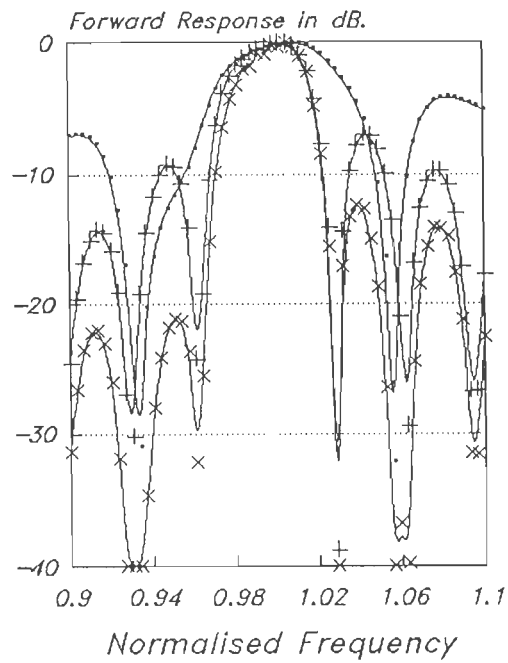
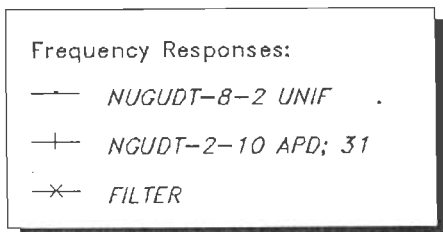


Fig. 5.8 Input admittance of uniform NUGDT-8-2, apodized NGUDT-2-10 and filter of both transducers.
Max Aperture is $7.3798E-4$ m.

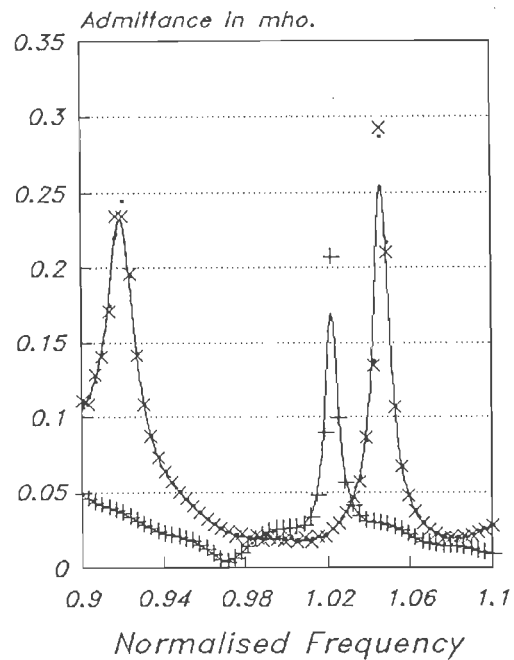
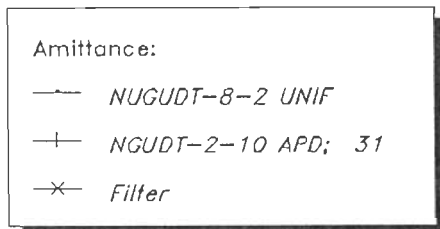


Fig. 5.9 Input phase response for uniform NUGUDT-8-2, apodized NGUDT-2-10 and filter of both. Max aperture is $7.3798E-4$ m.

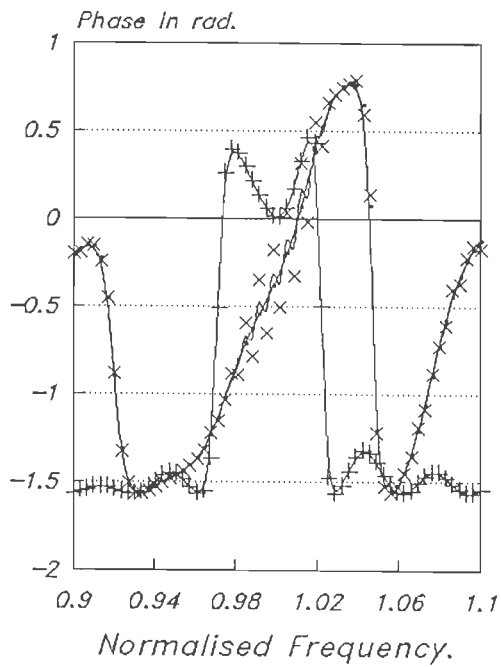
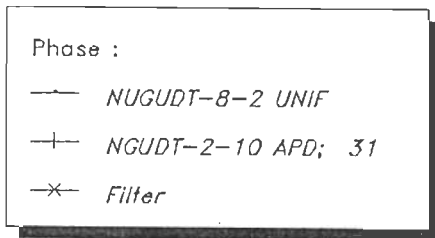
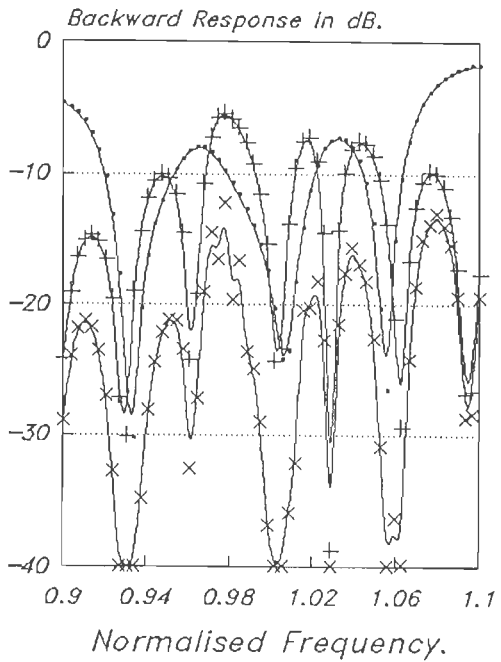
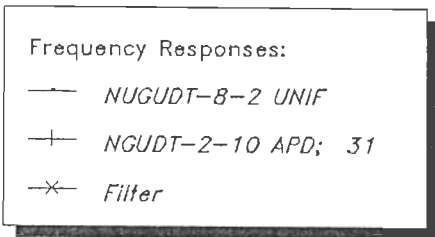


Fig. 5.10 Backward frequency response of uniform NUGUDT-8-2, apodized NGUDT-2-10 and filter of both transducers. Max aperture is $7.3798E-4$ m.



fingers per group - groups product number and with the increase of number of apodized groups for the same fingers per group - groups product number. While the fall bandwidth behaves the reverse way.

According to the requirements the ratios of the rise and fall bandwidths relative to 3dB bandwidth can be modified by changing the above parameters. It has to be noted that both ratios can not be considered alone without taking into consideration both sides (lower and upper) first side-lobes levels. By definition rise and fall bandwidths are measured at first right and first left side-lobes levels which are in most of the cases not at the same level.

Such improvements in the shape factor of the filter as well as reducing the difference between the rise and fall bandwidths of the apodized transducer and filter by increasing the number of groups is very much visible in the performances of transducers and filters shown in Figures 5.7 and 5.12. Figures 5.9, 5.10 and 5.11 show the phase response, backward response and relative directivity of uniform GUDT-8-3, SINC apodized GUDT-2-10 and their filter. The phase ripples (oscillations) can be seen in the filter phase response. The directivity of this filter is more flat than that of the apodized transducer and sharper than the uniform transducer directivity as can be seen from Figure 5.11.

Fig. 5.11 Relative directivity of uniform NUGUDT-8-2, apodized NGUDT-2-10 and filter of both. Max aperture is $7.3798E-4$ m.

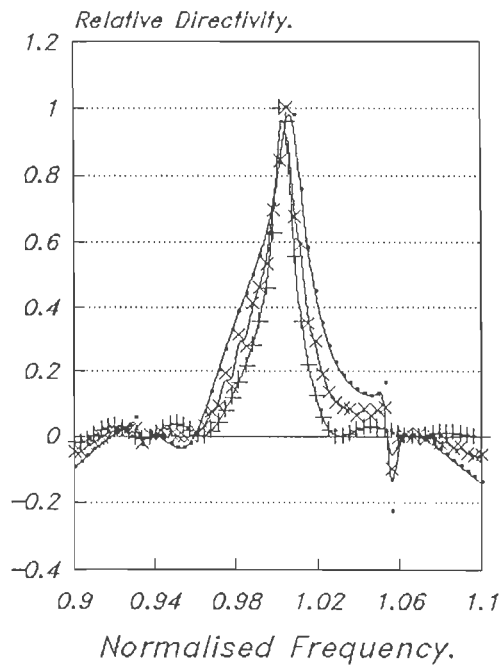
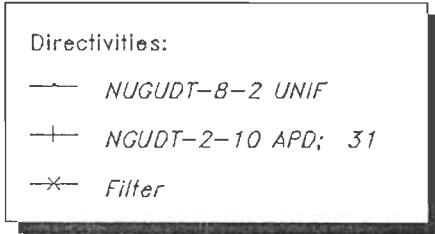
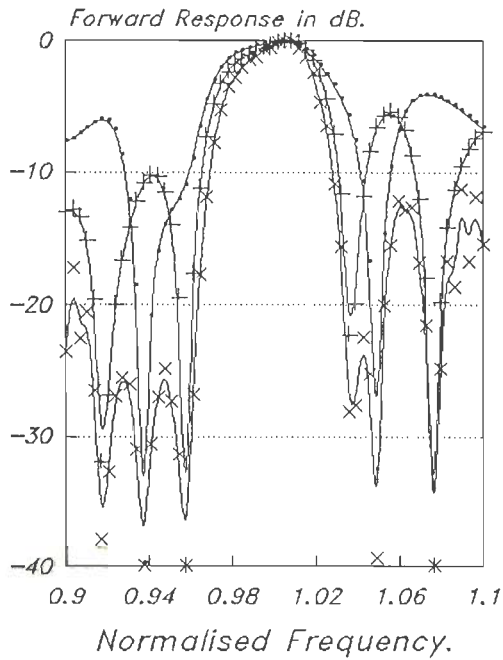
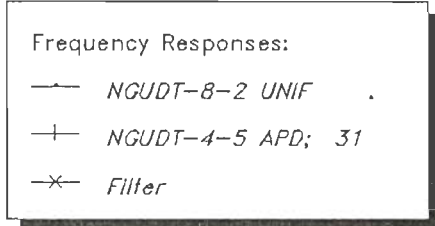


Fig. 5.12 Forward Frequency response of uniform NGUDT-8-2, apodized NGUDT-4-5 and filter of both transducers. Max. Aperture is $7.3798E-4$ m



In continuation of the study of apodization effect on improving filters performances, number of two three-phase unidirectional transducers filters have been simulated, with one apodized narrow band transducer and one uniform wider band transducer. Computational results of some of these filters are presented in Tables {5.10}, {5.11} and {5.12}. Performances of some of these filter and their corresponding uniform and apodized transducers performances are presented in Figure 5.13 to Figure 5.21. From the plots of forward frequency responses it can be seen that the filter forward frequency response is generally very close to the apodized transducer frequency response specially in the main lobe and differs in side-lobes levels and frequency locations. backward frequency response, admittance response..etc of the filter is generally different than that of the apodized transducer.

The effect of increasing the number of sections on transition and 3dB bandwidths is greatly visible from Tables and forward frequency responses plots of Figures 5.13 and 5.14. The effect of increasing the weighting (untruncated) length of the SINC function on increasing the rise bandwidth and decreasing the fall bandwidth is clear from Tables. This effect causes a great degradation in the shape factor. This is also clear from Figure 5.19 which

Table {5.10}

*Computed Rise, 3dB and Fall bandwidths of filters
of uniform and SINC apodized TPUDTs.*

Transducer type	Apodization type	Aperture in meter	RB per cent	3dB BW per cent	FB per cent
T-13	1	7.4526E-4	2.9608	6.7038	1.363
T-17	31				
T-16	1	4.9199E-4	2.324	5.698	1.3407
T-20	31				
T-16	1	4.9199E-4	2.5809	2.3240	0.2681
T-33	32				

Table {5.11}

*Computed left and right side lobes levels of filters
of uniform and SINC apodized TPUDTs.*

Transducer type	Apodization type	Aperture in meter	LSL in dB	RSL in dB
T-13	1	7.4526E-4	24.	21.
T-17	31			
T-16	1	4.9199E-4	26.4	23.4
T-20	31			
T-16	1	4.9199E-4	14.4	9.6
T-33	32			

Table {5.12}

Computed Rejection bandwidth and Shape factor of filters of uniform and SINC apodized TPUDTs.

Transducer type	Apodization type	Aperture in meter	RJ per cent	SHAPE factor
T-13	1	7.4526E-4	11.899	0.56337
T-17	31			
T-16	1	4.9199E-4	9.8323	0.5795
T-20	31			
T-16	1	4.9199E-4	6.1563	0.37749
T-33	32			

Fig. 5.13 Forward frequency response of uniform TPUDT-13, apodised TPUDT-17 and filter of both transducers. Max. Aperture is $7.45265E-4$ m

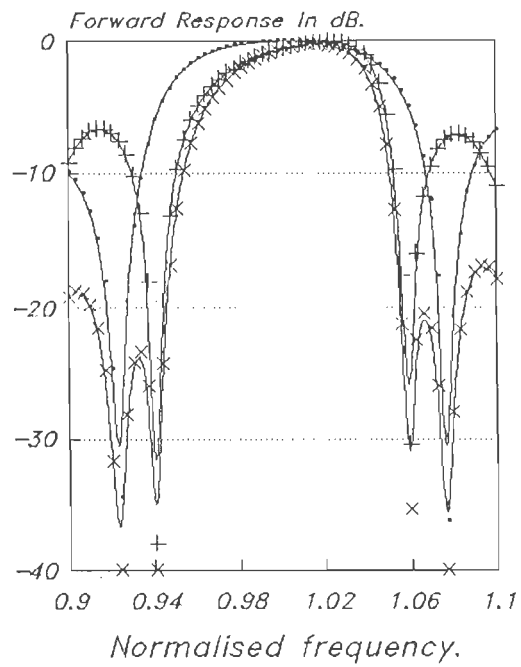
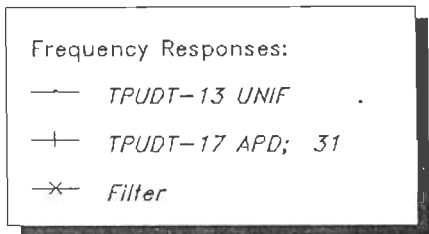


Fig. 5.14 Forward frequency response of uniform TPUDT-16, apodized TPUDT-20 and filter of both transducers. Max. Aperture is $4.9189E-4$ m

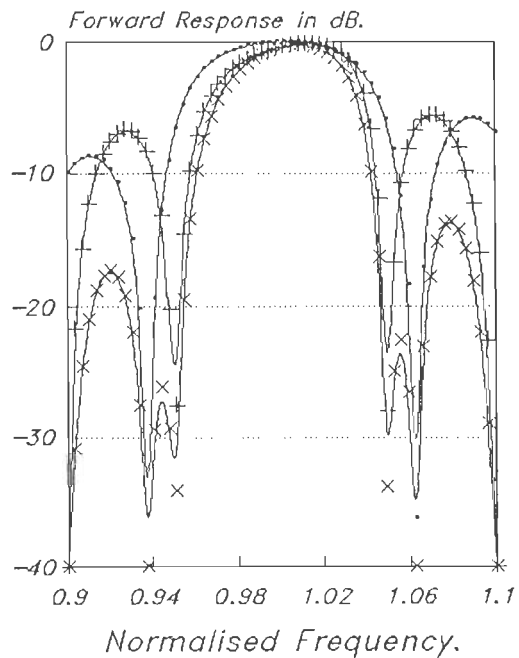
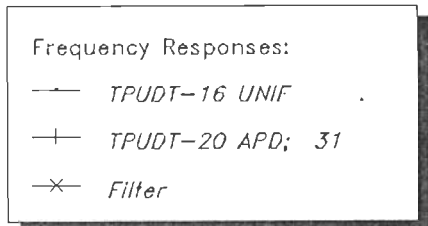


Fig. 5.15 Input admittance of uniform TPUDT-16, apodized TPUDT-20 (single crossing) and filter of both. Max aperture is $4.9199E-4$ m.

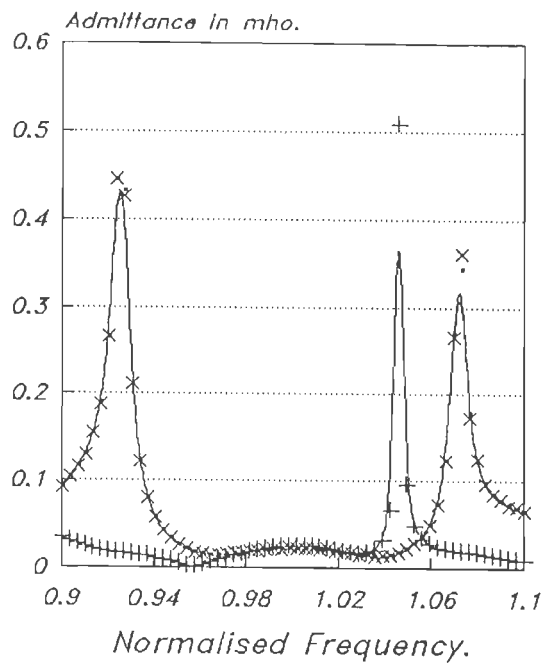
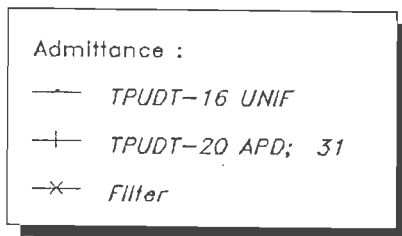
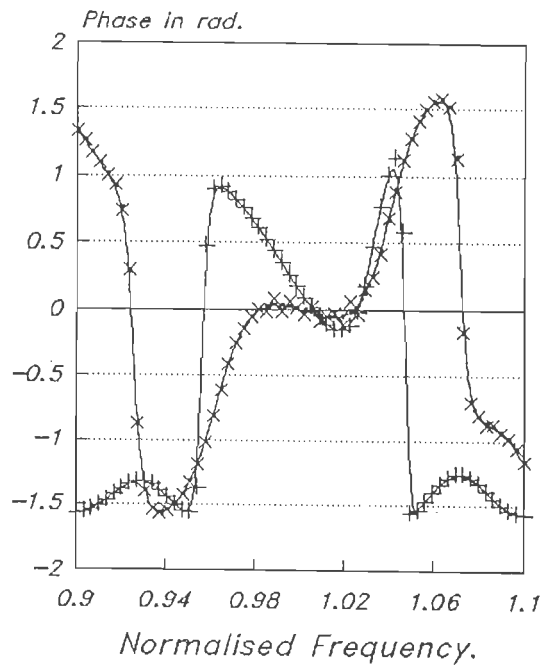
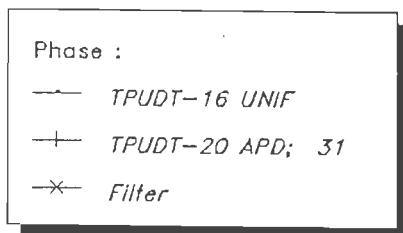


Fig. 5.16 Input phase response of uniform TPUDT-16, apodized TPUDT-20 and filter of both. Max aperture is $4.9199E-4$ m.



represents TPUDT-16/TPUDT-33 filter with the SINC function truncated at second zero crossing. This degradation can be improved by decreasing the rise band or in other words lower the rise to 3dB bandwidth ratio by increasing the number of sections to a proper number to bring rise and fall bandwidths as close to each other as possible. The effect of increasing the number of apodized sections or reducing the rise bandwidth can be seen from Figures 5.13 and 5.14.

The selection of the uniform transducer affects very much the side-lobes levels of the filter in addition to the effect of the apodized transducer. The frequency locations of side-lobes of both uniform and apodized transducers are very important in getting filter response with low side-lobes levels. Some times side-lobes frequency locations may cause cancellation of side-lobes close to the main lobe in the filter response causing separation between the main and side-lobes frequencies.

It has been found from the different simulated apodized transducers and filters that transition bandwidths are very much related to the number of sections and length of the SINC weighting function. The rise bandwidth increases with increasing the length of the SINC weighting function (reducing the truncation) and with decreasing the number of sections. When the rise bandwidth increases it may affect greatly both 3dB and fall bandwidths. If number of sections of the apodized transducer of the filter whose response shown in Figure 5.19 is reduced by enough number the

Fig. 5.17 Backward frequency response of uniform TPUDT-16, apodized TPUDT-20 and filter of both. Max aperture is $4.9199E-4$ m.

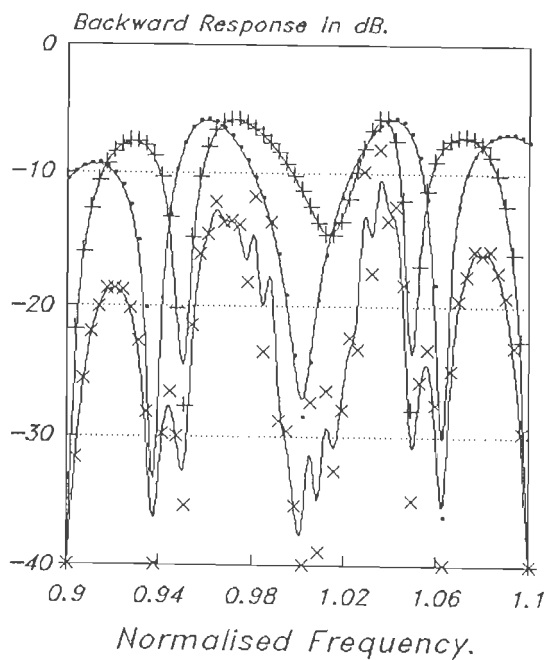
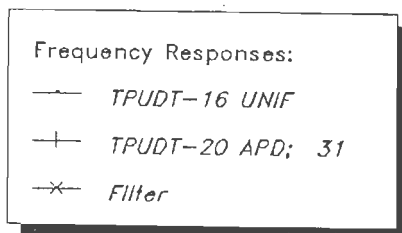


Fig. 5.18 Relative directivity of uniform TPUDT-16, apodized TPUDT-20 and filter of both. Max aperture is $4.9199E-4$ m.

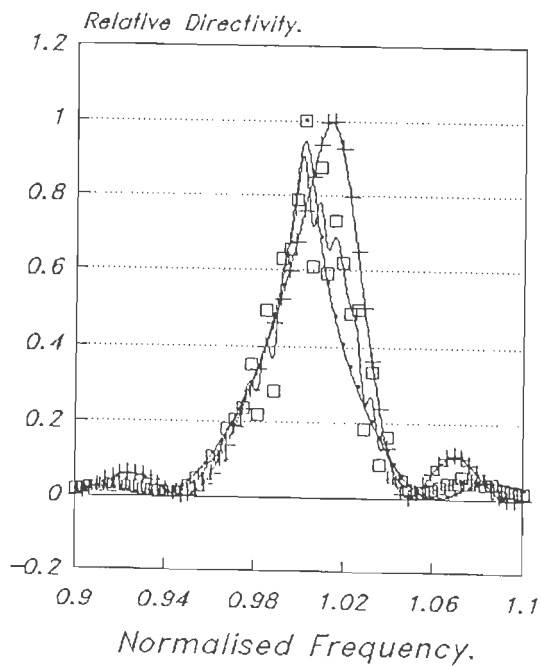
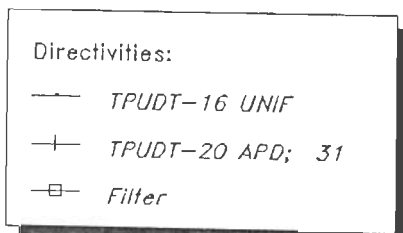


Fig. 5.19 Forward frequency response of uniform TPUDT-16, apodized TPUDT-33 (two zero crossing) and filter of both. Max. Aperture is $4.9199E-4$ m

Frequency Responses:
 — TPUDT-16 UNIF
 + TPUDT-33 APD; 32
 × Filter

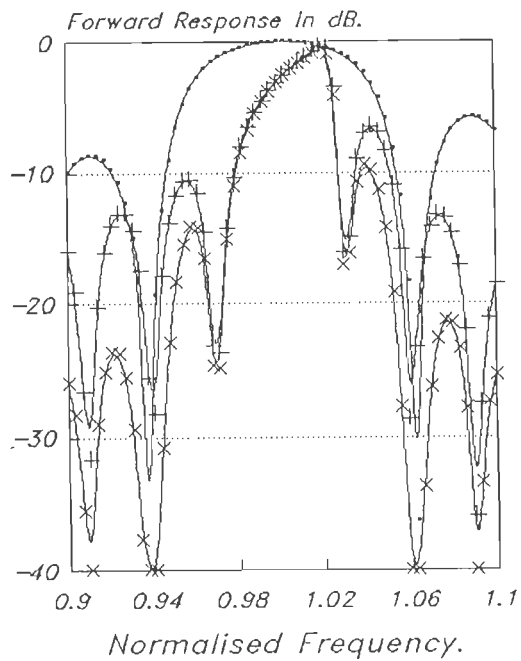
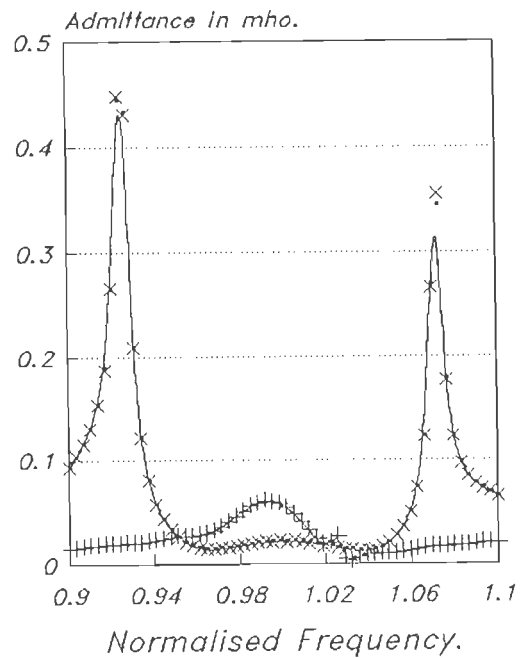


Fig. 5.20 Input admittance of uniform TPUDT-16, apodized TPUDT-33 (two zero crossing) and filter of both. Max. aperture is $4.9199E-4$ m.

Admittance:
 — TPUDT-16 UNIF
 + TPUDT-33 APD; 32
 × Filter



responses of both apodized transducer and filter may not have the chance to rise above the 3dB line and fall sharply causing a response with null 3dB bandwidth, very low fall bandwidth and high insertion loss although both apodized and uniform transducers are of low loss type and they are supposed to have zero insertion loss at f_0 !

Admittance, phase responses, backward and forward frequency responses and relative directivities of some of the simulated filters are presented in Figures 5.13 to 5.21. In Figures 5.17 and 5.18 frequency shifting of the apodized transducer backward response and relative directivity from the same uniform transducer responses can be seen. Some oscillation in these responses of the filter due to this shift can also be seen.

5.9 FILTERS OF COMBINATIONS OF UNIFORM AND APODIZED GUDT AND TPUDT TRANSDUCERS :

Filters of combinations of uniform and apodized GUDT and TPUDT transducers have been simulated. A wider band uniform GUDT or TPUDT transducer is used in combination with an apodized narrower band of a different type transducer to obtain the filters. Simulation results of some of these filters are listed in Tables {5.13}, {5.14} and {5.15}. Performances of these filters (in terms of different responses) and some other related graphs are shown in Figures 5.22 to 5.27. As was the case in the previous

Fig. 5.21 Input phase response of uniform TPUDT-16, apodized TPUDT-33 (two zero crossing) and filter of both. Max aperture is $4.9199E-4$ m.

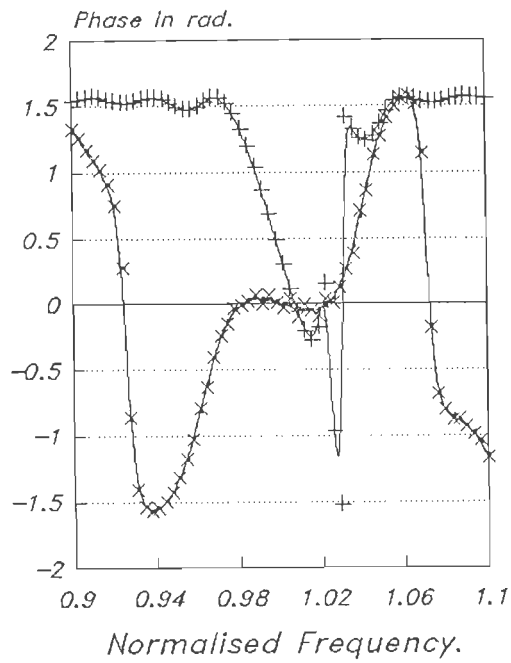
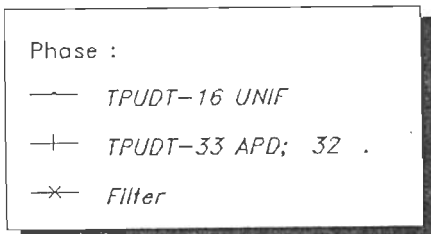


Fig. 5.22 Forward frequency response of uniform NGUDT-4-4, apodized TPUDT-17 and filter of both transducers. Max. Aperture is $7.3798E-4$ m

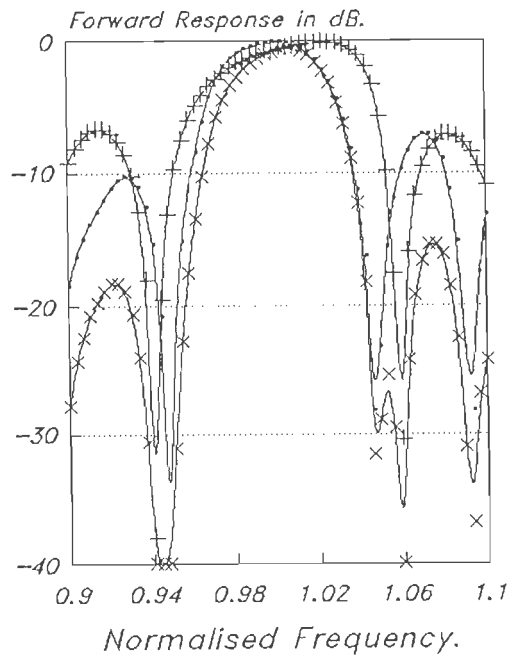
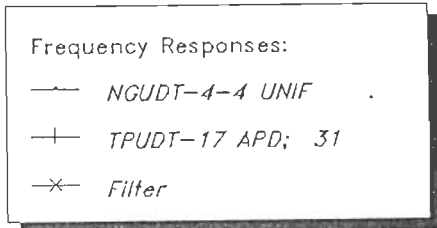


Table {5.13}
*Computed Rise, 3dB and Fall bandwidths of filters
of combinations of uniform and apodized
GUDT and TPUDT transducers.*

Transducer type	Apodization type	Aperture in meter	RB per cent	3dB BW per cent	FB per cent
N-4-4	1	7.3798E-4	2.324	4.469	1.6536
T-17	31				
T-13	1	7.4526E-4	1.6536	2.6815	0.2234
N-4-7	32				
T-16	1	4.9199E-4	1.6759	3.486	0.5474
N-4-6	31				
T-20	1	3.1487E-4	0.7932	2.9943	0.2793
N-4-8	31				

Table {5.14}

*Computed left and right side lobes levels of filters
of combinations of uniform and apodized
GUDT and TPUDT transducers.*

Transducer type	Apodization type	Aperture in meter	LSL in dB	RSL in dB
N-4-4	1	7.3798E-4	18.48	16.64
T-17	31			
T-13	1	7.4526E-4	11.96	5.52
N-4-7	32			
T-16	1	4.9199E-4	15.56	8.
N-4-6	31			
T-20	1	3.1487E-4	13.52	8.5
N-4-8	31			

Table {5.15}

Computed Rejection bandwidth and Shape factor of filters of combinations of uniform and apodized GUDT and TPUDT transducers.

Transducer type	Apodization type	Aperture in meter	RJ per cent	SHAPE factor
N-4-4	1	7.3798E-4	9.854	0.4535
T-17	31			
T-13	1	7.4526E-4	5.698	0.47058
N-4-7	32			
T-16	1	4.9199E-4	6.569	0.5306
N-4-6	31			
T-20	1	3.1487E-4	5.027	0.59553
N-4-8	31			

two articles, It can be seen from forward frequency responses that main lobes of filters responses are very close to their apodized transducers main lobes.

From the three tables and plots of forward frequency responses in Figures 5.23-5.24 the effect of increasing the number of apodized groups/sections on decreasing rise and 3dB bandwidths is very clear. The increase in fall bandwidth due to the decreased rise bandwidth is also very clear from tables and above mentioned figures. This cause a great improvement in the shape factor of the filter shown in Figure 5.24.

The cancellation of first side-lobe (or the free side-lobe band to the left of the main lobe) of the filter (whose forward frequency response is shown in Figure 5.22) is due to the different frequency locations of side-lobes of both uniform and apodized transducers from which the filter is constructed.

Such cancellation can also be seen in different frequency locations in filters responses shown in Figures 5.23 and 5.25.

In the filter whose frequency response is shown in Figure 5.25 with its apodized transducer SINC weighting function is truncated after two zero crossings, the number of apodized groups are not enough to reduce the ratio of rise to 3dB bandwidths. The rise bandwidth (and the ratio of rise to 3dB bandwidths) is related to the SINC weighting function length and the number of

Fig. 5.23 Forward frequency response of uniform TPUDT-16, apodized NGUDT-4-6 and filter of both.
Max. Aperture is $4.9199E-4$ m

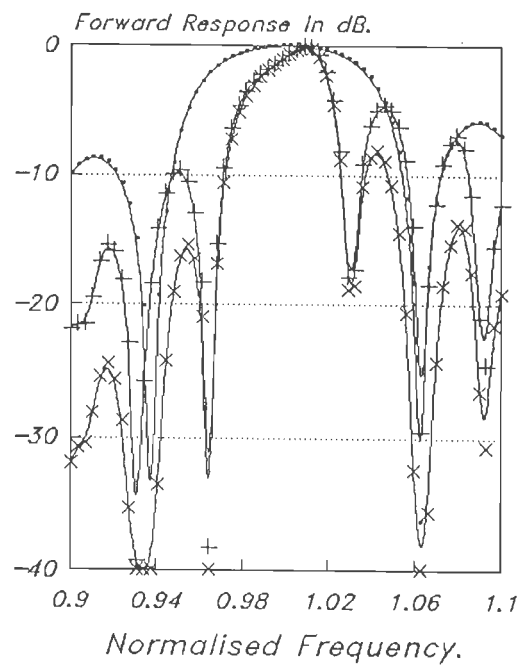
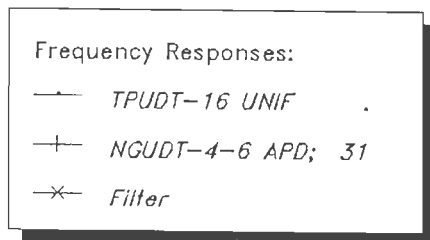


Fig. 5.24 Forward frequency response of uniform TPUDT-20, apodized NGUDT-4-8 and filter of both.
Max aperture is $3.1487E-4$ m.

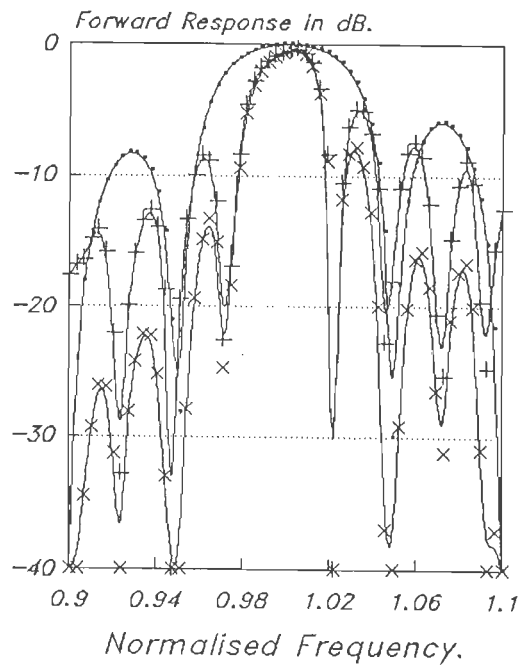
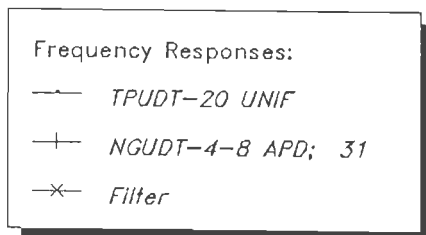


Fig. 5.25 Forward frequency response of uniform TPUDT-20, apodized NGUDT-4-13 (two zero crossing) and filter of both. Max aperture is $3.1487E-4$ m.

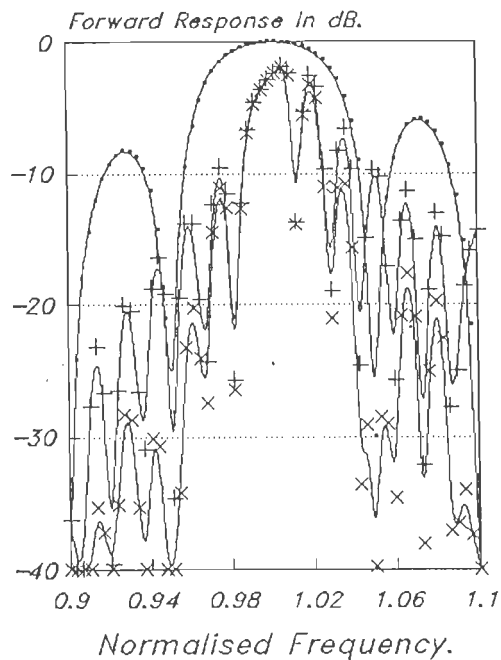
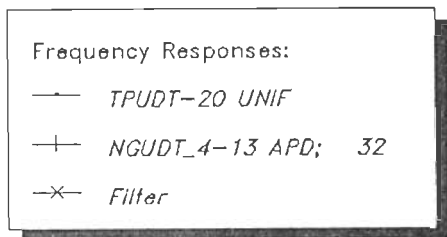
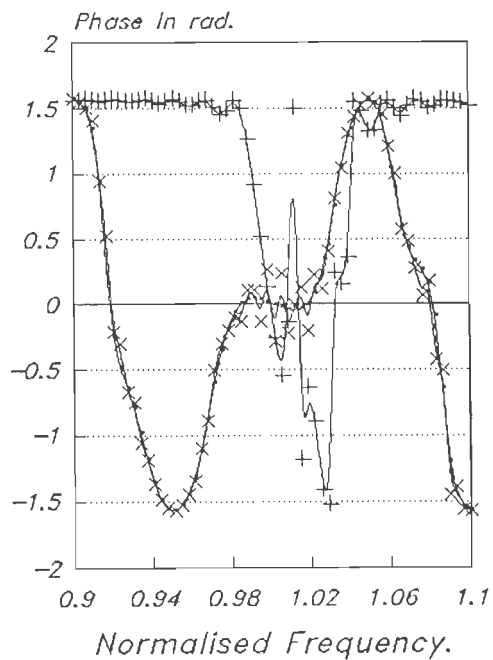
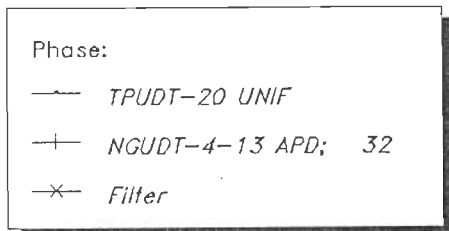


Fig. 5.26 Input phase response of uniform TPUDT-20, apodized NGUDT-4-13 (two zero crossing) and filter of both. Max aperture is $3.1487E-4$ m.



apodized groups/sections. The rise bandwidth in this filter is so wide that the response falls sharply just after crossing the 3dB line causing a very small 3dB bandwidth, very high RSL level up to 3dB and an insertion loss of more than 2 dB in both apodized transducer response as well as filter response although both transducers are low loss and supposed to be of zero insertion loss.

The filter response is so much deteriorated compared to the same combination of uniform transducers filter due to the improper selection of apodized groups with the selected SINC weighting function length. Increasing the number of apodized groups properly will improve the filter performance. This increase will cause a decrease in the ratio of rise to 3dB bandwidths and increase in the ratio of fall to 3dB bandwidths which in turn will improve the shape factor of both apodized transducer and filter.

Figure 5.26 shows the phase response of this filter and its uniform and apodized transducers. Figure 5.27 shows the effective aperture length of the 13 groups of apodized GUDT-4-13 transducer.

5.10 WINDOWING:

It is apparent that interdigital transducers of all SAW filter have a built in window function. That is the rectangular window function associated with the finite physical length of the

Fig. 5.27 Effective aperture length of apodized NGUDT-4-13 (two zero crossing).
Max. aperture is $3.1487E-4$ m.

Aperture pattern:
· NGUDT-4-13 APD; 32

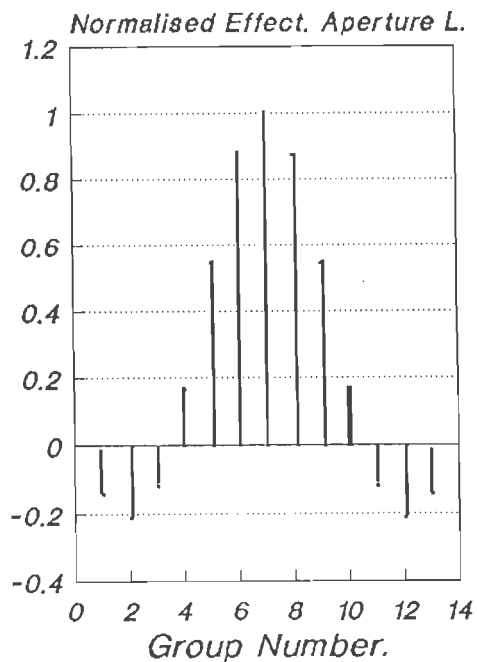
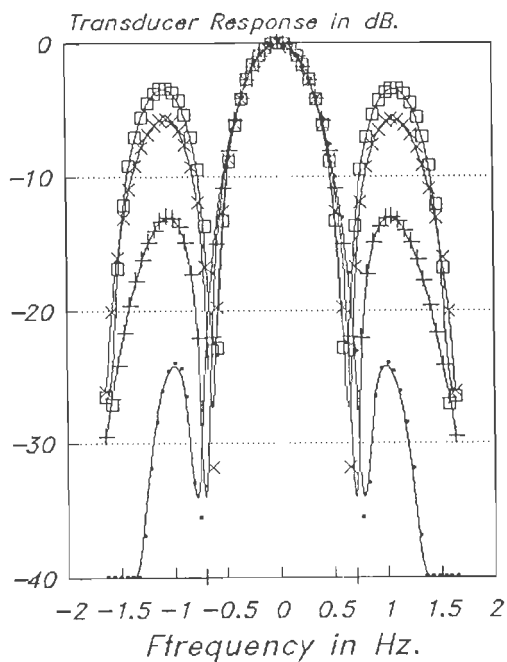


Fig. 5.28 Theoretical frequency responses of SINC apodized IDTs calculated using FFT.

FFT calculated Res.
 — Transducer1 APD; 31
 + Transducer2 APD; 32
 -x- Transducer3 APD; 33
 -□- Transducer4 APD; 34



IDT on the piezo electric substrate. It can be shown mathematically that the corresponding operation in the frequency domain is a convolution of the ideal response with the fourier transform of the IDT comb. This is called windowing because the original impulse response is effectively observed through a window, namely the sampling IDT. The synthesis amounts to the choice of a good impulse response in conjunction with a good window.

An all pass window with a SINC apodized transducer has the disadvantage of leaving scars, in the form of unwanted high frequency oscillations (usually called Gibbs) in the frequency response. More over the resultant frequency response is yet not as close as the ideal requirements. These Gibbs can be overcome and the frequency response can be improved up to some extent by the use of more elaborate windows.

In general it is desirable to obtain a brick-wall type (i.e rectangular) filter response which is simply a frequency translated rectangular function.

$$H(\omega) = \text{rect} \left[\frac{(\omega - \omega_o)}{BW} \right] \quad \dots (5.1)$$

where $H(\omega)$ is the transfer function.

ω, ω_o are angular frequencies.

BW is bandwidth.

The time function fourier transform of equation (5.1) is infinite and unrealizable. The procedure to get appropriate response close to the desirable is to pick a proper time truncation function or window to multiply the infinite time function.

In this chapter we will consider the COSINE function window which is described in equation (5.2) in time domain over a time interval from $-\tau/2$ to $\tau/2$.

$$W_{\text{COS}} = \cos (\pi t/\tau) \quad \dots(5.2)$$

There are many other COSINE windows such as Hamming, Blackman and others [44,46].

5.11 COSINE WINDOWING COMPUTATIONS :

To enable the software package that has been developed earlier to model and simulate apodized transducers, with SINC weighting-COSINE windowing apodization patterns, and two transducer filters with one of the transducers is apodized with one such pattern some additional development has been made to the said package. As in the case of simulating filters with SINC weighted apodized and uniform transducers the software calculates the proper number of finger pairs, sections, fingers per group or number of groups for the apodized transducer to secure matching of the two transducers.

An FFT computation facility has been included also in the package [46] to calculate the expected responses of apodized transducers regardless of the number of finger pairs, sections or groups (i.e assuming continuous $h(t)$). The software calculates the response from sampled rectangular, SINC and COSINE functions. The total length of weighting and windowing functions T is taken to be 1 which represents also the normalized number of pairs, sections or group in an IDT.

The graphs shown in Figure 5.28 represent the FFT calculated responses of SINC apodized IDTs with different lengths of the SINC weighting function. The weighting function in this Figure is truncated at first, second, third and fourth zero crossings. The apodization type is described in figure by a two-digit number. First digit of the apodization type number represents the weighting function and windowing if any, and the second digit represents the length of weighting\windowing function. In figure apodization type number of 31 and 34 represent SINC function weighted transducers with the SINC function truncated at first and fourth zero crossings, respectively.

Figure 5.29 represents the FFT calculated responses of SINC weighted-COSINE windowed IDTs with different lengths of the weighting-windowing functions. Both functions are truncated at first, second, third and fourth zero crossings as indicated by the apodization type number shown in figure. Apodization type number of 41 represents SINC weighting-COSINE windowing apodization type with both functions truncated at first zero crossings.

From both figures of 5.28 and 6,29 the improvement using COSINE function windowing is clear. It can be seen also that increasing the length of the SINC weighting function causes reduction in IDT bandwidth, high side-lobes and increases side-lobes bandwidths, while in the case of COSINE windowed transducers increasing the length of the SINC weighting-COSINE windowing functions increases transducer bandwidth, lower side-lobes levels and decrease side-lobes bandwidths.

In continuation with the study of the different ways of improving the performances of SAW two-transducer filters and to see the effect of COSINE windowing on improving these responses trough studying the responses of simulated SAW filters, different types of such filters having one uniform and one SINC weighted-COSINE windowed transducers have been modeled/simulated. Different combinations of low loss transducers have been used in constructing such filters (filters of GUDTs, TPUDTs and combinations of GUDTs and TPUDTs). In the following sections we present performances results of some of the simulated SINC weighted-COSINE windowed transducers, and filters consist of one such apodized transducer and the other uniform.

5.12 SINC WEIGHTED-COSINE WINDOWED APODIZED GUDTs :
--

Filters of different combinations of group unidirectional transducers with one uniform and another SINC weighted-COSINE

Fig. 5.29 Theoretical frequency responses of sinc apodized IDTs with cosine window function calculated using FFT.

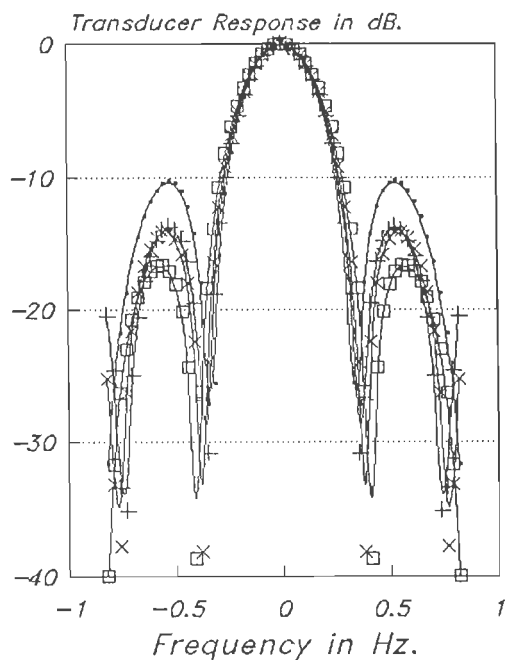
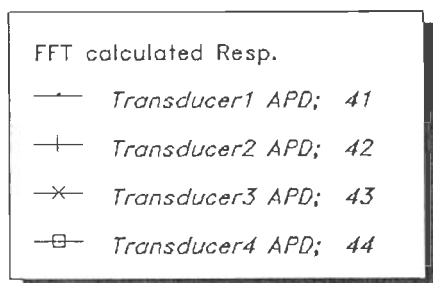
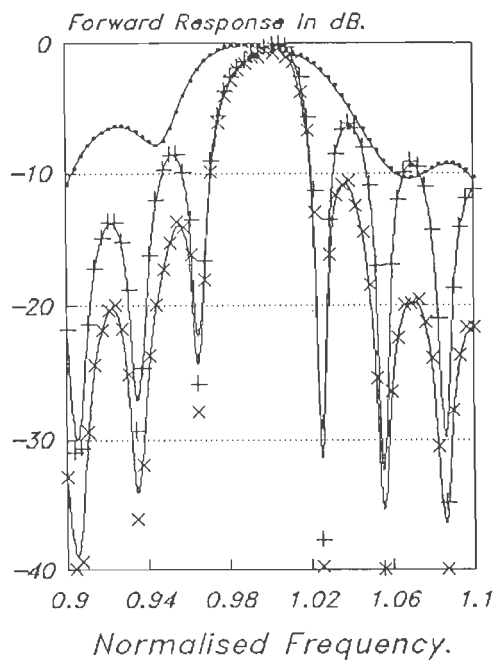
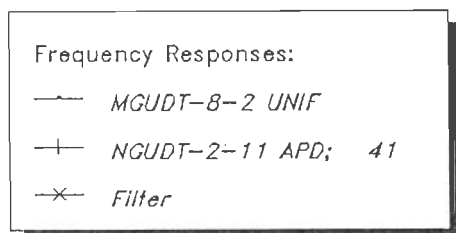


Fig. 5.30 Forward frequency response of uniform MGUDT-8-2, apodized & cosine windowed NGUDT-2-11 and filter of both. Max aperture is $7.3798E-4$ m.



windowed transducers having different numbers of fingers per group and groups have been simulated. Computational results of some of these SINC weighted-COSINE windowed GUDT transducers are presented in Tables 5.16, 5.17 and 5.18. Graphs of performances of some of these transducers are shown later in coming sections. Comparing the results reported in these three tables with results of SINC apodized GUDTs reported in Tables {5.1}, {5.2} and {5.3} one can see the improvements in transducers performances. results related to GUDT-4-5 and GUDT-4-7 in tables show significant improvement in frequency responses of the two transducers in terms of bandwidths and transducers shape factors.

The relation between increasing fingers per group - groups product number and increasing number of groups for constant fingers per group - groups product number on one side and rise, 3dB bandwidths and side-lobes levels on the other side still holds as in the cases of uniform and SINC apodized (unwindowed) GUDT transducers. In case of increasing the used length of the SINC weighting-COSINE windowing functions as in the last two transducers listed in Tables {5.16}, {5.17} and {5.18}, this increased length causes an increase in the rise bandwidth, or more correctly increases the rise to 3dB bandwidths ratio remarkably, which in turn affects negatively the shape factor of the transducer unless a proper increase in number of fingers per group - groups product and number of groups is made.

Table {5.16}

*Computed Rise, 3dB and Fall bandwidths of
SINC weighted-COSINE windowed GUDTs.*

Transducer type	Apodization type	Aperture in meter	RB per cent	3dB BW per cent	FB per cent
N-4-5	41	7.3798E-4	1.016	4.58	0.435
N-4-8	41	3.2799E-4	0.760	3.016	0.1117
N-2-11	41	7.3798E-4	0.8628	3.497	0.3351
N-2-17	41	3.2799E-4	0.4469	2.10	0.134
N-4-7	42	7.3798E-4	1.519	2.737	0.1117
N-4-9	42	4.9169E-4	1.173	1.452	0.1229

Table {5.17}

*Computed left and right side lobes levels of
SINC weighted-COSINE windowed GUDTs.*

Transducer type	Apodization type	Aperture in meter	LSL in dB	RSL in dB
N-4-5	41	7.3798E-4	10.	5.4
N-4-8	41	3.2799E-4	8.52	4.88
N-2-11	41	7.3798E-4	3.408	3.16
N-2-17	41	3.2799E-4	7.6	5.4
N-4-7	42	7.3798E-4	10.	4.08
N-4-9	42	4.9169E-4	11.2	3.69

Table {5.18}

*Computed Rejection bandwidth and Shape factor of
SINC weighted-COSINE windowed GUDTs.*

Transducer type	Apodization type	Aperture in meter	RJ per cent	SHAPE factor
N-4-5	41	7.3798E-4	7.932	0.577
N-4-8	41	3.2799E-4	6.122	0.492
N-2-11	41	7.3798E-4	6.134	0.570
N-2-17	41	3.2799E-4	4.022	0.522
N-4-7	42	7.3798E-4	5.698	0.4803
N-4-9	42	4.9169E-4	4.134	0.351

Table {5.19}

*Computed Rise, 3dB and Fall bandwidths of
SINC weighted-COSINE windowed TPU DTs.*

Transducer type	Apodization type	Aperture in meter	RB per cent	3dB BW per cent	FB per cent
T-19	41	7.3798E-4	2.368	5.237	0.614
T-22	41	4.9169E-4	1.285	4.8044	0.469
T-28	41	3.1467E-4	1.050	4.134	0.223
T-40	42	3.1467E-4	1.664	2.067	0.1675
T-40	43	4.9169E-4	2.592	1.1173	0.335

Table {5.20}

*Computed left and right side lobes levels of
SINC weighted-COSINE windowed TPUDTs.*

Transducer type	Apodization type	Aperture in meter	LSL in dB	RSL in dB
T-19	41	7.3798E-4	8.8	9.4
T-22	41	4.9169E-4	7.92	7.2
T-28	41	3.1467E-4	7.2	5.6
T-40	42	3.1467E-4	10.8	7.2
T-40	43	4.9169E-4	14.6	11.2

Table {5.21}

*Computed Rejection bandwidth and Shape factor of
SINC weighted-COSINE windowed TPUDTs.*

Transducer type	Apodization type	Aperture in meter	RJ per cent	SHAPE factor
T-19	41	7.3798E-4	10.446	0.5047
T-22	41	4.9169E-4	9.072	0.5295
T-28	41	3.1467E-4	7.217	0.5727
T-40	42	3.1467E-4	5.117	0.4039
T-40	43	4.9169E-4	5.094	0.2193

5.13 SINC WEIGHTED-COSINE WINDOWED APODIZED TPUDTs:
--

Many SINC weighted-COSINE windowed three phase unidirectional transducers with different numbers of sections have been simulated. Computational results of some of these transducers are reported in Tables {5.19} to {5.21}.

From these results the effect of increasing number of sections is clear on reducing rise, 3db, fall bandwidths, increasing fall to 3dB bandwidths ratio and decreasing rise to 3dB bandwidths ratio as well as improving the shape factor of the transducer. The effect of increasing the length of SINC weighting-COSINE windowing functions is obvious on increasing rise bandwidth, decreasing 3db and fall bandwidths, increasing rise to 3dB bandwidths ratio and decreasing fall to 3dB bandwidths ratio. This can be seen clearly from the last two transducers listed in tables. The corresponding degradation in transducer shape factor can also be observed.

5.14 FILTERS OF UNIFORM AND SINC WEIGHTED-COSINE WINDOWED (APODIZED) GUDTs :
--

Some of the filters that have been simulated having one uniform and another SINC weighted-COSINE windowed GUDT transducers are listed in Tables {5.22}, {5.23} and {5.24} with their

Table {5.22}
*Computed Rise, 3dB and Fall bandwidths of filters
of uniform and SINC weighted-COSINE windowed GUDTs.*

Transducer type	Apodization type	Aperture in meter	RB per cent	3dB BW per cent	FB per cent
N-8-2	1	7.3798E-4	1.944	3.91	1.452
N-4-5	41				
M-8-2	1	7.3798E-4	0.636	3.363	0.558
N-2-11	41				
N-8-3	1	3.2799E-4	1.340	2.5698	0.67
N-4-8	41				
N-8-3	1	3.2799E-4	1.117	2.011	0.368
N-2-17	41				
N-8-2	1	7.3798E-4	2.022	2.469	0.446
N-4-7	42				

Table {5.23}

Computed left and right side lobes levels of filters of uniform and SINC weighted-COSINE windowed GUDTs.

Transducer type	Apodization type	Aperture in meter	LSL in dB	RSL in dB
N-8-2	1	7.3798E-4	24.88	22.4
N-4-5	41			
N-8-2	1	7.3798E-4	13.76	10.8
N-2-11	41			
N-8-3	1	3.2799E-4	24.44	16.8
N-4-8	41			
N-8-3	1	3.2799E-4	19.2	9.6
N-2-17	41			
N-8-2	1	7.3798E-4	21.	10
N-4-7	42			

Table {5.24}

Computed Rejection bandwidth and shape factor of filters of uniform and SINC weighted-COSIN windowed GUDTs.

Transducer type	Apodization type	Aperture in meter	RJ per cent	SHAPE factor
N-8-2	1	7.3798E-4	7.932	0.493
N-4-5	41			
N-8-2	1	7.3798E-4	6.134	0.548
N-2-11	41			
N-8-3	1	3.2799E-4	6.122	0.4197
N-4-8	41			
N-8-3	1	3.2799E-4	4.022	0.5
N-2-17	41			
N-8-2	1	7.3798E-4	5.698	0.433
N-4-7	42			

corresponding computational results. The relevant performances and some other related responses of these filters and the group unidirectional transducers from which these filters have been constructed (in software) are given in Figures 5.30 to 5.39.

Comparing the computational results of GUDT-8-2/GUDT-4-5 filter given in tables {5.22} to {5.24} with the computational results of the filter of same combination of transducers but without COSINE windowing reported in Tables {5.7} to {5.9} one can see the marginal improvement in rise, 3dB and fall bandwidths which caused marginal improvement in the shape factor of the filter. This marginality (small improvement) is due to the low number of apodized groups used. It can also be seen that the side-lobes levels have been increased marginally due to the COSINE windowing. This increase can be reduced by increasing the length of the SINC weighting-COSINE windowing functions and choosing a proper fingers per group - groups product number and apodized groups number. The corresponding forward frequency response of this filter is shown in Figure 5.31 with its transducers forward responses.

In an attempt to get more improved performance than that of NUGUDT-8-2/GUDT-2-10 whose frequency response shown in Figure 5.7 earlier(its computational results listed in Tables {5.7} to {5.9}) in addition to the improvement caused by the COSINE windowing, the uniform transducer type has been changed by some other group unidirectional transducer. Modified type GUDT has been

Fig. 5.31 Forawrd frequency response of uniform NGUDT-8-2, sinc apodized and cosine windowed NGUDT-4-5 and filter of both. Max aperture is $7.3798E-4$ m.

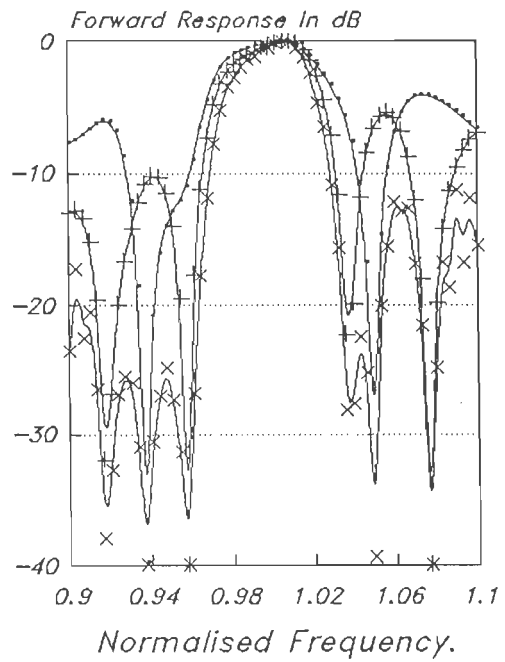
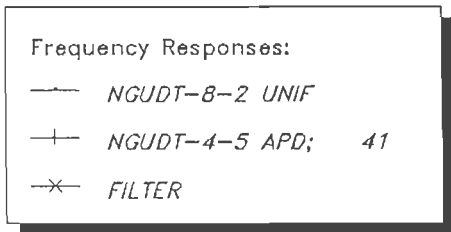
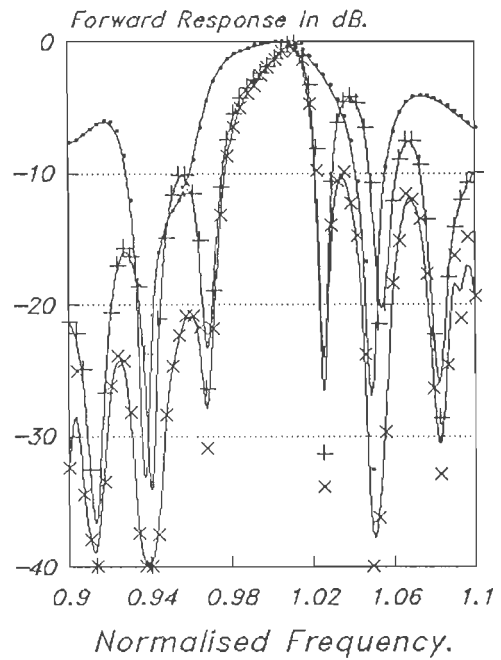
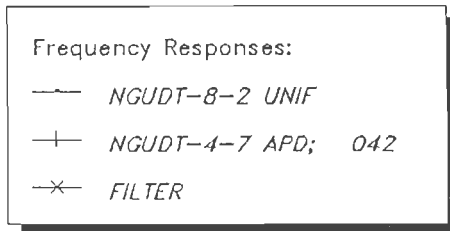


Fig. 5.32 Forward frequency response of uniform NGUDT-8-2, sinc apodized and cosine windowed (two zero crossing) NGUDT-4-7 and filter of both transducers. Max aperture is $7.3798E-4$ m.



used instead of the New type GUDT with the same finger and group numbers. Figure 5.30 shows the forward frequency response of this filter in addition to the forward responses of the two building transducers. From Figure and the corresponding computational results presented in Tables 5.22 to 5.24 it can be seen that an improvement has been achieved in the shape factor with reduction in rise, 3dB and fall bandwidths, lowering rise to 3db bandwidths ratio yet having higher side-lobes level which requires some more improvement.

The frequency response of GUDT-8-2/GUDT-4-7 filter shown in Figure 5.32 with the weighting-windowing functions of the apodized transducer truncated at second zero crossing shows very slow rise and very sharp fall. And although the rise to 3dB bandwidth ratio is high (0.818) still the shape factor is not bad. The performance of the filter can be improved by reselecting proper numbers of fingers and groups.

The filters GUDT-8-3/GUDT-4-8 and GUDT-8-3/GUDT-2-17 whose frequency responses are shown in Figures 5.33 and 5.36 and their computational results are given in Tables {5.22} to {5.24} show clearly how increasing the number of apodized groups (in approximately equal fingers per group - groups product number) can improve the shape factor of a filter of same combination of transducers types but with sacrificing side-lobe rejection levels as per this filter.

Fig.5.33 Forward frequency response of uniform NGUDT-8-3, sinc apodized and cosine windowed NGUDT-4-8 and filter of both. Max aperture is $3.2799E-4$ m.

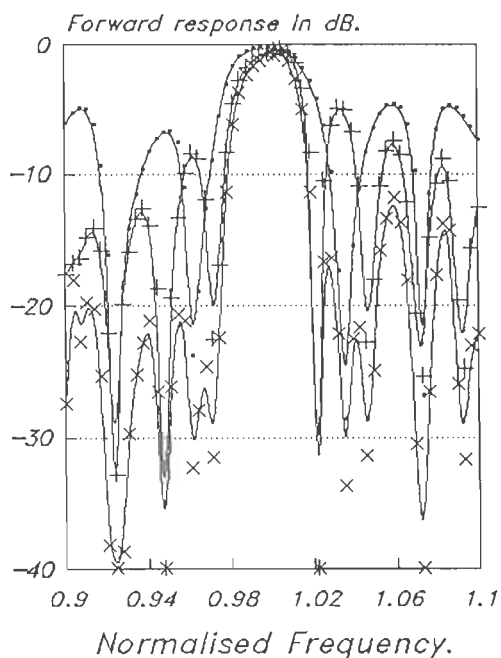
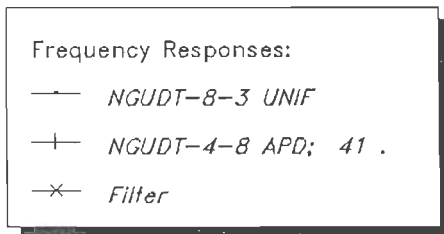


Fig. 5.34 Input admittance of uniform NGUDT-8-3, apodized and cosine windowed NGUDT-4-8 and filter of both transducers. Max aperture is $3.2799E-4$ m.

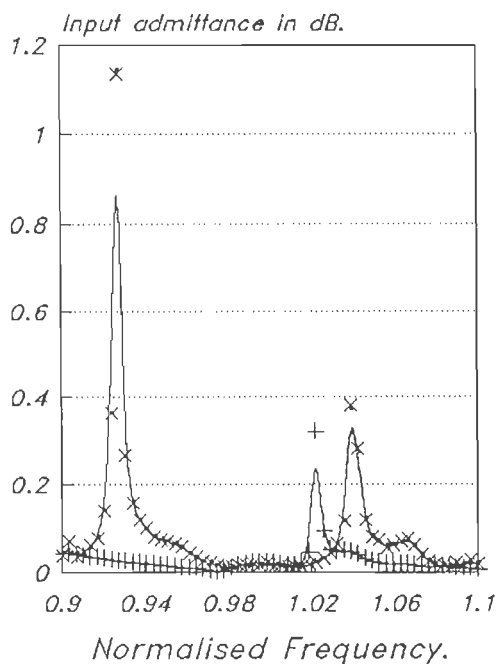
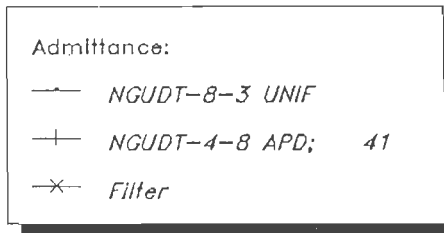


Fig. 5.35 Phase response of uniform NGUDT-8-3, sinc apodized and cosine windowed NGUDT-4-8 and filter of both transducers.

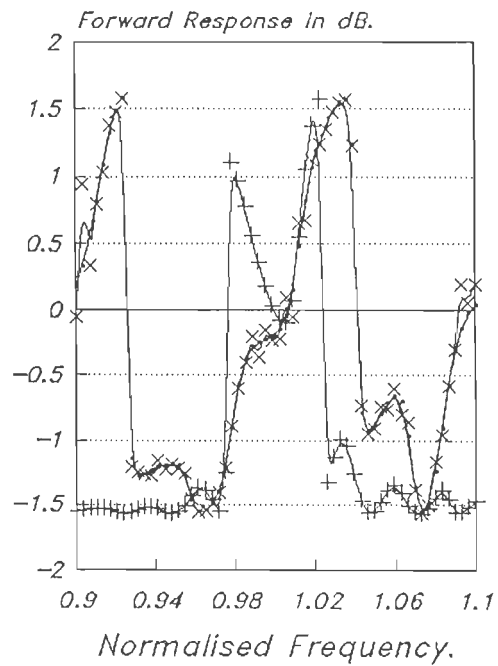
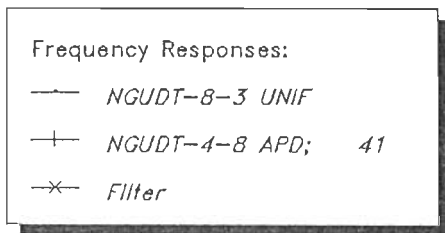


Fig. 5.36 Forward frequency response of uniform NGUDT-8-3, sinc apodized and cosine windowed NGUDT-2-17 and filter of both. Max aperture is $3.4799E-4$ m.

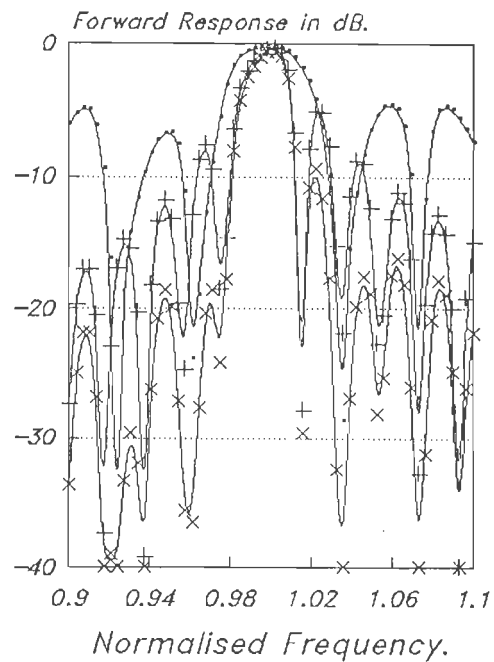
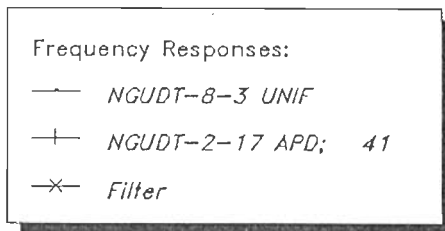


Fig. 5.37 Relative directivity of uniform NGUDT-8-3, apodized and cosine windowed NGUDT-2-17 and filter of both.

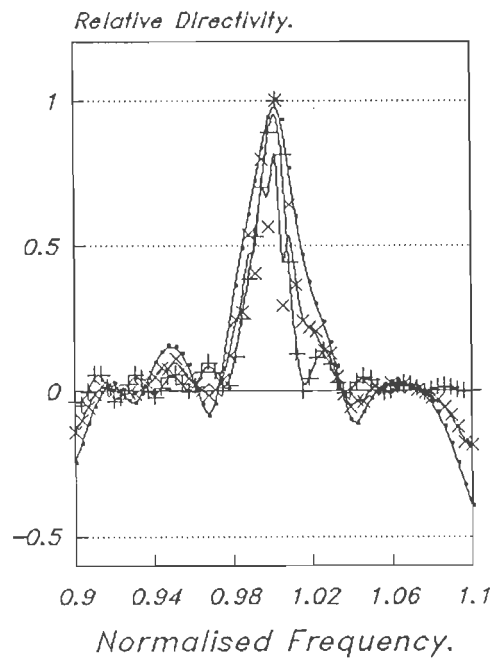
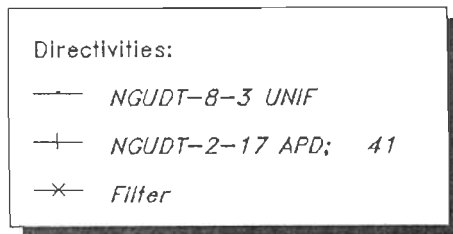
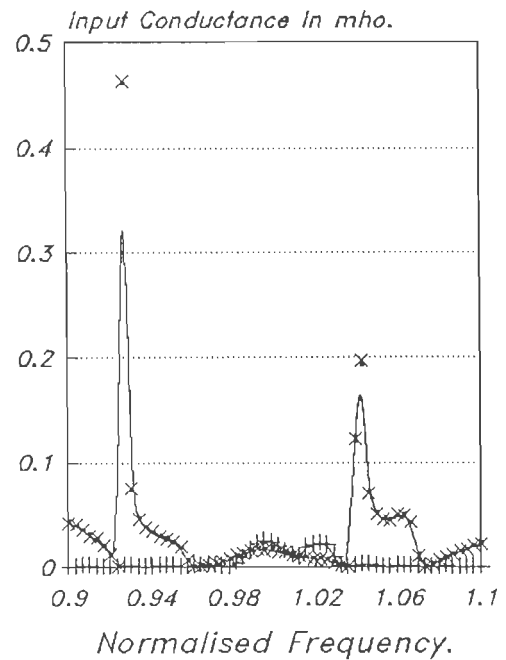
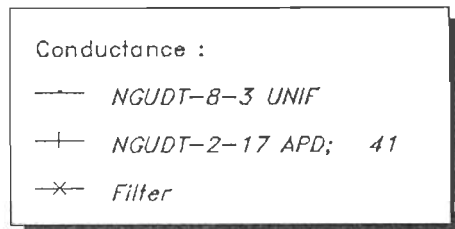


Fig. 5.38 Conductance response of uniform GUDT-8-3, apodized and cosine windowed GUDT-2-17 and their filter. Max aperture is $3.2799E-4$ m



Figures 5.34, 5.35, 5.38, 5.39 show admittance, phase, conductance, and susceptance responses, respectively of the above mentioned two filters. Differences in these responses between the uniform and the apodized (weighted and windowed) transducers are also observed. From figures it appears that although in forward response the filter response is very close to that of the apodized transducer in the above responses it follows the uniform transducer with some oscillations (ripples) in filters phase responses at and around f_0 .

The effect of both uniform and apodized transducer side-lobes having different frequency locations in giving low filter side-lobes levels (or even some times cancellation of some filter side-lobes) is very clear from responses shown in Figures 5.30 and 5.33.

Figure 5.37 shows a plot of the relative directivity of GUDT-8-3/GUDT-2-17 filter and those of its transducers. The directivity of the apodized transducer (in this filter) is sharper than that of the uniform transducer. The directivity plot of the filter is more sharp with many up-and-downs in the main lobe.

5.15 FILTERS OF UNIFORM AND SINC WEIGHTED-COSINE WINDOWED (APODIZED) TPUUTs :

A number of three phase unidirectional transducers filters with one uniform transducer and another (SINC weighted-COSINE

Fig. 5.39 Susceptance response of uniform GUDT-8-3, apodized and cosine windowed GUDT-2-17 and their filter.

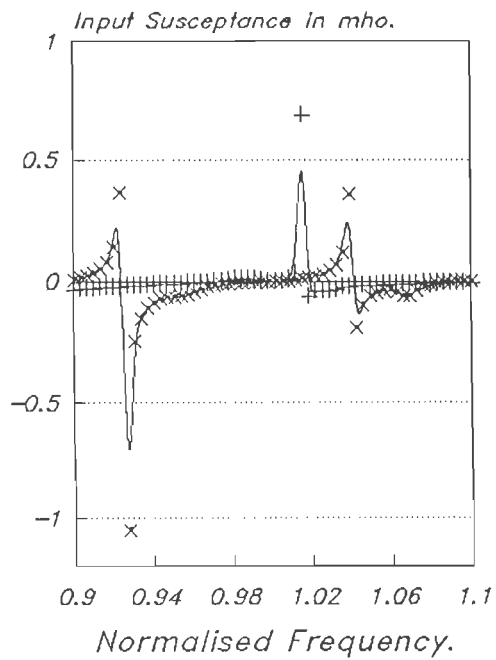
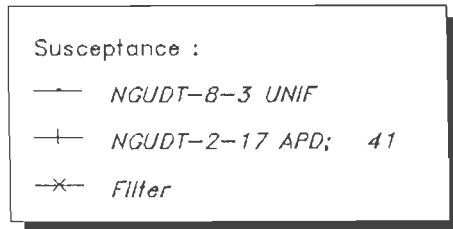
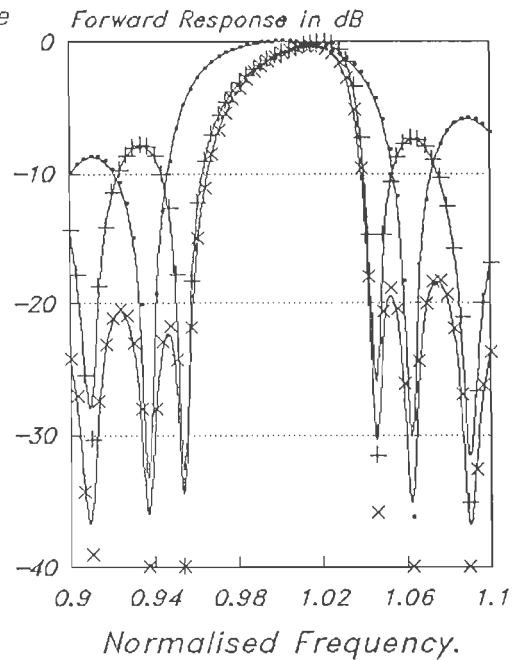
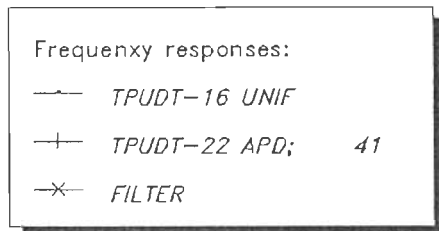


Fig. 5.40 Forward frequency response of uniform TPUDT-16, apodized and cosine windowed TPUDT-22 and their filter.



windowed) apodized transducer have been simulated. Some of these filters computational results are given in Tables {5.25}, {5.26} and {5.27} and some of their responses are shown in Figure 5.40 to 5.50.

Comparing the computational results of TPUDT-16/TPUDT-22 filter whose frequency response is shown in Figure 5.40 with that of Figure 5.14 and its relevant computational results given in Tables {5.10} to {5.12} we can see the deterioration in filter performance and shape factor when COSINE windowing is used due to the improper selection of number of sections. From filter forward response it can be seen that using the window function caused an increase in the rise to 3dB bandwidths ratio and a decrease in fall to 3db bandwidths ratio.

This response deterioration can be cured and the response can be further improved by increasing the number of sections, as we will see later. Figures 5.41 to 5.44 show admittance, phase and backward responses as well as the relative directivity of this filter and its transducers for comparison with same responses corresponding to the filter whose forward response is shown in Figure 5.14 and its other responses reported earlier in this chapter after the mentioned figure.

In agreement with the results obtained earlier from TPUDT/TPUDT weighted -unwindowed filters a deteriorated performance has been obtained when the apodized transducer of the

Table {5.25}

Computed Rise, 3dB and Fall bandwidths of filters of uniform and SINC weighted-COSINE windowed TPUDTs.

Transducer type	Apodization type	Aperture in meter	RB per cent	3dB BW per cent	FB per cent
T-16	1	4.9169E-4	2.88	4.357	0.12
T-22	41				
T-20	1	3.1467E-4	1.34	3.787	0.67
T-28	41				
T-20	1	3.1467E-4	1.564	2.067	0.279
T-40	42				
T-16	1	4.9169E-4	2.703	1.1173	0.39
T-40	43				

Table {5.26}

*Computed first left and right side lobes levels
of filters of uniform and SINC weighted-COSINE windowed
TPUDTS.*

Transdu- cer type	Apodizat- ion type	Aperture in meter	LSL in dB	RSL in dB	dB
T-16	1	4.9169E-4	20.	19.12	
T-22	41				
T-20	1	3.1467E-4	20.4	17.12	
T-28	41				
T-20	1	3.1467E-4	15.	10.	
T-40	42				
T-16	1	4.9169E-4	16.48	12.56	
T-40	43				

Table {5.27}

Computed Rejection bandwidth and Shape factor of filters of uniform and SINC weighted-COSINE windowed TPUDTs.

Transducer type	Apodization type	Aperture in meter	RJ per cent	SHAPE factor
T-16	1	4.9169E-4	9.072	0.48
T-22	41			
T-20	1	3.1467E-4	7.217	0.5247
T-28	41			
T-20	1	3.1467E-4	5.117	0.4039
T-40	42			
T-16	1	4.9169E-4	5.094	0.2192
T-40	43			

filter, whose frequency response is shown in Figure 5.40, has been apodized with increased SINC weighting-COSINE windowing functions length (without properly increasing the number of sections.). This is clear from the frequency response of TPUDT-16/TPUDT-40 filter with the weighting-windowing functions truncated at third zero crossing. Very slow response rise and so sharp fall with high rise to 3dB bandwidths ratio cause very low shape factor of 0.2192.

In an attempt to improve the performance of TPUDT-16/TPUDT-22 filter of Figure 5.40 discussed earlier a filter with the same type and same apodization profile with increased number of sections (to decrease the rise to 3dB bandwidths ratio and increase the fall to 3dB bandwidths ratio) has been simulated. The new filter with the increased number of sections is TPUDT-20/TPUDT-28.

Comparing the computational results of this filter given in Tables {5.25} to {5.27} and the corresponding forward frequency response shown in Figure 5.47 with that of TPUDT-16/TPUDT-22 one can see the extent of improvement. It can be seen also from both tables and Figure 5.47 that the response rise is still much slower than its fall compared to that of TPUDT-16/TPUDT-20 filter reported in Tables {5.10} to {5.12} earlier. Selecting still higher number of sections will improve both rise and fall to 3dB bandwidths ratios and therefore cause more improvement in filter response and shape factor.

Fig 5.41 Admittance response of uniform TPUDT-16, apodized and cosine windowed TPUDT-22 and their filter.

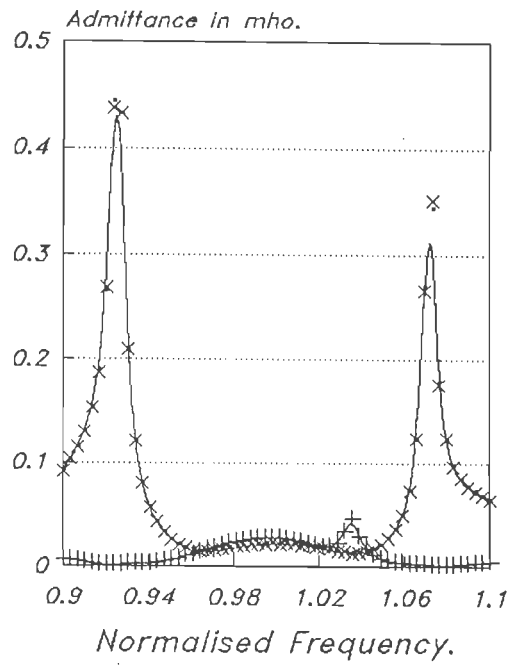
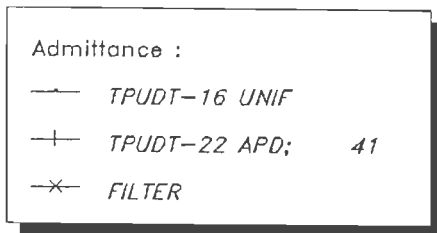


Fig. 5.42 Phase response of uniform TPUDT-16, apodized and cosine windowed TPUDT-22 and their filter.

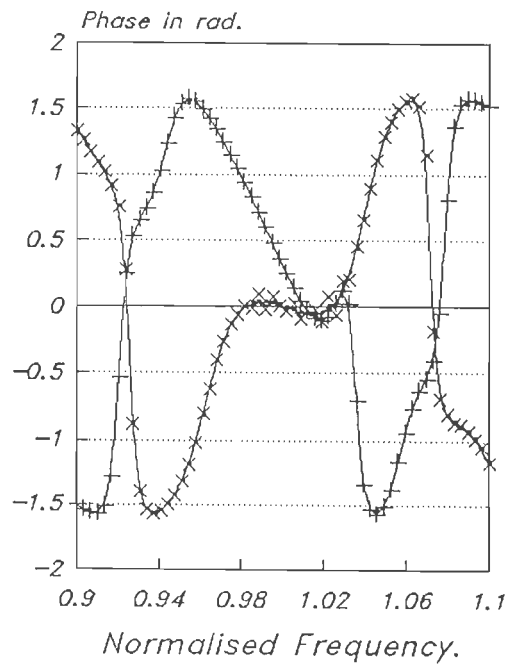
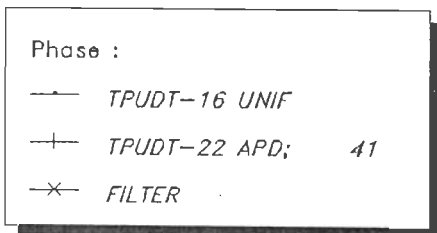


Fig. 5.43 Backward frequency response of uniform TPUDT-16, apodized and cosine windowed TPUDT-22 and their filter. Max aperture is $3.2799E-4$ m.

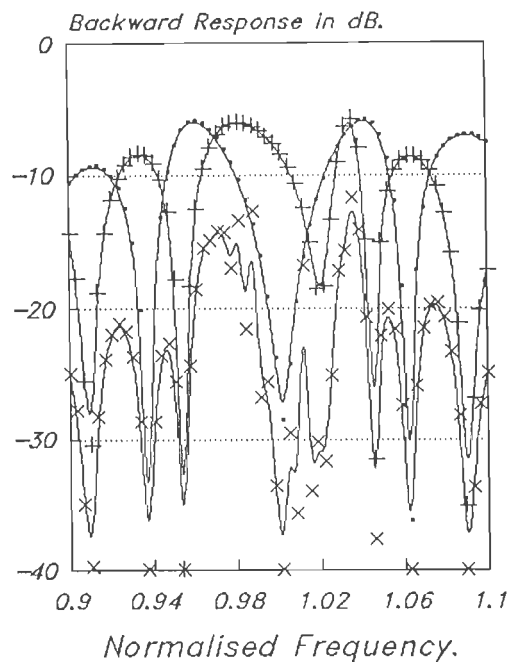
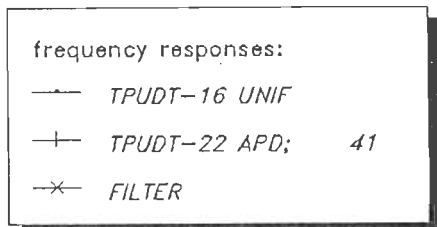


Fig. 5.44 Relative directivity of uniform TPUDT-16, apodized and cosine windowed TPUDT-22 and their filter.

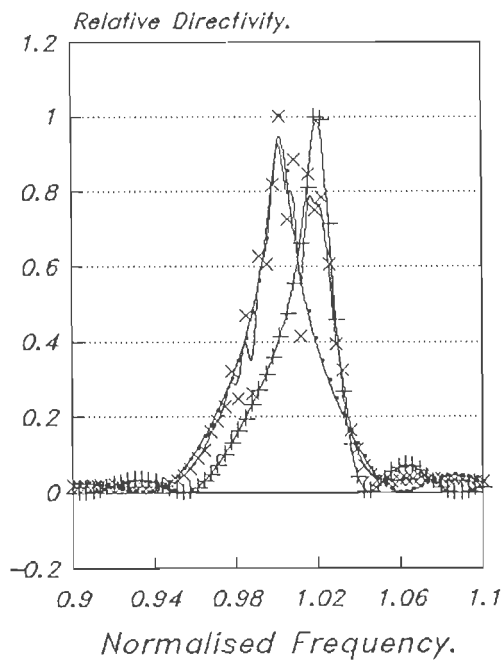
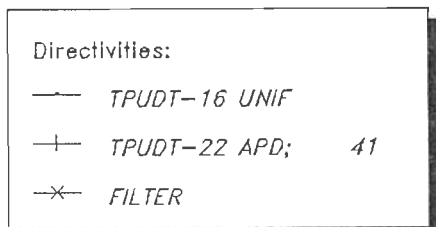


Fig. 5.45 Forward frequency response of uniform TPUDT-16 apodized and cosine windowed (three zero crossing) TPUDT-40 and their filter. Max aperture is $4.9199E-4$ m.

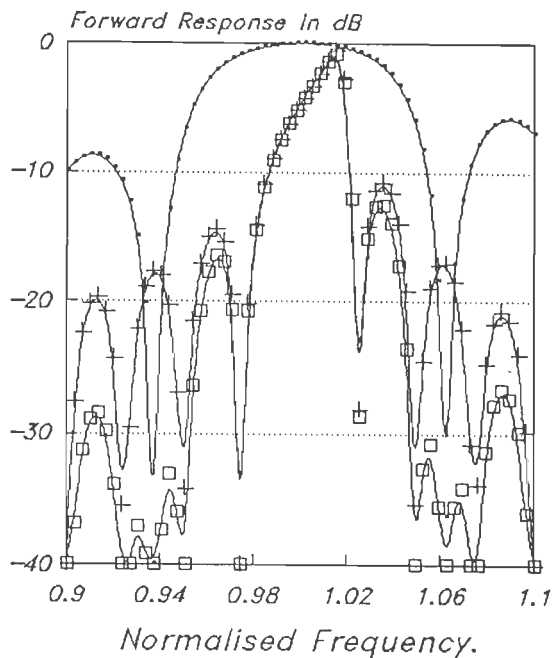
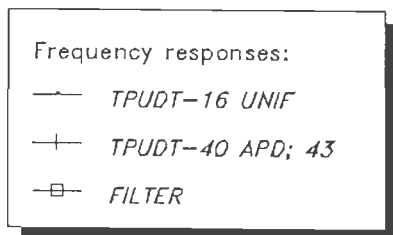
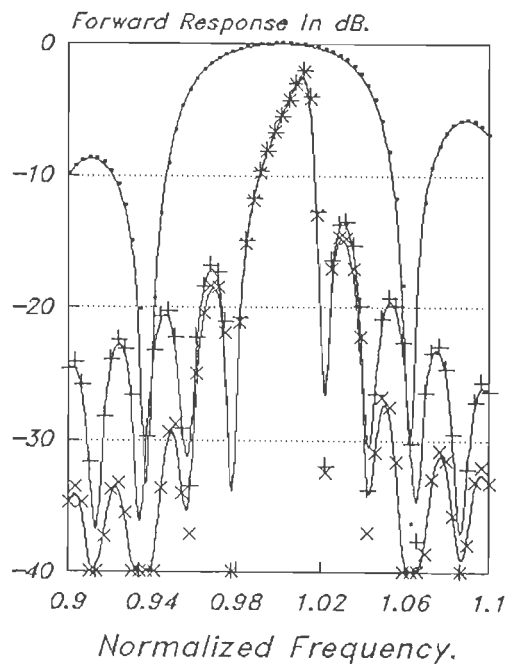
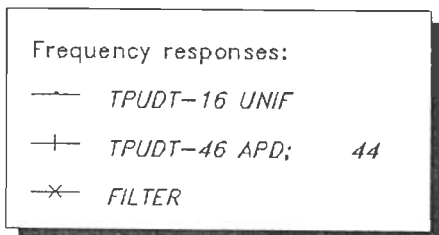


Fig. 5.46 Forward frequency response of uniform TPUDT-16, apodized and cosine windowed (four zero crossing) TPUDT-46 and their filter. Max. aperture is $4.9199E-4$ m.



For lowering filter side-lobes levels the apodization pattern of the apodized transducer has to be changed by increasing the length of weighting-windowing functions with a suitable additional increase in the number of sections to compensate the effect of this (weighting-windowing functions) lengthening on both rise and fall to 3dB bandwidths ratios.

Phase response and relative directivity of TPUDT-20/TPUDT-28 filter and its transducers are shown in Figures 5.48 and 5.49, respectively, for comparison with those of TPUDT-16/TPUDT-22 of apodization type number 41 and TPUDT-16/TPUDT-20 of apodization type number 31.

Increasing the length of weighting-windowing functions without increasing the number of sections properly will cause a filter performance similar to that of Figure 5.50. The apodization profile of TPUDT-20/TPUDT-28 filter has been changed by further lengthening the weighting-windowing functions one more zero crossing without increasing the number of sections to compensate the effect of low rise and sharp fall caused by this lengthening.

5.16 FILTERS OF COMBINATIONS OF UNIFORM AND SINC WEIGHTED-COSINE WINDOWED (APODIZED) GUDTs AND TPUDTs :

Many filters of mixed type of unidirectional transducers (GUDTs and TPUDTs) with the uniform transducer of one type and the apodized (SINC weighted-COSINE windowed) transducer of the other

Fig. 5.47 Forward frequency response of uniform TPUDT-20, apodized and cosine windowed TPUDT-28 and their filter. Max. aperture is $3.1487E-4$ m.

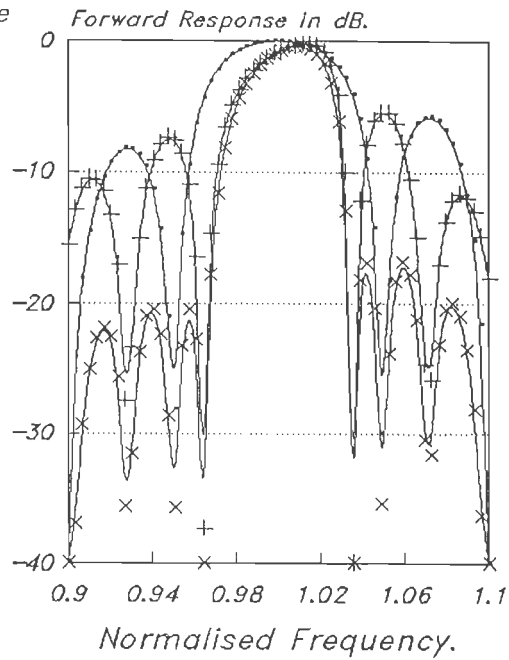
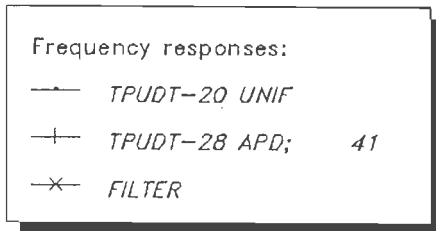


Fig. 5.48 Phase response of uniform TPUDT-20, apodized and cosine windowed TPUDT-28 and their filter. Max. aperture is $3.1487E-4$ m.

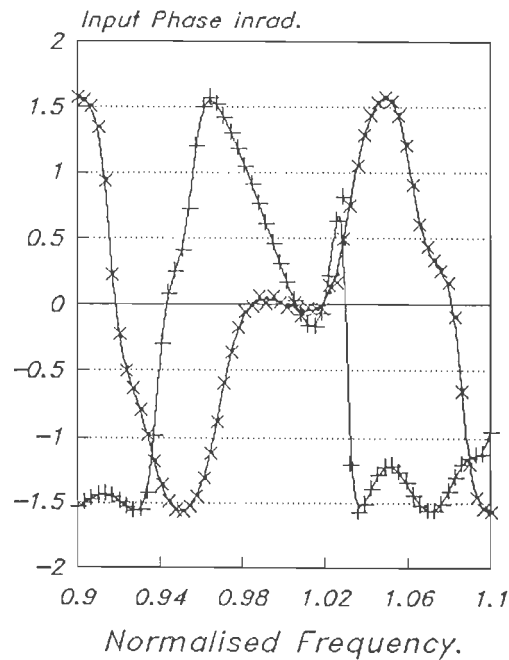
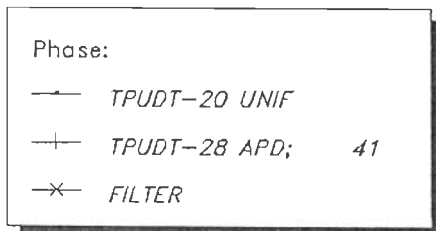


Fig. 5.49 Relative directivity of uniform TPUDT-20, apodized and cosine windowed TPUDT-28 and their filter.

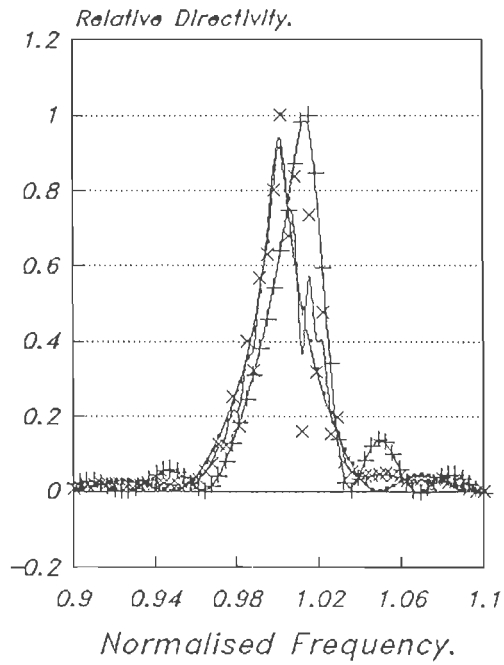
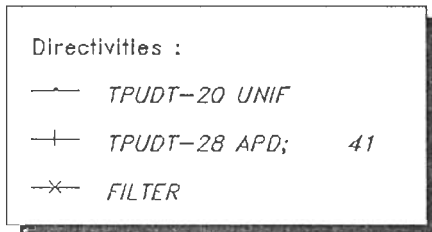
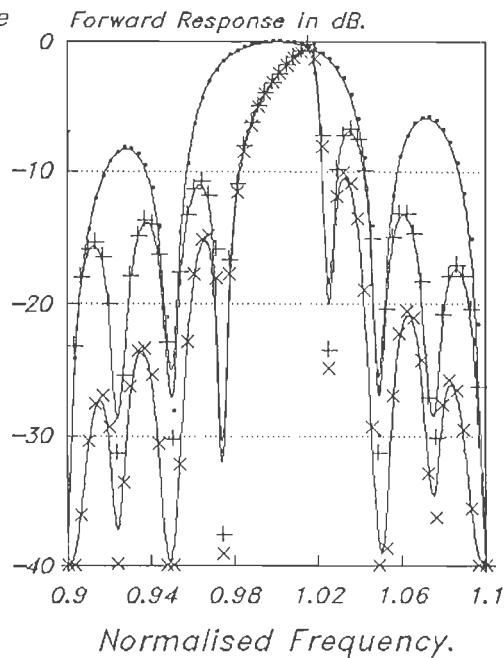
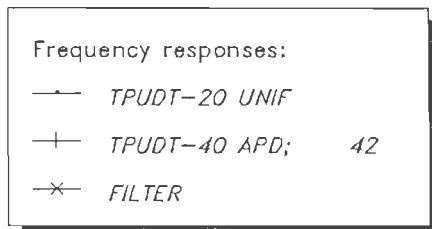


Fig. 5.50 Forward frequency response of uniform TPUDT-20, apodized and cosine windowed (two zero crossing) TPUDT-40 and their filter. Max. aperture is $3.1487E-4$ m.



type have been simulated. In Tables {5.28}, {5.29} and {5.30} we present the computational results of some of these transducers with their forward frequency responses shown in Figures 5.51, 5.53 and 5.54.

In all the filters presented here the uniform transducers are group type unidirectional transducers and the apodized transducers are three phase type unidirectional transducers. It can be seen from the frequency responses of uniform and apodized transducers of GUDT-8-2/TPUDT-19 filter and GUDT-8-3/TPUDT-28 filter shown in Figures 5.51 and 5.53 that the uniform transducers in both filters are either having narrower or comparable bandwidth to that of the apodized transducer of the same filter which gives a filter response that is not very close to either of the uniform or the apodized transducer.

It has been found from the different filters that have been simulated that for a better performance it is preferable to have a wider band uniform transducer with a narrower band apodized transducer. In this case the main lobe of the filter response will be very close to that of the apodized transducer. This makes the design of the filter easier by selecting the apodization profile and the number of groups/sections that will give apodized transducer response close to the required filter response.

Moreover the use of narrower and wider bands transducers in constructing a filter may give very low side-lobes levels

Table {5.28}

*Computed Rise, 3dB and Fall bandwidths of filters
of combinations of uniform and SINC weighted-COSINE windowed*

GUDT and TPUDT transducers.

Transdu- cer type	Apodizat- ion type	Aperture in meter	RB per cent	3dB BW per cent	FB per cent
N-8-2	1	7.3798E-4	2.547	3.798	1.396
T-19	41				
NU-8-3	1	3.2799E-4	1.765	3.296	0.983
T-28	41				
NU-8-3	1	3.2799E-4	2.145	1.843	0.446
T-40	42				

Table {5.29}

Computed first left and right side lobes levels of filters of combinations of uniform and SINC weighted-COSINE windowed GUDT and TPUDT transducers.

Transducer type	Apodization type	Aperture in meter	LSL in dB	RSL in dB
N-8-2	1	7.3798E-4	15.04	14.8
T-19	41			
NU-8-3	1	3.2799E-4	16.4	13.77
T-28	41			
NU-8-3	1	3.2799E-4	22.48	15.2
T-40	42			

Table {5.30}

Computed Rejection bandwidth and Shape factor of filters of combination of uniform and SINC weighted-COSINE windowed GUDT and TPUDT transducers.

Transducer type	Apodization type	Aperture in meter	RJ per cent	SHAPE factor
N-8-2	1	7.3798E-4	10.15	0.374
T-19	41			
NU-8-3	1	3.2799E-4	7.24	0.455
T-28	41			
NU-8-3	1	3.2799E-4	5.072	0.363
T-40	42			

Fig.5.51 Forward frequency response of uniform NGUDT-8-2, apodized and cosine windowed TPUDT-19 and their filter.
Max aperture is $7.3798E-4$ m.

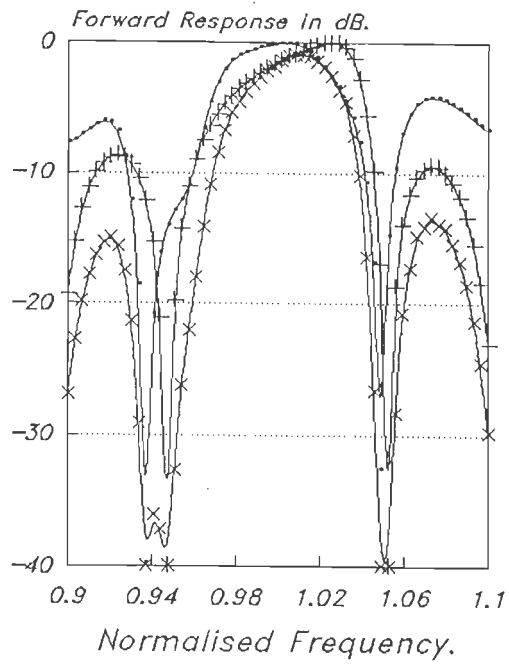
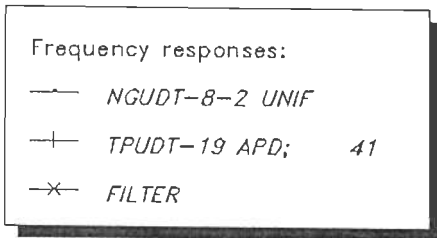
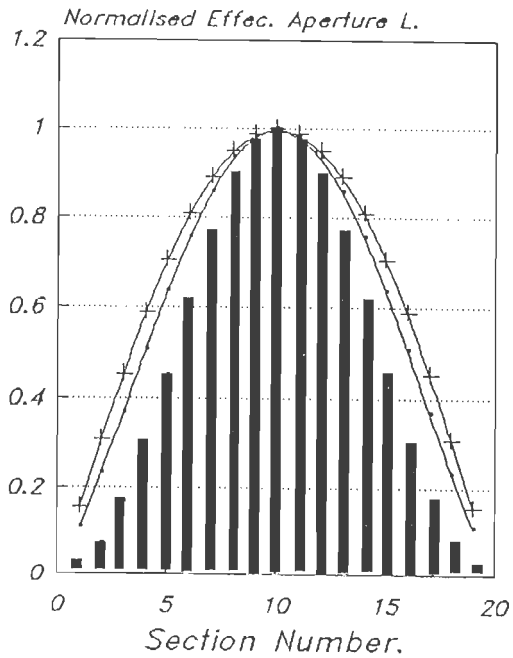
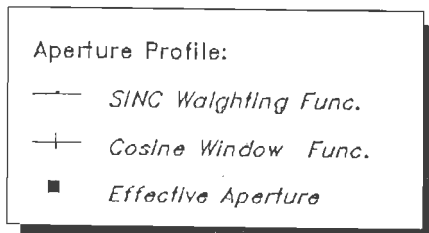


Fig. 5.52 Effective aperture of apodized and cosine windowed TPUDT-19.
Max. aperture is $7.3798E-4$ m.



(specially side-lobes close to the main lobe) or even cancellation of some of these side-lobes due to the different frequency locations of the two transducers side-lobes.

For this reason also it has been found that the performance of filters constructed from uniform GUDT and apodized TPUDT with the SINC weighting-COSINE windowing functions truncated at the first zero crossing is not as good as the performances of many filters constructed from uniform TPUDTs and apodized GUDTs with the same apodization profiles.

It can be seen also from the two mentioned Figures that the responses of apodized transducers in both filters have very slow rise and fast fall which gives low transducer and filter shape factor. This transducer performance can be improved by increasing the number of sections which may improves the filter performance. Here we would like to mention that we found that improving the performance of a filter of same type of uniform and apodized transducers is much easier than that of a filter with mixed combination of TPUDT and GUDT.

Figure 5.54 shows the forward response of NUGUDT-8-3/TPUDT-40 filter with the weighting-windowing functions truncated at second zero crossing. The main lobe of the filter response follows that of the apodized transducer because the uniform transducer is much wider. The filters side-lobes levels are so low compared to the previous two filters (see table {5.29}) due to the different

Fig. 5.53 Forward frequency response of uniform NUGUDT-8-3, apodized and cosine windowed TPUDT-28 and their filter. Max. Aperture is $3.2799E-4$ m

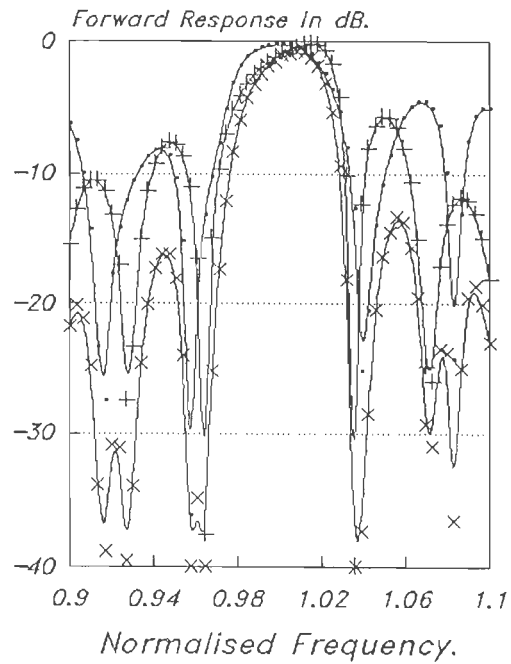
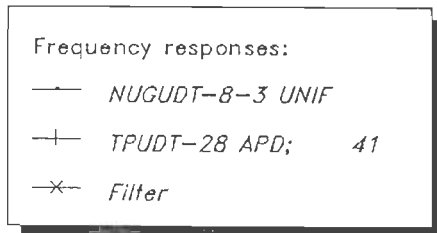
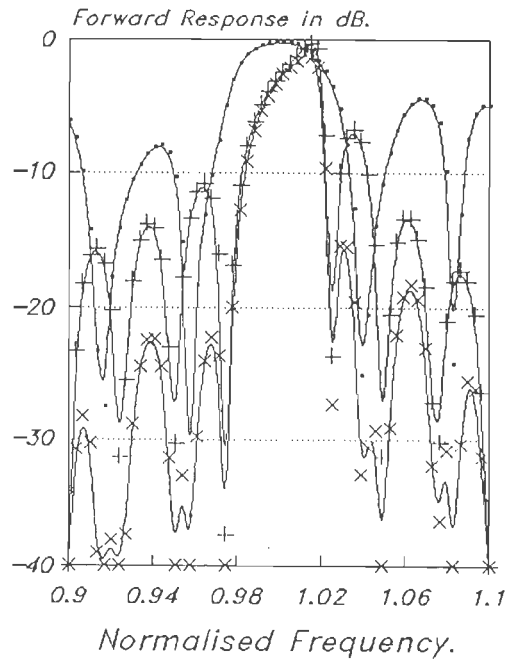
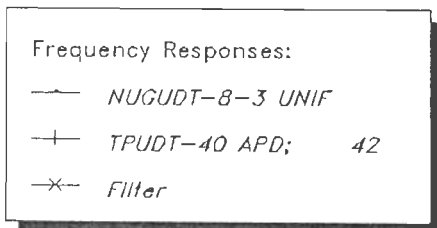


Fig. 5.54 Forward frequency response of uniform NUGUDT-8-3, apodized and cosine windowed (two zero crossing) TPUDT-40 and their filter. Max aperture is $3.2799E-4$ m.



frequency locations of the two transducers side-lobes. The shape factor of the filter is low due to the high rise to 3db bandwidths ratio caused by lengthening the weighting-windowing function. It is worth to mention that the shape factor is a measure of how close is the filter response to the brick-wall response. In some applications such as in channel-equalizer filters, such response with this low shape factor may be desirable.

For improving the shape factor of both the apodized transducer and filter compensation of the effect of lengthening the weighting-windowing functions is required. This can be done by increasing the number of apodized sections for the same apodization profile. Increasing the apodized sections of the TPUDT requires a suitable increase in the number of fingers per groups-groups product of the uniform GUDT transducer to secure matching.

Note that all numbers of fingers per group - groups product of GUDTs and number of sections of TPUDTs and transducers aperture lengths have been calculated so that transducers admittances at f_0 in all filters are equal to 0.002 mho or the transducers impedances are equal to 50 ohm.

5.17 CONCLUSION :

In order to study the performances of apodized transducers and filters with one apodized and one uniform transducers, the

performances of apodized and windowed transducers and filters with such transducers, and the improvement in transducers/filters responses caused by apodization and windowing techniques, both apodization and windowing techniques have been studied. SINC weighting and COSINE windowing have been considered and applied. The software package developed earlier has been improved to include the simulation of such filters. FFT computation facility has been also included to study windows in both time and frequency domains, and to calculate the theoretical responses of weighted and windowed transducers.

Filters of different combinations of low loss GUDTs and TPUDTs with one uniform and one apodized transducers have been simulated. Apodization has been performed in all cases studied in this chapter either using SINC weighting function only or using SINC weighting function along with COSINE window. Different apodization profiles have been used using the two functions with different lengths in performing the apodization. Fingers in each group/section have been kept constant in apodized unidirectional transducers and aperture variations have been performed per groups/sections and not per fingers in each.

Computational results and graphs of performances of these simulated filters and its uniform and apodized transducers along with some other related responses have been studied and reported. The results of both apodized and windowed transducers/filters gave an idea about the extent of improvement in performances using the

two techniques (SINC weighting and COSINE windowing). Many useful conclusions and remarks have been obtained from studying the different performances results of the simulated filters which we feel that it is very helpful in designing SAW apodized and COSINE windowed transducers/filters.

It has been found from the different filters that have been simulated that it is not only the apodization profile of the apodized transducer that decides the SAW filter response. Selecting the apodization profile means selecting either SINC weighting or COSINE windowing as well with different lengths of the weighting windowing functions. It has been found that there are many factors that affect the SAW filter response and it has to be taken into consideration when designing SAW filter using one or both mentioned techniques in addition to the selection of the proper apodization profile. some of these factors are the selection of the two transducers combinations, uniform transducer bandwidth relative to the apodized transducer bandwidth, number of apodized groups/sections, number of fingers per group, frequency locations of both transducers side-lobes...etc.

The numbers of sections/groups and fingers per group have great effect on apodized transducers/filters performances. It is not simply the effect of these numbers on rise, 3dB, fall bandwidths and side-lobes levels as the case in filters of two uniform transducers discussed in the previous chapter. Changing these numbers in apodized transducer/filters may cause drastic

changes in transducer/filter response because it affect greatly rise to 3dB bandwidths ratio and fall to 3dB bandwidth ratio in addition to the effect on these bandwidths which is the same effect as in uniform transducers/filters. Proper selection of number of pairs/sections/groups and fingers per group is very essential in getting good apodized/windowed transducer/filter response.

Changing the apodization profile by changing the length of the SINC weighting-COSINE windowing functions has great effect on the apodized transducer/filter performance. Increasing this length increases the rise to 3dB bandwidths ratio and decreases fall to 3dB bandwidths ratio. if the lengthening is performed with proper increase in apodized sections/groups numbers it will cause great improvement in apodized transducer/filter performance, shape factor and side-lobe levels as well in COSINE windowed transducers. Increasing number of sections/groups of apodized transducers compensates the effect of increasing the length of weighting-windowing function on rise to 3dB bandwidths ratio and fall to 3dB bandwidths ratio.

The behavior of rise and fall bandwidths of weighted-windowed transducers/filters have been found to be related but different. While both bandwidths and 3dB bandwidth are increasing or decreasing with the decrease or increase of number of sections/groups and fingers per group - groups product the ratio of rise to 3dB bandwidths decreases with the increase of number of

sections/groups and fingers per group - groups product. The fall to 3dB bandwidths ratio behaves the opposite way. Rise to 3dB bandwidths ratio increases with the increase of weighting-windowing functions length and fall to 3dB bandwidths ratio decreases with this increase. Right side-lobe level is related also to rise to 3dB bandwidths ratio. The level is high with high rise to 3dB bandwidths ratio. Rise, 3dB and fall bandwidths have great importance in determining the shape factor of weighted-windowed transducer/filter. Generally it is required to have very low and equal rise and fall to 3dB bandwidths ratios yet in some applications like equalizer filters high rise bandwidths may be required.

Filter side-lobes levels are determined from both uniform and apodized transducers side-lobes levels. Another factor of great effect on reducing filter side-lobes levels is the differences in frequency locations of the two transducers side-lobes. These differences in frequency locations causes great lowering of filter side-lobes levels and in some cases cancellation of some of these side-lobes creating side-lobe-free frequency bands.

If the uniform transducer frequency response is much wider than the apodized transducer response then these side-lobes cancellations or levels lowering will be close to filter main lobe. Selection of uniform filter response affects filter side-lobes levels as well as filter response in general.

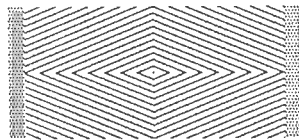
The selection of wider band uniform transducer simplifies the design of the SAW filter in the sense that the designer will worry about the apodized transducer response only, because in this case main lobe of filter response will be very close to the apodized transducer main lobe. In addition to that choosing a wider band uniform transducer response will lower filter side-lobes due to differences in frequency locations of both uniform and apodized transducers side-lobes as discussed earlier.

It has been found that due to the differences required between the the uniform and apodized bandwidths, if mixed types unidirectional transducers are to be used in constructing a filter then it is better for good filter performance to choose the TPU DT type transducer as uniform transducer and apodize the GUDT transducer in case the weighting-windowing function is truncated at first zero crossing, because in such length the apodized TPU DT bandwidth will be very close to or wider than the uniform GUDT bandwidth. The later will give filter response which is not close to either of transducers and with possible greater insertion loss. If SINC weighting-COSINE windowing functions are truncated after more than one zero crossing then any combination of TPU DT and GUDT can be used depending upon the required filter response.

It has been found that using a wide band uniform transducer with narrower band apodized transducer in constructing a filter, the different filter responses in the pass frequency band will be as follow: The forward frequency response will be very close to

the apodized transducer frequency response, Admittance, phase, conductance and susceptance responses will be very close to corresponding responses of the uniform transducer with some oscillations or ripples in the filter phase response unless dummy fingers are used. Filter backward frequency response and directivity response may or may not be close to either of uniform and apodized transducers.

So far in this chapter we have studied and discussed SINC function apodization and COSINE function windowing. In the next chapter we will discuss and present some other apodization profiles by using some other window functions.



CHAPTER SIX

6

Modified Bessel Function Window Family.

- 6.1 Introduction.
- 6.2 Windows For SAW Transducers.
- 6.3 Modified Bessel Function
Window Family.
- 6.4 Computation Of Modified Bessel
Function Window Family.
- 6.5 Characteristics Of Different
MBF Windows.
- 6.6 New Apodization Profiles Using
MBF Windows.
- 6.7 Apodized GUDTs
(SINC-COSINE-MBF Profiles).
- 6.8 Apodized IPUDTs
(SINC-COSINE-MBF Profiles).
- 6.9 Filters With Uniform And
(SINC-COSINE-MBF Profiles)
Apodized GUDTs.

- 6.10 Filters With Uniform And
($IIN\bar{C}-COIIN\bar{C}-MBF$ Profiles)
Spodized $IPUDI$ s.
- 6.11 Filters With Uniform $IPUDI$ s
And ($IIN\bar{C}-COIIN-MBF$ Profiles)
Spodized $GUDI$ s.
- 6.12 Conclusion.

MODIFIED BESSEL FUNCTION WINDOW FAMILY

6.1 INTRODUCTION:

Window functions have found extensive applications in digital signal processing, signal analysis, detection, estimation, etc. There is a variety of window functions for use in different signal processing applications. we have already considered the COSINE window and studied the responses of SAW transducers and filters windowed with this function.

In this chapter we are considering a generalized modified Bessel function that by varying certain parameters it yields a big family of windows that we call modified Bessel function (MBF) windows. Some of these windows are same as some commonly used windows such as Dolph-Chebyshev and Kaiser-Bessel window functions but with simpler expressions.

The generalized equation of these MBF windows is considered in this chapter with different window functions derived from it. The characteristics of many such window functions are studied

after calculating their fourier transforms using the FFT facility of the software modeling package. New apodization profiles are presented using SINC function for weighting with COSINE and one MBF window functions for windowing using different lengths of SINC-COSINE functions.

These apodization profiles are used in apodizing many GUDT and TPUDT transducers. The different performances of these transducers are presented and discussed. Many filters having one uniform and one apodized transducers apodized with such profiles have been simulated. The performances of such filters constructed from same transducers either GUDTs or TPUDTs or from combinations of both types are studied, presented and discussed.

6.2 WINDOWS FOR SAW TRANSDUCERS:

There is much signal processing devoted in detection, estimation, equalization, multichannel multiplexing / demultiplexing..etc. Often the signal under processing is complicated or is corrupted by interfering signals or noise. To facilitate such signal processing tasks certain filter responses are required. For getting the required frequency responses it is always true that a good response for a certain application is primarily due to the selection of a proper window.

There is a wide range of window functions available in literature, and many of them are widely used in designing

equipments for signal processing applications. Some of these windows are simple such as the triangular and the trigonometric window functions and some are complicated. Some are rarely used such as the two prementioned windows and some are widely used such as Kaiser-Bessel and Dolph-Chebyshev window functions. Harris [47] has listed and discussed many types of reported window functions.

COSINE window functions have been widely used to improve SAW transducers and filters frequency responses [44,48]. And although surface acoustic waves filters design is closely allied to that of antenna arrays and digital finite impulse response filters yet one can not find much work reported on SAW transducers and filters utilizing different types of window functions [49]. This can be reasoned if one is to consider the cost of constructing many SAW transducers/filters using different window functions for simply studying the use of these windows in designing SAW transducers/filters. This indicates the need for a simulator that is able to aid such studies and help in selecting the proper window for the specific application.

Reddy and Lahiri [49,50] proposed a generalized window function to be used in the design of digital and SAW_filters. The proposed window function takes the form of the widely used Kaiser-Bessel and Dolph-Chebyshev window characteristics for certain values of parameters. In both papers only time and frequency domains calculations of some of these window functions derived from the generalized window function have been reported. Built in rect window of SAW transducers, apodization type,

transducer number of pairs, transducer type and other parameters have not been taken into consideration.

In the coming sections we will derive some more new window functions from the proposed modified Bessel window generalized equation, study different apodization profiles and simulate different windowed apodized transducers.

6.3 MODIFIED BESSEL FUNCTION WINDOW FAMILY:

The Bessel function based generalized window function reported in [50] is given by;

$$\begin{aligned}
 w(t) &= (T^2 - t^2)^{n/2} I_n \left(b \sqrt{(T^2 - t^2)} \right) \quad |t| < T \\
 &= 0. \quad \quad \quad |t| > T
 \end{aligned}
 \tag{6.1}$$

where I_n is the modified Bessel function of the first kind and of order n .

b any number > 0 .

The fourier transform of $w(t)$ is

$$\begin{aligned}
 W(\omega) &= \sqrt{(\pi T/2)} (b T)^n (b^2 - \omega^2)^{-n/2-1/4} \times \\
 &\quad I_{n+1/2} \left(T \sqrt{(b^2 - \omega^2)} \right) \quad \omega < b
 \end{aligned}$$

$$W(\omega) = \sqrt{(\pi T/2) (b T)^n (\omega^2 - b^2)^{-n/2-1/4}} \times J_{n+1/2}(T \sqrt{(\omega^2 - b^2)}) \quad \omega > b$$

where J_n is the Bessel function of the first kind and of order n .

Equation (6.1) yields a family of window functions for different values of b and n .

It is to be noted that Kaiser-Bessel function is a special case of equation (6.1) for $n=0$., and the characteristics of the window function for $n=1$ correspond to Dolph-Chebyshev [49,50].

6.4 COMPUTATION OF
MODIFIED BESSEL FUNCTION
WINDOW FAMILY:

In order to study the characteristics of the Modified Bessel Function (MBF) window family and to make use of it later on in getting the required responses from windowed SAW transducers/filters many window functions belong to this window family (derived from the generalized MBF window equation (6.1)) have been calculated with the aid of FFT facility made available in the software simulator package.

For the purpose of studying the different parameters that

Fig. 6.1 Time domain plot of MBF windows of $b=3$ and n from 0 to 1.5.

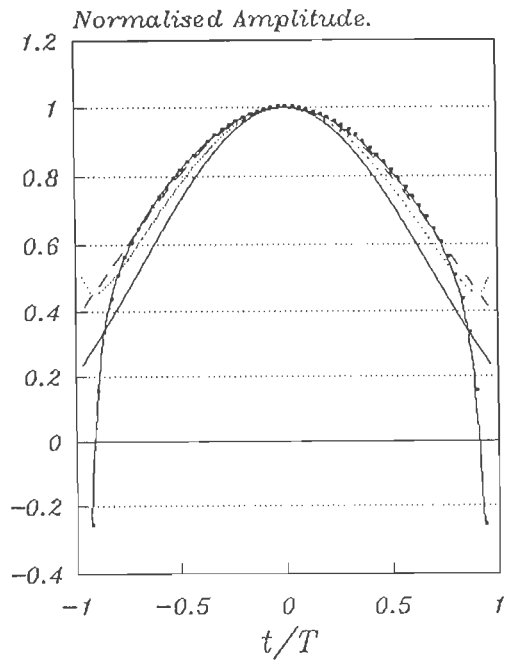
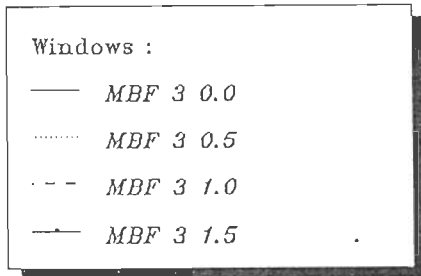


Fig. 6.2 Frequency domain plot of MBF windows of $b=3$ and n from 0 to 1.5.

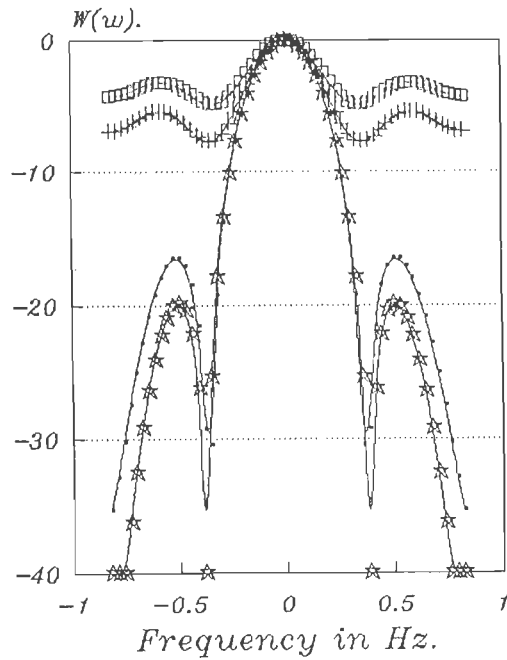
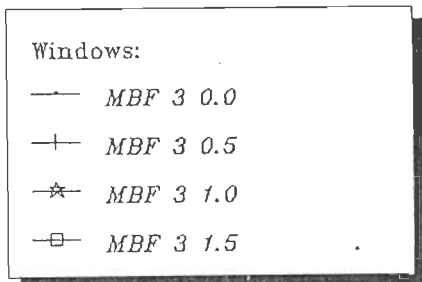


Fig. 6.3 Time domain plots of MBF windows of $b=4$ and n from 0.0 to 1.5.

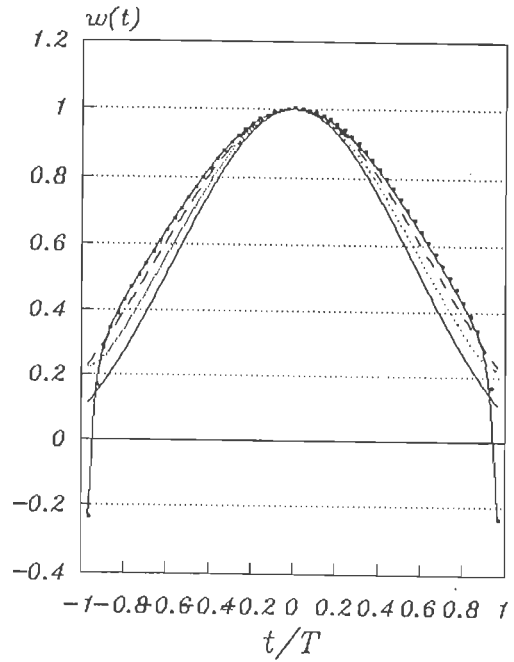
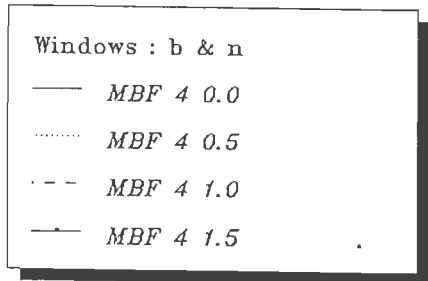
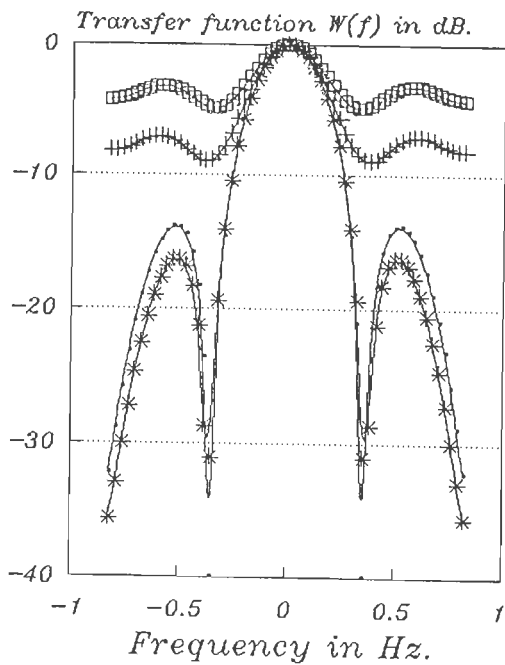
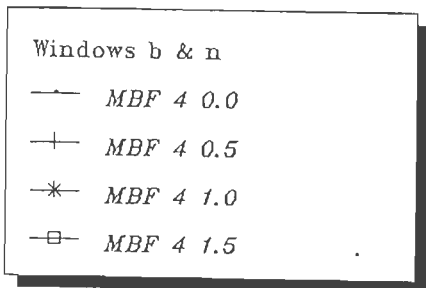


Fig. 6.4 Frequency domain plots of MBF windows of $b=4$ and n from 0.0 to 1.5.



affect the frequency responses of SAW filters, having one uniform transducer and other apodized, windowed with one of the MBF window functions in addition to the COSINE window discussed earlier, the package has been utilized to simulate such transducers and filters.

In the coming sections we present different FFT calculated window characteristics (in time and frequency domains), different apodization patterns using SINC weighting, COSINE windowing and one MBF window in calculating each pattern and more over expected (FFT calculated) transducers frequency responses. Also we present the results of different simulated SAW transducers and filters using such apodization patterns.

6.5 CHARACTERISTICS OF DIFFERENT MBF WINDOWS:
--

Referring to the generalized MBF window equation of (6.1), by changing b and n a large family of MBF windows can be generated. Odd numbered Figures 6.1 to 6.9 show time domain plots of number of MBF windows. In each figure a group of windows with constant b and with n having the values of 0., 0.5, 1. and 1.5 have been shown. In these figures b has been selected as 3., 4., 5., 6. and 7., respectively. The corresponding Fourier transforms of these window functions are shown in the even numbered Figures of 6.2 to 6.10.

Fig. 6.5 Time domain plot of MBF windows of $b=5$ and n from 0.0 to 1.5.

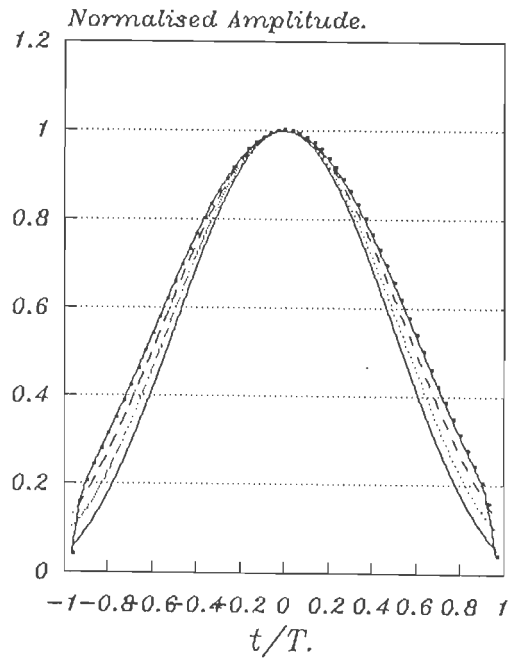
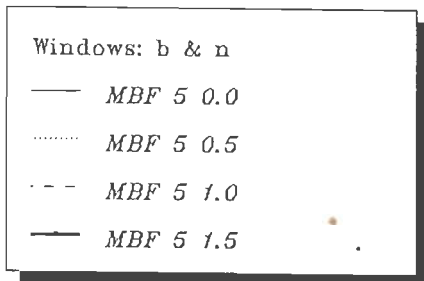


Fig. 6.6 Frequency domain plot of MBF windows of $b=5$ and n from 0.0 to 1.5.

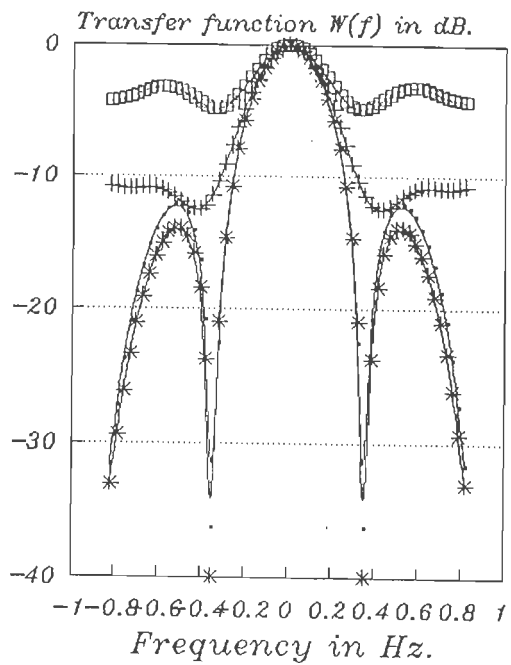
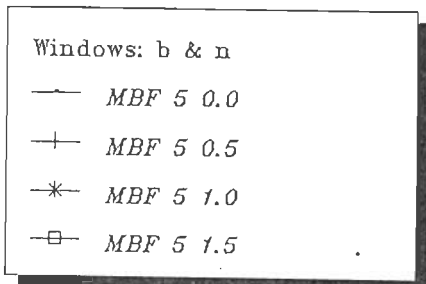


Fig. 6.7 Time domain plots of MBF windows of $b=6$ and n from 0.0 to 1.5.

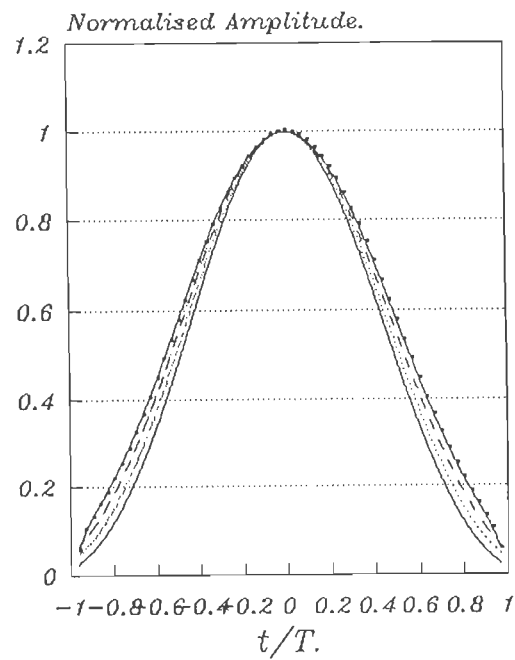
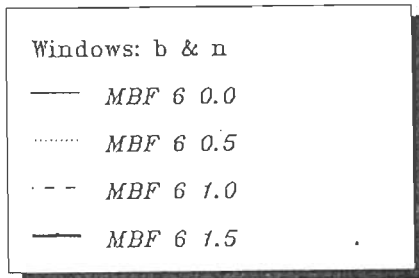
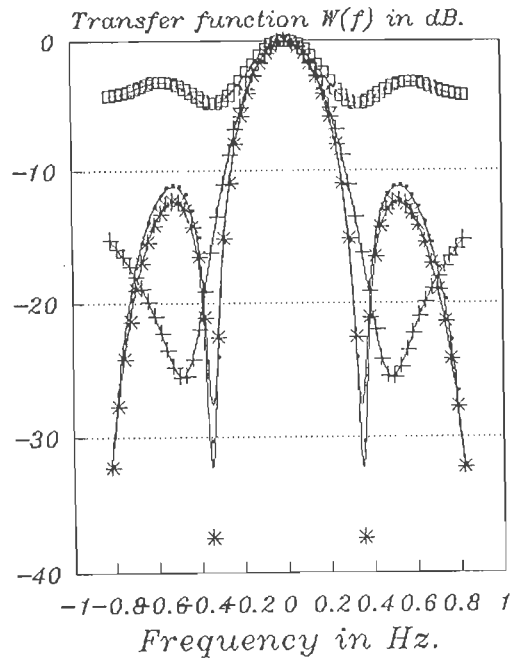
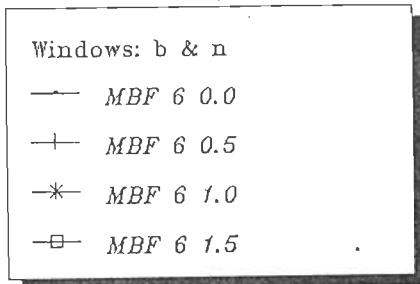


Fig. 6.8 Frequency domain plots of MBF windows of $b=6$ and n from 0.0 to 1.5.



b may take any value greater than zero and it is not necessary that the number is an integer. Figure 6.11 shows plots of windows of $n = 1$. and different fractional values of b along with one window of b equal to integer value (5.0) for comparison.

Figures 6.13 and 6.14 show some window functions with $n = 1$. and different b values (1., 3., 5. and 7.) and its fourier transforms.

In all the above mentioned figures the MBF windows are named by two numbers each; first number represents the value of b and the second number represents the value of n. It is to be noted that the value of n is always less or equal to zero yet we are always referring to the absolute values of n and not the real values for simplicity.

From the different MBF window functions that have been calculated it has been found that lower n and/or lower b means a more flat function regardless whether n or b are integers or fractionals. From the corresponding Fourier transforms it can be seen that lowering b generally means lower side lobes levels yet also lower shape factor. This is true whether b is integer or fraction. Higher integer n value means lower side lobes levels while the reverse can be expected with fractional n.

6.6 NEW APODIZATION PROFILES USING MBF WINDOWS:

If MBF windows are used with SINC apodization and COSINE windowing The designers of SAW devices for signal processing

Fig. 6.9 Time domain plots of MBF windows of $b=7$ and n from 0.0 to 1.5.

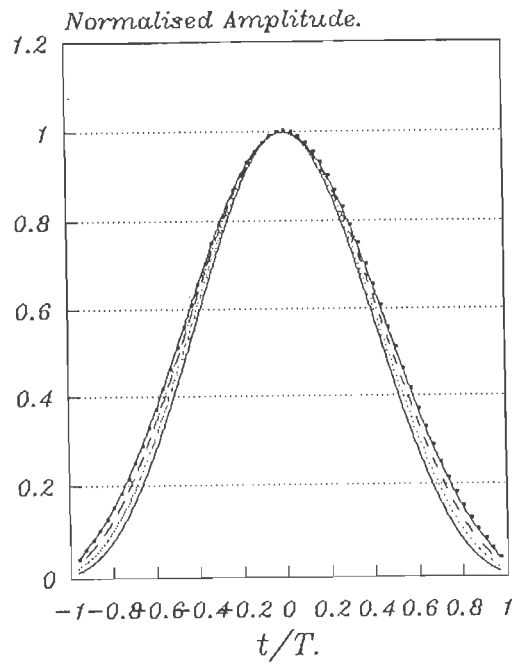
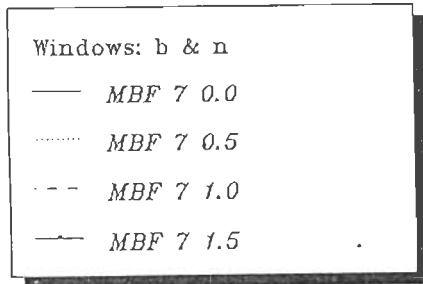


Fig. 6.10 Frequency domain plots MBF windows of $b=7$ and n from 0.0 to 1.5.

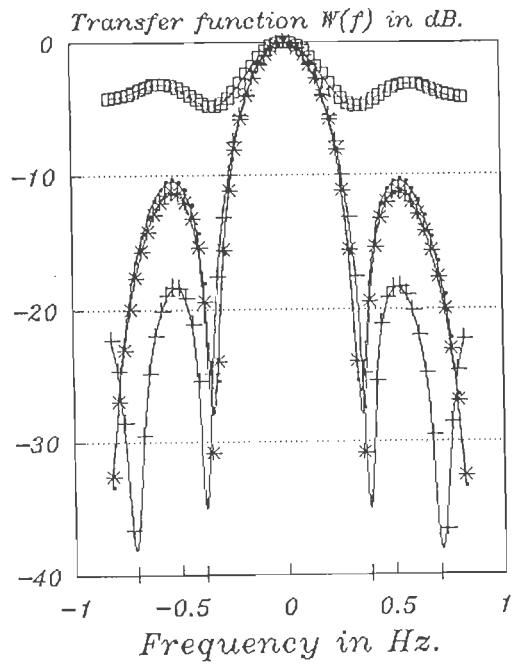
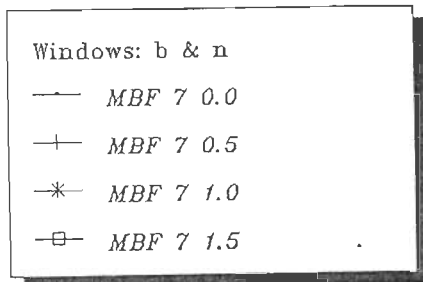


Fig. 6.11 Time domain plots of MBF windows of $n=1.0$ and b equal to 0.5, 2.5, 4.5 and 5.

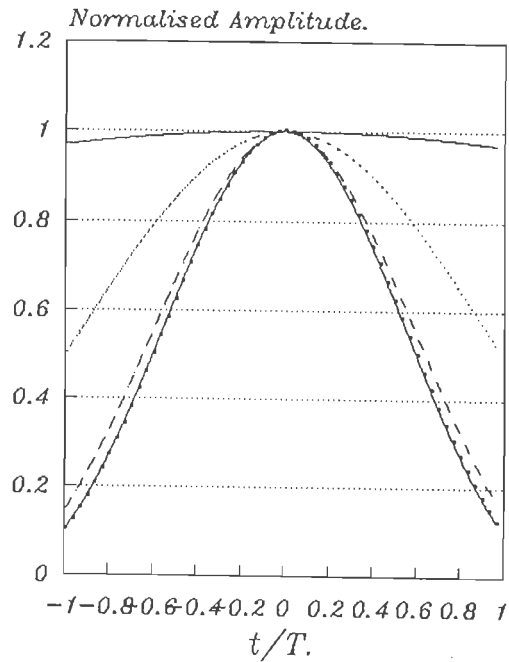
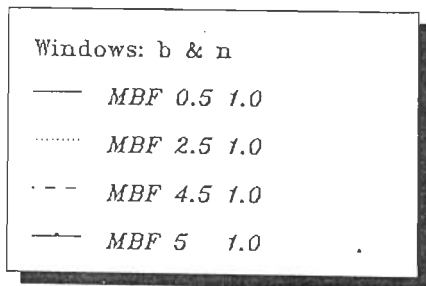


Fig. 6.12 Frequency domain plots of MBF windows of $n=1.0$ and b equal to 0.5, 2.5, 4.5 and 5.

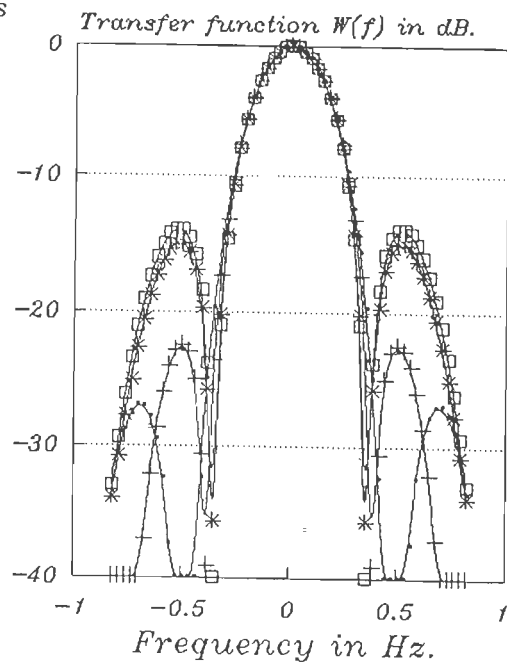
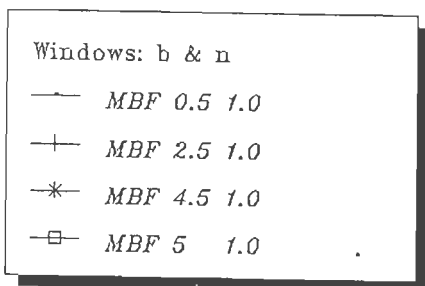


Fig. 6.13 Time domain plots of MBF windows of $n=1.0$ and b is 1, 3, 5 and 7.

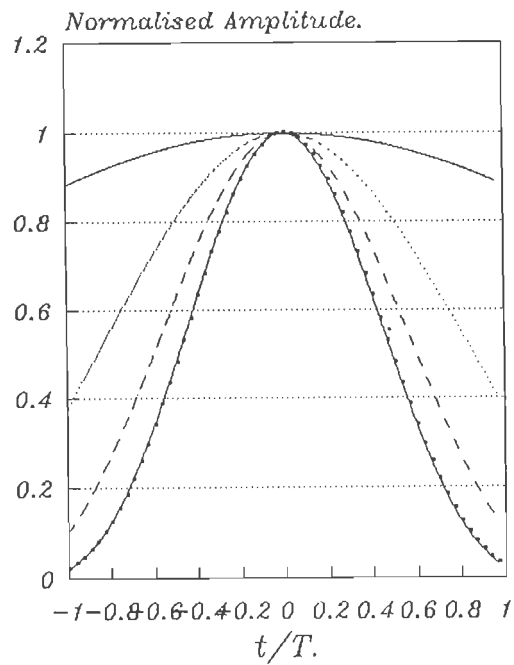
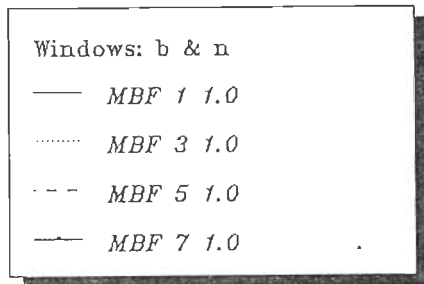
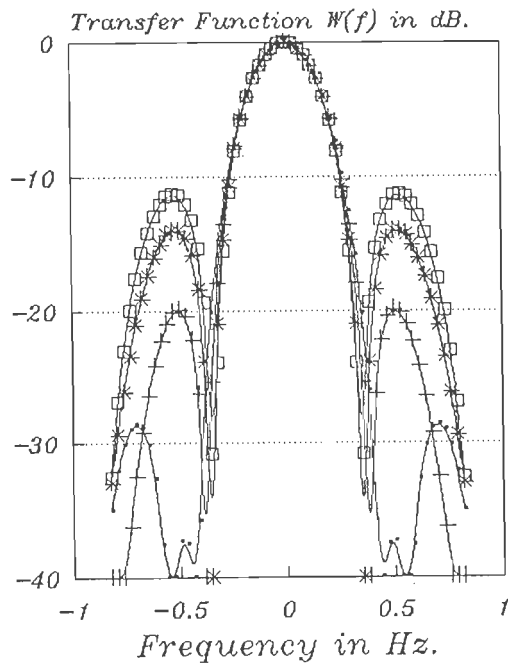
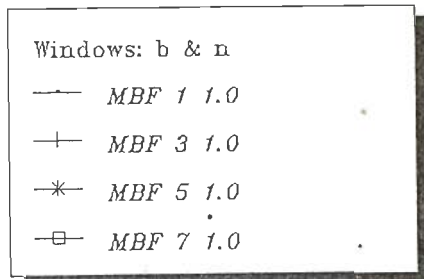


Fig. 6.14 Frequency domain plots of MBF windows of $n=1.0$ and b is 1, 3, 5, and 7.



applications can find a variety of apodization profiles from which they can select the one that may suit their applications and give the SAW transducer and filter responses that are required. By changing the MBF window (b and n) and the length of either or both of the SINC weighting function and COSINE windowing function, one can have different apodization profiles.

Although it is not necessary to use MBF windows with SINC weighting and COSINE windowing functions, for it can be used with any other weighting function alone or along with any other window, here we are considering the apodization profiles (or patterns) of the type mentioned above.

Figures 6.15 to 6.21 show plots of some of these apodization patterns or profiles by changing the value of n and b of the MBF windows and the lengths of SINC weighting and COSINE windowing functions. The apodization type number which defines every profile consists of four numbers. First number represents functions used in getting the profiles (1: No functions except the built in rect window i.e. uniform apodization, 2: uniform receiving transducer, 3: SINC weighting only, 4: SINC weighting and COSINE windowing apodization, 5: SINC weighting and COSINE & MBF windowing ..etc). Second number represents the length of SINC weighting-COSINE windowing functions in terms of number of zero crossings on each sides of functions. Third and fourth numbers are required only if MBF windows are used and these numbers represent values of b and n respectively. Both third and fourth numbers in the apodization type number can be integers or fractions.

Fig. 6.15 Apodization patterns of SINC weighting-COSINE+MBF windowing. MBF windows of $b=3$ and n equal to 0. and 1.5.

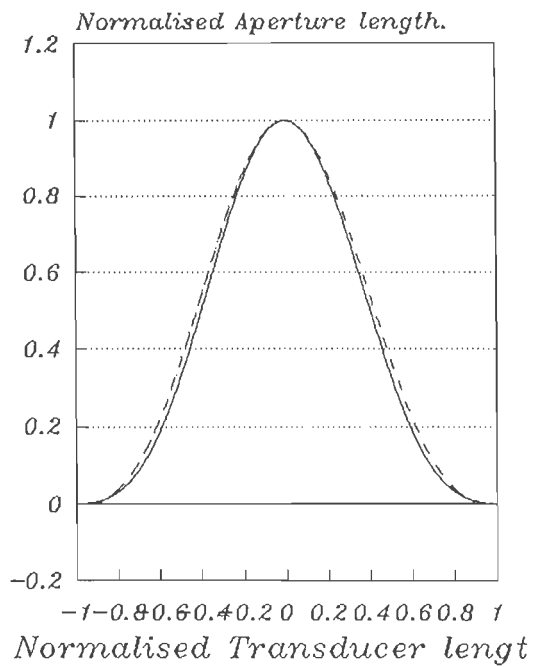
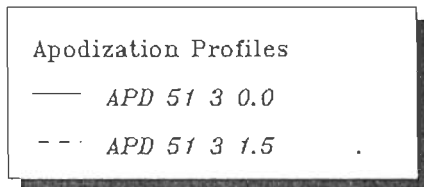


Fig. 6.16 Apodization patterns of SINC weighting-COSINE+MBF windowing. MBF windows of $b=4$ and n equal to 0.0 and 1.5. SINC-COSINE functions are truncated at first zero crossing.

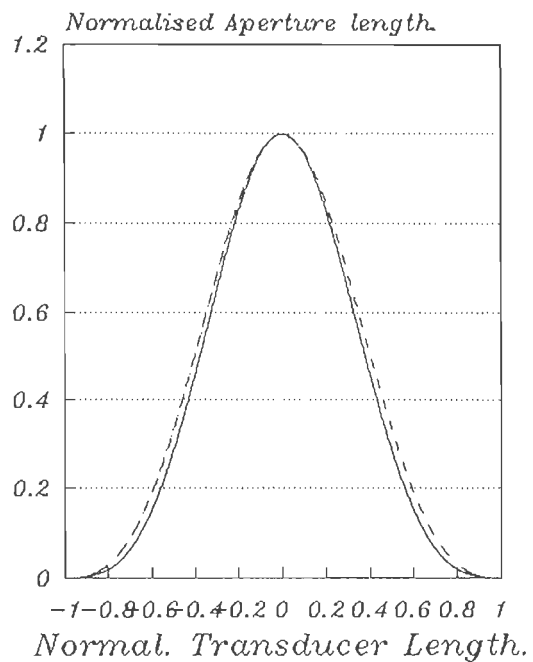
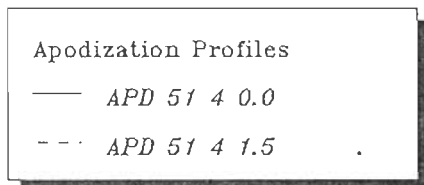


Fig. 6.17 Apodization patterns of SINC weighting-COSINE+MBF windowing. MBF windows are of $b=5$ and n 0.0 and 1.5.

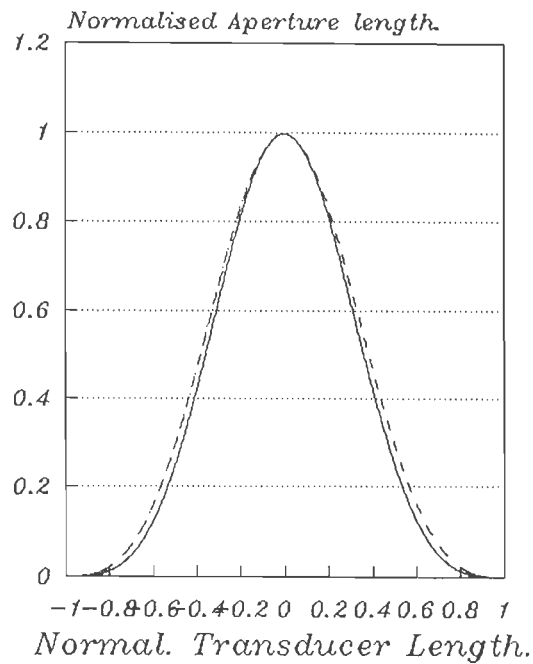
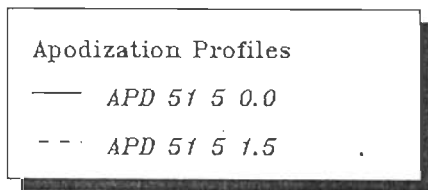


Fig. 6.18 Apodization patterns of SINC weighting-COSINE+MBF windowing. MBF windows are of $n=1.0$ and b of 1., 3., 5. and 7. SINC weighting function is truncated at first zero crossing.

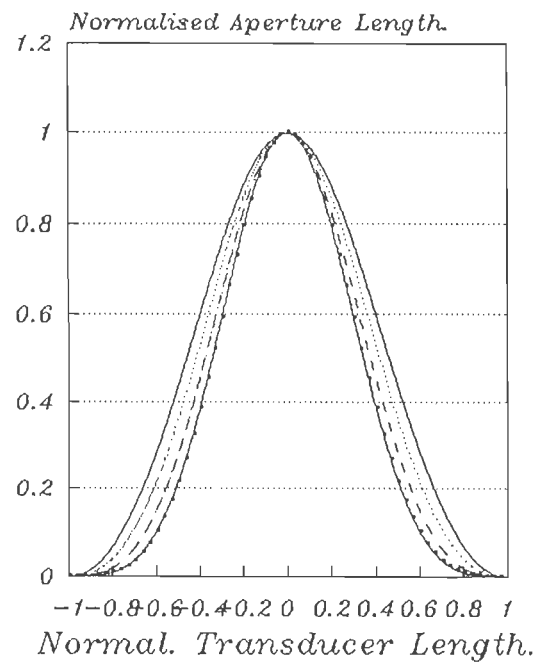
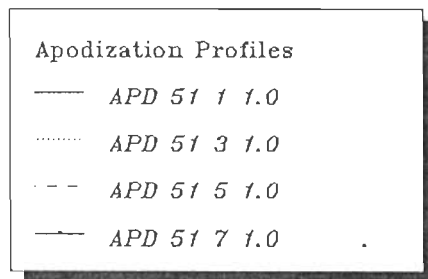


Fig. 6.19 Apodization patterns of SINC weighting-COSINE+MBF windowing. MBF windows are of $b=5$ and $n=1.0$. SINC-COSINE functions are truncated at 1, 2, 3 and 4 zero crossings.

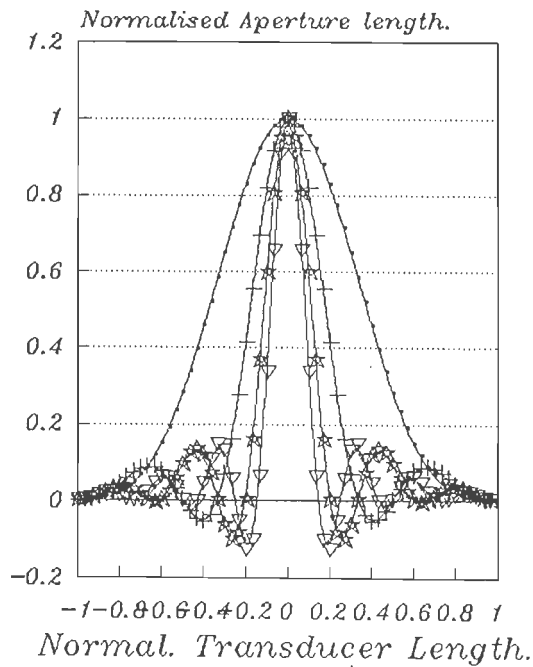
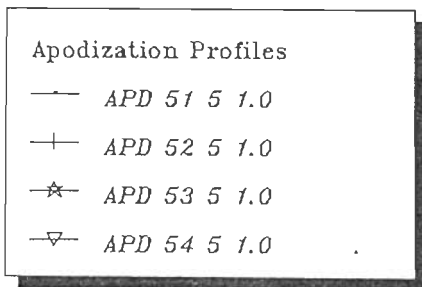


Fig. 6.20 Apodization patterns of SINC weighting-COSINE+MBF windowing. MBF windows are of $b=7$ and $n=1.0$. SINC-COSINE functions are truncated at first, second, third and fourth zero crossings.

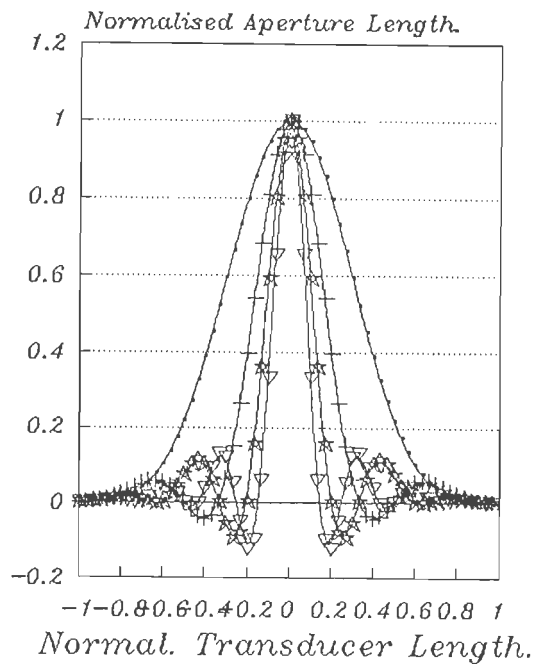
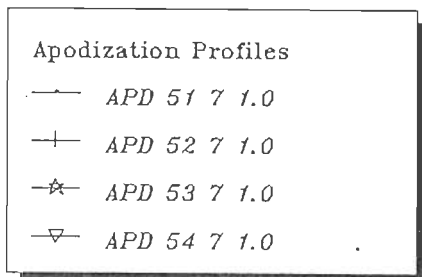


Fig. 6.21 Apodization profiles of SINC weighting-COSINE+MBF windowing. MBF windows are of $n=1.0$ and b of 0.5, 2.5, 4.5 and 5.0.

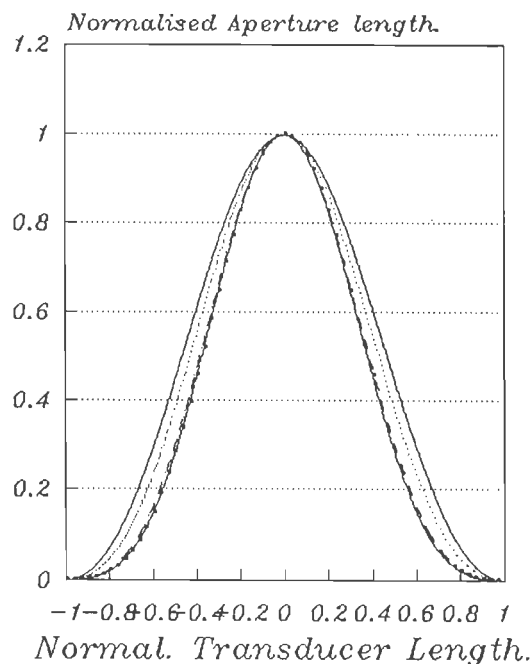
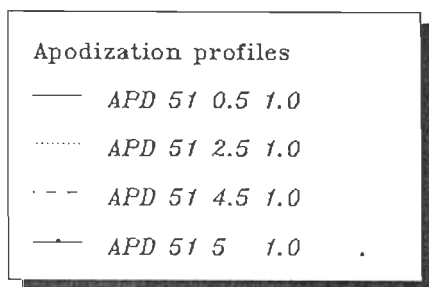


Fig. 6.22 FFT calculated Frequency response of SINC weighted-COSINE & MBF windowed transducers. MBF windows are of $n=1.0$ and b of 1 and 7. SINC weighting function is truncated at first zero crossing.

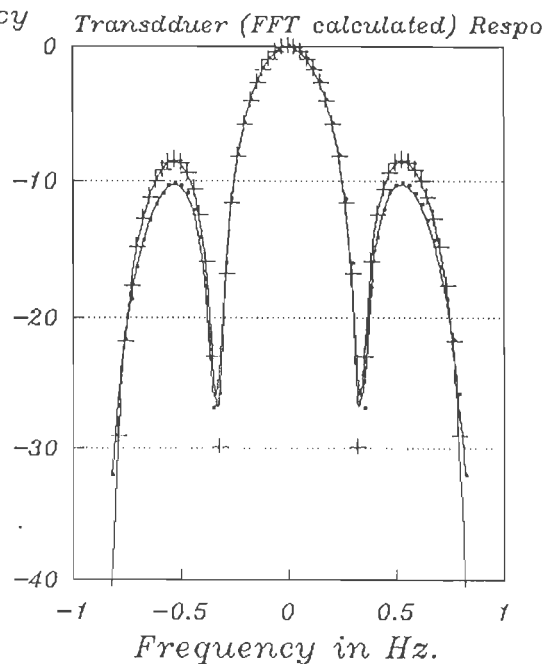
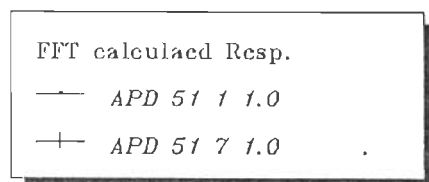


Figure 6.22 represents fourier transforms of two of these apodization profiles with the built-in rectangular window of SAW IDT.

6.7 APODIZED GUDTs (SINC-COSINE-MBF PROFILES):

To find out the effect of using the above apodization profiles on the performance of group type unidirectional transducers and to study the role of different IDT parameters on SAW GUDT transducers performances using such profiles, many SINC weighted-COSINE & MBF windowed GUDTs have been simulated. The computational results of some of these transducers are presented in Tables {6.1} to {6.3} in terms of rise, fall, 3dB, rejection bandwidths, first both sides lobes levels and transducers shape factors.

Comparing the results presented in the above mentioned tables with these presented earlier in tables {5.16} to {5.18} of SINC weighted-COSINE windowed transducers one can see the extent of improvement in terms of bandwidth and shape factor caused by using MBF windows.

Comparing the computational results of GUDT-4-5 with apodization type number of (51 5 1.) and same transducer with apodization type number of (41) one can see from tables such improvement although the number of apodized groups is small.

Table {6.1}

*Computed Rise, 3dB and Fall bandwidths of
SINC weighted-COSINE & MBF windowed GUDTs.*

Transdu- cer type	Apodizat- ion type	Aperture in meter	RB per cent	3dB BW per cent	FB per cent
N-4-6	5150	7.3798E-4	1.1843	3.754	0.2011
N-4-5	5151	7.3798E-4	1.0279	4.681	0.2458
N-4-8	5111	7.3798E-4	0.9497	2.709	0.1117
N-4-9	5150	3.2799E-4	1.3295	5.273	0.2234
N-4-9	5151	3.2799E-4	1.2848	5.251	0.2234
N-4-10	5171	3.4889E-4	1.1284	1.854	0.0558
N-2-19	5150	3.2799E-4	1.0167	4.134	0.2234
N-4-50	5151	1.1531E-5	0.346	2.044	0.6703

Table {6.2}

*Computed left and right side lobes levels of
SINC weighted-COSINE & MBF windowed GUDTs.*

Transdu- cer type	Apodizat- ion type	Aperture in meter	LSL in dB	RSL in dB
N-4-6	5150	7.3798E-4	9.69	4.4
N-4-5	5151	7.3798E-4	10.	7.32
N-4-8	5111	3.4889E-4	9.2	4.0
N-4-9	5150	3.2799E-4	8.48	4.0
N-4-9	5151	3.2799E-4	8.44	4.0
N-4-10	5171	3.4889E-4	10.	3.4
N-2-19	5150	3.2799E-4	7.8	4.28
N-4-50	5151	1.1531E-5	8.4	3.4

Table {6.3}

*Computed Rejection bandwidth and Shape factor of
SINC weighted-COSINE & MBF windowed GUDTs.*

Transdu- cer type	Apodizat- ion type	Aperture in meter	RJ per cent	SHAPE factor
N-4-6	5150	7.3798E-4	6.592	0.5694
N-4-5	5151	7.3798E-4	7.932	0.5901
N-4-8	5111	3.4889E-4	4.971	0.5449
N-4-9	5150	3.2799E-4	8.759	0.6020
N-4-9	5151	3.2799E-4	8.759	0.5994
N-4-10	5171	3.4889E-4	4.022	0.4611
N-2-19	5150	3.2799E-4	6.949	0.5948
N-4-50	5151	1.1531E-5	3.687	0.5545

SINC weighted-COSINE widowed GUDT-4-9 with weighting-windowing functions truncated at second zero crossing got so much improved in 3dB bandwidth and transducer shape factor when MBF window (5. 0.) has been used and with weighting-COSINE windowing functions truncated at first zero crossing.

GUDT-2-17 (of apodization type number 41) and GUDT-2-19 (of apodization type number (51 5. 0.)), the extent of improvement in 3dB bandwidth (as well as shape factor) is very much clear although the MBF windowed transducer is having little higher number of apodized groups.

It can be seen from Tables {5.17} and {6.2} that this improvement in bandwidth and transducer shape factor is with compromising side lobes levels. To reduce these side lobes levels one can increase the length of SINC weighting-COSINE windowing functions and increase in the same time the number of apodized groups to compensate the effect of increasing that length on rise to 3dB bandwidths ratio and on fall to 3dB bandwidths ratio.

From Tables {6.1} and {6.3} one can see the effect of increasing the number of apodized groups on improving both rise to 3dB bandwidths ratio and fall to 3dB bandwidths ratio using same apodization profile. This is clear from the computational results of GUDT-4-6 and GUDT-4-9 transducers (both using (51 5. 0.) apodization pattern) and GUDT-4-5 and GUDT-4-9 transducers (both using (51 5. 1.) apodization profile). GUDT-2-19 transducer computational results show that increasing the number of

apodization groups while keeping the product of effective fingers per group - groups constant may not cause such improvement.

It is worth to note here that it has been found that increasing the number of apodized groups beyond certain threshold may deteriorate the transducer shape factor due to the high increase in fall to 3dB bandwidths ratio and the decrease in rise to 3db bandwidths ratio, as can be seen from GUDT-4-50 (apodization type number (51 5. 1.)).

6.8 APODIZED TPU DTs (SINC-COSINE-MBF PROFILES) :
--

Some of the simulated apodized (SINC weighted-COSINE & MBF windowed) three phase unidirectional transducers are listed in Tables {6.4} to {6.6} along with its computational results in terms of rise, 3dB, fall, rejection bandwidths, side lobes levels and transducer shape factor.

It is clear from tables that with the increase of the value of b ; 3db bandwidth reduces, rise bandwidth increases, transducer shape factor decreases and both sides lobes levels increase. This conclusion is drawn from tables regardless the change occurring (due to matching calculations) to the number of apodized sections. The number of apodized sections is calculated according to uniform sections of 16 in all transducers listed in tables except TPU DT-28.

Table {6.4}

*Computed Rise, 3dB and Fall bandwidths of
SINC weighted-COSINE & MBF windowed TPUDTs.*

Transducer type	Apodization type	Aperture in meter	RB per cent	3dB BW per cent	FB per cent
T-23	5111	4.9199E-4	1.564	4.826	0.346
T-24	5131	4.9199E-4	1.698	4.536	0.770
T-25	5151	4.9199E-4	1.899	3.854	0.335
T-26	5170.5	4.9199E-4	2.346	3.139	0.458
T-25	5172	4.9199E-4	2.067	3.821	0.4025
T-28	5111	3.1487E-4	1.005	3.776	0.223

Table {6.5}

*Computed left and right side lobes levels of
SINC weighted-COSINE & MBF windowed TPUDTs.*

Transducer type	Apodization type	Aperture in meter	LSL in dB	RSL in dB
T-23	5111	4.9199E-4	8.2	7.6
T-24	5131	4.9199E-4	8.72	7.6
T-25	5151	4.9199E-4	10.	8.8
T-26	5170.5	4.9199E-4	11.6	10.4
T-25	5172	4.9199E-4	12.36	9.8
T-28	5111	3.1487E-4	7.6	5.44

Table {6.6}

*Computed Rejection bandwidth and Shape factor of
SINC weighted-COSINE & MBF windowed TPUDTs.*

Transducer type	Apodization type	Aperture in meter	RJ per cent	SHAPE factor
T-23	5111	4.9199E-4	8.513	0.5669
T-24	5131	4.9199E-4	8.424	0.5384
T-25	5151	4.9199E-4	7.888	0.4886
T-26	5170.5	4.9199E-4	7.798	0.4025
T-25	5172	4.9199E-4	7.843	0.4859
T-28	5111	3.1487E-4	7.150	0.5281

These transducers can be compared with TPUDT-22 of Tables {5-19} to {5-20}. The transducer admittance and number of sections has been calculated with reference to uniform sections number of 16 also. It can be seen that transducers TPUDT-23 (apodization type number (51 1. 1.)) and TPUDT-24 (apodization type number (51 3. 1.)) are having improved shape factors but high side lobes levels in the same time. TPUDT-23 (APD 51 1. 1.) is even having wider 3db bandwidth than TPUDT-22 (apodization type number 41).

Other transducers modelled with reference to uniform sections number 16 having apodization type numbers with b higher than 3 given in tables suffer from a high rise to 3dB bandwidths ratio and that is why it is having lower transducers shape factors. The shape factors of these transducers can be improved by increasing the number of apodized sections (calculate the number of apodized sections with reference to a higher number of uniform sections) so that to reduce the rise to 3db bandwidths ratio.

The effect of increasing the value of n on the performance of these filters can be seen from the computational results of TPUDT-26 (apodization type number (51 7. .5)) and TPUDT-25 (apodization type number (51 7. 2.)). This increase in this case caused a decrease in the number of apodized sections (same maximum aperture), an increase in 3dB bandwidth, decrease in rise and fall bandwidths, improved shape factor but higher side lobes levels.

TPUDT-28 transducers (with apodization type number of (51 1. 1.)), the number of apodized sections has been increased

(calculated with reference to uniform 20 sections). The apodization profile is exactly the same as TPUDT-23. An improvement in side lobes levels has been achieved (but with little compromise of transducer shape factor) as it can be seen from tables {6.4} to {6.6}.

6.9 FILTERS WITH UNIFORM AND (SINC-COSINE-MBF PROFILES) APODIZED GUDTs :
--

Tables {6.7},{6.8} and {6.9} list some of the filters constructed (in software) from one uniform and another SINC weighted-COSINE & MBF windowed apodized group unidirectional transducers. The corresponding computational results of these filters in terms of rise, fall, 3dB, rejection bandwidths, side lobes levels and filters shape factors are also given. The relevant forward frequency responses of these filters and the GUDT transducers from which it have been constructed along with other related responses are shown in Figures 6.23 to 6.32.

Comparing the performances of GUDT-8-2/GUDT-4-6 filter and GUDT-8-2/GUDT-4-5 filter (with apodization type numbers of (51 5. 0.) and (51 5. 1.) respectively) whose frequency responses are shown in Figures 6.23 and 6.33, the effect of the difference in frequency locations as well as bandwidths of side lobes of both uniform and apodized transducers on the shape, locations and levels of filter side lobes is very much clear. Although both

Table {6.7}

Computed Rise, 3dB and Fall bandwidths of filters of uniform and SINC weighted-COSINE & MBF windowed GUDTs.

Transducer type	Apodization type	Aperture in meter	RB per cent	3dB BW per cent	FB per cent
N-8-2	1	7.3798E-4	1.675	3.296	1.217
N-4-6	5150				
M-8-3	1	3.2799E-4	2.346	4.670	0.882
N-4-9	5150				
N-8-3	1	3.2799E-4	1.675	3.7988	0.983
N-2-19	5150				
N-8-2	1	7.3798E-4	1.921	3.787	1.474
N-4-5	5151				
N-8-3	1	3.2799E-4	2.402	4.536	0.930
N-4-9	5151				
N-16-8	1	1.1531E-5	0.569	1.765	0.916
N-4-50	5151				

Table {6.8}

*Computed left and right side lobes levels of filters
of uniform and SINC weighted-COSINE & MBF windowed GUDTs.*

Transducer type	Apodization type	Aperture in meter	LSL in dB	RSL in dB
N-8-2	1	7.3798E-4	22.44	14.2
N-4-6	41			
N-8-3	1	3.2799E-4	21.28	11.84
N-4-9	41			
N-8-3	1	3.2799E-4	16.08	7.68
N-2-19	41			
N-8-2	1	7.3798E-4	25.04	22.8
N-4-5	41			
N-8-3	1	3.2799E-4	21.2	11.68
N-4-9	41			
N-16-8	1	1.1531E-4	13.6	14.2
N-4-50	42			

Table {6.9}

Computed Rejection bandwidth and shape factor of filters of uniform and SINC weighted-COSIN & MBF windowed GUDTs.

Transducer type	Apodization type	Aperture in meter	RJ per cent	SHAPE factor
N-8-2	1	7.3798E-4	6.592	0.4999
N-4-6	5150			
N-8-3	1	3.2799E-4	8.759	0.5331
N-4-9	5150			
N-8-3	1	3.2799E-4	6.949	0.5466
N-2-19	5150			
N-8-2	1	7.3798E-4	7.932	0.4774
N-4-5	5151			
N-8-3	1	3.2799E-4	8.759	0.5178
N-2-9	5151			
N-16-8	1	1.1531E-4	3.687	0.4787
N-4-50	5151			

mentioned filters are having the same uniform transducers and there is a marginal difference between the main lobes of both filters apodized transducers (due to low number of apodized groups) still there is much difference between both filters side lobes (due to the difference in frequency locations and bandwidths of transducers side lobes) as can be seen from figures and read from tables.

By comparing computational results of these two filters and computational results of GUDT-8-2/GUDT-4-5 filter (with apodization type number of 41) given in the previous chapter one can see the differences between the three filters. It can be seen that (5. 0.) MBF window resulted in an improvement in the shape factor whereas (5. 1.) resulted in lower side lobes levels. The designer hence can select any of the filters depending on his requirements.

It is to be noted that this is not a general conclusion and it may be restricted to this case only because the difference in the number of apodized groups has it is own effect on the performances of filters also. This difference in the number of apodized groups has been calculated by the software package to secure matching.

In both filters one can see also that there is a great difference between rise to 3dB bandwidths ratio and fall to 3dB bandwidths ratio. If this is not required and some improvement in filters shape factors are required then increasing the number of

Fig. 6.23 Forward frequency response of uniform GUDT-8-2, apodized GUDT-4-6 and filter of both transducers. Apodization type number is 5150. Max aperture is $7.3798E-4$ m.

Frequency Responses:
 — NGUDT-8-2 UNIF
 + NGUDT-4-6 APD;5150.0
 * FILTER

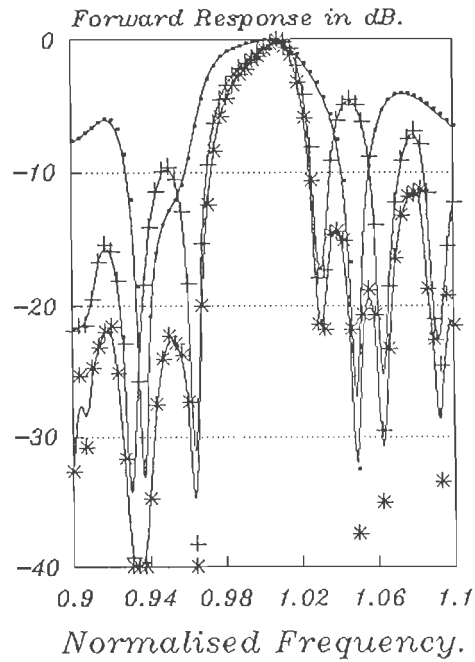


Fig. 6.24 Forward frequency response of uniform GUDT-8-2, apodized GUDT-4-5 and filter of both transducers. Apodization type number is 5151. Max aperture is $7.3798E-8$ m.

Frequency Responses:
 — NGUDT-8-2 UNIF
 + NGUDT-4-5 APD;5151.0
 * FILTER

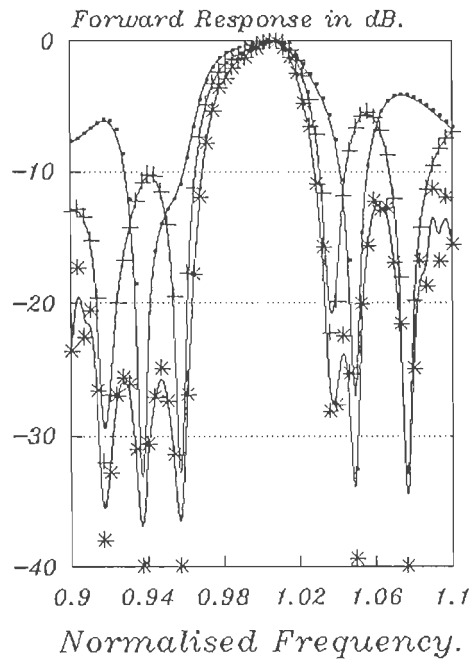


Fig. 6.25 Admittance response of uniform GUDT-8-2, apodized GUDT-4-5 and filter of both. Apodization number is 5151. Max aperture is $7.3798E-4$ m.

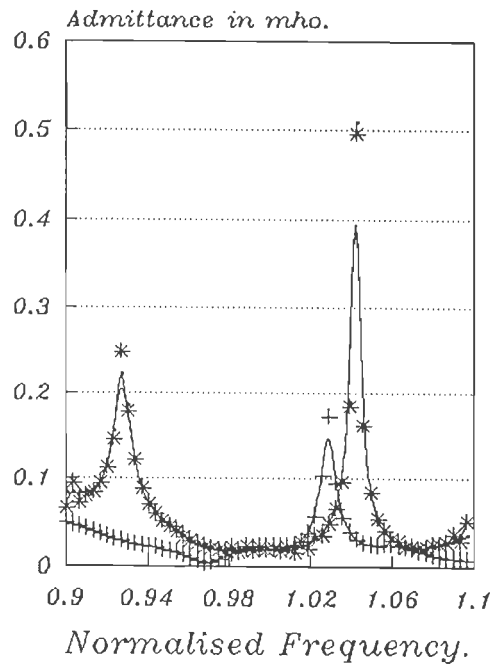
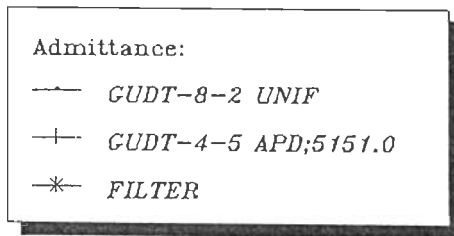
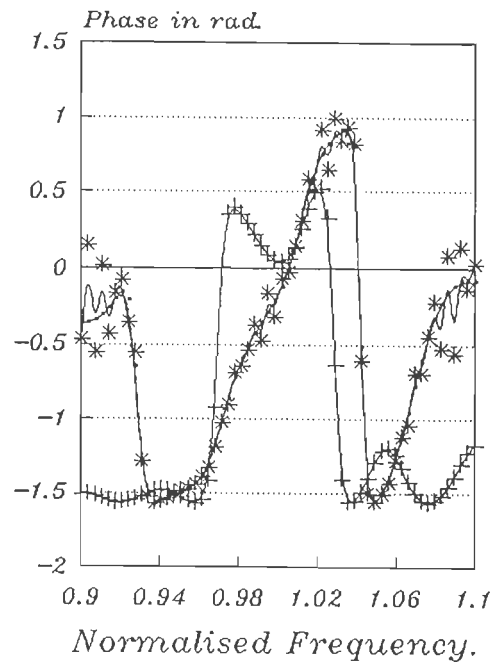
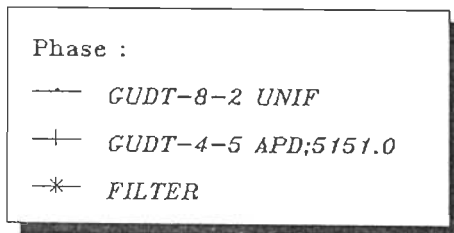


Fig. 6.26 Phase response of uniform GUDT-8-2, apodized GUDT-4-5 and filter of both transducers. Apodization number is 5151.



apodized groups (by increasing the number of effective fingers per group - group product) is one of the possible solutions.

Figures 6.25 and 6.26 show comparison between admittance and phase responses of GUDT-8-2/GUDT-4-5 filter (APD 51 5. 1.) and the corresponding responses of its uniform and apodized transducers. From the admittance response one can see that the value of the uniform transducer admittance is constant ($\cong 0.02$ mho) over a certain range of frequencies around the operating frequency. The range of which the apodized transducer admittance is having the same value is very much less. The filter admittance response is very close to that of the uniform transducer.

Great difference in phase ripples between both uniform and apodized transducers of the mentioned filter can be seen from their phase responses shown in Figure 6.26. The larger phase ripples of the apodized transducer causes oscillations (ripples) in the filter phase response. These ripples have to be reduced if not eliminated to improve the phase linearity of the filter so that the processed signal will not be distorted (unless this distortion is required intentionally in some applications). One method of reducing these ripples is to use dummy fingers.

Variation in effective aperture lengths (due to apodization) of apodized groups of GUDT-4-5 (APD 51 5. 2.) and GUDT-4-6 (APD 51 5. .5) transducers are shown in figures 6.27 and 6.28. It can be seen that in the case of even number of apodized groups the maximum aperture is less than the aperture of the uniform

Fig. 6.27 Effective aperture of GUDT-4-6 apodized transducer. Apodization Number is 5150.5. Max aperture is $7.3798E-4$ m.

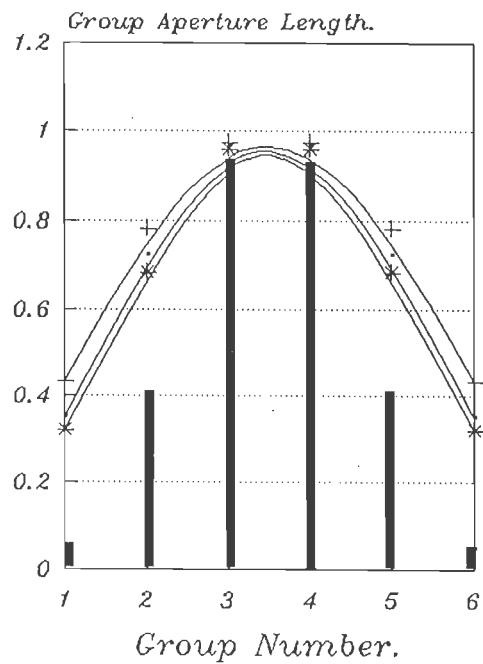
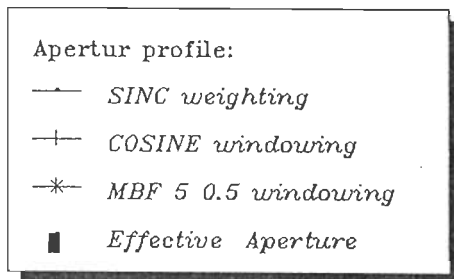
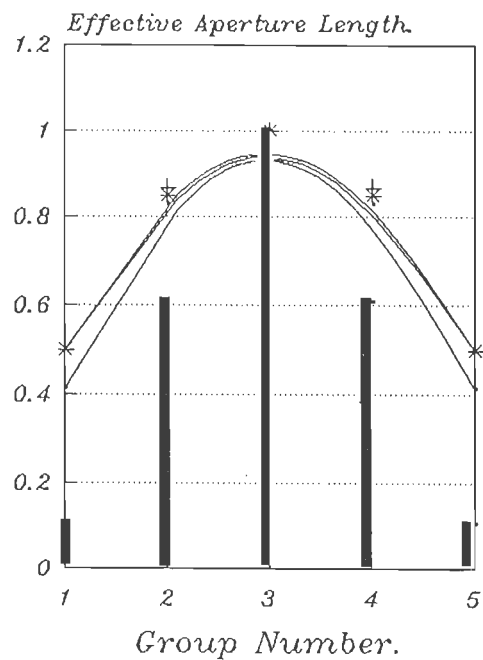
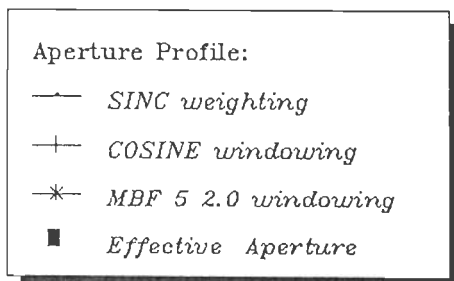


Fig. 6.28 Effective aperture of GUDT-4-5 apodized transducer. Apodization number is 5152. Max aperture is $7.3798E-4$ m.



transducer by an amount depending upon the number of apodized groups. In the transducer of Figure 6.27 effective aperture lengths of fingers of groups 3 and 4 are 10 percent less than the uniform transducer aperture length, which means that some of the acoustic energy transmitted by the uniform transducer are not passing through the apodized transducer, which is an additional loss. The difference between the max apertures of both the uniform and apodized transducers and this acoustic energy loss is lesser when the (even) number of apodized groups is larger.

It can be noted also that with less number of apodized groups it is difficult to shape the selected apodization profile (for the same reason why the curve fitting technique used in fitting the weighting and windowing functions of Figures 6.27 and 6.28 failed to give a closer fit to these functions due to the less number of points used in drawing these functions). As higher is the number of apodized groups used as closer is the effective aperture profile from the apodized profile selected.

It is worth to mention here that the software package has been developed in away that it will try several times to find the optimum effective aperture lengths (profile) which is as close as possible from the selected profile within the range of apodized groups that will provide the suitable impedance matching. Yet some times if the range of apodized groups number is so less (usually decided by the product number of fingers per group - groups of the uniform transducer and number of fingers per group of apodized transducer) that the optimum number calculated to be fractional

Fig. 6.29 Forward Frequency response of unifor GUDT-8-3, apodized GUDT-4-9 and filter of both transducers. Apodization number is 5150. Max aperture is $3.2799E-4$ m.

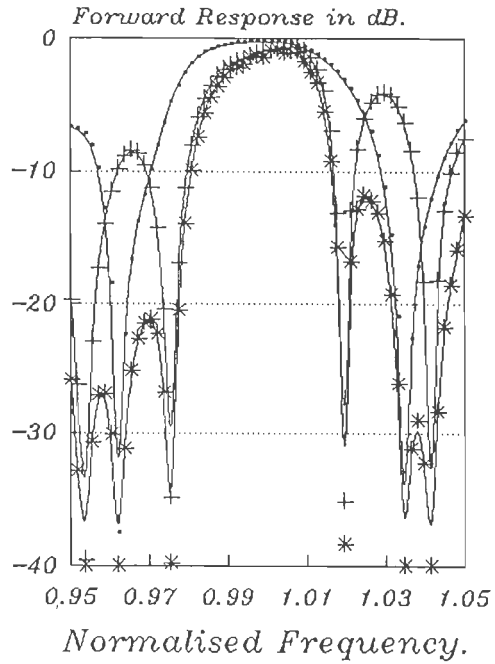
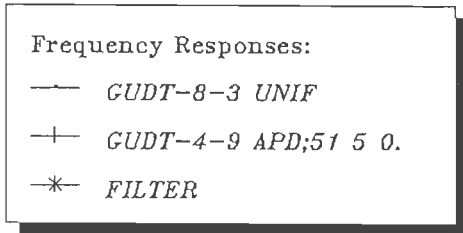
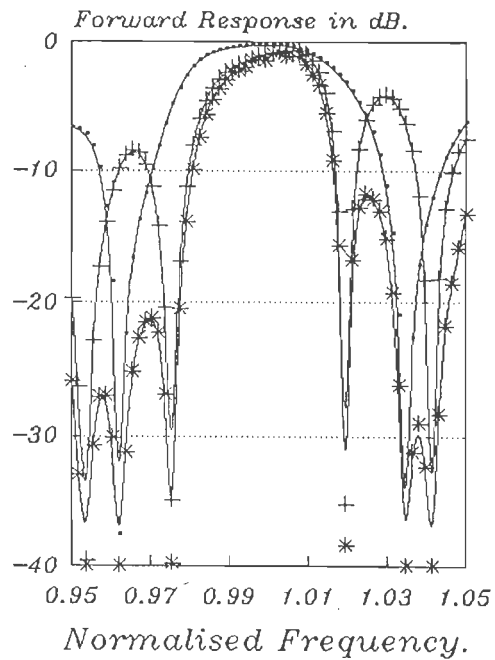
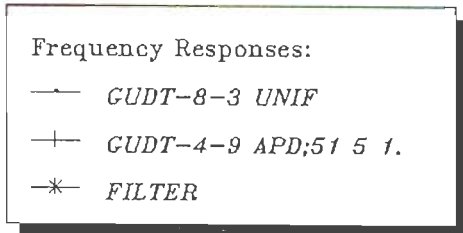


Fig. 6.30 Forward frequency response of uniform GUDT-8-3, apodized GUDT-4-9 and filter of both transducers. Apodization number is 5151. Max aperture is $3.2799E-4$ m.



centered mid way in between two integer numbers and the software will select any of both. If the number of apodized groups is small then this selection may cause a great deference.

Improvement in shape factors have been achieved in GUDT-8-3/GUDT-4-9 filters (with apodization type numbers (51 5. 0.) and (51 5. 1.)) compared to GUDT-8-2/GUDT-4-5 (APD 51 5. 1.) filter and GUDT-8-2/GUDT-4-6 (APD 51 5. 0.) filter by increasing the number of apodized groups. (51 5. 0.) apodization profile gave better improvement than (51 5. 1.) in this case. This can be seen from Figures 6.29 and 6.30 that show the forward frequency responses of both filters and from tables {6.7} to {6.9}. It can be seen that this improvement was due to improving the rise to 3dB bandwidths ratio. This improvement was combined with rise in filter side lobes levels due to the rise of apodized transducers side lobes levels and the change of their frequency locations and bandwidths. Side lobes levels can be improved by more increase in the number of apodized groups with lengthening of SINC weighting-COSINE windowing functions.

Increasing the number of apodized groups while keeping the product number of effective fingers per group - groups constant may not necessary improve the shape factor as it is the case with GUDT-8-3/GUDT-2-19 filter (with the apodization profile used in apodizing one of its transducers is 51 5. 0.) whose frequency response is shown in Figure 6.31.

It seems that there is a range of apodized groups number for each transducer after which any increase in the number of apodized

Fig. 6.31 Forward frequency response of uniform GUDT-8-3, apodized GUDT-2-19 and filter of both transducers. Apodization number is 5150. Max aperture is $3.2799\text{E-}4$ m.

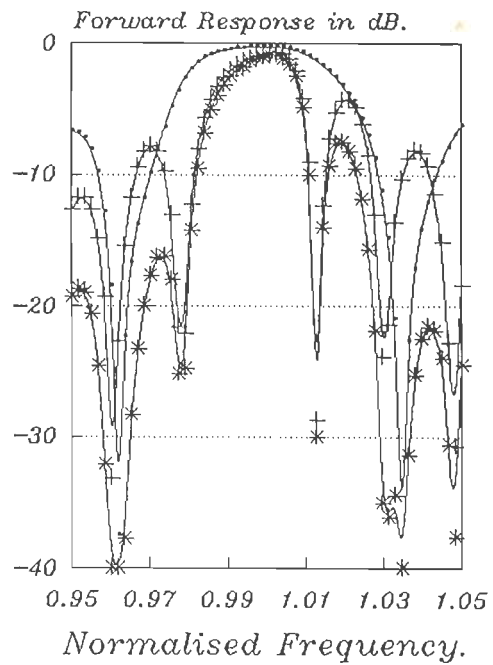
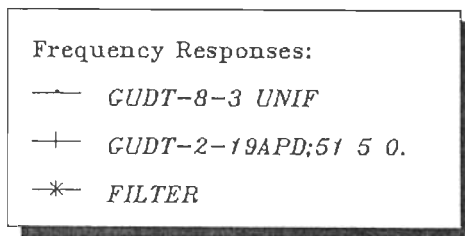


Fig. 6.32 Forward frequency response of uniform GUDT-16-8, apodized GUDT-4-50 and filter of both transducers. Apodization type number is 5151. Max aperture is $1.1531\text{E-}5$ m.

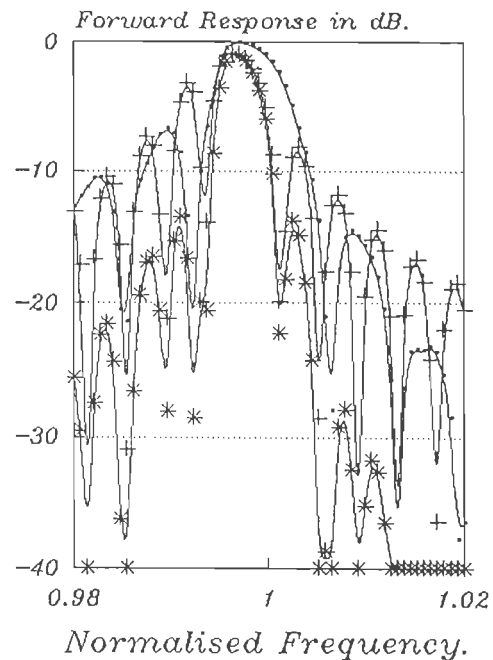
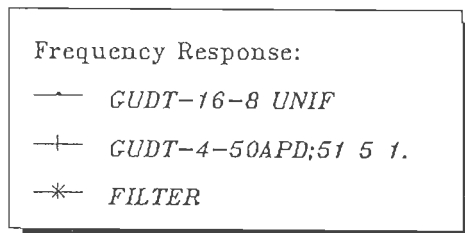


Fig. 6.33 Effective aperture of Apodized GUDT-4-50 transducer. Apodization type number is 5151. Max aperture is $1.1531\text{E-}5$ m.

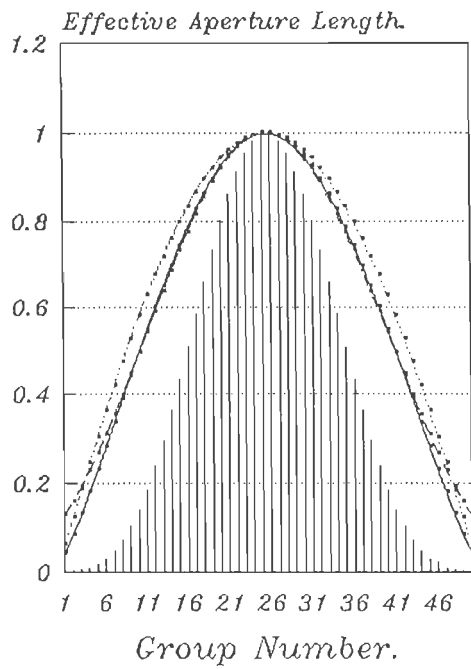
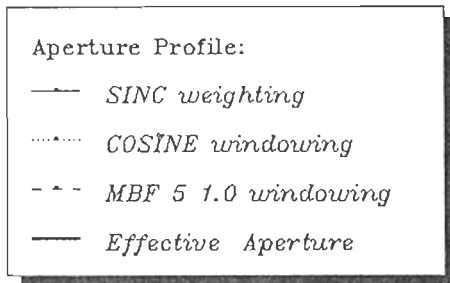
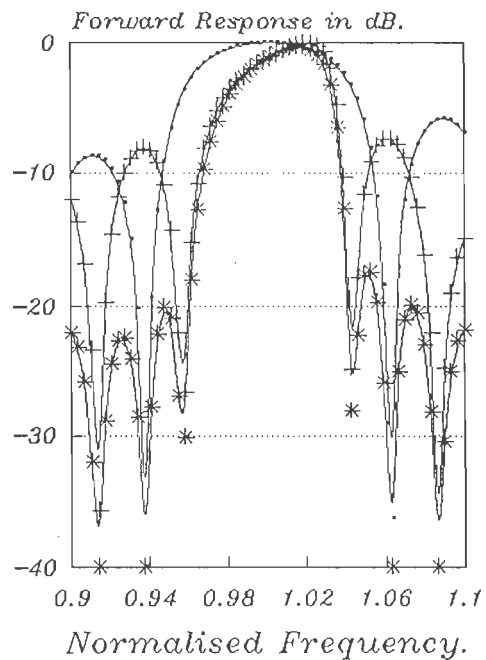
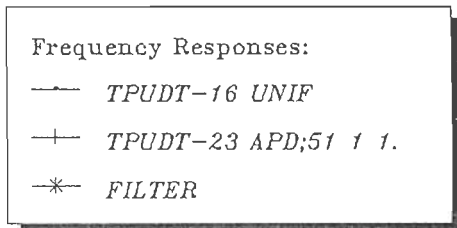


Fig. 6.34 Forward frequency response of uniform TPUDT-16, apodized TPUDT-23 and filter of both transducers. Apodization type number is 5111. Max aperture is $4.9199\text{E-}4$ m.



groups will deteriorate the apodized transducer and the filter shape factors, due to lowering rise to 3dB bandwidths ratio and increasing fall to 3dB bandwidths ratio in a way that the later is very much higher than the former. however such filter performances are also required in equalizing processes.

Such a case is same as GUDT-16-8/GUDT-4-50 filter (APD 51 5. 1.) whose frequency response is shown in Figure 6.32 and its computational results are given in prementioned tables. The effective aperture lengths of the apodized transducer groups of this filter are shown in Figure 6.33 along with plots of the weighting and windowing functions used in obtaining this profile.

6.10 FILTERS WITH UNIFORM AND (SINC-COSINE-MBF PROFILES) APODIZED TPUDTs :
--

To understand the effect of SINC-COSINE-MBF apodization profiles on the performances of filters of three phase unidirectional transducers having one uniform and one apodized transducers using one such profiles, a work of simulating and calculating different such filters responses has been carried out. The computational results of some of these simulated filters are presented in Tables {6.10} to {6.12}.

Comparing the computational results given in tables and frequency responses shown in Figures 6.34 to 6.36 of TPUDT-16/TPUDT-23 filter (apodization type number (51 1. 1.)),

Table {6.10}

Computed Rise, 3dB and Fall bandwidths of filters of uniform and SINC weighted-COSINE & MBF windowed TPUDTs.

Transducer type	Apodization type	Aperture in meter	RB per cent	3dB BW per cent	FB per cent
T-16	1	4.9199E-4	2.569	4.480	0.782
T-23	5111				
T-16	1	4.9199E-4	2.569	4.134	0.770
T-24	5131				
T-16	1	4.9199E-4	2.703	3.687	0.670
T-25	5151				
T-16	1	4.9199E-4	2.960	3.005	0.837
T-26	5170.5				
T-16	1	4.9199E-4	2.770	3.709	0.670
T-25	5172				
T-20	1	3.1487E-4	1.675	4.1343	3.932
T-28	5111				

Table {6.11}

Computed first left and right side lobes levels
of filters of uniform and SINC weighted-COSINE & MBF windowed
TPUDTS.

Transducer type	Apodization type	Aperture in meter	LSL in dB	RSL in dB
T-16	1	4.9199E-4	20.4	17.6
T-23	5111			
T-16	1	4.9199E-4	19.12	16.36
T-24	5131			
T-16	1	4.9199E-4	18.84	16.4
T-25	5151			
T-16	1	4.9199E-4	21.6	17.0
T-26	5170.5			
T-16	1	4.9199E-4	19.28	16.76
T-25	5172			
T-20	1	3.1487E-4	20.72	17.32
T-28	5111			

Table {6.12}

Computed Rejection bandwidth and Shape factor of filters of uniform and SINC weighted-COSINE & MBF windowed TPUDTs.

Transducer type	Apodization type	Aperture in meter	RJ per cent	SHAPE factor
T-16	1	4.9199E-4	8.513	0.5262
T-23	5111			
T-16	1	4.9199E-4	8.424	0.4907
T-24	5131			
T-16	1	4.9199E-4	7.888	0.4674
T-25	5151			
T-16	1	4.9199E-4	7.798	0.3853
T-26	5170.5			
T-16	1	4.9199E-4	7.843	0.4729
T - 25		5 1 72		
T-20	1	3.1487E-4	7.150	0.5781
T-28	5111			

Fig. 6.35 Forward frequency response of uniform TPUDT-16, apodized TPUDT-24 and filter of both transducers. Apodization type number is 5131. Max Aperture is $4.9199\text{E}-4$ m.

Frequency Responses:
 — TPUDT-16 UNIF
 + TPUDT-24 APD;51 3 1.
 * FILTER

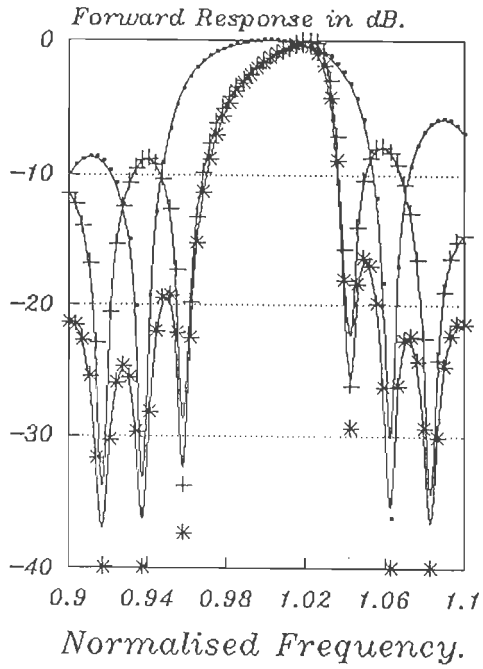
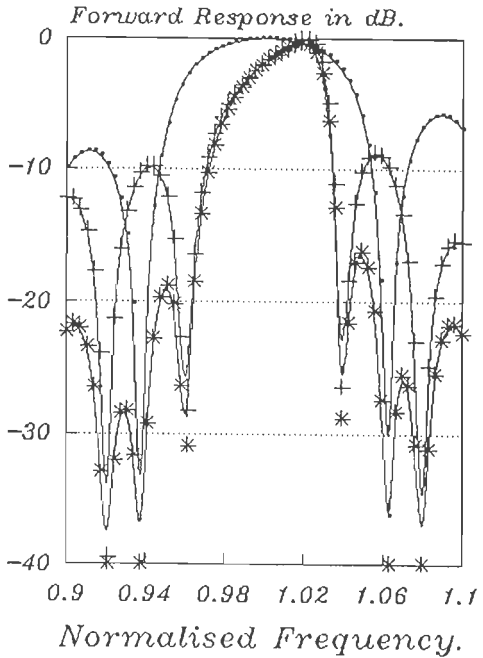


Fig. 6.36 Forward frequency response of uniform TPUDT-16, apodized TPUDT-25 and filter of both transducers. Apodization type number is 5151. Max aperture is $4.9199\text{E}-4$ m.

Frequency responses:
 — TPUDT-16 UNIF
 + TPUDT-25 APD;51 5 1.
 * FILTER



TPUDT-16/TPUDT-24 filter (APD 51 3. 1.) and TPUDT-16/TPUDT-25 filter (APD 51 5. 1.) on one hand and that of TPUDT-16/TPUDT-22 (apodization type number 41) given in Tables {5.25} to {5.27} whose frequency response is shown in Figure 5.40 on the other hand, one can see the improvement in filter performance using each of the above profiles with respect to the filter with SINC weighted-COSINE windowed transducer of Figure 5.40.

From these tables and figures it can be seen that with the increase in the value of b both 3dB bandwidth and shape factor are decreasing while side lobes levels are increasing. The increase in rise to 3dB bandwidths ratio can also be seen.

Figures 6.37 and 6.38 show increase in 3dB bandwidth and filter shape factor with the increase of the value of n . The performance shows some improvement in terms of side lobes levels with the decrease of the value of n .

In all the filters shown in Figures related to this section the effect of changing the frequency locations and bandwidths of apodized transducers side lobes by selecting different windows is very much clear.

The forward frequency responses of TPUDT-16/TPUDT-35 filter (APD 51 1. 1.) and TPUDT-20/TPUDT-28 shown in Figures 6.34 and 6.39 show clearly how frequency locations of apodized transducers side lobes resulted a uniform roll off while in other windows filters side lobes levels are going up and down as side lobes go away from the main lobe.

Fig. 6.37 Forward frequency response of uniform TPUDT-16, apodized TPUDT-26 and filter of both transducers. Apodization type number is 5170.5. Max aperture is $4.9199\text{E-}4$ m.

Frequency responses:
 — TPUDT-16 UNIF
 + TPUDT-26 APD;51 7 .5
 * FILTER

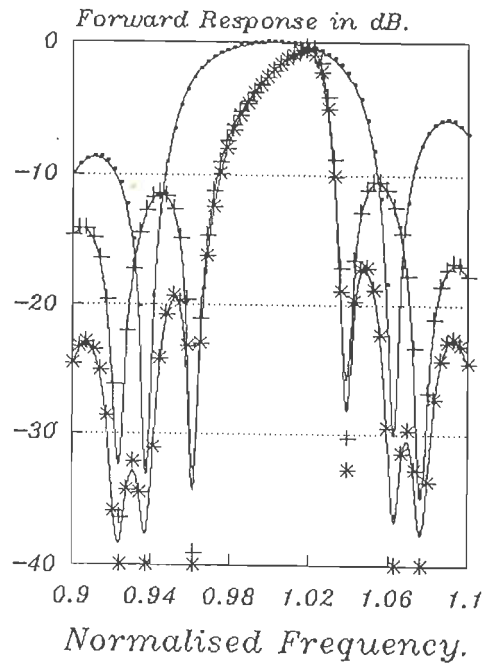


Fig. 6.38 Forward frequency response of uniform TPUDT-16, apodized TPUDT-25 and filter of both transducers. Apodization type number is 5172. Max aperture is $4.9199\text{E-}4$ m

Frequency Responses:
 — TPUDT-16 UNIF
 + TPUDT-25 APD;51 7 2.
 * FILTER

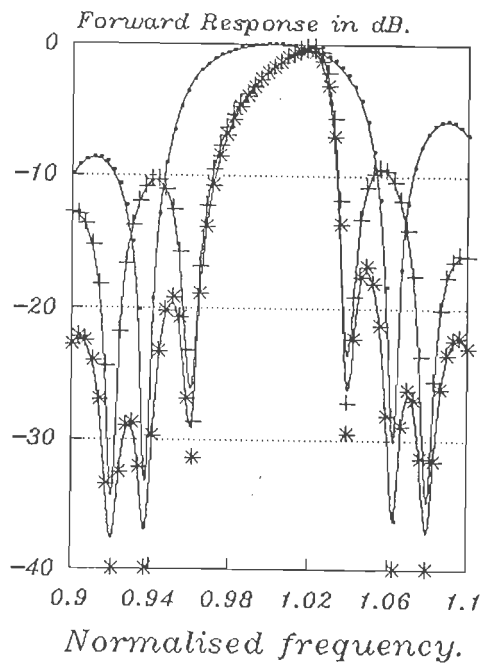


Fig. 6.39 Forward frequency response of uniform TPUDT-20, apodized TPUDT-28 and filter of both transducers. Apodization type number is 5111. Max aperture is $3.1487\text{E}-4$ m.

Frequency Responses:
 — TPUDT-20 UNIF
 + TPUDT-28 APD;51 1 1.
 * FILTER

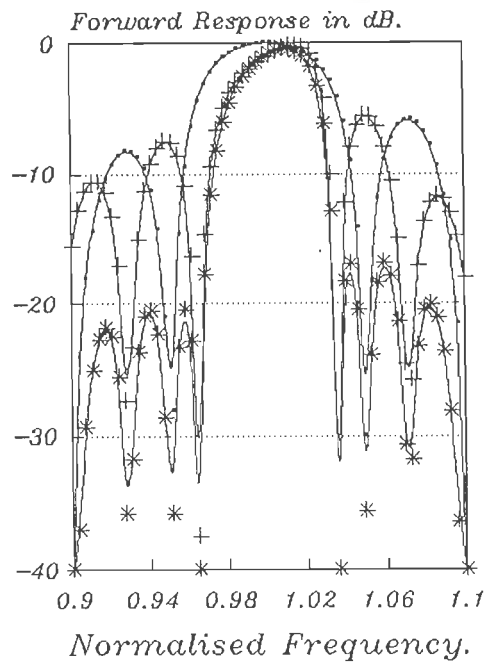


Fig. 6.40 Admittance response of uniform TPUDT-20, apodized TPUDT-28 and filter of both. Apodization type number is 5111. Max effect. apert. is $3.1487\text{E}-4$ m.

Admittance:
 — TPUDT-20 UNIF
 + TPUDT-28 APD;51 1 1.
 * FILTER

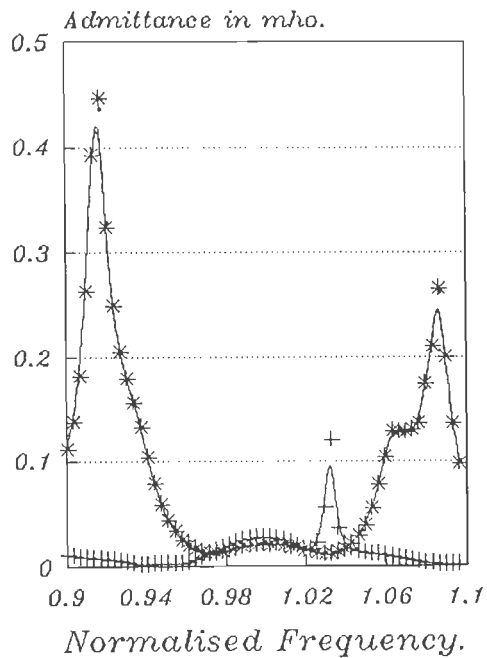


Fig. 6.41 *Relative Directivity of uniform TPUDT-20, apodized TPUDT-28 and filter of both. Apodization type number is 5111. Max Effec. Aper. is 3.1487E-4 m.*

Directivities:
 — TPUDT-20 UNIF
 + TPUDT-28 APD;51 1 1.
 * FILTER

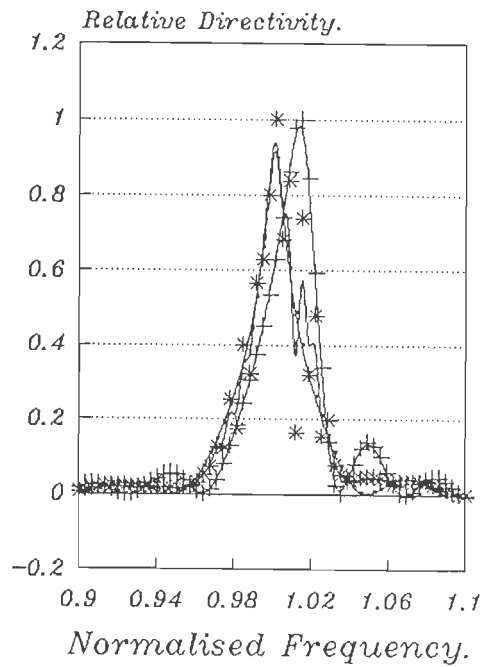
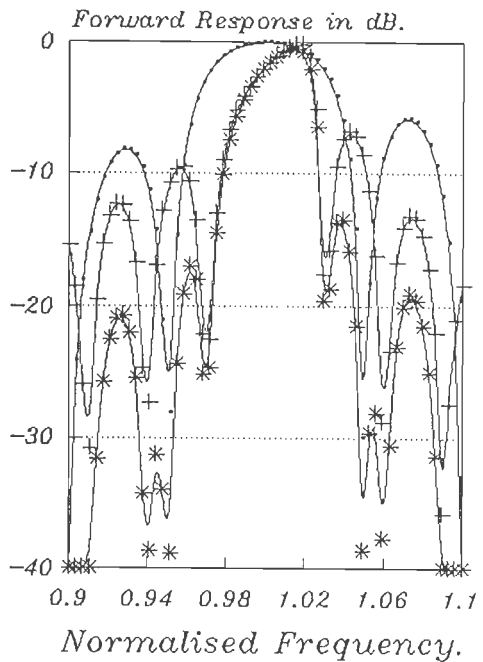


Fig. 6.42 *Forward frequency response of uniform TPUDT-20, apodized TPUDT-33 and filter of both transducers. Apodization type number is 5171. Max Aperture is 3.1487E-4 m.*

Frequency Responses:
 — TPUDT-20 UNIF
 + TPUDT-33 APD;51 7 1.
 * FILTER



Figures 6.40 and 6.41 show admittance and relative directivity responses of TPUDT-20/TPUDT-28 filter (APD 51 1. 1.).

6.11 FILTER WITH UNIFORM TPUDT AND (SINC-COSINE-MBF PROFILES) APODIZED GUDT :

Figures 6.43 to 6.49 give plots of different responses of simulated filters constructed from one uniform wide band three phase unidirectional transducer and narrower band (SINC-COSINE-MBF profiles) apodized group unidirectional transducer. Tables {6.13} to {6.15} give the computational results of two of such filters.

From tables and plots of frequency responses of these filters shown in Figures 6.43, 6.44 and 6,49 it can be seen that for the same uniform transducers the number of apodized groups may increase with the change of apodization profile with one of higher value of b . It can be seen also that with this change 3dB bandwidth decreases, rise bandwidth increases, filters shape factor lowers and side lobes levels increases.

It may be noted also from forward frequency responses of these filters that side lobes levels of these filters are generally high compared to filters of same transducers discussed earlier. This can be reasoned if one notices the frequency locations of apodized transducers side lobes. Because first both apodized transducer side lobes are located totally under the main lobe of the uniform TPUDT transducer we are not able to get the

Table {6.13}

*Computed Rise, 3dB and Fall bandwidths of filters
of combinations of uniform and SINC weighted-COSINE
& MBF windowed
GUDT and TPUDT transducers.*

Transducer type	Apodization type	Aperture in meter	RB per cent	3dB BW per cent	FB per cent
T-19	1	3.4889E-4	1.256	2.625	0.217
N-4-8	5111				
-19	1	3.4889E-4	1.284	1.854	0.089
N-4-10	5171				

Table {6.14}

*Computed first left and right side lobes levels of
filters of combinations of uniform and SINC weighted-COSINE
& MBF windowed GUDT and TPUDT transducers.*

Transducer type	Apodization type	Aperture in meter	LSL in dB	RSL in dB
T-19	1	3.4889E-4	13.28	6.4
N-4-8	5111			
T-19	1	3.4889E-4	12.4	4.6
N-4-10	5171			

Table {6.15}

Computed Rejection bandwidth and Shape factor of
 filters of combination of uniform and
 SINC weighted-COSINE & MBF windowed
 GUDT and TPUDT transducers.

Transducer type	Apodization type	Aperture in meter	RJ per cent	SHAPE factor
T-19	1	3.4889E-4	4.971	0.528
N-4-8	5111			
T-19	1	3.4889E-4	4.022	0.461
N-4-10	5171			

Fig. 6.43 Forward frequency response of uniform TPUDT-19, apodized GUDT-4-8 and filter of both transducers. Apodization type number is 5111. Max aperture is $3.4889\text{E-}4$ m.

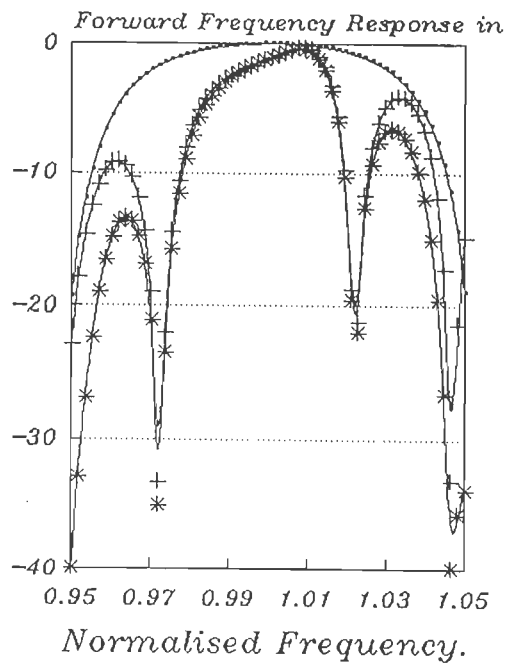
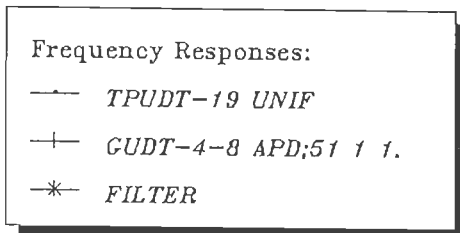


Fig. 6.44 Forward frequency response of uniform TPUDT-19, apodized GUDT-4-9 and filter of both. Apodization type number is 5131. Max Effective Aperture is $3.4889\text{E-}4$ m.

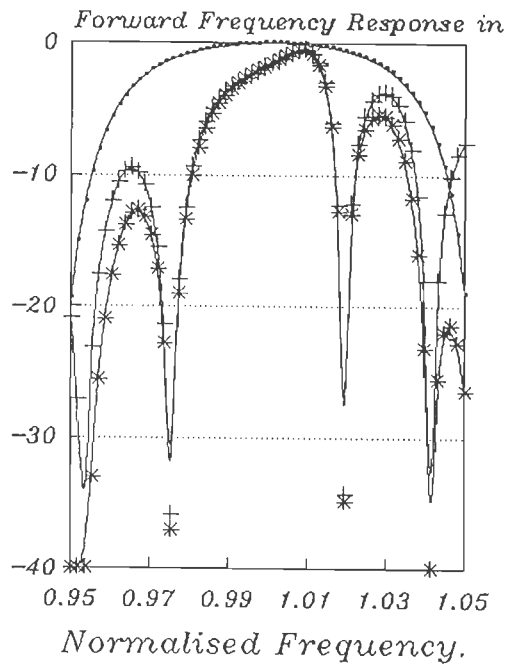
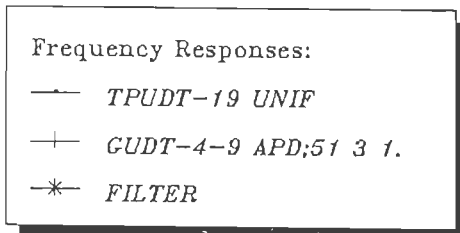


Fig. 6.45 Admittance response of uniform TPUDT-19, apodized GUDT-4-9 and filter of both. Apodization type number is 5131. Max aperture is 3.4889 m.

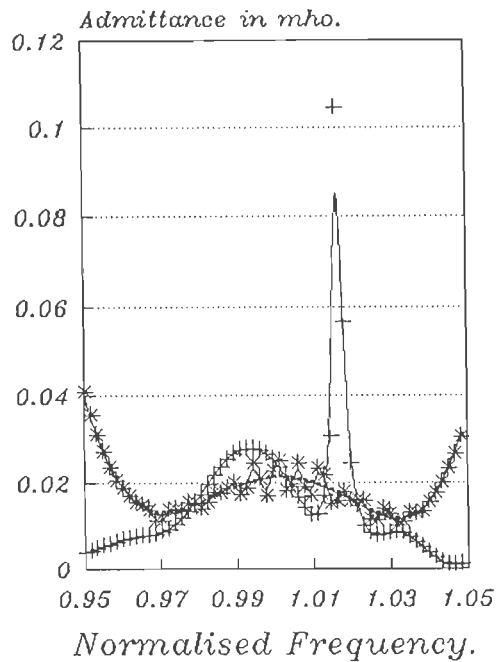
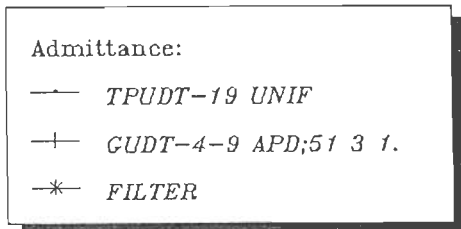


Fig. 6.46 Phase response of uniform TPUDT-19, Apodized GUDT-4-9 and filter of both. Apodization type number is 5131. Max aperture is 3.4889E-4 m.

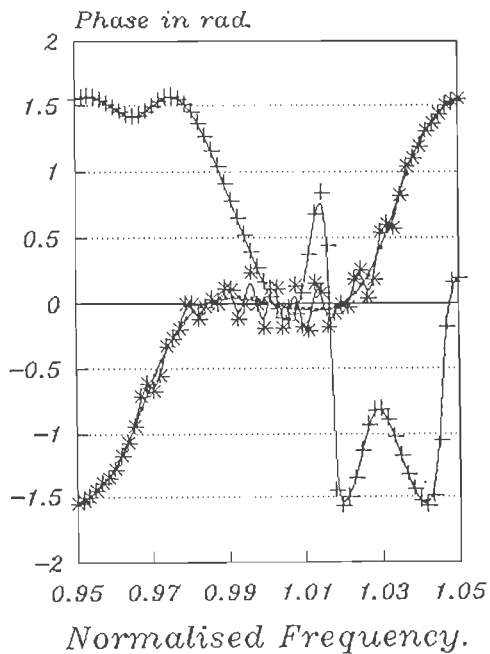
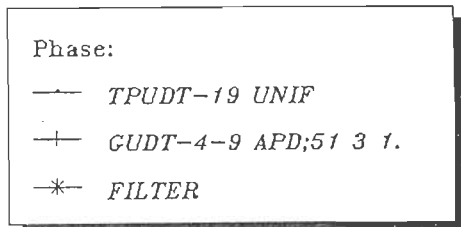


Fig. 6.47 Conductance response of uniform TPUDT-19, apodized GUDT-4-9 and filter of both. Apodization type number is 5131. Max aperture is $3.4889\text{E-}4$ m.

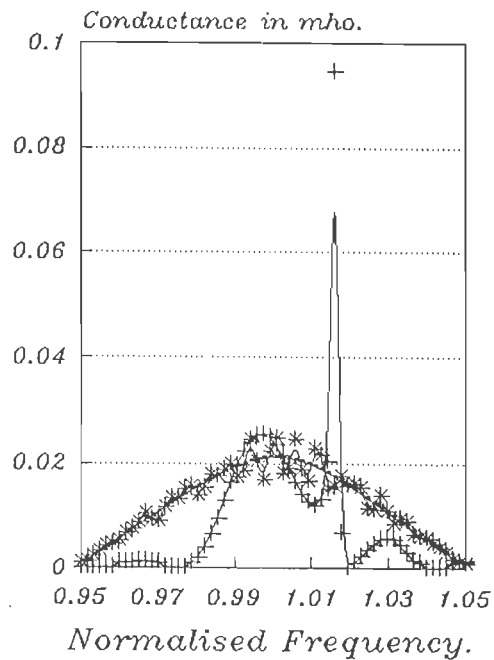
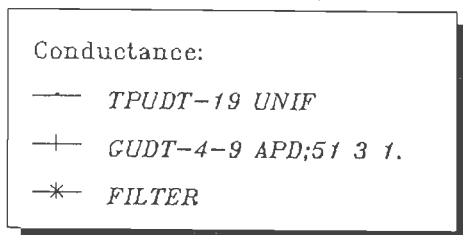
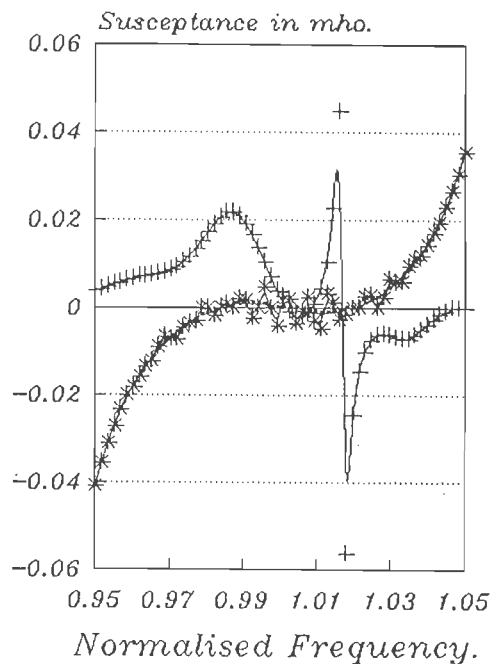
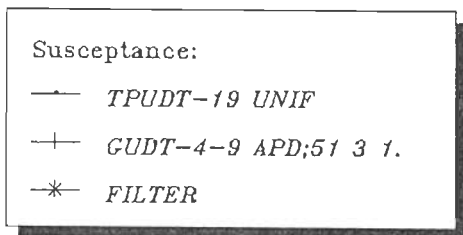


Fig. 6.48 Susceptance response of uniform TPUDT-19, apodized GUDT-4-9 and filter of both. Apodization type number is 5131. Max aperture is $3.4889\text{E-}4$ m.



appropriate side lobes levels reduction. This gives an advantage for filters having same type of uniform and apodized transducers.

Admittance, Phase, Conductance and susceptance responses of TPUDT-19/GUDT-4-9 filter (APD 51 3. 1.) along with corresponding responses of filter uniform and apodized transducers are shown in Figures 6.45 to 6.48. In all Figures, filter responses are oscillating around the uniform TPUDT responses.

6.12 CONCLUSION :

From the different window functions available in literature for different signal processing applications a generalized window function has been selected. This generalized function has been presented, studied and many Modified Bessel window Functions have been derived from.

Some of these window functions have been studied in both time and frequency domains. T in equation 6.1 has been taken as normalized 1.; b and n values have been varied. It has been found that lower n and/or lower b means a more flat window regardless whether the values of n and b are integers or fractionals.

In frequency domain it has been found that lowering b (by an integer or a fraction) yields lower side lobes levels but in the same time lower shape factor. Changing the value of n gives different responses depending on whether the value of n is integer or fractional. Side lobes levels are lower with lower integer n

values but it is higher with fractional n values. The value of n also affect side lobes roll off. Negative side lobes roll off has been noticed in windows with n greater than 1.

Many new apodization profiles have been calculated using SINC weighting, COSINE and one MBF windowing functions with different lengths of SINC-COSINE functions.

The profiles have been used in apodizing number of group and three phase unidirectional transducers. filters of one uniform transducer and one apodized with one such profiles have been simulated. The filters were having either both GUDT transducers, both TPUDT transducers or mixed combination of the two types.

From the different responses of these simulated apodized transducers and filters it has been found that the number of apodized groups or sections play a great role in changing the performance of apodized transducer or its filter. First of all this number should be quit enough to shape the selected profile otherwise another profile may be shaped if the number is so less.

The number of apodized groups or sections have been calculated according to the number of uniform groups and effective finger per group or number of uniform sections and the apodization profile selected in a way that the apodized groups or sections apertures will perform the selected profile shape while maintaining matching.

It has been found accordingly that selecting different apodization profiles some times requires changing the number of apodized groups or sections.

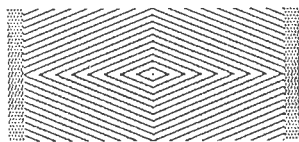
In general one can say from the different results we obtained that changing b requires always selection of a new number of apodized groups or sections so that to compensate for the change in rise to 3dB bandwidths ratio and improve the shape factor. Increasing the value of n will cause generally lowering rise, 3dB bandwidths, shape factor and side lobes level as well if this change does not cause a change in the number of apodized groups or sections, otherwise it may increase the bandwidth and shape factor.

It has been found that there are general guessings or expectations regarding the performance of apodized transducer or the filter it belongs to when certain profile is used in apodization, but still each case is having its own differences depending on the number of apodized groups or sections, how close it is shaping the selected profile and not another, and what is the value of rise to 3db bandwidths ratio in this specific case..etc.

For getting low filter side lobes levels it is recommended to make use of the effect of differences in transducers side lobes frequency locations and bandwidths. In the presented results for filters constructed from same type of unidirectional transducers such utilization can be observed. If the apodized transducer is

having so much wider bandwidth that both its first side lobes are included inside the main lobe of the uniform transducer no additional reduction can be gained from the difference in transducers side lobes frequency locations at least for the first left and right side lobes.

Finally we state that the apodization profiles that have been presented in this chapter are very less compared to the number of apodization profiles that can be provided by the MBF window family. Some more window functions can be generated by changing the values of T , b and n of equation 6.1 and some more apodization profiles one can get by changing the lengths of SINC or both SINC-COSINE functions or use MBF windows without the COSINE window..etc. The software modeling package is able to simulate SAW transducers and filters using the above mentioned profiles and with some minor modifications one can include any type of window and apodize with any selected profile according to design requirements.



CHAPTER SEVEN

7

Recapitulation And Conclusion

- 7.1 Introduction.
- 7.2 Modelling Of SAW Devices.
- 7.3 Simulation And Study Of
Performances Of Different types
Of SAW Transducers And Filters.
- 7.4 Discussing The Goals.
- 7.5 Future Scope.
- 7.6 Concluding Words.

RECAPITULATION AND CONCLUSION

7.1 INTRODUCTION :

Recapitulation of the work carried out and results obtained through the course of this study are presented and discussed. The goals that have been stated in the beginning of this work are discussed and verified with what has been achieved. Finally, recommendations and suggestions for future work are given.

7.2 MODELLING OF SAW DEVICES :

Different models commonly used for analyzing SAW devices (of field theory approach and circuit theory approach) have been briefly studied. The main goal of this work has been to try to find out a proper model and develop a simulator that can be used as an aidfull, quick and accurate tool for simulating and modelling incorporate different SAW devices, specially low loss transducers and filters with given specifications, to help designers of signal processing equipment using SAW devices to design using software and make the required modifications before the final fabrication.

Accordingly, and because time required by such simulator to perform the simulations of these designs is a very important factor (as well as the model accuracy) it has been decided to select the crossed field equivalent circuit as the basis for any model to be developed. The crossed field equivalent circuit model is not the most ideal one for analyzing SAW devices. The field theory approach models such as the coupled of modes theory model and the Green's function model are giving much more accurate results yet they require more computation effort and the modelling process is more complicated. The crossed field equivalent circuit model seemed to be the most appropriate for such task as far as a compromise between complexity and computational effort is concerned and with comparable results with the experiments.

The modelling work that has been carried out during the course of this study was in three approaches. In the first approach the surface acoustic wave interdigital transducer has been treated as a point scatterer located at the centre of the transducer. Two models have been presented, derived, discussed and studied. Both are based on the simplified equivalent circuit model and the scattering matrix theory. Accordingly, bidirectional transducers have been presented by a 3×3 scattering matrix with four independent scattering parameters, while unidirectional transducers required two more independent parameters to be represented by a similar matrix.

It has been found that the junction scattering matrix model capabilities are limited to the matched and tuned conditions. It

has been found also that the scattering matrix model provides many informations regarding the performances of SAW transducers such as forward and backward frequency responses, directivity, triple transit echo, acoustic transmission loss, electric mismatch loss..etc. of which some of them no other model can give directly. Moreover, the model has been found to be very fast in terms of computation time requirements, yet it is limited in its capability of representing many types of SAW transducers.

In the second approach, the gap between two fingers has been treated as a finger yet unmetalized. Both metalized and unmetalized fingers have been represented by three-ports networks with acoustic ports expressed in terms of waves and the electric port expressed in electrical terms; voltage and current.

The combination gap-finger-gap transfer matrix has been considered as the basic-unit matrix from which the full matrix of the full transducer can be derived through cascading this basic-unit.

The model was able to represent many types of bidirectional transducers, such as normal BIDT, split finger BIDT, CHIRP and COMB transducers and filters of such transducers from combinations of negative and positive voltage derived fingers. The model was not able to represent unidirectional transducers unless some more types of voltage derived basic-units such as the earthed finger unit and the phase shifted voltage derived finger unit are modelled, which leads to complexity.

In the chain matrix model, the acoustic terminals have been expressed in terms of acoustic force and particle velocity. The bidirectional transducer has been modelled by a four port network with two acoustic ports and two electric ports for input and output. It has been represented by a 4 x 4 Sittig's chain matrix. Group and three phase unidirectional transducers have also been modelled and represented by 6 x 6 and 8 x 8 matrices, respectively.

A SAW simulator has been developed to model and simulate many types of bidirectional and unidirectional transducers and filters built from combinations of these simulated transducers. The simulator allows the designers to simulate their devices and test its performances under different operational conditions by changing different parameters in the simulator such as electric load, transducer aperture, substrate material..etc. before fabricating the device, thus saving money and effort that may be spend on fabricating a device that has performance which is not up to the requirements.

7.3 SIMULATION AND STUDY OF PERFORMANCES OF DIFFERENT TYPES OF SAW TRANSDUCERS AND FILTERS :

Performances of normal and split-finger type uniform transducers and filters have been reported and briefly discussed. The results of these transducers and filters have been computed

with either scattering matrix or transfer matrix models.

Using the modelling software package that have been developed, many types of transducers and filters have been simulated. Performances of unidirectional transducers and filters constructed (in software) have been reported, studied and discussed. Different group types unidirectional transducers (Normal, Modified and New types) with different numbers of active fingers per group and different numbers of groups - either uniform, SINC apodized or windowed as well, with one or more of the windows discussed in this dissertation -have been simulated and performance results have been reported in tables or/and graph forms in terms of forward and backward frequency responses, directivity, admittance, phase, conductance, susceptance responses..etc. Results have been studied and deeply discussed.

Similarly, three phase unidirectional transducers have been simulated with different periodic sections, and using different apodization profiles starting with the uniform apodization. Results of three phase unidirectional transducers have been reported, studied and discussed in the same way we mentioned for GUDTs.

Number of two uniform transducer type filters as well as filters with one wide band uniform transducer and another narrow-band apodized transducer have been simulated. The combinations of transducers used have been either both transducers are of the same type or mixed combinations of group and three

phase unidirectional transducers.

In filter design for signal processing applications there are certain response requirements that are considered as goals for each specific application. Some of these filter responses required are those as close as possible from the ideal brick shape response. Some other applications require some different shape responses other than the brick-shape.

To study the different parameters that affect the performance of a SAW transducer and filter and to know how to get the required response or performance of a SAW transducer/filter that suits the aimed application, a study has been carried out on non-uniform finger overlapped transducers and filters. The functions that have been used in performing this non-uniform overlapping were SINC function for weighting, COSINE function as a window, in addition to many other window functions that have been derived from a generalized MBF equation. The characteristics of many of these MBF windows have been studied in both time and frequency domains, and many new apodization profiles using the three functions (SINC-COSINE-MBF) have been worked out.

Selection of an appropriate apodization profile using the proper window function is of a great importance for obtaining the required transducer/filter response for a specific signal processing application. Yet it has been found that it is not the only thing one has to care for when working to get such

transducer/filter responses, because it is not the only factor that affects transducer/filter performances. It has been found that there are many factors other than the apodization profile that affect greatly the SAW transducer/filter response. Some of these factors are the selection of the two transducers combination, uniform transducer bandwidth relative to the apodized transducer, number of apodized groups/sections, number of active fingers per group, frequency locations and bandwidths of both transducers side lobes, how close the apodized groups or sections are shaping the selected apodization profile, the value of rise to 3dB bandwidths ratio with all these factors...etc. It is needless to say that the input and output admittances of the filters play an important role in the design.

The selected number of sections/groups and fingers per group affect both uniform and apodized transducers. Yet these numbers in apodized transducers may cause drastic changes in transducer/filter responses compared to the uniform transducer response. It affect greatly rise to 3dB bandwidths ratio and fall to 3dB bandwidths ratio. these numbers may also be changed and used as a cure to ill responses obtained from apodized transducers. selecting the proper number of pairs/sections/groups and active fingers per group for a certain apodization profile is very much essential in getting good response from (weighted/windowed) apodized transducers.

The effect of the number of apodized pairs/groups/sections on the performance of apodized transducers is not limited to the

effect on transition to 3db bandwidths ratios. The number should be quite enough to give a close shape to the apodization profile selected so that the obtained response corresponds to that profile. There is a difference also in the cases where the number of apodized groups/sections/pairs is odd or even. Generally for even number of apodized pairs/sections/groups the maximum aperture of the apodized transducer is less than the computed or the uniform transducer aperture by an amount decreasing with the increase in this number. This difference in the two transducers apertures means that there will be some acoustic energy loss.

It has been found that the behaviour of rise and fall to 3db bandwidths ratios in apodized transducers is related but different. While both transition bandwidths and 3dB bandwidth are increasing or decreasing with the decrease or increase in number of pairs/sections/groups and fingers per group, both ratios are changing inversely with any increase or decrease in these numbers. Below a certain threshold for each transducer any increase in these numbers will cause a decrease in rise to 3dB bandwidths ratio and an increase in fall to 3dB bandwidth ratio. After the threshold things get reversed. Transition to 3db bandwidths ratios have relation with changing the truncated length of the weighting - windowing functions also.

Filters side lobes levels are determined from both transducers (constructing the filter) side lobes levels, whether both transducers are uniform or one of them is apodized. Yet there are other factors by which one can get still lower filter side

lobes levels. The differences in frequency locations and bandwidth of both transducers side lobes may cause great lowering of filter side lobes levels or even some times cancellation of some filter side lobes. In filters of both uniform transducers this can be achieved by having combinations of two types transducers with one wide band transducer and and the other narrower. In filters having one uniform and one apodized transducers this can be achieved with both same and mixed types of transducers. The passband of the apodized transducer can be controlled by selecting different apodization profiles. It is always better to have enough difference between both transducers passbands so that the filter pass band will be as close as possible to the apodized transducer passband for ease in design.

Apodization profiles that have been used in this study are either uniform overlapping, simply SINC function weighting with different truncation lengths, SINC function weighting with COSINE function windowing using different lengths of both functions, and finally the use of one more additional window from the MBF window family with the COSINE window and SINC weighting functions, also with different lengths of SINC and COSINE functions.

It has been found that although there are general expectations regarding the performance of an apodized transducer or the filter it belongs to when certain profile is used in performing the apodization, still each case is having its own differences depending on the number of apodized pairs/groups/sections, how close it is shaping the selected

profile and not another, and what is the value of rise to 3dB bandwidths ratio in that specific case..etc. Best - because there are so many factors to care for - is to use a simulator and simulate the apodized transducer and the filter it belongs to, and make sure that the designed transducer or filter is giving the required response and performance.

7.4 DISCUSSING THE GOALS :

Going back to the goals that have been stated for this work in the first chapter and comparing the work that has been achieved with respect to these goals one can see that most of the goals have been achieved. The simulator that have been developed - based on the chain matrix model of chapter four of this dissertation - has been found to be able to simulate a wide range of SAW transducers and filters . The package may be made to model single phase unidirectional transducers by including 'grattings' in the chain matrix model.

Filters with both apodized unidirectional transducers have not been modelled. Modelling of such filters has been tried using *channelization method* and scattering matrix theory, but the phase shifters which have been included in the basic modelling unit of both GUDT and TPUDT were great obstacles for such modelling.

Different apodization profiles have been worked out during this study, yet there are plenty more one can get by using

different window functions or even changing the weighting function as well giving rise to varied responses which may be needed in new signal processing applications.

7.5 FUTURE SCOPE :

A reliable, accurate and fast simulator to be used as an aiding tool by SAW signal processing designers can not be fulfilled fully and easily. The simulator that has been developed is able to cover wide range of SAW transducers and filters yet there are so many other types of SAW devices that have important signal processing applications such as single phase unidirectional transducers, resonators , Convolvers..etc.

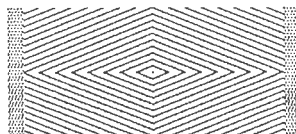
It is recommended that a similar work may be carried out using coupled of modes theory to include SPUDT and filters of such transducers and resonators. Some other models may also be used to include more SAW signal processing devices.

A simulator that is able to simulate SAW devices using different circuit and field theories approaches models with minimal errors and as close as possible to the real behaviour of the selected SAW device within acceptable time is a real aid to the designers of SAW signal processing devices. The work presented in this dissertation plus any work in the same line such as the work of Richie et al [48,51] are first steps towards such efficient simulator.

Lot of work can be done using the simulator presented in this dissertation. Some more apodization profiles may be derived and studied. A study of the different responses required in signal processing applications may be carried out and SAW filters that give such responses may be designed using the present simulator after selecting proper windows and apodization profiles.

7.6 CONCLUDING WORDS :

The model and the simulating package developed during the course of this study seems to be promising and expandable to include the modelling of few more SAW signal processing devices, and it is expected to be useful and helpful to the designers of SAW devices for signal processing applications. It is expected and hoped that the filters simulated in this work will have many applications. The filters using windowed apodization can have many important applications specially in multichannel systems where suppression of adjacent channels is very essential and in equalization where frequency dependent attenuation is required. Similarly proper selection of different pairs of UDTs and suitable apodization profiles may give very good convolver performances, when it is used to build up such convolvers, to be used in many communication and signal processing applications such as spread spectrum, cepstrum analysis, real time on-line filtering ..etc.



CHAIN MAT SIMULATOR

The simulation package developed and used during the course of this work consists of the following files;

CHAIN.EXE,
PCIQCT.EXE,
FTRES.EXE and
INQCT.DAT.

The software is run under DOS environment after typing CHAIN <RETURN>. It generates the following data files in the working directory;

TRES.DAT,
PNT.DAT and
PLT.DAT.

If the number of filters to be simulated is more than one the package will generate many PNT and TRES data files (i.e. PNT1.DAT, TRES1.DAT, PNT2.DAT, TRES2.DAT..etc.) up to the total required number of filters.

The input data can be edited either through the package or by editing INQCT.DAT by any unformatted word processor before running CHAIN.

PNTn.DAT files contain output data of simulated transducers and filters of the last run in terms of transducers/filters Insertion Losses, Backward Responses, Directivities, Input and Output transducers/filters Admittances (Magnitudes and Phases), Conductances and Susceptances.

FTRESn.DAT files contain output data of last FFT computations which include transducers (FFT Computed) responses, Apodization Profiles, Window functions in time and frequency domains..etc.

PLT.DAT file contains the plots of the results obtained from the last run of the simulator program.

The package is made to be menu driven and on line help is provided to make it user friendly. The selection of action is performed by arrows or option numbers. Figures A.1 to A.4 show screen print-outs of the package while in use.

CHAIN MAT SIMULATOR V 1.00
(SAW Transducers/Filters Simulator)

Written and Developed by HISHAM AL-RAWI

For Information, Consultations, Problems if any, and Suggestions CONTACT:
[(c) Copy right holders; 1992. All Rights Reserved.]

Dr. Jai Krishna Gautam
Dept. Electron. & Comp. Engg.
University Of Roorkee
Roorkee 247 667 INDIA

Hisham Al-Rawi
P.O.Box 7295
Baghdad - IRAQ
Tel. 00964-1-5378875

Press any key to start CHAIN MAT...

Figure A.1 Title and Copyright Screen.

Chain Matrix Menue

09/15/92 10:53:13

1. Edit Data.
2. Simulate Filter.
3. FFT Computation.
4. Exit.

Highlight Option By ↑ or ↓ And Press ←

Or Press Appropriate Menue Number.

Enter/Change Simulator Input Data.

Figure A.2 CHAIN MAT Simulator Main Menue.

Chain Simulation Menue

09/15/92 10:52:31

1. Run Simulator.
2. Show Results.
3. Print Results.
4. Exit.

Highlight Option By ↑ or ↓ And Press ↵

Or Press Appropriate Menue Number.

Calculate Transducer/Filter Different Responses.

Figure A.3 Transducer/Filter Simulation Menue.

FFT Computations Menue

09/15/92 10:54:04

1. Start FFT Computations.
2. Show Results.
3. Print Results.
4. Exit.

Highlight Option By ↑ or ↓ And Press ↵

Or Press Appropriate Menue Number.

Calculate Windows and Apodization Profiles.

Figure A.4 FFT Computation Menue.

REFERENCES

1. White R. M., and Voltmer F. W.; " Direct Piezoelectric Coupling To Surface Elastic Waves ", Appl. Phys. Lett. Vol.7, pp-314-316, 1965.
2. Krimholtz R. S.; " The Hybrid-Junction Interdigital Acoustic Surface Wave Transducer" , Ph.D. Dissertation Univ. Of California, U.S.A., 1971.
3. Matthews H. (Ed.); " Surface Wave Filters ", John Wiley, New York, 1977.
4. Datta S.; " Surface Acoustic Wave Devices ", Prentice-Hall, 1986.
5. Tancrell R. H., Schulz H. H., Davis L., Jr., and Holland M. G.; " Dispersive Delay Lines Using Ultrasonic Waves ", Proc. IEEE, Vol 57, PP-1211-1213, 1969.
6. Tancrell R. H. and Holland M. G.; " Acoustic Surface Wave Filters ", Proc. IEEE Vol 59, PP-393-409, 1971.
7. Redwood M. and Milson R. F.; " Piezoelectric Coupling Coefficient Of Interdigital Rayleigh Wave Transducer ', Electron. Lett., Vol 6, PP-437, 1970.
8. Lewis .M. F.; ' SAW Filters Employing Interdigitated Transducers, IIDT ', Proc. IEEE Ultrasonic Symposium, PP-12-17, 1982.

9. Collins J. H., Gerard H. M., Reader T. M. and Shaw H. J.; " Unidirectional Surface Wave Transducers ", Proc. IEEE Vol 57, PP-833-835, 1969.
10. Lewis M. F., West C. L., Deacon J. M. and Humphryes R. F. " Recent Developments In SAW Devices ", Proc. IEE Vol 131, Part A, PP-186-215, 1984.
11. Engan H.; " Interdigital Electric Transducers For The Excitation Of Elastic Surfaces In Piezoelectric Media." Research Lab, Norwegian Institute Of Technology, Norway, ELAR Report. TE-91, 1967.
12. Potter B. R. and Hartmann C. S.; " Low Loss SAW Filters ", IEEE Trans. Vol PHP-13, PP-348-353, 1977.
13. Yamanouchi K., Nyffeler F. M. and Shibayama K. " Low Insertion Loss Acoustic Surface Wave Filters Using Group Type Unidirectional IDT " Proc. IEEE Ultrasonic Symp., PP-317-321, 1975.
14. Yamanouchi K., Meguro T., and Gautam J. K.; " Low Loss GHz Range SAW Filter Using Group Type Unidirectional Transducers - New GUDT And New Phase Shifter ", Proc IEEE Ultrasonic Symp., PP-212-217, 1982.
15. Hartmann C. S., Wright P. V., Kansy R. J. and Garber E. M.; "Analysis Of IDTs With Internal Reflections And The Application To The Design Of Single Phase UDTs ", Proc. IEEE Ultrasonic Symp. PP-40-45, 1982.
16. Hartmann R. H., Bell D. T, and Rosenfeld R. C. " Impulse Model Design Of Acoustic Surface Wave Filters ", IEEE Trans. Vol MTT-20, PP-162-175, 1973.

17. Smith W. R. Gerard H. M., Collins J. H., Reader T. M. and Shaw H. T.;" Analysis Of Interdigital Surface Wave Transducers By Use Of An Equivalent Circuit Model ", IEEE Trans. Vol MTT-17, PP-856-864, 1969.
18. Smith W. R., Gerard H. M. and Jones W. R.;" Analysis And Design Of Dispersive Interdigital Surface Wave Transducers ", IEEE Trans, Vol MTT-20, PP-458-471, 1972.
19. Milson R. F., Reilly N. H. C. and Redwood, M.;" Analysis Of Generation And Detection Of Surface And Bulk Acoustic Waves By Interdigital Transducers ", IEEE Trans. Vol SU-24, PP-147-166, 1977.
20. Campbell C.;" Surface Acoustic Wave Devices And Their Signal processing Applications ", Academic Press, 1989.
21. Auld B. A. and Kino G. S.;" Normal Mode Theory For Acoustic Waves And Its Applications To Interdigital Transducer ", IEEE Trans. Vol. ED-18, PP-898-908, 1971.
22. Kogelnik H.;" Coupled Wave Theory for Thick hologram gratings " , Bell Sys. Tech. J., Vol 48, PP-2809-2947, 1969.
23. Kogelnik H. and Shank C. V.;" Coupled Wave Theory of Distributed Feedback Lasers ', J. Appl. Phys. Vol. 43, PP-2327-2335, 1972.
24. Thorvaldsson T. " Design And Analysis Of Surface Acoustic Wave Resonators And Resonator Filters ". Ph.D. Dissertation, ETH , Switzerland, 1988.
25. Morgan D. P.;" Quasi-Statistic Analysis Of Generalized SAW Transducers Using The Green's Function Method ", IEEE Trans. Vol. SU-27, PP-111-123, 1980.

26. Bahai-Wadji A. R., Selbuherrs S., and Safut F. J.; " Two Dimensional Green's Function Of A Semi Infinite Anisotropic Dielectric In The Wave Number Domain." ,IEEE Trans. Vol. UFFC-33, PP-315-317, 1986.

27. Ablot B. P., Hartmann C. S. and Malocha D. C.;" Tranduction Magnitude An Phase For COM Modeling Of SAW Devices." , IEEE Trans., Vol. UFFC-39, PP-54-60, 1992.

28. Chen E. M., Takenchi M, and Yamanochi K.; " Analysis Of The Filter Thickness Dependence Of A Single Phase Unidirectional Transducer Using Coupled Of Modes And Finite Element Method.", IEEE Trans., Vol. UFFC-39, PP-82-94, 1992.

29. Visinein G., Baghi-Wadji A. R., and Männe O.; " Modular Two-Dimensional Analysis Of SAW Filters, Part I; Theory.", IEEE Trans, Vol. UFFC-39, PP-61-72, 1992.

30. Feldmann M. and Henaff J.; " Surface Acoustic Waves For Signal Processing ", Artech House, London, 1989.

31. Slobodnik A. J.; " A Review Of Material Trade-Offs In The Design Of Acoustic Surface Wave Devices At VHF And Microwave Frequencies. ", IEEE Trans. , Vol. SU-20, PP-315-323, 1973.

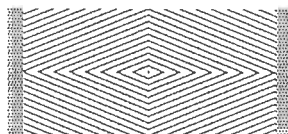
32. Rosenberg R. L.; " Wave - Scattering Properties Of Interdigital SAW Transducers. ", IEEE Trans., Vol. SU-28, PP-26-41, 1981.

33. Waldron R. A.; " Scattering Matrix Theory Of The Performance Of Acoustic Surface Interdigital Transducers. ", Microwaves, Optics And Acoustics, Vol. 3, PP-259-264, 1979.

34. Waldron R. A.; " Scattering Matrix Theory Of Dispersive Interdigital Transducers For Pulse Compression Radar ", IEE Proc. Vol. 127, Part H, PP-15-19, 1980.

35. Joshi S. G. and Sudhakar P.; " Scattering Parameters Of Interdigital Surface Acoustic Wave Transducers ", IEEE Trans, Vol. SU-24, PP-201-206, 1977.
36. Gautam J. K.; " Modelling of SAW Devices, Lectures And Notes ", University Of Roorkee, 1990.
37. Debnath N. C., Ajmera R. C., Hribsek M. F. and Newcomb R. W.; " Scattering And Admittance Matrices Of SAW Transducers. ", Circ., Sys. and Sign. Processing (USA), Vol. 2, PP-161-177, 1983.
38. Nyffeler M. F. and Gautam J. K.; " Personal Notes On Transfer Matrix." E.T.H., Zürich, Switzerland, 1989.
39. Jones W. S., Hartmann C. S. and Sturdivant T. D.; " Modified Equivalent Circuit Model For Ultrasonic Surface Wave Interdigital Transducers " , Proc. IEEE MTT Symp., P58-59, 1971.
40. Krairojatan T. and Redwood M.; " Equivalent Electrical Circuits Of Interdigital Transducers For Piezoelectric Generation And Detection Of Rayleigh Waves ", Proc. IEEE, Vol. 118, PP-305-310, 1971.
41. Sato H., Yamanouchi K., Shibayama K. And Nishiyama S.; " On The Design Of Electric Surface Wave Filters With No Tuning Coil." , Proc. Of 28th Symp. Of Frequency Contral, PP-286-298, 1974.
42. Gautam J. K.; " Low Loss Surface Acoustic Wave Transducers and Their Applications ", D. Engg. Dissertation, Tohoku University, Japan, 1984.

43. Sittig E. K. ; " Transmission Parameters Of Thickness-Driven Piezoelectric Transducers Arranged In Multilayer Configarations. ", IEEE Trans, Vol. SU-14, PP-167-174, 1967.
44. Malocha D. C.; " Theory and Design Of Surface Acoustic Wave Transducers And Filters, Collected Lectures ", University of Central Florida, 1989.
45. Malocha D. C. and Bishop C. D.; " The Classical Truncated Cosine Series Functions With Application To SAW Filters ", IEEE Trans., Vol. UFFC-34, PP-75-85, 1987.
46. Gekinli N. C. and Yavuz D., " Discrete Fourroer Transformation And Its Applications To Power Spectra Estimations. ", E.S.P., 1983.
47. Harris F. J.; " On The Use Of Window For Harmonic Analysis With Discrete Fourier Transforms." , Proc. IEEE Vol. 66 PP-51-83, 1978.
48. Richie S. M.; A design Automation System For Surface Acoustic Wave Filters Using Bidirectional Transducers." , Ph.D. Dissertation , University Of Central Florida, USA, 1989.
49. Reddy A. R.; " Design Of SAW Bandpass Filters Using New Window Functions ". IEEE Trans. Vol. UFFC-35, PP-50-56, 1988.
50. Reddy A. R. and Lahiri S. K.; " On Window Functions ", International J. Electronics, Vol. 56, PP-805-813, 1981.
51. Richie S. M. and Malocha D. C.; " A First Generation CAD Compiler For Surface Acoustic Wave Filters Using Bidirectional Transducers. ", Proc. Ultrasonic Symp., PP-173-178, 1989.



VITA OF THE AUTHOR

- * Name : Hisham Al-Rawi.
- * Father's Name : Sherif Abdullatif.
- * Date Of Birth : 28th. June. 1957.
- * Place Of Birth : Baghdad - IRAQ.
- * Nationality : Iraqi.
- * Permanent Address : 71/13/1, Haifa St., Baghdad - IRAQ.
Tel. 00964-1-5378875
- * Mailing Address : P.O Box 7295 Baghdad - IRAQ.
- * Academic And Business Record ;
 - I joined the *Department of Electrical Engineering (Light Current Section)*, University Of Technology, Baghdad - IRAQ, in 1975, and graduated in 1980 with B.Sc.Engg. & Tech. Electrical Engineering.
 - Jan. 1981, I joined the Post Graduate Studies (Communication Group) in the above Department. Jan. 1982 and Jan. 1984, I received my High Diploma Sc.Engg. & Tech. and M.Sc.Engg. & Tech. in Communications Engineering, respectively.
 - Feb. 1984 till Dec. 1985, I worked in the *Arab Gulf Academy For Mary Time Studies*, Basra - IRAQ, as a lecturer of Electronic Circuits and Communications, for the Naval Engineering College and academy post graduate (First Officer and Captain Courses) students.
 - Dec. 1985 up to date, lecturer (Electronic Circuits, Digital Electronics and Communications); in the *School Of Education Engineering*, Electrical Engineering Section, University Of Technology, Baghdad - IRAQ.
 - For the period from Dec. 1985 to Dec. 1986, I joined research groups - as part time assistant researcher - in *The Scientific Research Council*, Baghdad - IRAQ.
 - The period from Jan. 1987 to Jun. 1989, I worked as part time senior engineer in *A.E.C. Company for Engineering Designs And Services*, Baghdad - IRAQ, in the PABXs and Office Communications Section.
 - Aug. 1989 till date, Research scholar, *Department Of Electronics And Computer Engineering*, University Of Roorkee, Roorkee - INDIA.